

**The Production and Evaluation of
Microcapsules from Biological
Sources**

Katrina M. Bakker

PhD

University of York

Chemistry

June 2014

Abstract

The outer walls of pollen and spores are formed from sporopollenin: a strong, chemically inert biopolymer. In this thesis, several methods were applied to a range of pollen and spore species with the primary aim of removing all non-sporopollenin material, which may elicit an allergic response in some humans. The ultimate goal was to produce hollow, sporopollenin microcapsules from both pollen and spores and subsequently evaluate their properties and potential uses.

Microcapsules were prepared from *Lycopodium clavatum* spores according to a published base and acid treatment. The base step of this treatment caused notable damage to the pollen species investigated. Acetolysis was evaluated as an alternative method. It successfully removed most non-sporopollenin material, but turned all pollen and spore species investigated dark brown. As lighter-coloured microcapsules are usually desirable, acetolysed pollen and spores could not be used as microcapsules without bleaching.

A published enzyme treatment applied to pollen failed to remove most non-sporopollenin material and caused pollen from one species to crack. This method was therefore not considered suitable to produce microcapsules from the pollen species studied.

Attempts were made to encapsulate *Lactobacillus* bacteria inside enzyme-treated *Betula fontinalis* pollen. Light microscopy indicated that although encapsulation possibly took place, further analysis, as well as optimisation of the encapsulation method, would be desirable.

Pollen and spores from a range of species were successfully differentiated according to their fluorescence emission spectra. All contained several similar, intense emission peaks, attributed to sporopollenin. Rhodamine B's emission shifted to longer wavelength after binding to pollen and spores, and also quenched emission from sporopollenin. Rhodamine B bound preferentially to pollen walls rather than their protoplasts. Fluorescence studies confirmed *p*-coumaric acid and ferulic acid as potential sporopollenin proxies.

Contents

Abstract	i
List of Figures	vii
List of Tables	xix
Acknowledgements	xxii
Author's declaration	xxiii
1 Introduction	1
1.1 Pollen and spore structure	1
1.1.1 Pollenkitt	2
1.1.2 Exine and exospore	2
1.1.3 Intine and endospore	5
1.1.4 Protoplast	6
1.1.5 Apertures and nano-channels	6
1.1.6 Size and shape	8
1.2 Chemical composition of pollen and spores	9
1.2.1 Exine and exospore	9
1.2.2 Intine and endospore	12
1.2.3 Protoplast	13
1.3 Physical properties of pollen and spores	13
1.4 Emptying pollen and spores	14
1.4.1 Pre-treatment	14
1.4.2 Acetolysis	15
1.4.3 Acid and alkali treatments	16
1.4.4 Treatments involving 4-methylmorpholine N-oxide	19
1.4.5 Enzymatic treatments	21
1.4.6 Physical treatments	22
1.5 Microencapsulation and surface functionalization	22
1.5.1 Foods and dietary supplements	24
1.5.2 Pharmaceuticals	25
1.5.3 Biological material	27
1.5.4 Surface functionalization	29
1.6 Analytical techniques	31
1.6.1 Light microscopy	31
1.6.2 Scanning electron microscopy	33

1.6.3	Transmission electron microscopy	35
1.6.4	Laser scanning confocal microscopy	36
1.6.5	Spectrofluorometry	39
1.7	Fluorescence	40
1.7.1	Basic theory of fluorescence	40
1.7.2	Measurement of fluorescence in pollen and spores	42
2	Aims of the project	47
3	Emptying pollen and spores	51
3.1	Introduction	51
3.2	Analysis of untreated pollen and spores	51
3.2.1	<i>Lycopodium clavatum</i> spores	52
3.2.2	<i>Secale cereale</i> pollen	55
3.2.3	<i>Juglans nigra</i> pollen	57
3.2.4	<i>Ambrosia artemisiifolia</i> pollen	60
3.2.5	<i>Betula fontinalis</i> pollen	63
3.3	Acetolysis	67
3.3.1	Acetolysis of <i>Lycopodium clavatum</i> spores	69
3.3.2	Acetolysis of <i>Secale cereale</i> pollen	70
3.3.3	Acetolysis of <i>Juglans nigra</i> pollen	71
3.3.4	Acetolysis of <i>Betula fontinalis</i> pollen	72
3.3.5	Acetolysis: summary of results	73
3.4	Base and acid treatments	74
3.4.1	Base and acid treatment applied to <i>Lycopodium clavatum</i> spores	77
3.4.2	Base and acid treatment applied to <i>Secale cereale</i> pollen	86
3.4.3	Base and acid treatment applied to <i>Juglans nigra</i> pollen	92
3.4.4	Base and acid treatment applied to <i>Ambrosia artemisiifolia</i> pollen	96
3.4.5	Base and acid treatments: summary of results	99
3.5	Treatments involving enzymes	100
3.5.1	Enzyme treatment applied to <i>Juglans nigra</i> pollen	104
3.5.2	Enzyme treatment applied to <i>Betula fontinalis</i> pollen	109
3.5.3	Enzyme treatment applied to <i>Secale cereale</i> pollen	119
3.5.4	Treatments involving enzymes: summary of results	124
3.6	Conclusions	124
4	Encapsulation of <i>Lactobacillus</i> bacteria into enzyme-treated <i>Betula fontinalis</i> pollen	128

4.1	Introduction	128
4.2	Materials and methods	128
4.3	Results	129
4.4	Conclusions	134
5	Fluorescent microcapsules produced from pollen and spores	136
5.1	Introduction	136
5.2	Materials and methods	139
5.3	Visual observations	140
5.3.1	Visual observations: summary of results	145
5.4	Analysis by Spectrofluorometry	146
5.4.1	Spectrofluorometry of untreated pollen and spores	146
5.4.1.1	Spectrofluorometry of untreated pollen and spores: summary of results ..	151
5.4.2	Spectrofluorometry of untreated, enzyme-treated and base & acid-treated pollen and spores	152
5.4.2.1	Spectrofluorometry of untreated, enzyme-treated and base and acid-treated pollen and spores: summary of results	159
5.4.3	Spectrofluorometry of untreated, enzyme-treated, and base and acid-treated pollen and spores, treated with Rhodamine B	159
5.4.3.1	The effect of changing the solvent used to dissolve Rhodamine B	167
5.4.3.2	The effect of changing the concentration of Rhodamine B applied	170
5.4.3.3	The effect of changing the genus of pollen and spores.....	177
5.4.3.4	Spectrofluorometry of untreated, enzyme-treated, and base and acid-treated pollen and spores, treated with Rhodamine B: summary of results.....	181
5.4.4	Spectrofluorometry of models for sporopollenin: <i>p</i> -coumaric acid and ferulic acid.	182
5.4.4.1	Spectrofluorometry of models for sporopollenin: summary of results	189
5.5	Analysis by laser scanning confocal microscopy (LSCM)	190
5.5.1	Single track LSCM	190
5.5.1.1	LSCM of untreated pollen and spores	190
5.5.1.2	LSCM of enzyme-treated pollen.....	195
5.5.1.3	LSCM of untreated pollen and spores, treated with Rhodamine B	197
5.5.1.4	Single-track LSCM: summary of results	199
5.5.2	Multi-track LSCM of untreated and enzyme-treated <i>Betula fontinalis</i> pollen treated with aqueous and ethanolic solutions of Rhodamine B	200

5.5.2.1 Enzyme-treated <i>Betula fontinalis</i> pollen, treated with aqueous solutions of Rhodamine B	200
5.5.2.2 Enzyme-treated <i>Betula fontinalis</i> pollen, treated with ethanolic solutions of Rhodamine B	207
5.5.2.3 Untreated <i>Betula fontinalis</i> pollen, treated with aqueous solutions of Rhodamine B	211
5.5.2.4 Untreated <i>Betula fontinalis</i> pollen, treated with ethanolic solutions of Rhodamine B	215
5.5.2.5 Multi-track LSCM of untreated and enzyme-treated <i>Betula fontinalis</i> pollen treated with aqueous and ethanolic solutions of Rhodamine B: summary of results	218
5.6 Conclusions	220
6 Conclusions	223
6.1 Emptying pollen and spores	223
6.2 Attempted encapsulation of <i>Lactobacillus</i> bacteria	224
6.3 Fluorescence studies.....	224
6.4 Concluding remarks and future work.....	226
7 Experimental.....	228
7.1 Materials.....	228
7.2 Methods.....	230
7.2.1 Acetolysis applied to <i>Lycopodium clavatum</i> spores and <i>Secale cereale</i> , <i>Juglans nigra</i> & <i>Betula fontinalis</i> pollen.....	230
7.2.2 Base and acid treatments.....	230
7.2.2.1 Standard base and acid treatment applied to <i>Lycopodium clavatum</i> spores and <i>Secale cereale</i> and <i>Juglans nigra</i> pollen.....	230
7.2.2.2 Acid and base treatment applied to <i>Ambrosia artemisiifolia</i> pollen.....	232
7.2.3 Enzyme treatment applied to <i>Juglans nigra</i> , <i>Betula fontinalis</i> and <i>Secale cereale</i> pollen.....	233
7.2.4 Application of solutions of Rhodamine B to <i>Lycopodium clavatum</i> spores (untreated) and enzyme-treated <i>Betula fontinalis</i> pollen (untreated and enzyme-treated).....	234
7.2.5 Preparation of saturated solutions of <i>p</i> -coumaric and ferulic acid (with and without Rhodamine B).....	235
7.2.6 Addition of freeze-dried yogurt culture to enzyme-treated <i>Betula fontinalis</i> pollen	235

7.3	Techniques and analysis.....	235
7.3.1	Light microscopy	235
7.3.1.1	Preparation of slides.....	235
7.3.2	Scanning electron microscopy	236
7.3.2.1	Sample preparation	236
7.3.3	Transmission electron microscopy	237
7.3.3.1	Preparation of sections.....	237
7.3.3.2	Staining of sections.....	237
7.3.4	Laser scanning confocal microscopy.....	238
7.3.4.1	Sample preparation	239
7.3.5	Spectrofluorometry	239
7.3.5.1	Sample preparation	239
8	Abbreviations.....	242
9	References	245

List of Figures

Figure 1.1: Cross-sections of the layers present within spores and pollen grains	2
Figure 1.2: Transmission electron micrographs of pollen from (a) <i>Salix fragilis</i> (brittle willow); (b) <i>Corylus avellana</i> (common hazel); (c) <i>Fraxinus excelsior</i> (common ash); (d) <i>Platanus × hispanica</i> (common plane); (e) <i>Syringa vulgaris</i> (common lilac); and (f) <i>Quercus robur</i> (English oak)	4
Figure 1.3: Scanning electron micrographs of <i>Secale cereale</i> (rye) pollen at (a) low magnification and (b) higher magnification, showing its annulus and pore .	7
Figure 1.4: Transmission electron micrograph of <i>Lopezia lopezoides</i> pollen.....	8
Figure 1.5: (a) Zeaxanthin; (b) canthaxanthin; and (c) echinone	10
Figure 1.6: Structure of (a) <i>p</i> -coumaric acid and (b) ferulic acid.....	11
Figure 1.7: Mass spectra of <i>Pinus mugo</i> pollen (a) untreated and (b) treated to remove non-sporopollenin material ³⁵	12
Figure 1.8: Scanning electron micrograph of the <i>Beilschmiedia</i> pollen (a) before acetolysis and (b) after acetolysis. Scale bars = 1 μm ⁵⁶	16
Figure 1.9: Summary of processes involved in the base and acid treatment protocol published by Atkin <i>et al.</i> ⁵⁷	18
Figure 1.10: Structure of 4-methylmorpholine <i>N</i> -oxide (MMNO)	19
Figure 1.11: Scanning electron micrographs of <i>Lilium longiflorum</i> pollen (a) acetone washed (yellow dashed line shows the position of the aperture); (b) during protoplast release; and (c) after protoplast release ¹⁴	20
Figure 1.12: Structure of cyclohexylamine (CHA)	21
Figure 1.13: Generic structure of a microcapsule	23
Figure 1.14: A flowchart to demonstrate the range of materials used to form microcapsules.	23
Figure 1.15: Scanning electron micrograph of untreated <i>Lycopodium clavatum</i> spore (yellow lines highlight the trilete scar)	28
Figure 1.16: Structure of three <i>Lycopodium clavatum</i> spore-immobilised Schiff bases prepared by Kocak <i>et al.</i> in preparation for Vanadium (IV) sorption studies (spores indicated by blue circles) ⁷⁵	30
Figure 1.17: Structure of two <i>Lycopodium clavatum</i> spore-immobilised Schiff bases prepared by Kocak <i>et al.</i> in preparation for Ruthenium (III) sorption studies (spores indicated by orange circles) ⁸⁸	30

Figure 1.18: Light micrographs of untreated <i>Juglans nigra</i> pollen ($\times 400$ magnification) in (a) a dehydrated and (b) a hydrated state.....	32
Figure 1.19: Schematic representation of the preparation of a microscope slide for light microscopy analysis of hydrated pollen and spores	33
Figure 1.20: Schematic representation of a scanning electron microscope.....	34
Figure 1.21: Schematic representation of a transmission electron microscope.....	36
Figure 1.22: Schematic representation of the preparation of a microscope slide for laser scanning confocal microscopy.....	37
Figure 1.23: Schematic representation of a laser scanning confocal microscope	38
Figure 1.24: LSCM images (multi-track mode, $\times 630$ magnification) of enzyme-treated <i>Betula fontinalis</i> pollen stained with Rhodamine B; (a) excitation λ 405 nm; (b) excitation λ 561 nm; and (c) images from (a) and (b) stacked	39
Figure 1.25: Schematic representation of the sample preparation required for front-face excitation fluorescence measurements: (a) side-on view; and (b) aerial view	39
Figure 1.26: Schematic representation (aerial view) of front-face excitation geometry	40
Figure 1.27: Simplified Jablonski diagram representing fluorescence processes	41
Figure 1.28: Excitation and emission spectra of (a) corn pollen; (b) mulberry pollen; (c) pecan pollen; (d) ragweed pollen; (e) sporopollenin particles from <i>Lycopodium</i> spores; and (f) puff ball spores ⁹⁹	43
Figure 2.1: Structure of Rhodamine B	48
Figure 2.2: Structures of (a) <i>p</i> -coumaric acid and (b) ferulic acid	49
Figure 3.1: Light micrographs of untreated <i>Lycopodium clavatum</i> spores ((a) $\times 200$ and (b) $\times 400$ magnification).....	52
Figure 3.2: Scanning electron micrographs of untreated <i>Lycopodium clavatum</i> spores:	53
Figure 3.3: Transmission electron micrographs of untreated <i>Lycopodium clavatum</i> spores.	54
Figure 3.4: Light micrographs of untreated <i>Secale cereale</i> pollen ((a) and (b) $\times 400$ magnification).....	55
Figure 3.5: Scanning electron micrographs of untreated <i>Secale cereale</i> pollen:	56
Figure 3.6: Transmission electron micrographs of untreated <i>Secale cereale</i> pollen.....	57
Figure 3.7: Light micrographs of untreated <i>Juglans nigra</i> pollen ((a) $\times 100$ and (b) $\times 400$ magnification).....	58
Figure 3.8: Scanning electron micrographs of untreated <i>Juglans nigra</i> pollen:	59
Figure 3.9: Transmission electron micrographs of untreated <i>Juglans nigra</i> pollen.....	60

Figure 3.10: Light micrographs of untreated <i>Ambrosia artemisiifolia</i> pollen ((a) and (b) × 100 magnification; (c) and (d) × 400 magnification).....	61
Figure 3.11: Scanning electron micrographs of untreated <i>Ambrosia artemisiifolia</i> pollen:	62
Figure 3.12: Transmission electron micrographs of untreated <i>Ambrosia artemisiifolia</i> pollen.	63
Figure 3.13: Light micrographs of untreated <i>Betula fontinalis</i> pollen ((a) and (b) × 400 magnification).....	64
Figure 3.14: Scanning electron micrographs of untreated <i>Betula fontinalis</i> pollen:	65
Figure 3.15: Transmission electron micrographs of untreated <i>Betula fontinalis</i> pollen.	67
Figure 3.16: Light micrographs of untreated <i>Lycopodium clavatum</i> spores ((a) × 200 and (b) × 400 magnification).....	69
Figure 3.17: Light micrograph of acetolysed <i>Lycopodium clavatum</i> spores (× 100 magnification).....	70
Figure 3.18: Light micrographs of untreated <i>Secale cereale</i> pollen ((a) and (b) × 400 magnification).....	71
Figure 3.19: Light micrographs of acetolysed <i>Secale cereale</i> pollen ((a) × 100 and (b) × 400 magnification)	71
Figure 3.20: Light micrographs of untreated <i>Juglans nigra</i> pollen ((a) × 100 and (b) × 400 magnification)	72
Figure 3.21: Light micrographs of acetolysed <i>Juglans nigra</i> pollen ((a) × 100 and (b) × 400 magnification)	72
Figure 3.22: Light micrographs of untreated <i>Betula fontinalis</i> pollen ((a) and (b) × 400 magnification).....	73
Figure 3.23: Light micrographs of acetolysed <i>Betula fontinalis</i> pollen ((a) × 100 and (b) × 400 magnification)	73
Figure 3.24: Summary of the base and acid treatment protocol applied to <i>Lycopodium clavatum</i> spores, published by Atkin <i>et al.</i> ⁵⁷	75
Figure 3.25: Summary of the base and acid treatment protocol applied to <i>Ambrosia trifida</i> pollen, published by Fletcher <i>et al.</i> ¹²⁴	76
Figure 3.26: Scanning electron micrographs of untreated <i>Lycopodium clavatum</i> spores:	78
Figure 3.27: Scanning electron micrographs of <i>Lycopodium clavatum</i> spores after step 1	79

Figure 3.28: Scanning electron micrographs of <i>Lycopodium clavatum</i> spores after step 2	80
Figure 3.29: Scanning electron micrographs of <i>Lycopodium clavatum</i> spores after step 3, part (i)	81
Figure 3.30: Scanning electron micrographs of <i>Lycopodium clavatum</i> spores after step 3, part (iii)	82
Figure 3.31: Transmission electron micrographs of untreated <i>Lycopodium clavatum</i> spores	83
Figure 3.32: Transmission electron micrographs of <i>Lycopodium clavatum</i> spores after step 1	84
Figure 3.33: Transmission electron micrographs of <i>Lycopodium clavatum</i> spores after step 3, part (iii)	85
Figure 3.34: Transmission electron micrographs of <i>Lycopodium clavatum</i> spores after step 4	86
Figure 3.35: Light micrographs of untreated <i>Secale cereale</i> pollen ((a) and (b) × 400 magnification)	87
Figure 3.36: Light micrographs of <i>Secale cereale</i> pollen after step 1 ((a) × 100 and (b) × 400 magnification)	87
Figure 3.37: Light micrographs of <i>Secale cereale</i> pollen after step 2 ((a) & (b) × 100, and (c) and (d) × 400 magnification)	88
Figure 3.38: Light micrographs of <i>Secale cereale</i> pollen after step 2 (2 h, room temperature) ((a), (b), (c) and (d) × 400 magnification)	89
Figure 3.39: Light micrographs of <i>Secale cereale</i> pollen after step 2 (4 h 30 min, without stirring). Slide stained with Ruthenium Red. ((a) and (b) × 100, and (c) × 400 magnification)	90
Figure 3.40: Transmission electron micrographs of untreated <i>Lycopodium clavatum</i> spores, highlighting their laminated exospore	91
Figure 3.41: Transmission electron micrographs of untreated <i>Secale cereale</i> pollen, highlighting its columellate infratectum	91
Figure 3.42: Schematic representing the columellate exine of <i>Secale cereale</i> pollen and the lamellar exospore of <i>Lycopodium clavatum</i> spores	92
Figure 3.43: Light micrographs of untreated <i>Juglans nigra</i> pollen ((a) × 100 and (b) × 400 magnification)	93
Figure 3.44: Light micrographs of <i>Juglans nigra</i> pollen after step 1 ((a) × 100 and (b) × 400 magnification)	93

Figure 3.45: Light micrographs of <i>Juglans nigra</i> pollen after step 2 ((a) and (b) × 100 magnification).....	93
Figure 3.46: Light micrographs of <i>Juglans nigra</i> pollen after step 3 ((a) and (b) × 100 magnification).....	94
Figure 3.47: Light micrograph of <i>Juglans nigra</i> pollen after step 2 (4 h 30 min, room temperature) (× 400 magnification).....	95
Figure 3.48: Light micrographs of <i>Juglans nigra</i> pollen after step 2 (6 h, without stirring). ((a) and (b) × 100 and (c) and (d) × 400 magnification)	96
Figure 3.49: Schematic representing the granular infratectum of <i>Juglans nigra</i> pollen	96
Figure 3.50: Light micrographs of untreated <i>Ambrosia artemisiifolia</i> pollen ((a) and (b) × 100 magnification; (c) and (d) × 400 magnification).....	97
Figure 3.51: Light micrographs of <i>Ambrosia artemisiifolia</i> pollen after step 1 ((a) × 100 and (b) × 400 magnification).....	98
Figure 3.52: Light micrographs of <i>Ambrosia artemisiifolia</i> pollen after step 3 ((a) × 100 and (b), (c) and (d) × 100 magnification)	98
Figure 3.53: Schematic representing the columellate infratectum and lamellar endexine of <i>Ambrosia artemisiifolia</i> pollen.....	99
Figure 3.54: Structure of (a) 4-methylmorpholine <i>N</i> -oxide (MMNO) and (b) cyclohexylamine (CHA).....	101
Figure 3.55: Summary of the enzyme method published by Loewus <i>et al.</i> ⁶⁴	102
Figure 3.56: Potter-Elvehjem tissue grinder.....	103
Figure 3.57: Light micrographs of untreated <i>Juglans nigra</i> pollen ((a) × 100 and (b) × 400 magnification)	105
Figure 3.58: Light micrographs of enzyme-treated <i>Juglans nigra</i> pollen after step 5 (iv) (ten pestle cycles, 16 h in enzyme suspension) ((a) and (b) × 400 magnification).....	105
Figure 3.59: Light micrographs of enzyme-treated <i>Juglans nigra</i> pollen after step 5 (iv) (ten pestle cycles, 42 h in enzyme suspension) ((a) and (b) × 400 magnification).....	105
Figure 3.60: Light micrographs of enzyme-treated <i>Juglans nigra</i> pollen after step 5 (v) (ten pestle cycles) ((a) and (b) × 100 magnification, and (c) × 400 magnification).....	106
Figure 3.61: Light micrographs of enzyme-treated <i>Juglans nigra</i> pollen after step 5 (iv) (thirty pestle cycles, 20 h in enzyme suspension) ((a) × 100 magnification, and (b) and (c) × 400 magnification).....	107

Figure 3.62: Light micrographs of enzyme-treated <i>Juglans nigra</i> pollen after step 5 (iv) (ten pestle cycles, 24 h in doubled mass of enzyme suspension) ((a) and (b) × 400 magnification)	108
Figure 3.63: Light micrographs of enzyme-treated <i>Juglans nigra</i> pollen after step 5 (iv) (ten pestle cycles, 48 h in doubled mass of enzyme suspension) ((a) and (b) × 400 magnification)	108
Figure 3.64: Light micrographs of untreated <i>Betula fontinalis</i> pollen ((a) and (b) × 400 magnification).....	109
Figure 3.65: Light micrographs of MMNO and CHA-treated <i>Betula fontinalis</i> pollen after step 3 (v) (ten pestle cycles) ((a) and (b) × 400 magnification).....	110
Figure 3.66: Light micrographs of enzyme-treated <i>Betula fontinalis</i> pollen after step 5 (iv) (ten pestle cycles) ((a) and (b) × 400 magnification).....	110
Figure 3.67: Light micrographs of MMNO and CHA-treated <i>Betula fontinalis</i> pollen after step 3 (iv) (thirty pestle cycles) ((a) and (b) × 400 magnification) ...	111
Figure 3.68: Light micrographs of enzyme-treated <i>Betula fontinalis</i> pollen after step 5 (iv) (thirty pestle cycles) ((a) and (b) × 400 magnification).....	111
Figure 3.69: Transmission electron micrographs of untreated <i>Betula fontinalis</i> pollen.	112
Figure 3.70: Transmission electron micrographs of <i>Betula fontinalis</i> pollen after step 5 (iv).	113
Figure 3.71: LSCM images of untreated <i>Betula fontinalis</i> pollen: (a) and (b) excitation wavelength 405 nm; (c) and (d) excitation wavelength 633 nm.	115
Figure 3.72: LSCM images of <i>Betula fontinalis</i> pollen after step 5 (iv): (a) and (b) excitation wavelength 561 nm; (c) and (d) excitation wavelength 405 nm.	116
Figure 3.73: LSCM images of <i>Betula fontinalis</i> pollen (a) untreated and (b) enzyme-treated, excitation wavelength 405 nm. Scale bars = 25 μm	117
Figure 3.74: LSCM z-stack images of <i>Betula fontinalis</i> pollen after step 5 (iv), taken perpendicular to the z-axis.....	118
Figure 3.75: Light micrographs of untreated <i>Secale cereale</i> pollen ((a) and (b) × 400 magnification).....	119
Figure 3.76: Light micrographs of MMNO and CHA-treated <i>Secale cereale</i> pollen after step 3 (v) (10 pestle cycles) ((a) and (b) × 100 magnification)	119
Figure 3.77: Light micrographs of enzyme-treated <i>Secale cereale</i> pollen after step 5 (iv) (10 pestle cycles) ((a) and (b) × 100 magnification)	120

Figure 3.78: Light micrographs of enzyme-treated <i>Secale cereale</i> pollen after step 5 (iv) (10 pestle cycles, 18 h in enzyme suspension) ((a), (b) and (c) × 400 magnification).....	121
Figure 3.79: Light micrographs of enzyme-treated <i>Secale cereale</i> pollen after step 5 (iv) (10 pestle cycles, 40 h in enzyme suspension) ((a) and (b) × 400 magnification).....	121
Figure 3.80: Light micrographs of enzyme-treated <i>Secale cereale</i> pollen after step 5 (iv) (thirty pestle cycles, 20 h in enzyme suspension) ((a) and (b) × 100, and (c) and (d) × 400 magnification).....	122
Figure 3.81: Light micrographs of enzyme-treated <i>Secale cereale</i> pollen after step 5 (iv) (10 pestle cycles, 24 h in enzyme suspension, double mass of enzymes) ((a) and (b) × 400 magnification).....	123
Figure 3.82: Light micrographs of enzyme-treated <i>Secale cereale</i> pollen after step 5 (iv) (10 pestle cycles, 48 h in enzyme suspension, double mass of enzymes) ((a) × 100 and (b) and (c) × 400; magnification)	123
Figure 4.1: Light micrographs of enzyme-treated <i>Betula fontinalis</i> pollen stirred with yogurt culture in MRS broth (24 h).....	130
Figure 4.2: Light micrographs of enzyme-treated <i>Betula fontinalis</i> pollen stirred with yogurt culture in MRS broth (48 h).....	131
Figure 4.3: Light micrographs of enzyme-treated <i>Betula fontinalis</i> pollen stirred with yogurt culture in MRS broth (72 h).....	132
Figure 4.4: Transmission electron micrographs of enzyme-treated <i>Betula fontinalis</i> pollen containing unidentified organisms.....	133
Figure 5.1: Structure of Rhodamine B	137
Figure 5.2: Emission spectra of untreated <i>Betula fontinalis</i> pollen (excitation λ 300 nm, 350 nm longpass filter), Rhodamine B (1×10^{-4} mol dm ⁻³ in EtOH, excitation λ 543 nm) and Rhodamine B (1×10^{-4} mol dm ⁻³ in water, excitation λ 548 nm).....	139
Figure 5.3: Photographs of untreated pollen from (a) <i>Betula fontinalis</i> ; (b) <i>Secale cereale</i> ; (c) <i>Juglans nigra</i> ; (d) <i>Taraxacum officinale</i> ; (e) <i>Ambrosia artemisiifolia</i> ; and spores from (f) <i>Lycopodium clavatum</i>	140
Figure 5.4: Photographs of <i>Betula fontinalis</i> pollen (a) untreated and (b) after enzyme treatment; <i>Ambrosia artemisiifolia</i> pollen (c) untreated and (d) after enzyme-treatment	141

Figure 5.5: Photograph of <i>Lycopodium clavatum</i> spores (a) untreated and (b) after base and acid treatment.....	141
Figure 5.6: Photograph of enzyme-treated <i>Betula fontinalis</i> pollen treated with ethanolic solutions of RhB.	142
Figure 5.7: Photograph of enzyme-treated <i>Betula fontinalis</i> pollen treated with aqueous solutions of RhB.	142
Figure 5.8: Photograph of untreated <i>Betula fontinalis</i> pollen treated with aqueous solutions of RhB.	143
Figure 5.9: Photograph of untreated <i>Juglans nigra</i> pollen treated with aqueous solutions of RhB.....	143
Figure 5.10: Photograph of untreated <i>Betula fontinalis</i> pollen treated with ethanolic solutions of RhB.	143
Figure 5.11: Photograph of untreated <i>Juglans nigra</i> pollen treated with ethanolic solutions of RhB.	144
Figure 5.12: Photograph of untreated <i>Lycopodium clavatum</i> spores treated with ethanolic solutions of RhB.	145
Figure 5.13: Photograph of base and acid-treated <i>Lycopodium clavatum</i> spores treated with ethanolic solutions of RhB.	145
Figure 5.14: Fluorescence emission spectra of untreated <i>Lycopodium clavatum</i> spores and untreated <i>Betula fontinalis</i> , <i>Juglans nigra</i> , <i>Secale cereale</i> , <i>Taraxacum officinale</i> and <i>Ambrosia artemisiifolia</i> pollen (excitation λ 300 nm, 350 nm longpass filter applied)	147
Figure 5.15: Structure of (a) <i>p</i> -coumaric acid and (b) ferulic acid.....	148
Figure 5.16: Emission spectra of saturated ethanolic solutions of ferulic acid (excitation λ 385 nm) and <i>p</i> -coumaric acid (excitation λ 450 nm).....	148
Figure 5.17: Structure of (a) flavone and (b) lycopene	149
Figure 5.18: Summary of the orders, genera and species under investigation.	151
Figure 5.19: Fluorescence emission spectra of untreated and enzyme-treated <i>Betula fontinalis</i> pollen (excitation λ 300 nm, 350 nm longpass filter).....	153
Figure 5.20: Fluorescence emission spectra of untreated and enzyme-treated <i>Taraxacum officinale</i> pollen (excitation λ 300 nm, 350 nm longpass filter).....	153
Figure 5.21: Fluorescence emission spectra of untreated and enzyme-treated <i>Ambrosia artemisiifolia</i> pollen (excitation λ 300 nm, 350 nm longpass filter)	154

Figure 5.22: Fluorescence emission spectra of untreated and base and acid treated <i>Lycopodium clavatum</i> spores (excitation λ 300 nm, 350 nm longpass filter)	156
Figure 5.23: Fluorescence emission spectra of untreated and base and acid treated <i>Betula fontinalis</i> pollen (excitation λ 300 nm, 350 nm longpass filter)	157
Figure 5.24: Diagram to demonstrate the samples prepared from <i>Betula fontinalis</i> pollen for spectrofluorometry and the excitation wavelengths used to produce spectra.....	160
Figure 5.25: Emission spectra of untreated <i>Betula fontinalis</i> (<i>Bf</i>) pollen, treated with aqueous solutions of RhB of varying concentrations (excitation λ 300 nm, 350 nm longpass filter).....	161
Figure 5.26: Emission spectra of untreated <i>Betula fontinalis</i> (<i>Bf</i>) pollen, treated with aqueous solutions of RhB of varying concentrations (excitation λ 543 nm)	161
Figure 5.27: Emission spectra of enzyme-treated <i>Betula fontinalis</i> (<i>Bf</i>) pollen, treated with aqueous solutions of RhB of varying concentrations (excitation λ 300 nm, 350 nm longpass filter).....	162
Figure 5.28: Emission spectra of enzyme-treated <i>Betula fontinalis</i> (<i>Bf</i>) pollen, treated with aqueous solutions of RhB of varying concentrations (excitation λ 543 nm).....	162
Figure 5.29: Emission spectra of untreated <i>Betula fontinalis</i> (<i>Bf</i>) pollen, treated with ethanolic solutions of RhB of varying concentrations (excitation λ 300 nm, 350 nm longpass filter).....	163
Figure 5.30: Emission spectra of untreated <i>Betula fontinalis</i> (<i>Bf</i>) pollen, treated with ethanolic solutions of RhB of varying concentrations (excitation λ 548 nm)	163
Figure 5.31: Emission spectra of enzyme-treated <i>Betula fontinalis</i> (<i>Bf</i>) pollen, treated with ethanolic solutions of RhB of varying concentrations (excitation λ 300 nm, 350 nm longpass filter).....	164
Figure 5.32: Emission spectra of enzyme-treated <i>Betula fontinalis</i> (<i>Bf</i>) pollen, treated with ethanolic solutions of RhB of varying concentrations (excitation λ 548 nm).....	164
Figure 5.33: Emission spectra of RhB in solution with water at a range of concentrations. (Excitation λ 548 nm).....	169

Figure 5.34: Emission spectra of RhB in solution with EtOH at a range of concentrations. (Excitation λ 543 nm).....	170
Figure 5.35: The intensity of fluorescence emission related to the concentration of RhB within a sample. (a) High concentration and (b) low concentration of RhB	171
Figure 5.36: Simplified Jablonski diagram illustrating the process of reabsorption....	173
Figure 5.37: Emission spectrum of a fluorochrome demonstrating reabsorption at increasing fluorochrome concentrations (indicated by the arrow). Inset: Absorption and emission spectra of the same fluorochrome, demonstrating that a good overlap between the two is required for reabsorption to take place ¹⁶⁵	173
Figure 5.38: Absorption spectrum of a fluorochrome, demonstrating the increased absorption of aggregates (indicated by the arrow) compared to monomer fluorochromes as the concentration of the fluorochrome is increased. Inset: Absorption of monomer (●) and of aggregate (○) fluorochromes ¹⁶⁵	174
Figure 5.39: Comparison of the peak emission wavelengths of aqueous solutions of RhB and untreated & enzyme-treated <i>Betula fontinalis</i> pollen, treated with aqueous solutions of RhB. Concentrations of RhB range from 1×10^{-3} to 1×10^{-6} mol dm ⁻³	175
Figure 5.40: Comparison of the peak emission wavelengths of ethanolic solutions of RhB and untreated & enzyme-treated <i>Betula fontinalis</i> pollen, treated with ethanolic solutions of RhB. Concentrations of RhB range from 1×10^{-3} to 1×10^{-6} mol dm ⁻³	176
Figure 5.41: Emission spectra of untreated <i>Juglans nigra</i> (<i>Jn</i>) pollen, treated with aqueous solutions of RhB of varying concentrations (excitation λ 300 nm, 350 nm longpass filter).....	178
Figure 5.42: Emission spectra of untreated <i>Juglans nigra</i> (<i>Jn</i>) pollen, treated with aqueous solutions of RhB of varying concentrations (excitation λ 530 nm)	178
Figure 5.43: Emission spectra of untreated <i>Lycopodium clavatum</i> (<i>Lc</i>) spores, treated with aqueous solutions of RhB of varying concentrations (excitation λ 300 nm, 350 nm longpass filter).....	179
Figure 5.44: Emission spectra of untreated <i>Lycopodium clavatum</i> (<i>Lc</i>) spores, treated with aqueous solutions of RhB of varying concentrations (excitation λ 530 nm).....	179

Figure 5.45: Comparison of peak emission wavelengths of untreated <i>Betula fontinalis</i> and <i>Juglans nigra</i> pollen and <i>Lycopodium clavatum</i> spores, treated with aqueous solutions of RhB at various concentrations	181
Figure 5.46: Emission spectra of saturated ethanolic solutions of <i>p</i> -coumaric acid (excitation λ 450 nm) and ferulic acid (excitation λ 385 nm); and RhB in ethanol (1×10^{-3} mol dm ⁻³) (excitation λ 543 nm).....	183
Figure 5.47: Emission spectra of saturated ethanolic solutions of <i>p</i> -coumaric acid (CA) mixed with equal volumes of ethanolic solutions of RhB of varying concentrations (excitation λ 450 nm)	184
Figure 5.48: Emission spectra of saturated ethanolic solutions of <i>p</i> -coumaric acid (CA) mixed with equal volumes of ethanolic solutions of RhB of varying concentrations (excitation λ 540 nm)	184
Figure 5.49: Emission spectra of saturated ethanolic solutions of ferulic acid (FA) mixed with equal volumes of ethanolic solutions of RhB of varying concentrations (excitation λ 385 nm)	186
Figure 5.50: Emission spectra of saturated ethanolic solutions of ferulic acid (FA) mixed with equal volumes of ethanolic solutions of RhB of varying concentrations (excitation λ 540 nm)	186
Figure 5.51: Peak emission wavelengths of RhB in ethanol at varying concentrations when combined with saturated, ethanolic solutions of <i>p</i> -coumaric acid (excitation λ 450 nm), ferulic acid (excitation λ 540 nm) or untreated <i>Betula fontinalis</i> pollen. Data taken from Figure 5.30, Figure 5.48 and Figure 5.50	188
Figure 5.52: Structure of riboflavin.....	189
Figure 5.53: Emission spectra of Rhodamine B and a Rhodamine B – riboflavin conjugate (excitation λ 445 nm) ¹⁷⁷	189
Figure 5.54: LSCM images of untreated <i>Betula fontinalis</i> pollen: (a) and (b) excitation wavelength 405 nm; (c) and (d) excitation wavelength 633 nm.	191
Figure 5.55: LSCM images of untreated <i>Juglans nigra</i> pollen: (a) and (b) excitation wavelength 405 nm; (c) and (d) excitation wavelength 633 nm.	192
Figure 5.56: LSCM images of untreated <i>Secale cereale</i> pollen: (a) and (b) excitation wavelength 561 nm.....	193
Figure 5.57: LSCM images of untreated <i>Ambrosia artemisiifolia</i> pollen: (a) and (b) excitation wavelength 405 nm; (c) and (d) excitation wavelength 561 nm.	194

Figure 5.58: LSCM images of untreated <i>Lycopodium clavatum</i> spores: (a) and (b) excitation wavelength 405 nm; (c) and (d) excitation wavelength 561 nm.	195
Figure 5.59: LSCM images of enzyme-treated <i>Betula fontinalis</i> pollen: (a) and (b) excitation wavelength 405 nm; (c) and (d) excitation wavelength 561 nm.	196
Figure 5.60: LSCM images of <i>Betula fontinalis</i> pollen (a) untreated and (b) enzyme-treated, excitation wavelength 405 nm.	197
Figure 5.61: Laser scanning confocal micrographs of untreated <i>Betula fontinalis</i> pollen treated with an aqueous solution of RhB (1×10^{-3} mol dm ⁻³). Excitation wavelength 561 nm.	198
Figure 5.62: Laser scanning confocal micrographs of untreated <i>Juglans nigra</i> pollen treated with RhB (1×10^{-3} mol dm ⁻³). Excitation wavelength 561 nm.	199
Figure 5.63: Emission spectra of enzyme-treated <i>Betula fontinalis</i> (<i>Bf</i>) pollen, and enzyme-treated <i>Bf</i> pollen treated with an aqueous solution of RhB (1×10^{-3} mol dm ⁻³) (excitation λ 300 and 405 nm)	205
Figure 5.64: Emission spectra of enzyme-treated <i>Betula fontinalis</i> (<i>Bf</i>) pollen, and enzyme-treated <i>Bf</i> pollen treated with an aqueous solution of RhB (1×10^{-3} mol dm ⁻³) (excitation λ 543 and 561 nm)	206
Figure 5.65: Emission spectra of untreated <i>Betula fontinalis</i> (<i>Bf</i>) pollen, treated with ethanolic solutions of RhB of varying concentrations (excitation λ 300 nm, 350 nm longpass filter)	218
Figure 7.1: Schematic representation of the preparation of a microscope slide for light microscopy analysis and the application of water or a stain solution	236
Figure 7.2: Summary of multi-track mode LSCM	238
Figure 7.3: Schematic representation of the preparation of a microscope slide for laser scanning confocal microscopy.....	239
Figure 7.4: Schematic representation (aerial view) of 90 ° excitation geometry	240
Figure 7.5: Schematic representation of the sample preparation required for front-face excitation fluorescence measurements	240
Figure 7.6: Schematic representation (aerial view) of front-face excitation geometry	240

List of Tables

Table 1.1: Summary of analytical techniques used to evaluate pollen and spores.....	31
Table 1.2: Summary of the possible sources of emission observed in pollen and spore fluorescence analysis ⁹⁵	44
Table 3.1 Summary of coloured arrows used to highlight features within light micrographs	104
Table 5.1: Summary of treatments applied to pollen and spores	138
Table 5.2: Emission intensities at 370 nm and 470 nm and calculated peak ratios of untreated and enzyme-treated <i>Betula fontinalis</i> , <i>Ambrosia artemisiifolia</i> and <i>Taraxacum officinale</i> pollen. Data taken from Figure 5.19 - Figure 5.20.	155
Table 5.3: Emission intensities at 370 nm and 470 nm and calculated peak ratios of untreated and base and acid-treated <i>Lycopodium clavatum</i> spores and <i>Betula fontinalis</i> pollen. Data taken from Figure 5.22 and Figure 5.23	158
Table 5.4: Summary of peak emission wavelengths of untreated <i>Betula fontinalis</i> pollen, treated with aqueous solutions of RhB at varying concentrations. Data taken from Figure 5.25 and Figure 5.26.....	165
Table 5.5: Summary of peak emission wavelengths of enzyme-treated <i>Betula fontinalis</i> pollen, treated with aqueous solutions of RhB at varying concentrations. Data taken from Figure 5.27 and Figure 5.28.....	166
Table 5.6: Summary of peak emission wavelengths of untreated <i>Betula fontinalis</i> pollen, treated with ethanolic solutions of RhB at varying concentrations. Data taken from Figure 5.29 and Figure 5.30.....	166
Table 5.7: Summary of peak emission wavelengths of enzyme-treated <i>Betula fontinalis</i> pollen, treated with ethanolic solutions of RhB at varying concentrations. Data taken from Figure 5.31 and Figure 5.32.....	167
Table 5.8: Emission intensities at 370 nm and 470 nm and calculated peak ratios of untreated <i>Betula fontinalis</i> pollen treated with aqueous and ethanolic solutions of RhB at varying concentrations. Data taken from Figure 5.25 and Figure 5.29; peak emission wavelengths used taken from Table 5.4 and Table 5.6	168
Table 5.9: Emission intensities at 370 nm and 470 nm and calculated peak ratios of enzyme-treated <i>Betula fontinalis</i> pollen treated with aqueous and ethanolic solutions of RhB at varying concentrations. Intensity data taken from Figure	

5.27 and Figure 5.31; peak emission wavelengths used taken from Table 5.5 and Table 5.7	168
Table 5.10: Summary of peak emission wavelengths in solutions of RhB at varying concentrations with water (excitation λ 548 nm), or ethanol (excitation λ 543 nm) as the solvent	170
Table 5.11: Summary of peak emission wavelengths of untreated <i>Betula fontinalis</i> and <i>Juglans nigra</i> pollen and <i>Lycopodium clavatum</i> spores, all treated with aqueous solutions of RhB of varying concentrations	180
Table 5.12: Summary of peak emission wavelengths for the fluorescence of a saturated solution of <i>p</i> -coumaric acid with Rhodamine B. All solutions prepared in ethanol	185
Table 5.13: Summary of peak emission wavelengths for the fluorescence of a saturated solution of ferulic acid with Rhodamine B. All solutions prepared in ethanol	187
Table 5.14: Summary of samples prepared for multi-track LSCM.....	200
Table 5.15: LSCM images of enzyme-treated <i>Betula fontinalis</i> pollen, with and without treatment with aqueous solutions of RhB. LSCM settings were maintained between samples of the same magnification. Excitation λ 405 nm.....	202
Table 5.16: LSCM images of enzyme-treated <i>Betula fontinalis</i> pollen, with and without treatment with aqueous solutions of RhB. LSCM settings were maintained between samples of the same magnification. Excitation λ 561 nm.....	203
Table 5.17: Excitation wavelength and range over which emission was collected for both spectrofluorometry and LSCM (applicable to all samples).....	204
Table 5.18: LSCM images of enzyme-treated <i>Betula fontinalis</i> pollen, with and without treatment with ethanolic solutions of RhB. LSCM settings were maintained between samples of the same magnification. Excitation λ 405 nm.....	208
Table 5.19: LSCM images of enzyme-treated <i>Betula fontinalis</i> pollen, with and without treatment with ethanolic solutions of RhB. LSCM settings were maintained between samples of the same magnification. Excitation λ 561 nm.....	209
Table 5.20: LSCM images of untreated <i>Betula fontinalis</i> pollen, with and without treatment with aqueous solutions of RhB. LSCM settings were maintained between samples of the same magnification. Excitation λ 405 nm.....	213
Table 5.21: LSCM images of untreated <i>Betula fontinalis</i> pollen, with and without treatment with aqueous solutions of RhB. LSCM settings were maintained between samples of the same magnification. Excitation λ 561 nm.....	214

Table 5.22: LSCM images of untreated <i>Betula fontinalis</i> pollen, with and without treatment with ethanolic solutions of RhB. LSCM settings were maintained between samples of the same magnification. Excitation λ 405 nm.....	216
Table 5.23: LSCM images of untreated <i>Betula fontinalis</i> pollen, with and without treatment with ethanolic solutions of RhB. LSCM settings were maintained between samples of the same magnification. Excitation λ 561 nm.....	217
Table 5.24: Summary of findings from LSCM	219
Table 7.1: Summary of materials used and associated suppliers	229
Table 7.2: Summary masses of each species used, the volumes of base and solvents applied and the percentage yields achieved.....	232
Table 7.3: Summary of the number of pestle cycles (x) applied to each species during enzyme treatment.....	234
Table 7.4: Summary of pollen and spores treated with aqueous and ethanolic solutions of Rhodamine B.....	234

Acknowledgements

Without the funding of the Engineering and Physical Sciences Research Council, this research would not have been possible and I am grateful for the Council's generous support.

I offer my warm thanks to Professor John Goodby, FRS, for accepting me to undertake this project, and for his invaluable guidance and advice. I also thank Dr Stephen Cowling, Dr Verena Gortz and Dr Isabel Saez for their helpful input. The members of the Advanced Materials Group at The University of York provided a great deal of cheerful support, and I am especially grateful to them for helping me to develop my practical skills.

The Bioscience Technology Facility at The University of York carried out TEM sample preparation and analysis, as well as training me on the best use of their SEM and LSCM. In particular, I thank Karen Hodgkinson, Dr Graeme Park and Meg Stark for their support in analysing my numerous samples.

Professor High Dickinson (University of Oxford) generously hosted me for two days, and I am grateful for his assistance with the TEM analysis of *Lycopodium clavatum* spores. I thank Carol Furness (Royal Botanic Gardens, Kew) for providing me with the protocol for her acetolysis method as well as kindly allowing me to visit her laboratory.

This work was proofread by my father. As a technical writer rather than a chemist, he carefully uncovered my many errors. Thanks to both my mother and father for their encouragement throughout my lengthy period in higher education. I also thank my many friends in York and beyond for their unstinting support.

Professor Pete Dowding initially persuaded me to pursue a research career and I am grateful for his continuing advice, motivation and good humour.

Finally, thanks to Elsie for her great company and for sitting on the computer regularly to encourage me to take a break from pollen.

Author's declaration

I confirm that the work presented in this thesis, both written and experimental, is my own and has not been submitted for publication elsewhere. The following exceptions apply:

- Meg Stark (The Bioscience Technology Facility, The University of York) followed the method described in section 7.3.3.1 to prepare samples for Transmission Electron Microscopy.
- Meg Stark and Professor Hugh Dickinson (Department of Plant Sciences, The University of Oxford) performed the transmission electron microscopy in this thesis.
- The acetolysis method described in section 7.2.1 was provided by Carol Furness, Royal Botanic Gardens, Kew.
- A talk entitled 'Pollen and spore exines: potential new microencapsulants' was presented at the Linnean Society Palynology Specialist Group Meeting in London, UK (November 2011).
- A poster entitled 'The production and evaluation of pollen microcapsules containing fluorochromes' was presented at the Linnean Society Palynology Specialist Group Meeting in London, UK (November 2012).
- A poster entitled 'The Production and Evaluation of Fluorescent Pollen Microcapsules' was presented at the Bruker Poster Competition in The Department of Chemistry, The University of York (March, 2013).
- A talk entitled 'Fluorescent Microcapsules Produced from Pollen' was presented at the RSC MC11 conference in Warwick, UK (July 2013).

Chapter 1:

Introduction

1 Introduction

Pollen and spores protect the genetic information and form part of the reproductive cycles of flowering plants, fungi, mosses, some bacteria and protozoans. They also act as vectors to transport this genetic information. Understanding the structural features and chemical composition of pollen and spores enables us to relate structure to function. This knowledge facilitates the selection of suitable species for use as microcapsules. It is also key to determining the extent to which methods applied are able to remove material from pollen and spores to produce these microcapsules.

1.1 Pollen and spore structure

The structural features of pollen and spores are considered to be broadly interchangeable. They both consist of a wall, made up of several layers, which surrounds the cytoplasmic contents. A cross-section of the layers present in both pollen and spores is shown in Figure 1.1. A good understanding of the structures present allows a careful evaluation of the effects of a range of treatments applied to both pollen and spores (see section 1.4).

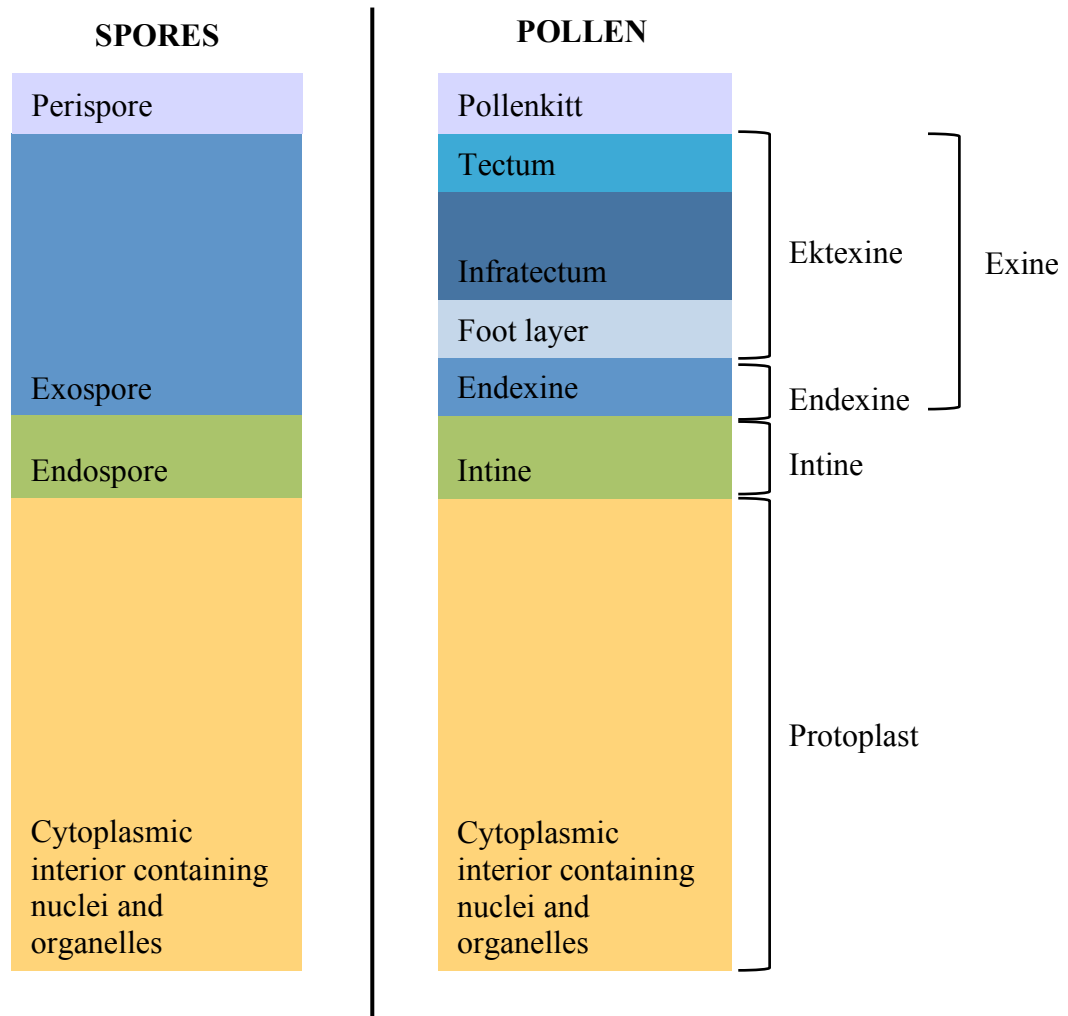


Figure 1.1: Cross-sections of the layers present within spores and pollen grains

1.1.1 Pollenkitt

Pollenkitt is a sticky lipid substance that can be found on the surface of some species of pollen, but not on spores. For example, pollen from the genus *Lilium* has this coating, but it is absent from the pollen in the Poaceae family.¹ Its functions are numerous and include: (1) facilitating pollination; (2) protecting pollen from ultraviolet (UV) radiation and pathogens; and (3) limiting water loss from grains.^{2,3}

1.1.2 Exine and exospore

The outermost wall layer present in pollen is the exine and in spores it is the exospore. The function of the exine and exospore is to protect the contents of the pollen grain or

spore while facilitating processes such as dehydration and rehydration and the movement of materials into and out of the spore or pollen grain. These wall layers are composed of a chemically and physically resilient biopolymer termed sporopollenin. The structure of this substance remains hotly debated and is discussed in more detail later in this chapter (see section 1.2.1).

The exine of pollen grains can be further sub-divided into two layers, in terms of composition and function: the endexine and ektexine. The endexine is a layer in its own right, whereas the ektexine is composed of the foot layer; the infratectum; the tectum; and any pollenkitt present.⁴ Most species exhibit this layered structure, with all elements present. However, in some species layers may be missing, or completely homogeneous.^{5, 6} Transmission electron microscopy highlights how differently the exine (and other wall components) can appear in various genera (Figure 1.2).⁷ Care must be taken when assigning these layers *via* transmission electron microscopy (TEM).⁸

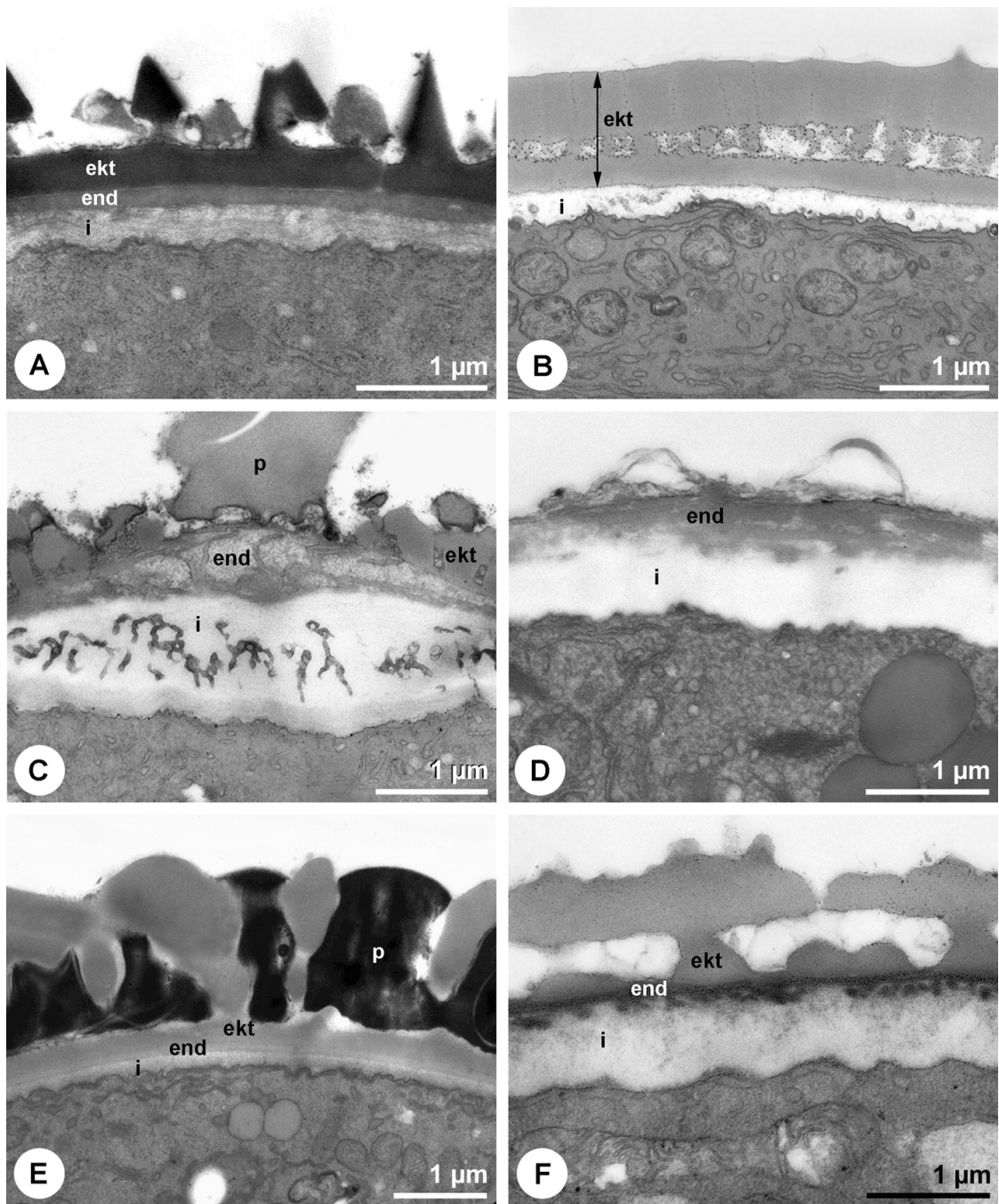


Figure 1.2: Transmission electron micrographs of pollen from (a) *Salix fragilis* (brittle willow); (b) *Corylus avellana* (common hazel); (c) *Fraxinus excelsior* (common ash); (d) *Platanus* × *hispanica* (common plane); (e) *Syringa vulgaris* (common lilac); and (f) *Quercus robur* (English oak)

ekt = ektexine, end = endexine, i = intine; and p = pollenkit⁷

The tectum is part of the ektexine and is a structural feature that can also support additional sculpting. This sculpting varies enormously between species and greatly assists in the differentiation of species. Extensive classification work has been carried out in the fields of palynology and paleopalynology, where comparing modern and

fossil pollen respectively can give an indication of historic plant life. The early work of G. Erdtman (1897 – 1973) that describes the morphology of pollen and spores is particularly noteworthy and underpins many modern studies.^{9, 10} Sculptural features of the tectum continue to be studied in increasing detail as the resolution and magnification of scanning electron microscopes continues to improve.

The infratectum is the middle layer of the ectexine and lies between the foot layer and the tectum. Its internal structure varies between species, or is sometimes absent altogether.¹¹ Its role is to support the sculpting of the tectum.

The layer of the ectexine lying closest to the intine is the foot layer. This can cover the whole grain (continuous), may be missing in parts (discontinuous) or is sometimes absent altogether. This layer appears to have been little studied and many of the key textbooks in this area, including Faegri *et al.*'s 'Textbook of pollen analysis' and Hesse *et al.*'s more modern 'Pollen Terminology: An Illustrated Handbook', make only passing reference to it.^{4, 11}

The percentage of a spore or pollen grain that is composed of exine material varies between species; for example, *Lycopodium clavatum* (club moss) spores have been found to be 23.4 % exine, whereas *Narcissus pseudonarcissus* (wild daffodil) pollen is thought to be 1.9 % exine by mass.^{12, 13} This difference in composition may explain why some species have tougher exines compared to others.

1.1.3 Intine and endospore

The intine (found in pollen) and endospore (found in spores) are considered synonymous. The intine lies between the foot layer and the protoplast and does not contribute to the outward appearance of the pollen or spore. It is largely composed of polysaccharides, including cellulose and pectin.¹⁴ It is thought to make up between 2 and 25 % by mass of a pollen or spore wall (the percentage varies between species).¹⁵ The intine can be readily differentiated from the protoplast and exine using TEM.

1.1.4 Protoplast

As well as two nuclei, the protoplast of both pollen and spores contains other cytoplasmic organelles, including endoplasmic reticula, the vacuole, golgi apparatus and mitochondria.² Unlike seeds, pollen and spores do not contain sufficient nutrients to sustain prolonged growth. Their function is merely to act as a vector for genetic information, and provide just enough energy (sometimes in the form of starch or lipid bodies) for pollen tube growth following fertilization.² Despite containing two nuclei, pollen and spores behave as if they were single-celled organisms.

1.1.5 Apertures and nano-channels

Apertures are present in both pollen and spores from many species and take the form of pores and furrows. The function of these micron-sized channels through the pollen or spore wall is twofold: firstly, they facilitate the movement of water and other materials into and out of the grain. This allows the grain to switch between its hydrated and dehydrated state (the harmomegathic effect). Secondly, apertures provide a weakened region of the wall, through which the pollen tube grows during fertilization in flowering plants.¹⁶ The number of apertures present varies between species.

An aperture in a pollen grain is usually sealed by the endexine, and may sometimes contain additional exine material. If this material is in the form of a discrete plug that fills most of the aperture, it is termed the operculum. The ectexine surrounding an aperture is often thicker, and sometimes a thickened 'donut' shaped region termed an annulus is present. This can be observed around the single pore of *Secale cereale* (rye) pollen (Figure 1.3).

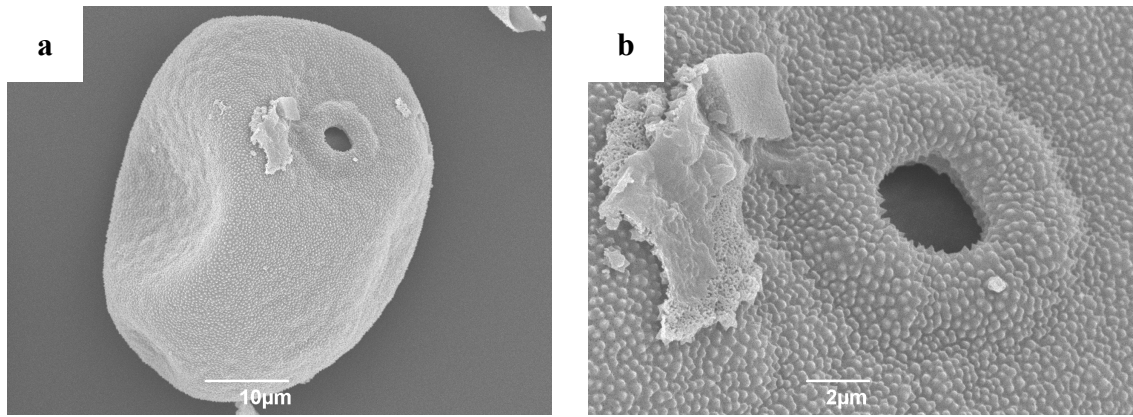


Figure 1.3: Scanning electron micrographs of *Secale cereale* (rye) pollen at (a) low magnification and (b) higher magnification, showing its annulus and pore

As well as apertures, some species possess nano-channels, which traverse all or part of the exine and intine. For example, these can be seen in the exine of *Lopezia lopezioides* (a member of the evening primrose family) pollen (Figure 1.4).¹⁷ These channels provide an additional route for the movement of material between the interior and exterior of the spore or pollen grain.¹⁸ Compared to apertures, the purpose of nano-channels has been less well researched.

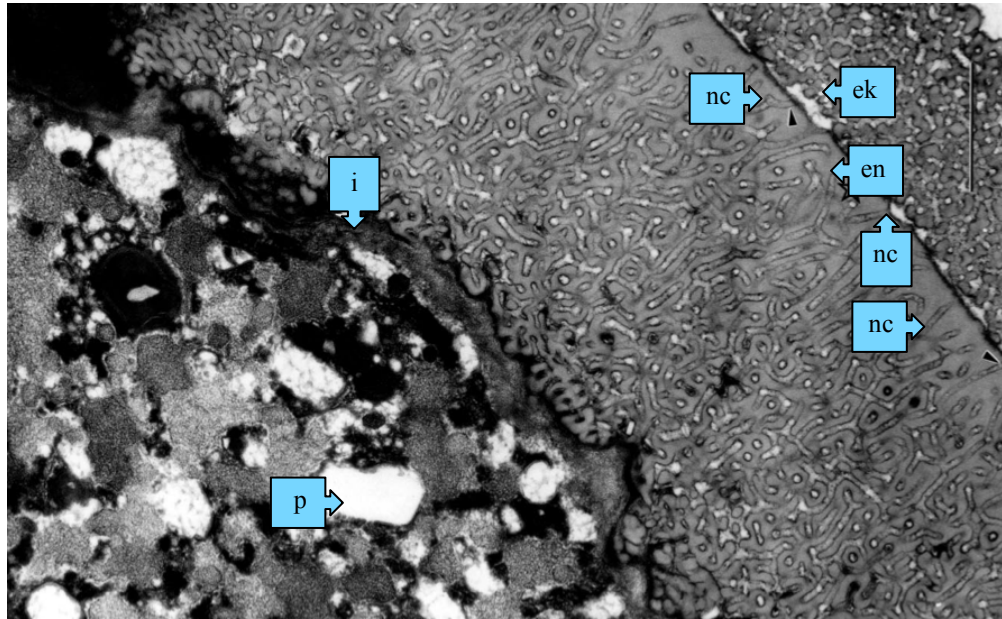


Figure 1.4: Transmission electron micrograph of *Lopezia lopezioides* pollen.

Scale bar = 1 μm ek = ektexine; en = endexine; i = intine;
nc = nano-channel; and p = protoplast¹⁷

1.1.6 Size and shape

The external sculptural features of the exine of pollen and spores have evolved to optimize their dispersal in a variety of habitats. As a result, the range of shapes and sizes of pollen and spore is substantial. For example, *Helianthus annuus* (sunflower) pollen is pollinated by insects. Its pollen has an oily surface with pointed sculptural elements that enable it to stick to pollinating insects. In contrast, wind and water pollinated species have much smoother surfaces.

It is challenging to measure the dimensions of pollen and spores in a consistent manner, as they are three-dimensional structures with a wide variety of shapes. However, they generally range in size from about 2 μm (genus: *Myosotis* (forget-me-not)), to greater than 100 μm (genus: *Cucurbita* (pumpkin)), with a range of sizes in between. Within each species, grains are almost monodisperse in size. Laser diffraction and microscopic image analysis have been used to demonstrate the narrow size distribution of *Lycopodium clavatum* spores.¹⁹ However, preparatory techniques for sample analysis (e.g. fixation, dehydration and embedding) can influence the size of both pollen and

spores. Therefore, care must be taken when selecting a preparation method and when analysing results.²⁰

1.2 Chemical composition of pollen and spores

1.2.1 Exine and exospore

The exine and exospore are composed of sporopollenin, which has been described as ‘Probably the most resistant organic material of direct biological origin found in nature’.²¹ John²² and Braconnot²³ first documented sporopollenin’s strength in the early 1800s after they observed that the exine was tougher than other layers of the pollen wall. They found that it was composed of carbon, hydrogen and oxygen. However, its chemical structure remains poorly understood and is still widely debated.

It is difficult to obtain sporopollenin in its pure form, as completely removing all non-exine material from pollen and spores is challenging. Methods that do remove all non-sporopollenin material are often found to alter sporopollenin’s chemical structure. For example, treating spores with sulfuric or hydrochloric acid introduces sulfur or chlorine respectively into sporopollenin’s structure.¹³

Many techniques have been applied in an attempt to elucidate sporopollenin’s structure, including: carbon and proton NMR,²⁴⁻²⁷ solid state carbon NMR;²⁸ ultraviolet-visible (UV-vis) and infra-red (IR) spectroscopy; X-ray photoelectron spectroscopy (XPS);²⁹ gas chromatography-mass spectrometry (GC-MS); and matrix-assisted laser desorption ionization time-of-flight mass spectrometry (MALDI ToF MS).³⁰ This analysis indicates that sporopollenin is likely to be a highly conjugated, organic polymer, consisting of an aliphatic backbone and aromatic, phenol, carboxylic acid, alkene, ester, ketone and ether functional groups.

Early work by Zetsche *et al.* focused on elucidating the degradation products of sporopollenin to provide insight into its structure.^{31, 32} They found sporopollenin to be a highly unsaturated polymer with hydroxyl, oxygen-containing and methyl functional groups. By treating pollen with ozone, followed by hydrogen peroxide, sporopollenin

was broken down into a series of mono- and di-carboxylic acids with both straight and branched chains. However, merely analysing degradation products provided limited structural information about sporopollenin.

Pollen develops in the anthers of flowering plants. Some studies have noted that the concentration of carotenoids and carotenoid esters found in the anthers is particularly high during pollen development.³³ These studies suggest that, as a result, sporopollenin could be composed of these building-block molecules.³⁴ In order to test this theory, a range of carotenoids (including zeaxanthin and canthaxanthin) and carotenoid esters (including echinone) (Figure 1.5) were polymerized.^{12, 13} These polymers were found to have similarities to naturally occurring sporopollenin, for example solvent solubility, products of ozonisation, elemental analysis, chemical resistance and infra-red spectra. However, none of the synthesised structures were found to be identical to sporopollenin. Therefore, although sporopollenin may have carotenoid components, it is unlikely that these are the sole building blocks of this complex system. This work suggests that merely attempting to synthesize sporopollenin from its likely precursors can provide only limited information.

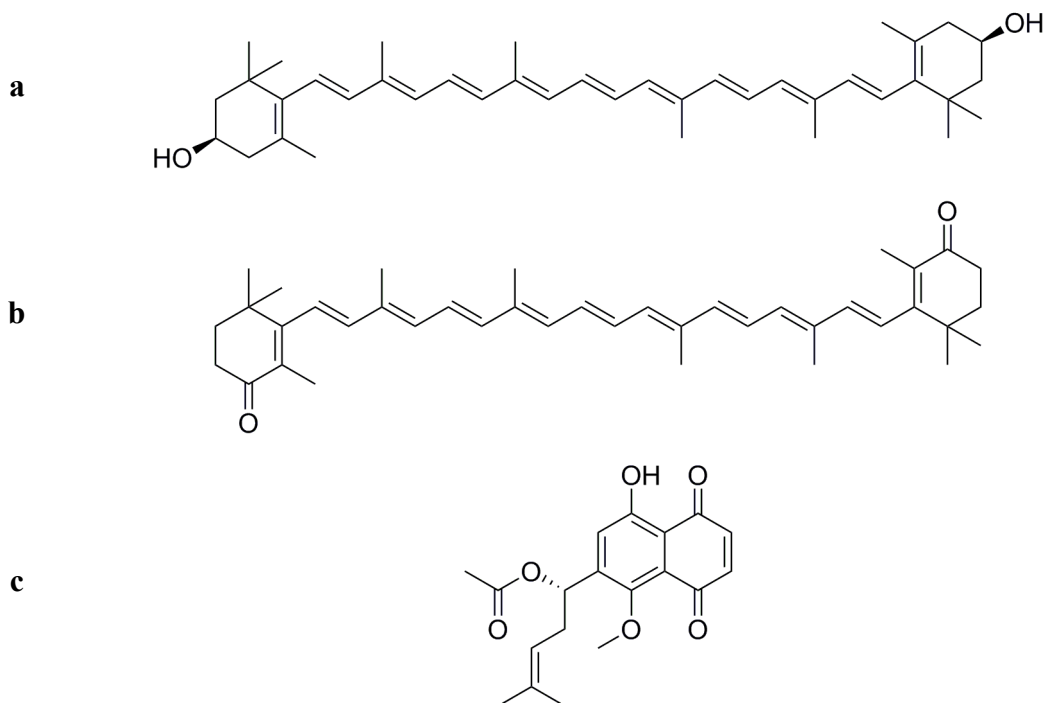


Figure 1.5: (a) Zeaxanthin; (b) canthaxanthin; and (c) echinone

Convincing evidence has been presented for the presence of *p*-coumaric acid (Figure 1.6) within sporopollenin's structure. Both untreated *Pinus mugo* (mountain pine) pollen and pollen treated to remove non-sporopollenin material was analysed by Curie-point pyrolysis mass-spectrometry.³⁵ Spectra show that peaks corresponding to *p*-coumaric acid were present in both samples (Figure 1.7), indicating the acid's presence in sporopollenin, rather than the intine or protoplast. The peak at m/z 164 corresponds to the molecular ion peak of *p*-coumaric acid and at the peak at m/z 120 corresponds to its decarboxylation product that forms during ionisation. After what the authors describe as a gentle degradation method involving AlI_3 , followed by a harsher saponification procedure, chromatographic and spectroscopic analysis still confirmed *p*-coumaric acid was the dominant component present. The authors postulate that due to the results observed during saponification, the acid moieties may be bound by ether linkages.³⁶ This extensive analysis provided strong evidence that *p*-coumaric acid is a major structural component of sporopollenin. More recent work by Boom *et al.* using a range of mass spectroscopic techniques has provided additional evidence for the presence of these acids within sporopollenin. Sporopollenin from *Isoetes killipi* C. Morton megaspores was found to be similar to a *p*-coumaric acid-based dehydrogenation polymer, and small differences were explained by the presence of ferulic acid moieties within the megaspore walls.³⁷



Figure 1.6: Structure of (a) *p*-coumaric acid and (b) ferulic acid

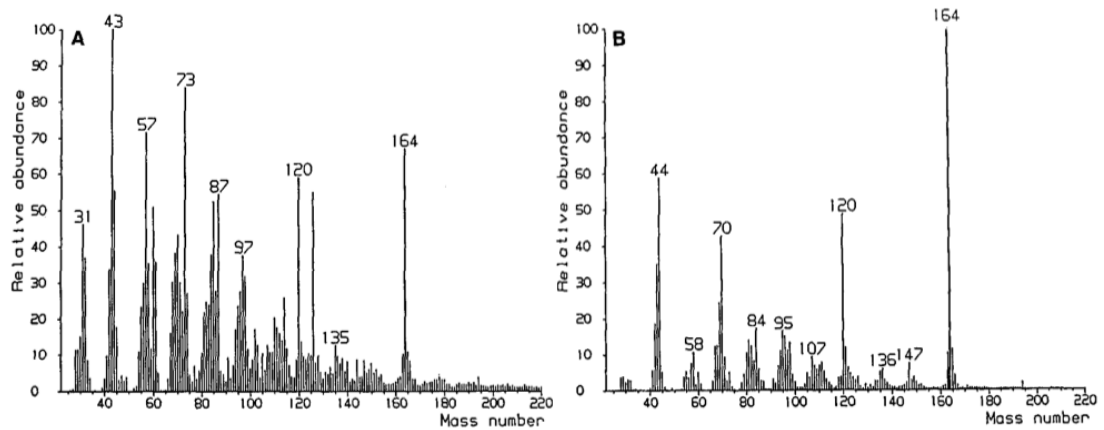


Figure 1.7: Mass spectra of *Pinus mugo* pollen (a) untreated and (b) treated to remove non-sporopollenin material³⁵

Recently, Rozema *et al.* and Blokker *et al.* used *p*-coumaric acid and ferulic acid (Figure 1.6) as sporopollenin proxies to predict sporopollenin's historic response to solar ultraviolet-B (UV-B) radiation.^{38, 39} Although these acids are unlikely to be the sole component of sporopollenin, they are well-studied structures, which could act as a simplified model of sporopollenin for analysis.

Sporopollenin is unlikely to be a single molecule, but rather a class of similar molecules that differ according to species. Its structure varies during a plant's lifecycle.⁴⁰ As some methods can result in chemical modifications to sporopollenin, it is recognised that the methods used to prepare sporopollenin for analysis can considerably influence the analytical results achieved.⁴¹ It is clear from published work that its structure remains far from being confirmed.

1.2.2 Intine and endospore

Early work suggested that the intine was primarily composed of cellulose, as demonstrated *via* a positive histological stain of iodine and concentrated sulphuric acid. Cellobiose (a classic, acid-hydrolysis product of cellulose) was identified after the acid hydrolysis of the intine of pollen.⁴² More recent studies have indicated that glucans, proteins and peptic polysaccharides may also be present in the intine or endospore.^{43, 44} Thin strands of cellulose known as microfibrils, were identified *via* electron microscopy.³³ In contrast to the sporopollenin exine, the intine or endospore is much more susceptible to chemical and physical degradation.

1.2.3 Protoplast

The protoplast contains a complex mixture of organelles, made up of a range of constituents. Proteins (including enzymes) ribonucleic acid (RNA), lipids (including phospholipids), starch, carbohydrates and water have all been found to be present.² Trace quantities of metal ions and inorganic salts, crucial to the function of metabolic processes have also been found.

1.3 Physical properties of pollen and spores

The exine wall of pollen and the exospore of spores survive intact for millions of years as fossils in rock. These have therefore frequently been exposed to high temperatures and pressures.⁴⁵ For example, in experiments *Lycopodium clavatum* spores retained a recognisable morphology after being exposed to temperatures of 300 °C and pressures of 1 kb for 100 hours.⁴⁶

The walls of pollen and spores act to protect their delicate protoplasts by reducing the levels of ultraviolet (UV) light transmitted. Pollen walls from a range of species were found to absorb strongly in the range 250 – 350 nm, which correlates with the wavelength range of UV type A and B radiation.^{38, 47}

As well as absorbing light, pollen and spores strongly autofluoresce between ~250 – 400 nm (the exact emission depends on the species). Autofluorescence is the natural fluorescence of materials without the addition of other fluorescent species e.g. fluorescent stains. This autofluorescence has been used to differentiate between species.⁴⁸ This effect is particularly useful during seasonal analysis of pollen field trials, where identifying and counting individual species using light microscopy is technically challenging and time-consuming.⁴⁹ Spectrofluorometry has been used to analyse the contents of *Lycopodium clavatum* spores. The peak emission of untreated spores was found to be 498 – 510 nm, whereas after treatment with phosphoric acid (85 %), this shifted to 548 – 558 nm.⁵⁰ The authors suggested that this shift correlates with the removal of cellulose, although acid treatment is likely to remove far more than cellulose alone. Although transmission electron microscopy is a more useful technique to elucidate the structural contents of pollen and spores, the work by van Gijzel *et al.*

highlighted the range of fluorescent species present and how their fluorescence can be influenced by chemical treatments.

1.4 Emptying pollen and spores

It is possible to remove some or all non-sporopollenin material from pollen and spores in order to produce microcapsules (see section 1.5). This can be achieved using a range of physical, chemical and biological processes. Microcapsules produced from both pollen and spores are termed ‘exine shells’ in some parts of the literature, despite spores possessing an exospore rather than an exine. However, the term will be used here for both pollen and spores for consistency.

It is usually desirable to recover only the pure, sporopollenin exine or exospore as this leaves hollow microcapsules, free of any potentially allergenic materials. The nature of the material recovered depends on the processes employed and the pollen or spore species used; not all species react to treatments in the same manner. The process selected to produce microcapsules depends on the type of microcapsule required. For example, microcapsules to be used in pharmaceutical or food applications must be white, intact and devoid of all non-sporopollenin material. Microcapsules used in engine lubricant additives could be coloured and could still contain allergenic components as they are unlikely to come into contact with humans. Some methods described in this section produce cracked exine shells, which could not be used as microcapsules (their contents would rapidly leak out). However, the surface of these cracked shells could be functionalized for a variety of applications (see section 1.5.4).

1.4.1 Pre-treatment

Pollen and spores are harvested together with other plant material e.g. leaves and stalks. This material must be separated out before any further treatments are considered, and this is usually done before pollen and spores material are sold to suppliers. In the case of Graminex (USA), the exact methods used during harvesting and separation are proprietary, but do involve drying harvested material, sieving it and then storing it under temperature and humidity controlled conditions.⁵¹ Patents have been granted that

describe the use of cyclone filtration bags to both harvest pollen and remove extraneous plant material.⁵² Smaller, laboratory-scale methods of removing contaminants include using fine metal sieves and suspending collected material in carbon tetrachloride or ether to remove soil particles.⁵³ Pollen and spores that are free of contaminants can be purchased from suppliers such as Sigma Aldrich (UK) and Allergon (Sweden).

1.4.2 Acetolysis

The acetolysis technique was first proposed by G. Erdtman and it is the most common preparatory technique used by palynologists to prepare pollen and spores for analysis by microscopy.⁵⁴ Its primary aim is not to produce microcapsules. The classical method involves heating pollen to 70 °C in a 9:1 mixture of acetic anhydride and sulphuric acid for one to two minutes, followed by centrifugation and washing with water.⁸ Slight modifications to the method have also been proposed, some of which describe washing pollen and spores in glacial acetic acid prior to acetolysis.⁵⁵

Acetolysis usually removes a large proportion of non-sporopollenin material, leaving hollow exine shells. TEM analysis is rarely carried out with the primary aim of demonstrating that the shells are completely devoid of non-sporopollenin material. Therefore, it is difficult to evaluate how successful the method is in removing intine and protoplast material. For example, acetolysis of pollen from the *Beilschmiedia* genus destroys the intine, but leaves the exine intact (Figure 1.8).⁵⁶

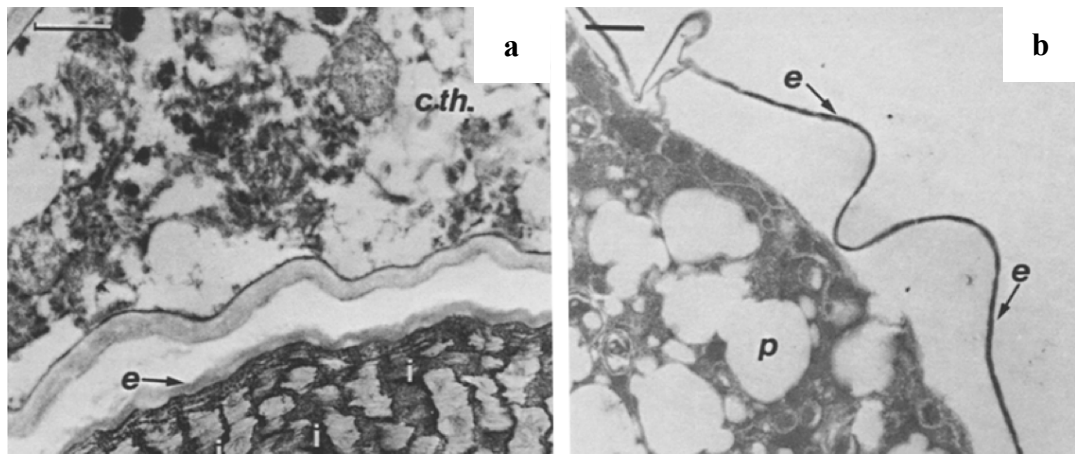


Figure 1.8: Scanning electron micrograph of the *Beilschmiedia* pollen (a) before acetolysis and (b) after acetolysis. Scale bars = 1 μm ⁵⁶
 e = exine; p = protoplast; and i = intine

Acetolysis almost always turns pollen and spores dark brown. The exine shells produced often require bleaching to make them sufficiently transparent for substantial analysis by light microscopy.⁴⁵ The fact that pollen and spores are turned dark brown suggests that the chemical structure of sporopollenin may have been altered, although this has not been confirmed experimentally. It is possible that bleaching could alter sporopollenin's structure. For most applications, for example pharmaceutical, food and visual displays, light-coloured or white microcapsules are desirable. Therefore, the dark brown exine shells produced by acetolysis are unlikely to be suitable for use in such applications.

1.4.3 Acid and alkali treatments

The most widely published methods used to produce exine shells from spores involve acids and alkalis. Unlike acetolysis, the primary aim of these treatments is usually the synthesis of microcapsules, rather than for the production of material for palynological analysis.

Zetzsche *et al.* first used an acid and alkali treatment to produce exine shells for microscopic analysis. Spores (*Lycopodium clavatum* and *Pinus sylvestris* (Scots pine)) were treated with hot acetone followed by hot alkali and then warmed for one week in phosphoric acid (85 %). Histological staining and microscopy suggest that the cellulosic

intine and the protoplast were successfully removed.⁴² However, work was largely limited to two species of spore.

More recently, Atkin *et al.* treated *Lycopodium clavatum* spores with organic solvents, acids and bases with the primary aim of producing exine shells for use as microcapsules. The method follows the general process flow outlined in Figure 1.9.⁵⁷ Laser scanning confocal microscopy (LSCM) analysis suggests that most non-sporopollenin material was successfully removed, but the resolution achieved means that this cannot be conclusively confirmed. However, scanning electron micrographs (SEMs) show that the surface morphology of *Lycopodium clavatum* spores was not damaged by the treatment. Limited transmission electron micrographs (TEMs) were presented and these were of low magnification, meaning that the complete absence of intine cannot be verified.⁵⁸ Combustion elemental analysis indicates a lack of nitrogen in treated spores.⁵⁹ This suggests that the protoplast and surface allergenic proteins, both of which have high nitrogen contents, were successfully removed. Exine shells were demonstrated to be devoid of allergenic proteins by matrix assisted laser desorption/ionization–time of flight mass spectrometry (MALDI-ToF-MS) and electrospray ionisation coupled with quadrupole-quadrupole time-of-flight mass spectrometry (ESI-QqTOF-MS).⁵⁹

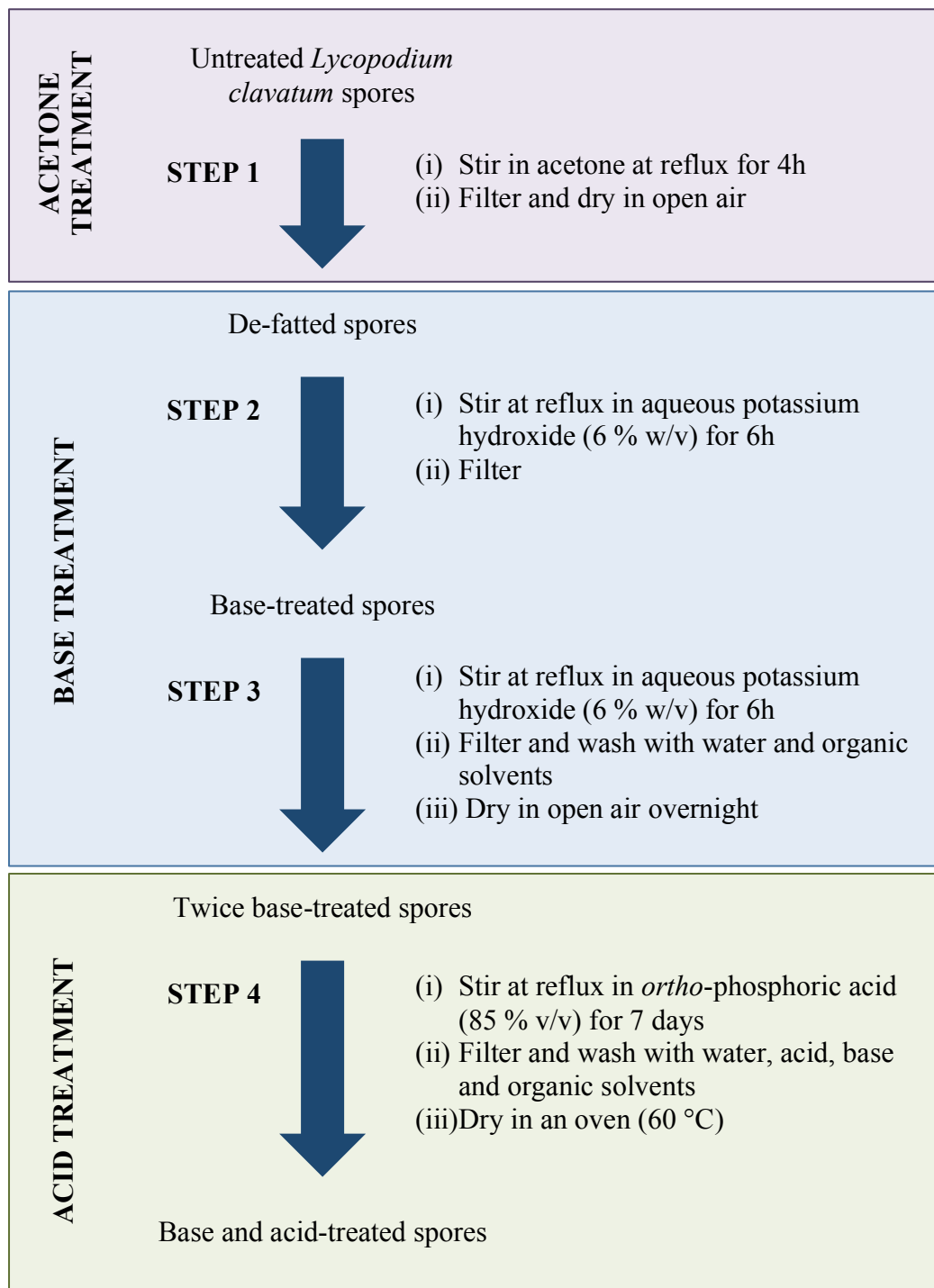


Figure 1.9: Summary of processes involved in the base and acid treatment protocol published by Atkin *et al.*⁵⁷

Although the base and acid treatment method proposed by Atkin *et al.* has been widely published and is now patented, it has only ever been used to isolate exine shells from *Lycopodium clavatum* spores. Atkin *et al.* propose that this method can be used to isolate exine shells from other species of pollen and spore, although this is not supported by published evidence.⁶⁰ Work has probably focussed on *Lycopodium clavatum* spores as they are widely available, inexpensive and well studied. It may be

that *Lycopodium clavatum* spores are robust enough to withstand this prolonged acid and base treatment, which could destroy other more fragile species.

Hydrogen fluoride (HF) has also been proposed as a method of producing intact exine from pollen. Pollen from *Pinus pinaster* (maritime pine), *Betula alba* (silver birch), *Ambrosia elatior* (common ragweed), *Zea mays* (maize) and *Capsicum annuum* (chilli) was heated at 40 °C for 5 hours in a mixture of pyridine and dry HF.⁶¹ The recovered exine shells were washed in ethanol. SEMs show that the morphology of most species was retained after treatment. Although *Zea mays* pollen became flattened after processing, its recognisable surface texture remained. Fourier transform infrared (FTIR) spectroscopy was used in an attempt to demonstrate that the cellulosic component of the intine was removed. Although treatment with HF would be expected to remove the protoplast and intine, no TEM evidence was provided to support this. Due to the toxicity and highly corrosive nature of HF, this method will not be investigated further in this thesis.

1.4.4 Treatments involving 4-methylmorpholine N-oxide

4-Methylmorpholine *N*-oxide (MMNO) (Figure 1.10) has been described as an effective solvent for cell wall polysaccharides, including cellulose.^{62, 63} As the intine is largely composed of cellulose, MMNO has been used to try and dissolve the intine of pollen, producing cracked pollen shells and protoplasts as a result

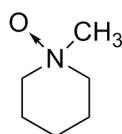


Figure 1.10: Structure of 4-methylmorpholine *N*-oxide (MMNO)

Pollen from *Lilium longiflorum* (lily) (0.1 – 0.2 µg) was treated with acetone and then suspended in 4-methylmorpholine *N*-oxide monohydrate (MMNO·H₂O, 200 µl).¹⁴ The suspension was heated to the desired temperature (between 70 – 100 °C) within 30 seconds, and the reaction subsequently observed *via* light microscopy. The primary aim of this work was to produce intact protoplasts (rather than exine shells), and this was achieved. MMNO was found to induce cracking along the aperture of the *Lilium*

longiflorum, which is probably the point at which the pollen is structurally weakest (Figure 1.11). As a majority of the intine and protoplast material was probably removed, the cracked exine shells could be used as ‘pure’ sporopollenin supports for surface functionalization (see section 1.5.4). Further analysis using (TEM) as well as spectroscopic techniques would be required to confirm the absence of all non-sporopollenin material. In addition, other species may be more amenable to treatment with MMNO.

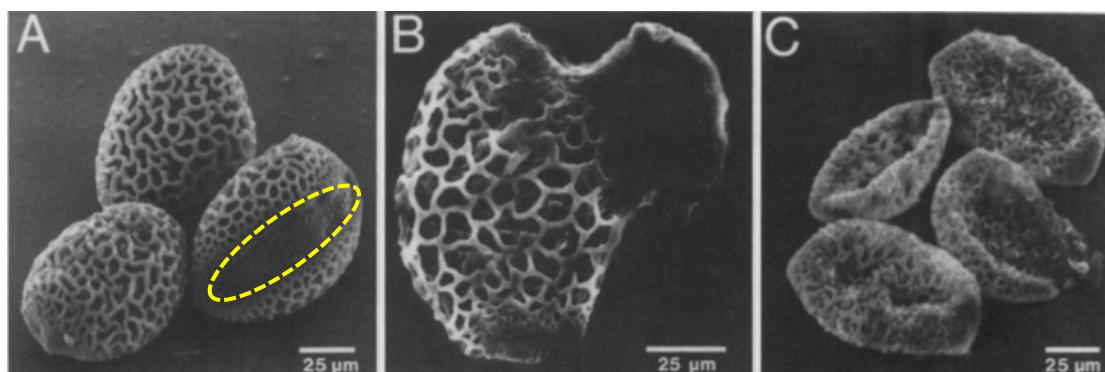


Figure 1.11: Scanning electron micrographs of *Lilium longiflorum* pollen (a) acetone washed (yellow dashed line shows the position of the aperture); (b) during protoplast release; and (c) after protoplast release¹⁴

Pollen from a range of genera was sieved and suspended in an aqueous solution of MMNO and cyclohexylamine (Figure 1.12). The pollen was then ground in a Potter-Elvehjem tissue grinder with a polytetrafluoroethylene (PTFE) pestle and glass mortar to detach the swollen exine shells from the protoplasts. Subsequently, the pollen was treated with cellulysin and macerase enzymes, plus bovine serum albumin (BSA) in order to digest the attachment between the intine and exine. The treated pollen was subjected to centrifugation over a density step gradient in order to separate out full, partially emptied and emptied pollen.⁶⁴ The primary aim of this treatment was to produce intact, pure sporopollenin exine shells for analysis. Pollen and spores from some species, including *Lycopodium clavatum* and *Fraxinus excelsior* (ash), were recovered intact. Others, including *Pinus monticola* (western white pine) and *Osmunda claytoniana* (interrupted fern), were quite damaged by the processing. The yield of completely empty exine shells recovered *via* this process was not reported and it is likely that this will differ between genera due to their varying compositions.

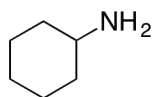


Figure 1.12: Structure of cyclohexylamine (CHA)

1.4.5 Enzymatic treatments

Enzymes are biological molecules that selectively catalyse chemical processes. They usually operate within a narrow temperature and pH range. Material (such as the protoplast and intine) can be efficiently removed from pollen and spores by selecting suitable enzymes to catalyse digestion. The gentle nature of most enzymes means that the chemical and physical structure of the exine shell is unlikely to be altered. Enzymes can be used alone, or with other reagents in order to enhance their properties.

Pollen from the genus *Tulipa* (tulip) was incubated with the following enzymes: pronase (to digest proteins); cellulase and pectinase (to digest cellulose and pectin); amylase and amyloglucosidase (to digest starch); and lipase and BSA (to digest lipids).⁶⁵ The aim of that work was to produce sporopollenin for analysis, rather than synthesising exine shells, therefore the morphology of the treated pollen was not evaluated.

In an alternative method, *Corylus avellana* (hazelnut) pollen was ground in a homogeniser in tris-hydrochloride buffer and then sonicated.⁶⁶ Pollen fragments were separated *via* centrifugation over a discontinuous glycerol gradient. The pollen was treated with pronase, lipase, cellulase, amylase and cellulysin enzymes. Homogenisation and sonication were used to rupture the intact pollen grains, allowing the release of digested protoplasts and intine material. Although analysis suggests that all non-exine material was removed, cracked grains were produced, which are not suitable as microcapsules. This method has more than thirty preparatory steps and uses costly enzymes, making it undesirable to further evaluate. Other, similarly long, enzyme methods have also been published.⁶⁷

1.4.6 Physical treatments

Many chemicals can alter the structure of sporopollenin, for example hydrochloric acid introduces chlorine into its structure.¹³ By only applying physical treatments, such as heating and centrifugation, sporopollenin's structure is expected to remain unchanged.

Pollen from a variety of genera was shaken in water for between six and twenty-four hours, then autoclaved (103 kPa, 121 °C, 15 minutes), centrifuged and then re-suspended in water.⁶⁸ Pollen was separated by centrifugation over a series of sucrose density gradients. Most pollen recovered by this method was ruptured, and therefore is unsuitable for producing pollen microcapsules. However, the primary aim of that study was not to recover intact exine shells.

1.5 Microencapsulation and surface functionalization

Microcapsules act to improve the properties of encapsulated materials, e.g. shelf life, controlled release profiles, resistance to external environmental pressures, ease of processing and handling, visual appearance and the masking of unpleasant odours or flavours.⁶⁹⁻⁷¹ They consist of the core material to be encapsulated, surrounded by a single or multi-layered wall (Figure 1.13). Specific microcapsules are selected to deliver the desired properties to the encapsulated material. They can be synthesised in numerous ways, but can be broadly broken down into two categories: water soluble and non-water-soluble (Figure 1.14).⁷² One of the first examples of microcapsules used commercially was carbonless copy paper.⁷³

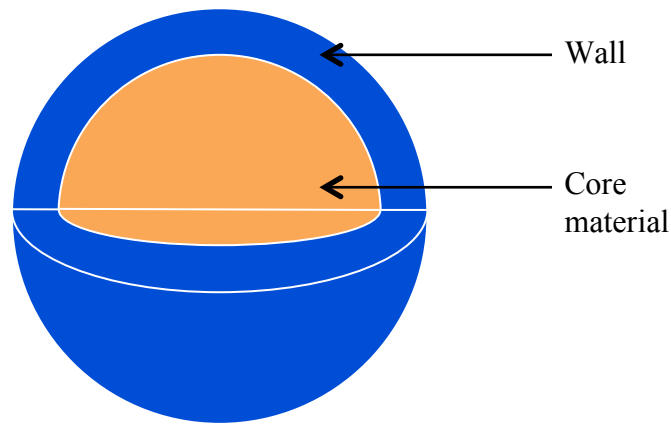


Figure 1.13: Generic structure of a microcapsule

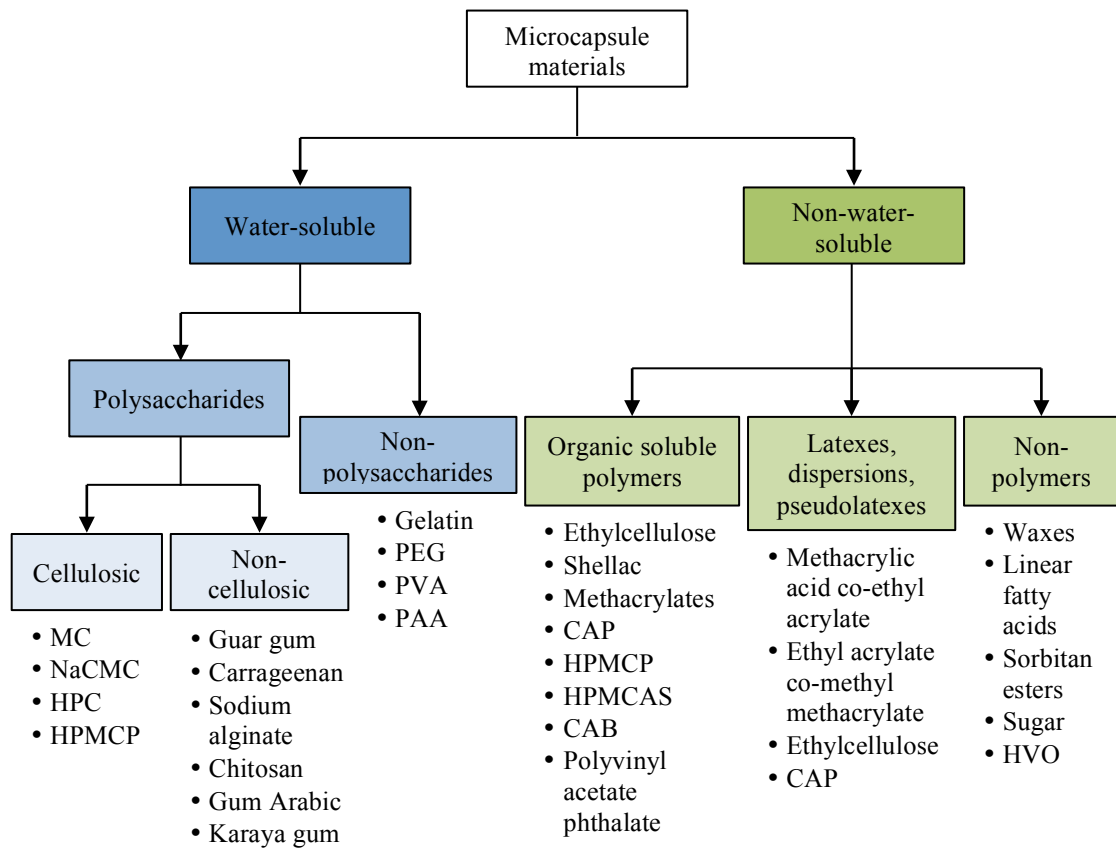


Figure 1.14: A flowchart to demonstrate the range of materials used to form microcapsules.

CAB = cellulose acetate butyrate; CAP = cellulose acetate phthalate;
 HPC = hydroxypropyl cellulose; HPMCAS = hydroxypropyl methyl cellulose acetate succinate; HPMCP = hydroxypropyl methylcellulose phthalate; HVO = hydrogenated vegetable oil; MC = methylcellulose; NaCMC = sodium carboxymethyl cellulose; PAA = polyacrylic acid; PEG = polyethylene glycol; and PVA = polyvinyl alcohol⁷²

It has been demonstrated that exine shells can be synthesised from *Lycopodium clavatum* spores and used as microcapsules for a range of materials.^{57, 74} These shells have been shown to absorb some materials e.g. fish oils, passively. Other techniques to increase loading levels and decrease surface contamination of the exine shell include dissolving the material to be encapsulated in a solvent, or applying a vacuum. The surface of *Lycopodium clavatum* exine shells has been functionalized with a variety of materials, including Schiff bases.⁷⁵ In addition, untreated *Lycopodium clavatum* spores have been used as microcapsules and as supports for other materials. However, to our knowledge, spore microcapsules have yet to be made available commercially, so microcapsules made from alternative materials currently supply all of the commercial market.

Microcapsules produced from pollen and spores may have several advantages over existing microcapsule technologies. Their tough sporopollenin outer wall means that such microcapsules are likely to survive harsh chemical and physical treatments and a range of environmental conditions. Within each species, pollen and spores are uniformly disperse; a property that can be difficult to engineer into synthetic microcapsules. Across species and genera, pollen and spores are available in a range of sizes and morphologies, meaning that a species could be selected to match almost any potential application. Pollen and spore microcapsules are produced from a renewable resource and may therefore be more environmentally friendly than microcapsules produced from petrochemicals. *Lycopodium clavatum* microcapsules can be produced using acids, bases and organic solvents, in a process which is simpler than that used to produce some existing microcapsule technologies. Commonly used species, for example *Lycopodium clavatum* spores, are inexpensive to purchase and are available in large (multi Kg) quantities.

1.5.1 Foods and dietary supplements

Foods and dietary supplements are sometimes microencapsulated to improve their properties, such as taste, texture, colour, fragrance and absorption in the body.⁷⁶ For spore exine shells to be considered as microcapsules in this field, they would need to be devoid of any proteins that could trigger allergenic responses in humans. They should usually be white or light in colour so as not to alter the colour of the material they are

added to. In order to fulfil these requirements, *Lycopodium clavatum* exine shells synthesised using acid and base hydrolysis are used almost exclusively.

A vacuum (10 hectopascals (hPa)) was applied to a homogeneous mixture of an edible fish oil and *Lycopodium clavatum* exine shells.⁵⁷ The shells were observed to absorb the fish oil and were then stained and evaluated using laser scanning confocal microscopy (LSCM). At a 1:1 weight/weight (w/w) loading, exine shells were reported to have absorbed most of the oil, with very little remaining on the outer surface. Other studies have found that loading fats above 1:1 (w/w) left material on the surface of exine shells, but that repeated washings with water reduced this surface contamination.⁵⁸

Solvents were used to facilitate the uptake of sunflower oil into exine shells. A 0.5 g tablet of *Lycopodium clavatum* exine shells readily absorbed a mixture of ethanol (1 mL) and sunflower oil (1 mL) in twenty seconds. Sunflower oil took longer to be absorbed when mixed with other solvents including petroleum ether (3 hours), hexane (3 hours), toluene (2 minutes 15 seconds) and dichloromethane (35 seconds).⁷⁷ Why ethanol is such a good solvent for this application remains unclear.

The ability of exine shells to shield their contents from UV radiation was used to reduce the rate at which cod liver, sunflower, rapeseed and soybean oils turned rancid.^{60, 78} Encapsulation notably reduced the degree of oxidation of the oils (measured by peroxide values) when they were exposed to UV radiation. These results indicate that encapsulating some foods within exine shells could extend their shelf lives.

1.5.2 Pharmaceuticals

Pharmaceuticals are often encapsulated to facilitate their movement to a particular location within the body; to mask undesirable tastes; and to allow for the controlled release of a drug over a predictable timescale. For example, to improve its palatability, diclofenac (a commonly prescribed non-steroidal anti-inflammatory drug) was encapsulated inside microcapsules synthesised from ethylcellulose, diethylphthalate and polyethyleneglycol.⁷⁹ Encapsulation was found not to slow the release of the drug into patients.

Acid and base treated *Lycopodium clavatum* spores have been filled with a range of pharmaceuticals. Most recently, ibuprofen was encapsulated in these shells at a 1:1 w/w loading.⁵⁹ Extensive analytical analysis demonstrated that the surface of the exine shells was not contaminated with ibuprofen and that the shells effectively masked the taste of the drug.

A gadolinium (III) magnetic resonance imaging (MRI) contrast agent was encapsulated in acid and base treated *Lycopodium clavatum* exine shells.⁸⁰ The aim of this work was to provide an oral delivery route for the contrast agent with a predictable, controlled release profile. The filled shells were incubated *in vitro* in human plasma for thirty minutes. SEM analysis was performed both before and after this incubation. Micrographs demonstrated that the shells broke down in human plasma. The authors suggested that enzymes found in blood plasma facilitated this degradation. The magnetic resonance relaxivity of a solution of filled exine shells in human plasma was compared to filled shells in a buffer solution over a period of eight hours. The relaxivity of the buffered solution remained almost constant. However, the relaxivity of the plasma solution increased almost three-fold over the period of analysis. This indicates that the plasma digested the exine shells, releasing the contrast agent thus showing an increase in measured relaxivity.

In vivo analysis of exine shell breakdown was performed. Two volunteers consumed exine shells (1 g each) and blood samples were then taken at thirty-minute intervals for two hours.⁷⁷ The samples were centrifuged to remove the blood serum fraction and the remaining solids were then examined by light microscopy. As the experiment progressed, the number of intact exine shells observed decreased, but the fraction of shells recovered as fragments increased. These results show that exine shells can pass intact from the digestive system into the blood and that once there, they are broken up.

Several patents have been granted to Mackenzie *et al.*, which describe the encapsulation of a range of other pharmaceuticals, including thyroxine, human recombinant growth hormone and insulin.⁷⁷ They also hint at the wide scope of delivery routes for filled exine shells, such as inhalation and oral, dermal and intravenous administration.^{19, 77}

1.5.3 Biological material

It is often desirable to encapsulate biological materials to protect them from their surrounding environment and prolong their viability. For example, probiotic bacteria have been encapsulated in an attempt to protect them from the acidic environment of the human stomach.⁸¹

Enzymes are nature's catalysts and usually only operate within a narrow pH and temperature range. They can easily be denatured (irreparably damaged) by exposure to conditions outside of their normal operating range. It is sometimes desirable to encapsulate enzymes to maintain high levels of activity, increase the range of conditions they can operate in and to limit damage to the enzymes. In some cases, encapsulated enzymes can also be recovered.⁸²

The enzymes alkaline phosphatase (ALP) and streptavidin-horseradish peroxidase (sHRP) were encapsulated in microcapsules synthesised from *Lycopodium clavatum* spores.⁵⁸ The activity of the enzymes was measured after they were recovered from the microcapsules by extraction into an aqueous buffer. Enzyme activity decreased between 3 – 9 % (sHRP) and 1 – 3 % (ALP), suggesting that encapsulation and recovery did not considerably affect enzyme activity. An additional 42 – 48 % activity loss was attributed to freeze-drying: an optional preparation step. In the same study, the enzyme α -amylase was stained with Evans blue (a fluorescent, anionic, protein-staining dye⁸³) and encapsulated inside the same spore microcapsules. Upon examination by LSCM, the stained α -amylase appeared to be fully encapsulated, with no material remaining on the surface of the exine shells.

Candida rugosa lipase (CRL) is an enantioselective enzyme. Tutar *et al.* successfully adsorbed this enzyme to the surface of untreated *Lycopodium clavatum* spores (as shown by SEM) with an optimum spore-to-enzyme ratio of 0.3.⁸⁴ After immobilisation, the pH for optimum activity of CRL shifted from 6.0 to 7.0. The optimum operating temperature also shifted from 35 °C to 40 °C, and CRL maintained a far longer storage stability time after immobilisation.

In a second study, CRL was encapsulated in a sol-gel matrix both in the presence and absence of either untreated, or acid and base treated *Lycopodium clavatum* spores.⁸⁵

Sol-gel encapsulation involves the formation of a gel matrix from a hydrolysed colloidal or polymeric solution. SEM demonstrated that CRL filled the surface cavities of untreated spores more efficiently, compared to acid and base treated spores. This encapsulated lipase showed many times the level of activity of free CRL or adsorbed CRL previously prepared by Tutar *et al.*⁸⁴ The encapsulated lipase was used to catalyse the enantioselective hydrolysis of Naproxen (a non-steroidal anti-inflammatory drug), with the immobilisation and encapsulation providing the optimum conditions for this reaction. These results show that exine shells can be used to facilitate reactions where enzymes are merely associated with the surface of the exine shell and are not necessarily encapsulated in its interior.

In addition to enzymes, base and acid treated *Lycopodium clavatum* spores were treated with bakers' yeast (*Saccharomyces cerevisiae*).⁷⁴ Exine shells were compressed and then mixed into a suspension of yeast in ethanol. A vacuum was applied for one hour and the exine shells were then left to re-inflate. An SEM of two cracked exine shells indicates that yeast cells were encapsulated in at least some of the shells. The authors suggest that the comparatively large yeast cells were able to enter the spores by means of *Lycopodium clavatum*'s trilete scar (Figure 1.15). The encapsulated yeast was found to still be biologically active, but not as active as unencapsulated yeast.

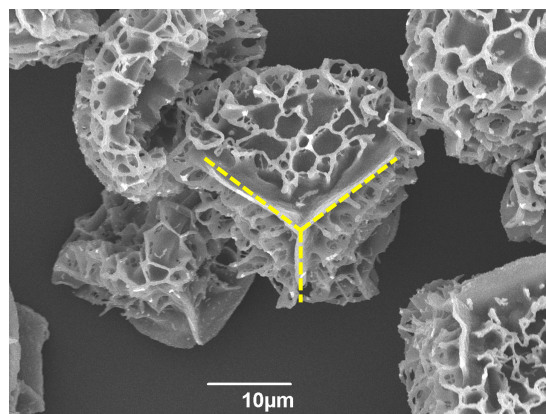


Figure 1.15: Scanning electron micrograph of untreated *Lycopodium clavatum* spore (yellow lines highlight the trilete scar)

1.5.4 Surface functionalization

The functional groups (predominantly –OH and –COOH) on the sporopollenin exine allow for the easy functionalization of the surface of spores.⁴² Functionalized spores are primarily used in separation chemistry. Spores make ideal supports for chromatography materials because, within each species, they have a consistent shape and size (providing a constant and predictable flow rate) and are largely inert.⁸⁶ Untreated *Lycopodium clavatum* spores are typically used, probably because they retain their structure and morphology despite extensive chemical treatment, are inexpensive and can be readily purchased in large volumes.

Gürten *et al.* prepared carboxylated diaminoethyl *Lycopodium clavatum* spores bound to cobalt (II) ions for use as a ligand exchange solid phase in liquid chromatography.⁸⁷ Isomers of nitroalanine were successfully separated. In similar work, ion exchange and ligand exchange supports were prepared from *Lycopodium clavatum* spores in order to separate nucleosides, nucleotides, amino acids and transition metals.⁸⁶ Although these approaches proved successful, chromatographic techniques based on the use of spores have not yet moved into the mainstream.

Inert, solid supports (modified silica gel, polymers, zeolites) treated with Schiff bases have been used to adsorb vanadium (IV) (the most harmful oxidation state of vanadium). These solid supports are easy to recover from aqueous solutions. *Lycopodium clavatum* spores were selected as an alternative to these solid supports. The spores were treated with acetone and their surfaces then functionalized with a range of Schiff bases (Figure 1.16). When these functionalized spores were exposed to aqueous solutions of vanadium (IV) ions, they successfully adsorbed the ions.⁷⁵ In a similar piece of work, tridentate Schiff bases were attached to acetone-treated *Lycopodium clavatum* spores (Figure 1.17). These functionalized spores adsorbed Ruthenium (III) ions from aqueous solutions.⁸⁸ That work indicates that functionalized spores could be used as easily recoverable supports for Schiff bases, which facilitate the adsorption of a range of metal ions from aqueous solutions.

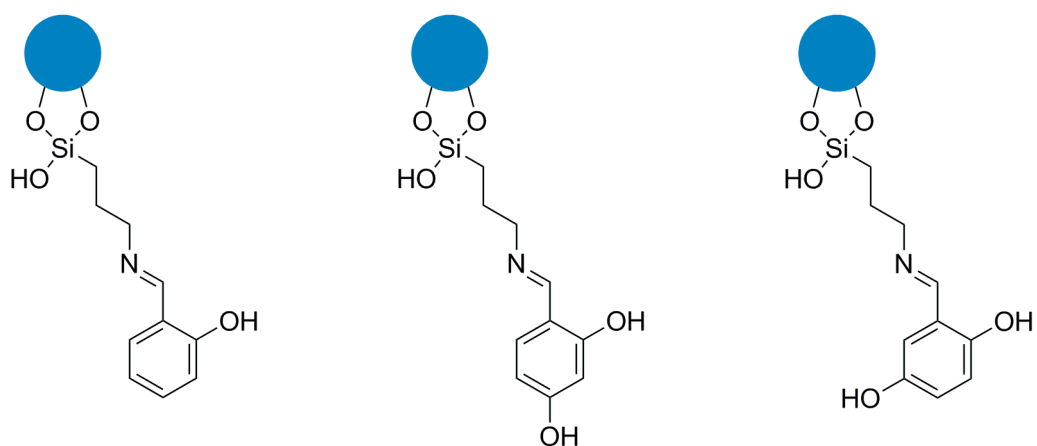


Figure 1.16: Structure of three *Lycopodium clavatum* spore-immobilised Schiff bases prepared by Kocak *et al.* in preparation for Vanadium (IV) sorption studies (spores indicated by blue circles)⁷⁵

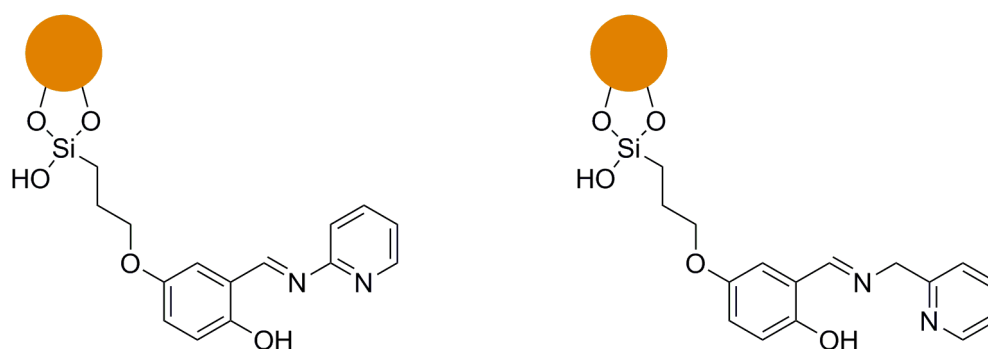


Figure 1.17: Structure of two *Lycopodium clavatum* spore-immobilised Schiff bases prepared by Kocak *et al.* in preparation for Ruthenium (III) sorption studies (spores indicated by orange circles)⁸⁸

As well as Schiff bases, calixarenes are used to recover inorganics from solution. Untreated *Lycopodium clavatum* spores were bound to calix[4]arene *via* a hexamethylene diisocyanate linker and were found to adsorb sodium dichromate ($\text{Na}_2\text{Cr}_2\text{O}_7$) ions from aqueous solution.⁸⁹ That work could provide easily recoverable particles able to separate harmful chromium (VI) species from groundwater.

Most recently, Mackenzie *et al.* functionalized the surface of base and acid treated *Lycopodium clavatum* spores with the aim of furthering the understanding of functional groups present on sporopollenin's surface.⁹⁰ FTIR evidence presented indicates that carboxylic acids on the surface of sporopollenin were converted to amides and subsequently reduced to primary amines. Combustion elemental analysis and solid-state

^{15}N & ^{13}C NMR support these results. This work represents a departure from previous approaches used to determine the structure of sporopollenin (see section 1.2.1).

1.6 Analytical techniques

A wide array of analytical techniques have been attempted in order to assess the structure and morphology of pollen and spores (Table 1.1). These techniques have been applied to assess surface morphology, internal structure or chemical composition of pollen and spores.

Table 1.1: Summary of analytical techniques used to evaluate pollen and spores

Analytical technique	Characteristic evaluated		
	Surface morphology	Internal structures	Chemical composition
Scanning electron microscopy (SEM)	✓✓	✓*	
Transmission electron microscopy (TEM)		✓✓	✓
Light microscopy (LM)	✓	✓	✓^
Laser scanning confocal microscopy (LSCM)	✓	✓	✓^
Spectrofluorometry			✓✓
Ultra-violet visible (UV-vis) spectroscopy			✓✓
Infrared (IR) spectroscopy			✓✓

✓✓ Provides a large amount of detailed information

✓ Provides a limited amount of less detailed information

* The internal composition of cracked spores has been evaluated⁷⁴

^ When combined with histological stains relevant to the features studied⁸³

1.6.1 Light microscopy

The most frequently used technique to analyse pollen and spores is light microscopy (LM). It can provide information on both the surface morphology and internal components of pollen and spores. In order to derive a true representation of pollen and spore structure, grains must usually be examined in their hydrated state. Dehydrated

grains appear very different to hydrated grains under the light microscope. This is illustrated with *Juglans nigra* (black walnut) pollen: it is much more difficult to observe surface detail or internal contents in the dehydrated pollen compared to the hydrated grains (Figure 1.18).

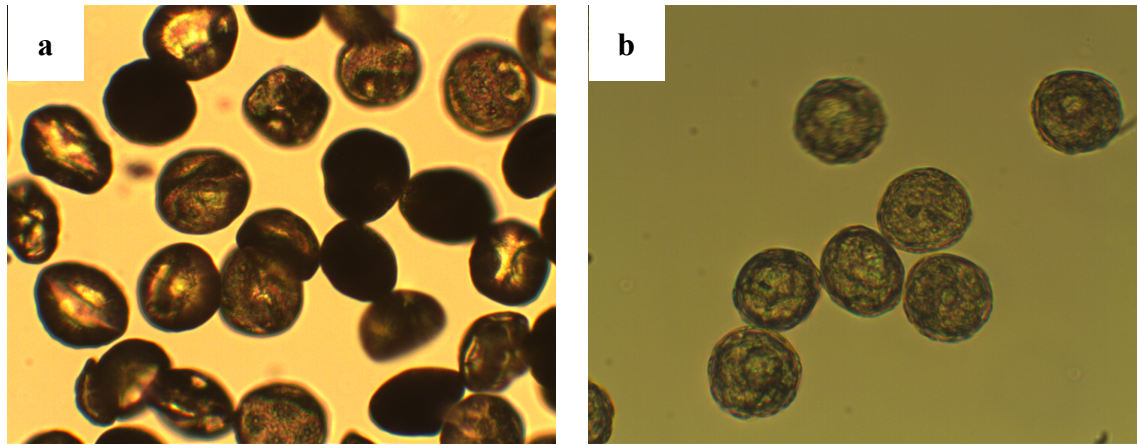


Figure 1.18: Light micrographs of untreated *Juglans nigra* pollen ($\times 400$ magnification) in (a) a dehydrated and (b) a hydrated state

In order to examine pollen and spores in their hydrated state, grains are suspended in water, and then a drop of this suspension placed on a glass microscope slide and covered with a glass coverslip (Figure 1.19). Over time ($>$ five minutes), as the slide is exposed to the heat of a microscope lamp, water evaporates and grains dehydrate. They can easily be rehydrated by the addition of water to the edge of the coverslip, which is then readily taken up *via* capillary action. If slides are to be kept for longer periods of time ($>$ one day), material should be suspended in glycerine jelly and prepared as described above.⁹¹ Glycerine limits potentially hazardous bacterial growth, which occurs readily in aqueous suspensions.

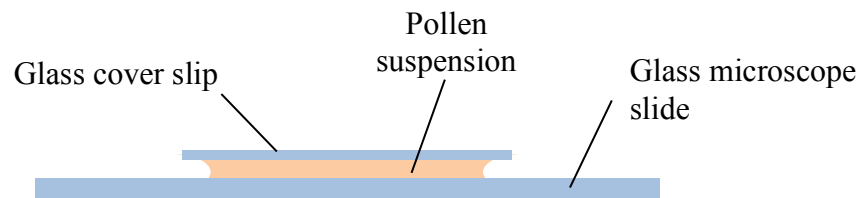


Figure 1.19: Schematic representation of the preparation of a microscope slide for light microscopy analysis of hydrated pollen and spores

1.6.2 Scanning electron microscopy

Scanning electron microscopy (SEM) enables the visualisation of sub-micron surface features of both pollen and spores. It can provide information on how treatments applied in order to produce microcapsules alter the sporopollenin exine. After LM, it is probably the next most commonly used technique used in palynology.

The SEM fires a high-energy beam of electrons towards a sample (Figure 1.20). These electrons are condensed into a beam and then focussed by a series of magnetic lenses. The incident beam is scanned over the sample and a range of signals is produced as a result of the incident beam-sample interactions. These signals include secondary electrons, X-rays, photons, backscattered electrons and heat. It is primarily the secondary electrons that are collected and converted into a digital image.

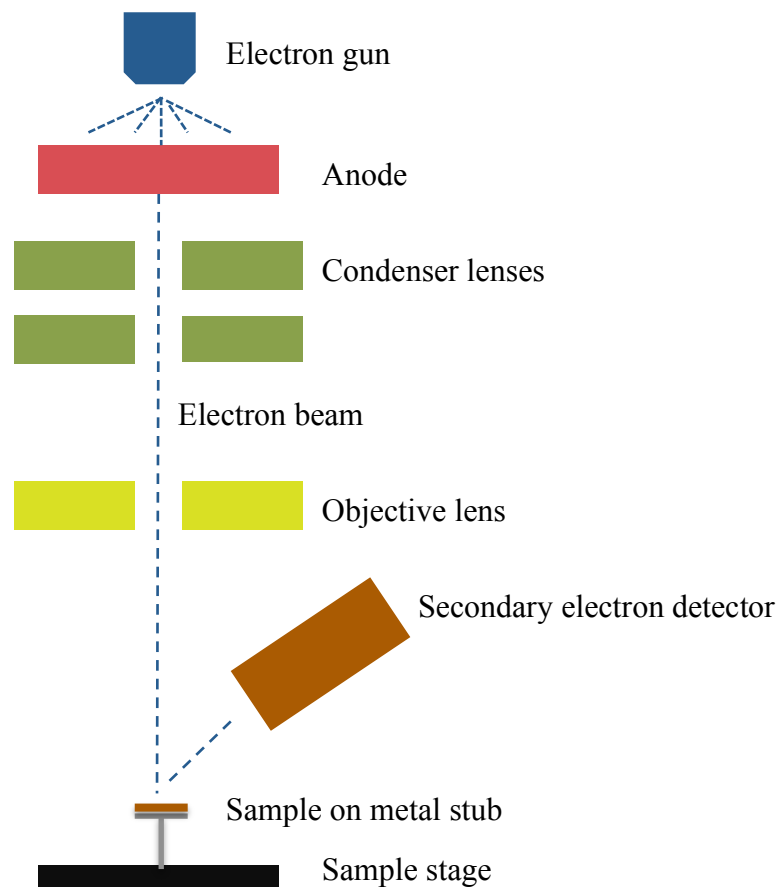


Figure 1.20: Schematic representation of a scanning electron microscope

SEM Samples must be electrically conductive and grounded, so pollen and spores are usually dusted onto metal stubs and coated with gold or palladium using a sputter coater. Most SEMs operate under vacuum, meaning that samples must also be fixed and dehydrated. Fixation aims to preserve material in its natural state and halt any continuing biological processes. As a result of this preparation, grains may appear to be collapsed and sculptural features are more difficult to distinguish. However, low-vacuum or ‘environmental’ SEMs are available, such as the JEOL 6490 LV in the Bioscience Technology Facility, The University of York. These eliminate the need for fixation and dehydration and do not deflate grains, allowing more meaningful analysis to be performed. The amount of sample preparation required is greater than for light microscopy, but SEM almost always yields more useful information about the morphology of grains.

1.6.3 Transmission electron microscopy

Transmission electron microscopy (TEM) provides information about the internal contents of pollen and spores. When used in conjunction with heavy metal stains, it can also give details about the chemical composition of components.

Before analysis, pollen and spores must be fixed. Samples are then dehydrated and embedded (usually in a resin) and then sliced into thin (0.2 – 2 μm) sections. Dehydration is necessary as most TEMs operate under vacuum. Heavy metal stains are used to provide contrast and different stains bind selectively to different components. These stains can be applied during fixation and dehydration or directly to thin sections.⁹² A commonly used fixative, which also acts as a stain, is osmium tetroxide. Sample preparation required for TEM is extensive and the array of fixation, embedding and staining protocols is vast, especially as different species respond differently to the same method.^{11, 93}

Inside the TEM, a high-energy beam of electrons is condensed and focussed towards the thin section by a series of magnetic lenses (Figure 1.21). A majority of the electrons pass through the sample without deviation. However, some are scattered due to the presence of heavy metals in the section. These heavy metals rarely occur naturally in a sample, but are of course found in the heavy metal stains applied. The unscattered electrons are detected and used to form a digital image of the section. Unscattered electrons show up as lighter areas, whereas regions of the section from which electrons have been scattered appear darker.

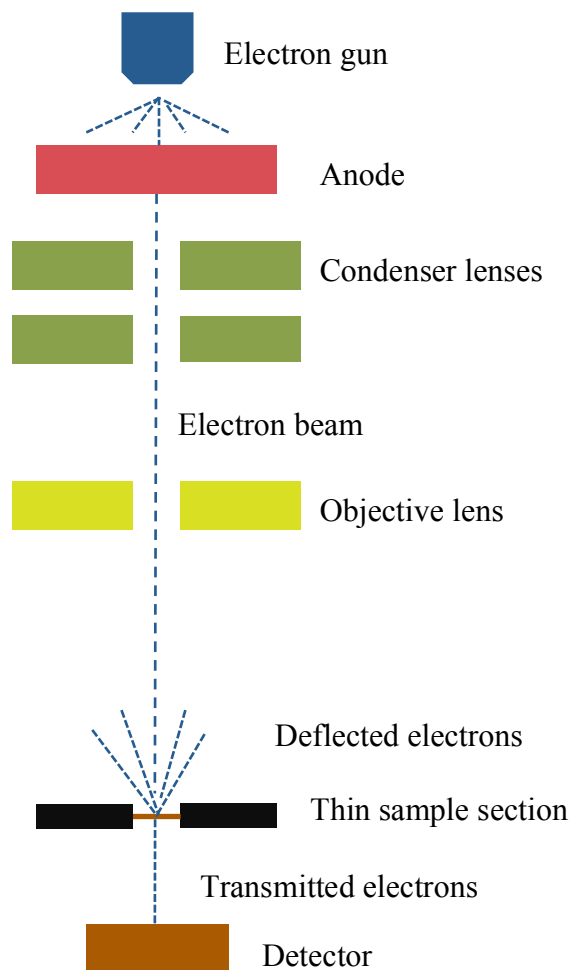


Figure 1.21: Schematic representation of a transmission electron microscope

1.6.4 Laser scanning confocal microscopy

A laser scanning confocal microscope (LSCM) uses the fluorescence emission of biological organisms (including pollen and spores) to investigate their internal structures. It works to eliminate all out-of-focus light from a sample so that only light emitted from a single focal plane is observed, so providing sharp images. Images of single planes can be built up to generate a three-dimensional representation (z-stack) of the sample.

Usually, biological samples do not possess intense natural fluorescence, and must therefore be selectively stained with fluorochromes (fluorescent molecules). For example, 4',6-diamidino-2-phenylindole (DAPI) selectively binds to DNA found within nuclei and has a fluorescence emission maximum at around 461 nm.⁹⁴ Pollen and spores naturally autofluoresce, meaning that stains are not essential, but may be applied to

selectively stain - and therefore highlight - specific components.⁹⁵ Minimal sample preparation is required, and pollen and spores are examined in an aqueous suspension, with the slide prepared as in Figure 1.19. Preparation required for analysis on an inverted LSCM (as available in the Bioscience Technology Facility, The University of York) is similar to that required for light microscopy. However, the slide is instead rotated 180 ° before being placed on the microscope stage (Figure 1.22), so that the incident excitation beam hits the slide first rather than the coverslip.

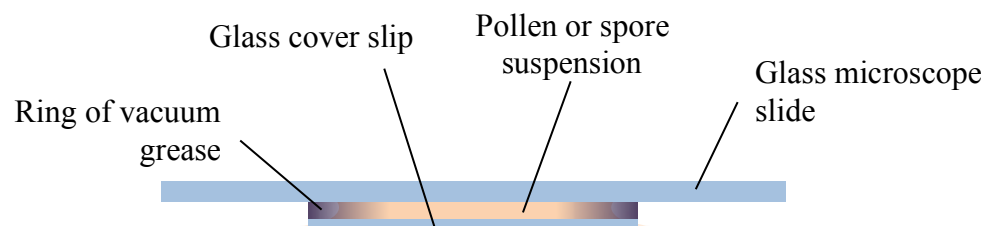


Figure 1.22: Schematic representation of the preparation of a microscope slide for laser scanning confocal microscopy

To collect fluorescence emission from a single focal plane, the LSCM must work to eliminate light emitted from other planes (Figure 1.23). Monochromatic light is emitted from the light source (usually a laser) and passes through a dichroic mirror. This light is focussed towards the sample by the objective lens. Structures within the bulk of the sample absorb this incident light and emit fluorescent light. The dichroic mirror selectively reflects emitted light towards the detector. The pinhole eliminates any fluorescence that does not originate from the selected plane of focus, so only fluorescence from the plane of focus is collected and converted to a digital image. Careful selection of lasers and the addition of filters allow specific fluorochromes within a sample to be observed.⁹⁶

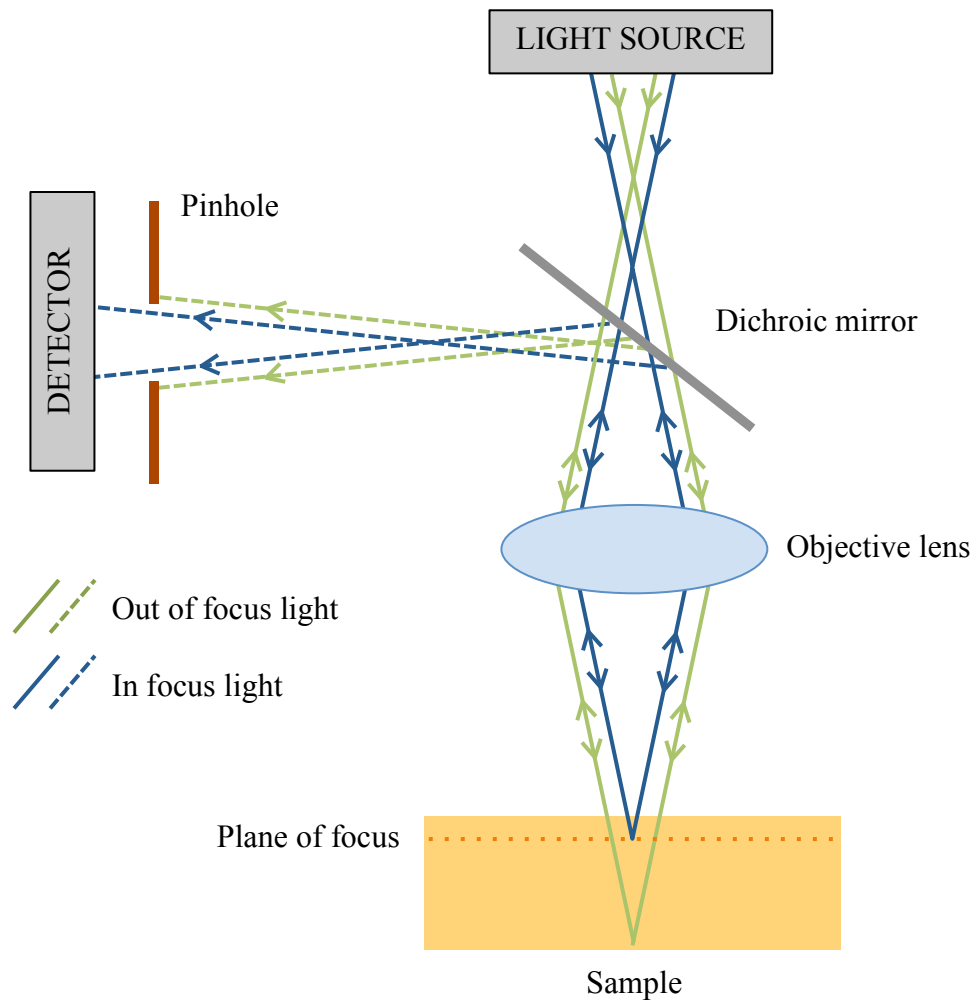


Figure 1.23: Schematic representation of a laser scanning confocal microscope

The LSCM can be set up to collect fluorescence from a single fluorochrome (single-track mode) or multiple fluorochromes (multi-track mode). Multi-track mode is used when several fluorochromes exist in a sample, but it is desirable to collect the emission from each one individually. It involves exciting and collecting emission from one fluorochrome, and then sequentially doing the same for other fluorochromes in the sample. A sequence of images (such as that in Figure 1.24) illustrates this technique. Images of enzyme-treated *Betula fontinalis* pollen stained with the fluorochrome Rhodamine B were collected after sequential excitation at 405 nm and 561 nm (Figure 1.24 (a) and (b) respectively). These were stacked together to create an overall image (Figure 1.24 (c)) that highlights the fluorescence present in both regions of the spectrum.

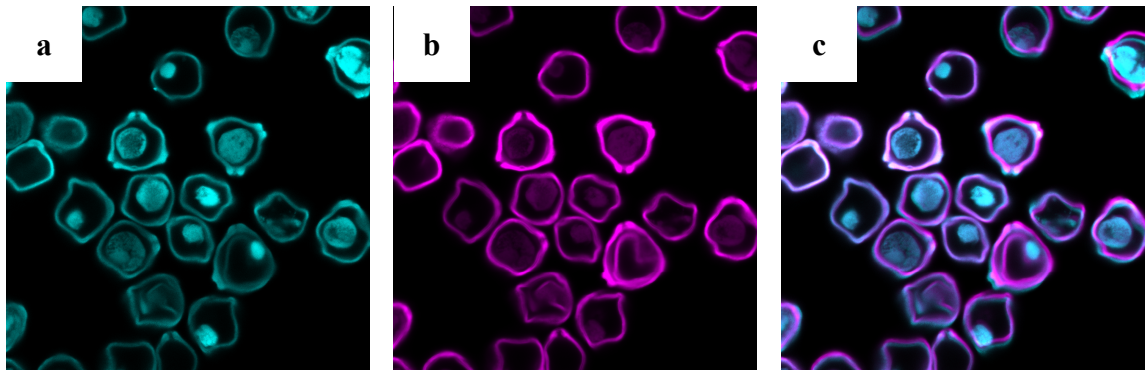


Figure 1.24: LSCM images (multi-track mode, $\times 630$ magnification) of enzyme-treated *Betula fontinalis* pollen stained with Rhodamine B; (a) excitation λ 405 nm; (b) excitation λ 561 nm; and (c) images from (a) and (b) stacked

1.6.5 Spectrofluorometry

Spectrofluorometry allows the measurement of the absorption and emission of fluorochromes within a sample. Usually, dilute aqueous solutions are used for analysis as this minimises interactions between fluorochromes that could cause shifts in absorption and emission. In order to analyse intact spores and pollen grains, solid, undiluted samples can be sandwiched between two cut-down glass microscope slides (dimensions of slides approximately 2.5 x 2.5 cm) (Figure 1.25). These must be secured together, and by using tape to do this the setup can be easily disassembled. As a result, samples can be used for additional analysis, meaning that this is a non-destructive technique. Analysis of solid, opaque samples (including pollen and spores) - prepared as in Figure 1.25 - is usually performed using a front-face excitation geometry (Figure 1.26).⁹⁷

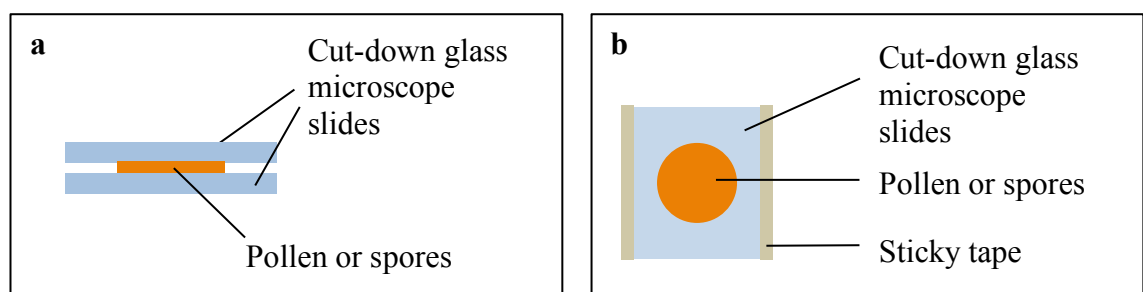


Figure 1.25: Schematic representation of the sample preparation required for front-face excitation fluorescence measurements: (a) side-on view; and (b) aerial view

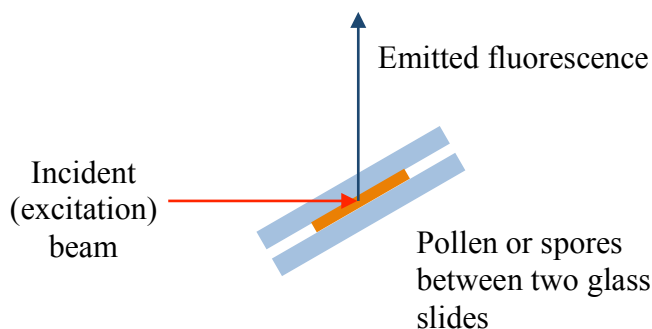


Figure 1.26: Schematic representation (aerial view) of front-face excitation geometry

A longpass filter is often placed between the sample and the detector. This filter attenuates light of shorter wavelengths. For example, a 350 nm longpass filter reduces the amount of light with a wavelength shorter than 350 nm that reaches the detector. These filters are used to reduce peaks observed in emission spectra that arise as a result of scattering interactions with the sample, rather than its fluorescence. For example, in aqueous samples, Raman scattering occurs at about 34 nm longer ($2.9 \times 10^5 \text{ cm}^{-1}$ lower) than the incident wavelength.⁹⁸ Therefore, an excitation wavelength of 300 nm ($3.3 \times 10^4 \text{ cm}^{-1}$) would show Raman scattering at 334 nm ($3.0 \times 10^4 \text{ cm}^{-1}$). A 350 nm longpass filter would therefore eliminate this Raman scattering.

1.7 Fluorescence

The components of pollen and spores (exine, intine and protoplast) all fluoresce to some degree, although the exine shows exceptionally high levels of fluorescence. Inspecting pollen and spores using a LSCM gives details of fluorescent structures. Analysis by spectrofluorometry can provide information about the fluorescent molecules present and their various interactions in a more quantitative fashion than LSCM.

1.7.1 Basic theory of fluorescence

Fluorescence occurs when a fluorochrome (a fluorescent molecule) absorbs light and re-emits light at a longer wavelength (i.e. at lower energy). This process can be explained by means of a simplified Jablonski diagram, which represents the quantised electronic states within a molecule and their associated vibrational fine structure (Figure 1.27). In

the first step, a molecule absorbs a photon that has sufficient energy to promote an electron from its ground state (usually the highest occupied molecular orbital (HOMO)) to an excited state (usually the lowest unoccupied molecular orbital (LUMO)). The electron then drops down to the lowest vibrational energy level within the excited state in a process termed vibrational relaxation, which is a radiationless transition that does not emit energy to its surroundings. Light is then emitted as the electron drops from this level back to the ground state. The emission of light is known as fluorescence.

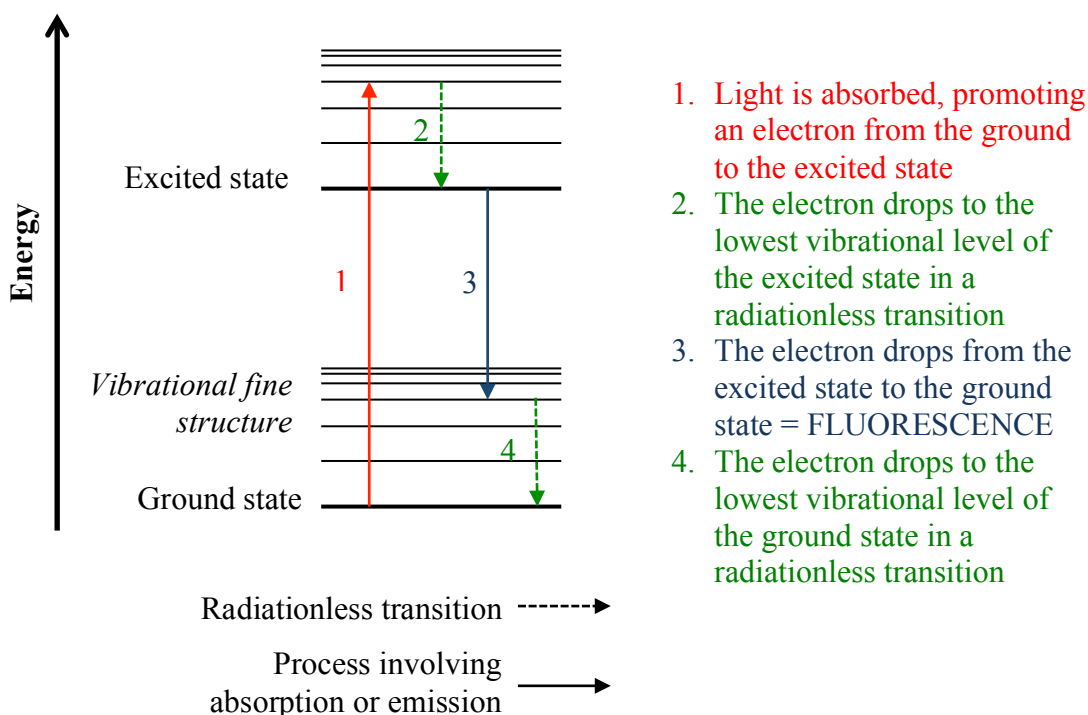


Figure 1.27: Simplified Jablonski diagram representing fluorescence processes

The energy of the light absorbed must be greater than or equal to the energy difference between the ground and excited states. The energy of light emitted is lower than that of the absorbed light. The absorption and emission wavelengths of the fluorochrome are influenced by its structure, as well as its local surroundings; for example, solvent, pH, concentration, crystal structure and other local fluorochromes.⁹⁷ Although fluorochromes vary widely in structure, they almost always possess a high degree of conjugation (alternating single and multiple bonds).

1.7.2 Measurement of fluorescence in pollen and spores

The fluorescence of a range of pollen and spores has been studied, primarily with the aim of furthering the understanding of their internal structures and chemical composition. Almost all species demonstrate a broad autofluorescence (natural fluorescence produced without the addition of fluorochromes) emission spectrum, from about 350 – 700 nm, with peak emission occurring around 460 – 600 nm.⁵⁰ The emission and excitation spectra of a range of pollen and spores were collected for aerobiological research: a maximum of around 400 nm was generally observed, with some species showing broader bands between 500 – 700 nm (Figure 1.28).⁹⁹ Recent work by Sodeau *et al.* analysed the fluorescence emission of several taxonomic orders of pollen (Poales, Fagales, Pinales, Rosales) and spores (Capnodiales and Eurotiales).⁹⁵ The authors found that pollen species within the same order displayed similar emission profiles, but that emission varied sufficiently for individual species to be distinguished.

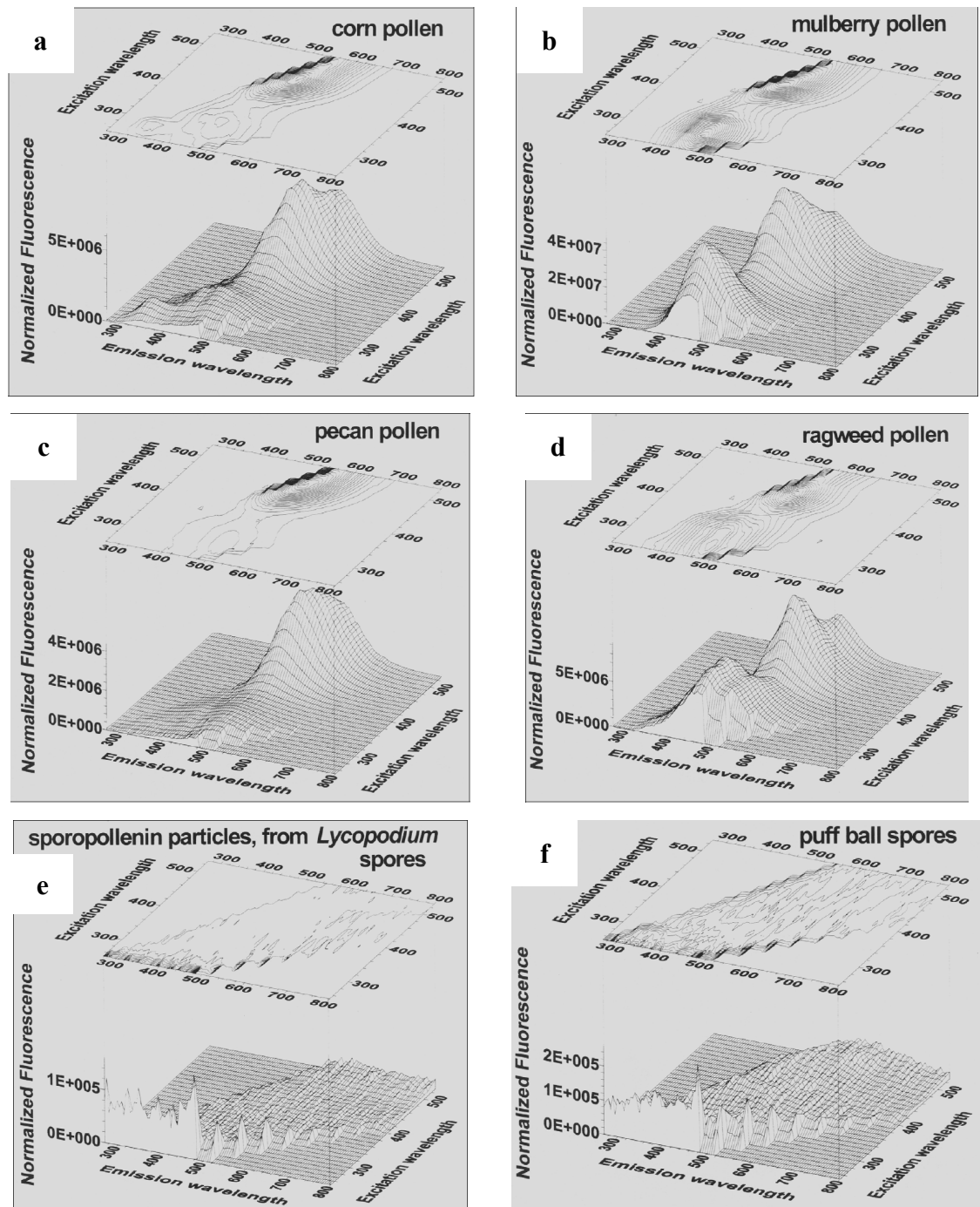


Figure 1.28: Excitation and emission spectra of (a) corn pollen; (b) mulberry pollen; (c) pecan pollen; (d) ragweed pollen; (e) sporopollenin particles from *Lycopodium* spores; and (f) puff ball spores⁹⁹

Identifying the source of particular bands within fluorescence emission spectra is challenging due to the large number of components present in pollen and spores that fluoresce. Emission patterns vary between individual pollen grains or spores from identical species, as each may contain slightly different amounts of fluorescent material.⁴⁸ The contents and chemical composition of spores and pollen vary during their lifetimes, causing a change in emission.⁵⁰ Fluorescence analysis of *Lycopodium*

clavatum spores revealed that the application of various chemical treatments shifted the peak fluorescence emission wavelength. For example, treatment with 85 % phosphoric acid shifted peak emission from 498 – 510 nm to 548 – 558 nm (excitation wavelength 365 nm).⁵⁰

In their recent work, Sodeau *et al.* suggested the source of fluorescent peaks, but these assignment bands were broad (often 50 – 100 nm wide) (Table 1.2).⁹⁵ The fluorescence of each species should be considered individually to identify where specific peaks lie within these bands. Sporopollenin is the most highly fluorescent component of pollen and spores, but its exact chemical nature remains unknown (see 1.2.1). The authors have suggested that sporopollenin may have coumaric and ferulic acid components.³⁸ *p*-Coumaric acid shows peak emission at around 435 nm and ferulic acid at approximately 420 nm.^{100, 101} Therefore, if sporopollenin is considered to be composed - at least in part - of coumaric and ferulic acid monomer units, then emission around 250 - 350 nm could be attributed to sporopollenin.

Table 1.2: Summary of the possible sources of emission observed in pollen and spore fluorescence analysis⁹⁵

Fluorescence region / nm	Possible assignment
415 – 420	DNA, phenols and terpenoids
450 – 500	Nicotinamide adenine dinucleotide (NADH), nicotinamide adenine dinucleotide phosphate (NADPH), cellulose, folic acid, arachidonic terpenoids and flavonoids
500 - 600	Carotenoids, lipopigments and flavins
620 – 640	Azulenes
675 – 680	Chlorophyll-a

Recent work has involved measuring the autofluorescence of pollen and spores as part of a technique used to rapidly detect and quantify airborne allergens.⁴⁸ This method presents a more efficient alternative to traditional pollen traps that involve manual counting and identification of pollen and spores using a light microscope.¹⁰² The ratio of red to blue autofluorescence of a common species of pollen in Japan that causes allergies was measured.¹⁰³ The authors suggested this as a novel approach to quickly discriminate between species. Pollen and spore autofluorescence has also been widely

used to gauge how environmental conditions may have changed over geological time scales.¹⁰⁴ All of this work illustrates that pollen and spore fluorescence is well studied and that these particles show substantial autofluorescence that differs between species.

Recent work by Walt *et al.* described the use of *Escherichia coli* bacteria - genetically engineered to produce fluorescent proteins - in devices used to encode messages.¹⁰⁵ Pollen and spores have the potential to be used as autofluorescent particles in similar messaging devices, where small differences in fluorescence could be measured and used to impart encoded information. An array of different fluorescent particles could be produced if commercially available fluorochromes were to be encapsulated inside microcapsules synthesised from pollen and spores (see section 1.4).

Chapter 2:

Aims of the project

2 Aims of the project

Pollen and spores both have outer walls composed of sporopollenin. The structure of this organic biopolymer is complex and varies between species, and its exact structure is yet to be elucidated. It possesses many desirable material properties, including chemical and physical resilience; shielding of UV radiation; flexibility; and selective permeability. Work has been published that indicates that all non-sporopollenin material can be removed from *Lycopodium clavatum* (club moss) spores to produce hollow exine microcapsules.^{57, 58} These microcapsules have been filled with a range of materials, including edible oils, pharmaceuticals, yeasts, enzymes and MRI contrast agents. However, to date, no reports of pollen grains being used as microcapsules appear to have been published.

The most widely published method used to produce microcapsules from *Lycopodium clavatum* spores involves solvents, bases and acids to both digest non-sporopollenin components and wash them out of the spores. Researchers suggest that this method is also applicable to pollen. This thesis aims to fully evaluate the effect of that published protocol on *Lycopodium clavatum*. Using transmission electron microscopy and scanning electron microscopy, the intention is to investigate to what extent the non-sporopollenin components of the spore are removed. In order to determine the suitability of this method for pollen, the process will be applied to *Juglans nigra* (black walnut), *Betula fontinalis* (water birch) and *Secale cereale* (rye) pollen and the products inspected.

Methods have been published that describe the removal of non-sporopollenin material from pollen and spores, with the primary aim of preparing sporopollenin for analysis, rather than for creating microcapsules. These methods include acetolysis and treatments involving enzymes, and will be applied to *Lycopodium clavatum* spores and *Secale cereale*, *Juglans nigra* and *Betula fontinalis* pollen. The products of these methods will be compared to those produced from base and acid treatments.

Pollen and spores are known to autofluoresce, with sporopollenin demonstrating the most intense autofluorescence of all components, with peak emission at around 470 nm. The fluorescence of untreated pollen and spores will be measured *via*

spectrofluorometry. In order to confirm the location of fluorescent components within spores and pollen grains, these particles will be inspected using laser scanning confocal microscopy (LSCM). The effect of base and acid treatments on the fluorescence of spores, and enzyme treatments on the fluorescence of pollen, will also be evaluated.

Rhodamine B (RhB) is a well-studied fluorescent dye (Figure 2.1), which, when prepared as an aqueous or ethanolic solution, emits intensely at around 600 nm. Untreated *Lycopodium clavatum* spores and untreated and enzyme-treated *Betula fontinalis* pollen will be treated with both aqueous and ethanolic solutions of RhB. The concentrations of the solutions applied will be varied. The fluorescence of solid samples produced will be measured using both spectrofluorometry and LSCM. As RhB and sporopollenin emit in different regions of the spectrum, it will be possible to measure the emission of these fluorochromes independently. In addition, as the emission spectrum of sporopollenin overlaps the absorption spectrum of RhB, these fluorochromes are likely to interact, and this potential interaction will be evaluated. By varying the solvent and concentration of the RhB solutions used, further information is expected to be gleaned regarding the emission of both RhB and pollen and spores.

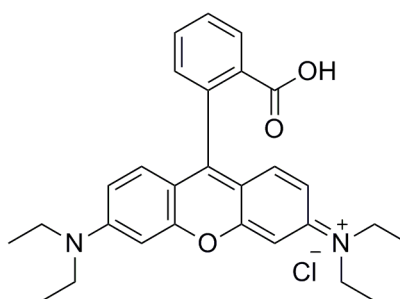


Figure 2.1: Structure of Rhodamine B

The fluorochromes *p*-coumaric acid and ferulic acid have been proposed as constituents of sporopollenin (Figure 2.2). They have been used to predict the effects of changing atmospheric conditions and solar radiation on pollen and spores. The fluorescence of solutions of these fluorochromes will be measured using spectrofluorometry and compared to that of pollen and spores to evaluate their suitability to mimic sporopollenin. RhB will be added to solutions of *p*-coumaric acid and ferulic acid to determine whether they show similar shifts in fluorescence compared to pollen and spores treated with RhB. This will provide further evidence regarding their suitability as materials to simulate sporopollenin.

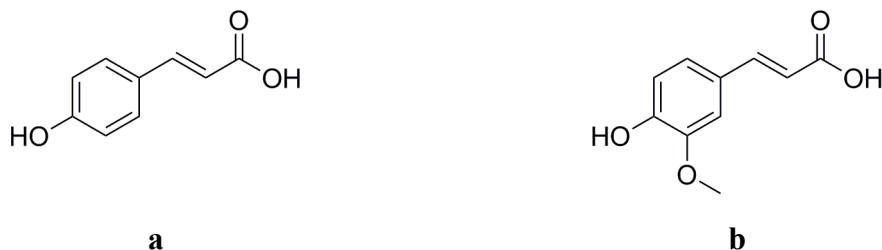


Figure 2.2: Structures of (a) *p*-coumaric acid and (b) ferulic acid

Published work reports that base and acid treated *Lycopodium clavatum* spores have been successfully filled with yeast cells. In order to determine whether pollen also can be filled with biological organisms, enzyme-treated *Betula fontinalis* pollen will be treated with yogurt cultures containing bacteria. Treated pollen will be inspected using light microscopy to detect the presence or absence of bacteria inside the cavity of the pollen grains.

By evaluating the properties of pollen and spores exposed to the treatments described here, it should be possible to gain further insight into their suitability as microcapsules. In particular, pollen may come to be used as a microcapsule for the first time. By adding the fluorescent dye RhB to pollen and spores, more information should be gleaned regarding their autofluorescence and how their interaction with RhB influences the emission from sporopollenin, as well as from RhB. Only a limited number of species will be studied here due to the time available for study. Species were selected to reflect a range of genera, as it was predicted that these would possess different chemistry, and are known to exhibit different morphologies. A much wider range of species is available for purchase and other species would be expected to display different properties to the species studied here.

Chapter 3:

Emptying pollen and spores

3 Emptying pollen and spores

3.1 Introduction

A wide variety of materials have been encapsulated in microcapsules produced from spores.^{74, 80} To date, there is no published research on the use of pollen as microcapsules, although pollen and spores share many structural and chemical similarities.¹⁰⁶ In order to produce microcapsules from spores and pollen, any allergenic components should first be removed in order to prevent allergic reactions in humans exposed to such microcapsules.² The microcapsules produced should not be damaged or cracked to ensure that there is no leakage or uncontrolled release of the encapsulated materials. Many applications for microcapsules, e.g. pharmaceuticals, cosmetics and displays, require microcapsules that are close to white in colour. Techniques applied to produce microcapsules should therefore ideally give light-coloured products, as close to white in colour as possible. Published methods evaluated in this chapter include acetolysis, base and acid treatments, and treatments involving enzymes.

3.2 Analysis of untreated pollen and spores

In order to analyse the effects of treatments used to empty pollen and spores, it was necessary to evaluate untreated pollen and spores. Light microscopy was used to inspect the general shape of spores and pollen grains, and to determine whether they were intact. Light micrographs collected throughout this thesis were collected using different light microscope settings, meaning that the brightness and background colour of micrographs varied. Scanning electron microscopy (SEM) provided greater detail about surface morphology and ornamentation. Transmission electron microscopy (TEM) was used to inspect sections of untreated pollen and spores, in order to evaluate both their contents and wall structure. Fluorescent components, and details such as pores, were highlighted using laser scanning confocal microscopy (LSCM).

3.2.1 *Lycopodium clavatum* spores

Untreated *Lycopodium clavatum* spores were suspended in water and inspected using light microscopy (Figure 3.1). However, as these spores are particularly opaque, light microscopy provides little information. Spores were examined using SEM (Figure 3.2), which shows that the spores are almost monodisperse in size and that most are intact. The distal face of the spore is covered with muri that surround lumina (Figure 3.2 (b) and (d)). A murus is a ridge on the surface of a spore or pollen grain, which surrounds the space referred to as the lumen. The walls of the muri contain ‘bridges’ and ‘windows’. The proximal face also has muri and lumina, but is dominated by a trilete scar, formed from three laesura (Figure 3.2 (c)). Each spore is approximately 25 μm in diameter.

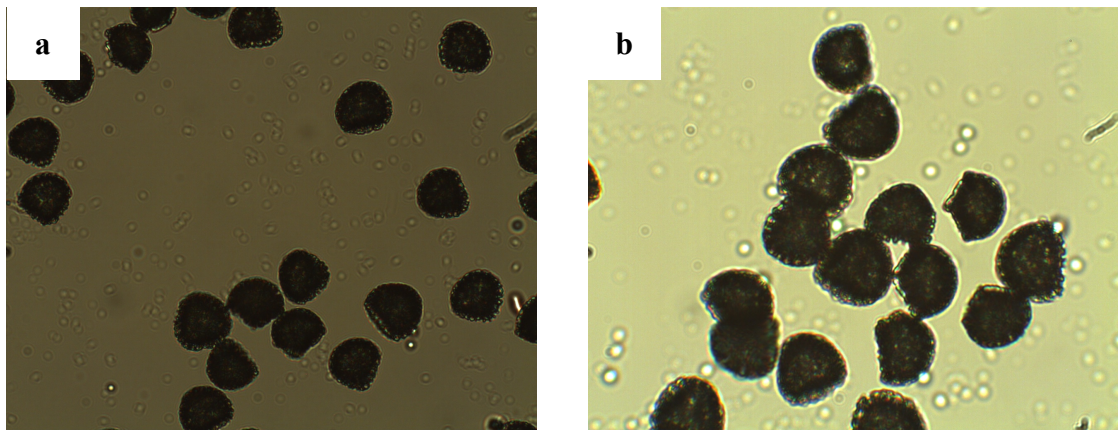


Figure 3.1: Light micrographs of untreated *Lycopodium clavatum* spores ((a) $\times 200$ and (b) $\times 400$ magnification)

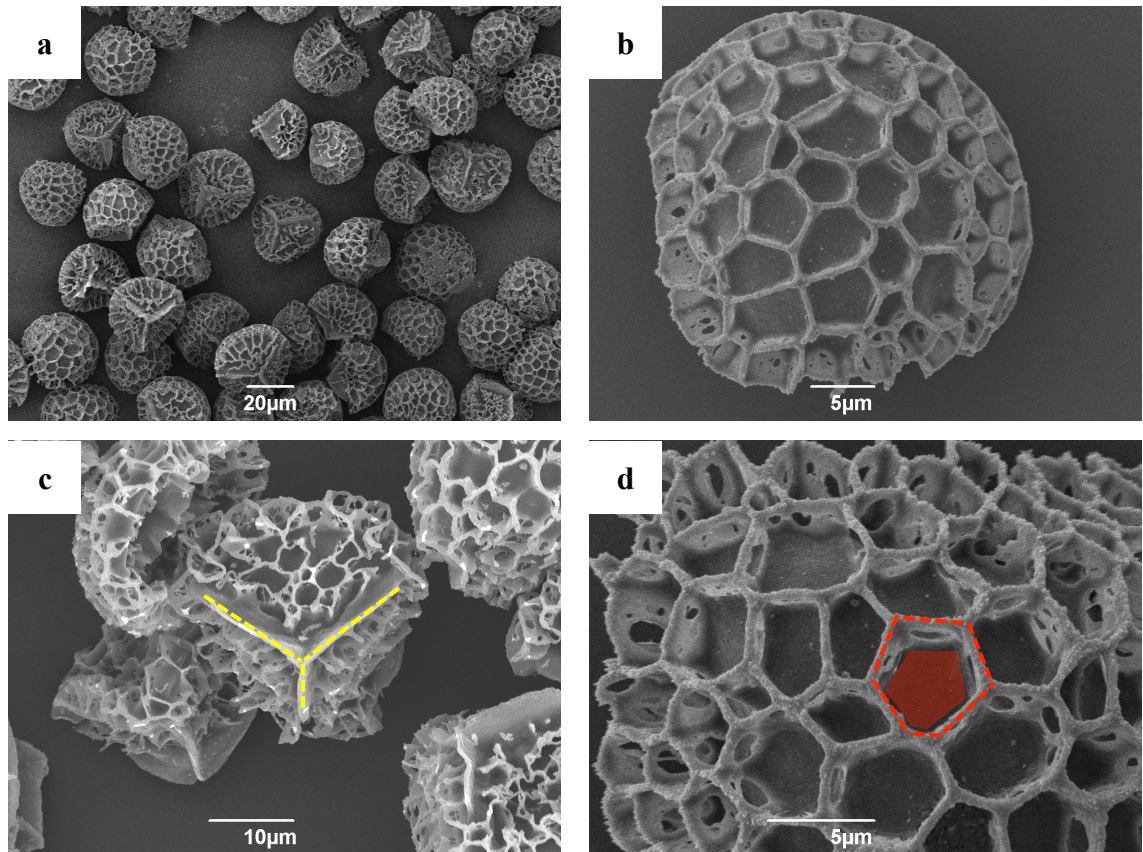


Figure 3.2: Scanning electron micrographs of untreated *Lycopodium clavatum* spores: (a) low magnification image; (b) distal face of spore; (c) proximal face of spore with three laesura forming a trilete scar, highlighted by broken yellow lines; and (d) high magnification image with a murus highlighted by a broken red line and a lumen shaded in red

Lycopodium clavatum spores were inspected using TEM. Identification of surface features was aided by a paper by Uehara and Kurita.¹⁰⁷ The appearance of the spores' distal and proximal faces (Figure 3.3 (a)) is determined by the development of the spores within tetrads. The plasma membrane encloses the nucleus, lipid bodies and other cellular structures (Figure 3.3 (b) and (c)), not all of which are observable in the cross-sections presented here. The wall of the spore is made up of an exospore and an endospore (Figure 3.3 (d) and (e)). The exospore possesses an obvious granular component – the exospore granular layer. The exospore is laminated in places (Figure 3.3 (f), (g) and (h)). Although nano-channels that pass through the walls of spores have been reported in other species from the *Lycopodium* genus, they are not present in the sections presented here.¹⁸

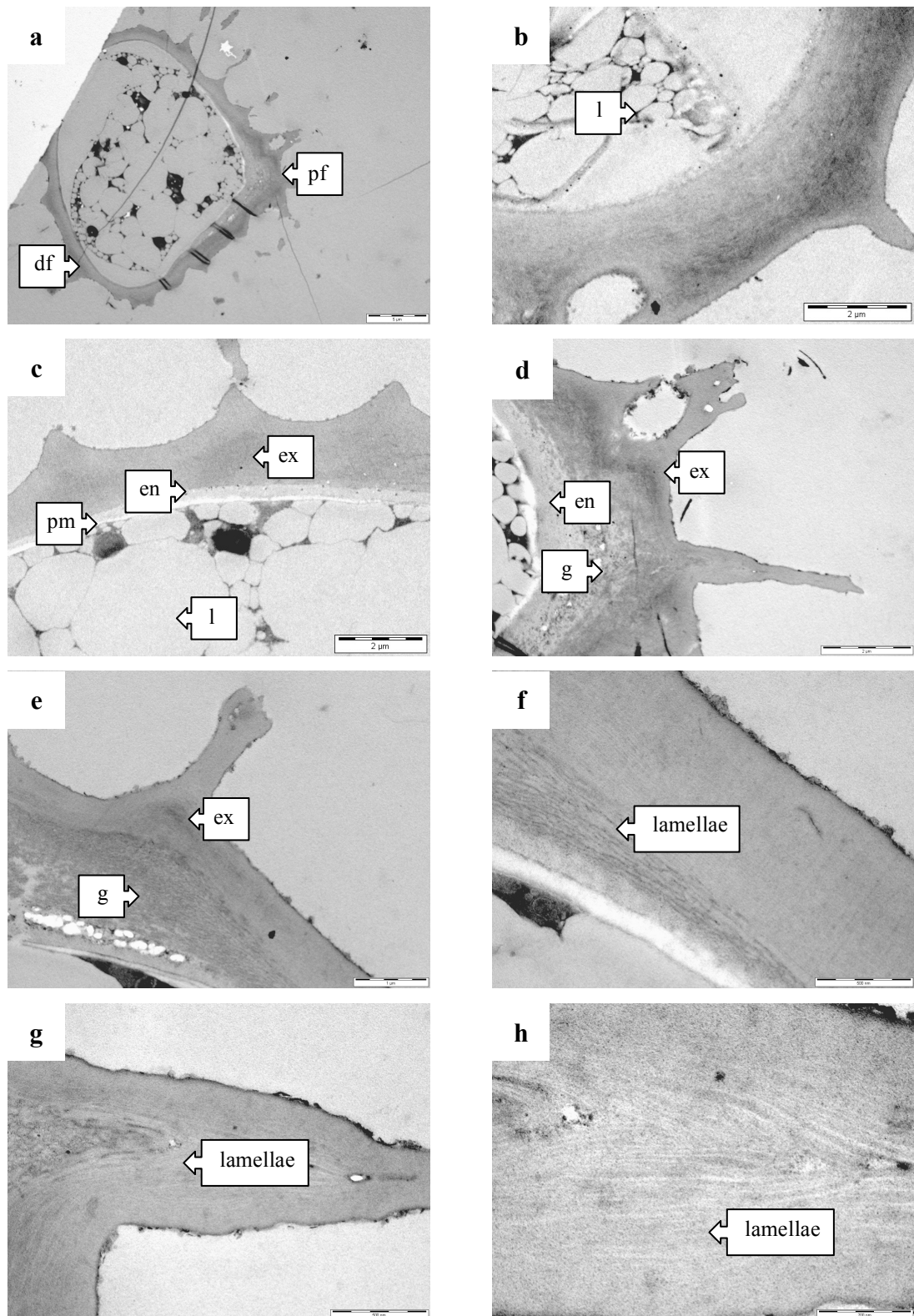


Figure 3.3: Transmission electron micrographs of untreated *Lycopodium clavatum* spores.

Scale bar (a) = 5 μm ; (b) = 2 μm ; (c) = 2 μm ; (d) = 2 μm ; (e) = 1 μm ; (f) = 500 nm;

(g) = 500 nm; and (h) = 200 nm

df = distal face; en = endospore; ex = exospore; g = exospore granular layer;

l = lipid body; pf = proximal face ; and pm = plasma membrane

3.2.2 *Secale cereale* pollen

Light microscopy of *Secale cereale* pollen shows that grains are translucent under illumination, but little can be discerned about their morphology (Figure 3.4). SEM analysis was therefore performed (Figure 3.5). Each grain is approximately 50 μm from pole to pole (along its longest axis), although many grains are shrunken and deformed (Figure 3.5 (a)). This is because SEM requires samples to be dry and grains are therefore observed in their dehydrated state. Each grain has a single pore surrounded by a thickened ‘donut’ region, known as an annulus (Figure 3.5 (b), (c) and (d)).¹¹ The literature suggests that each pore should be filled with a discrete plug of exine material known as an operculum.¹⁰⁸ However, the pollen examined here appears to be missing these opercula. The surface of *Secale cereale* pollen grains are described as having microechinate ornamentation, meaning that the pollen’s surface is covered in spines or points, each less than 1 μm in height or width.^{108, 109}

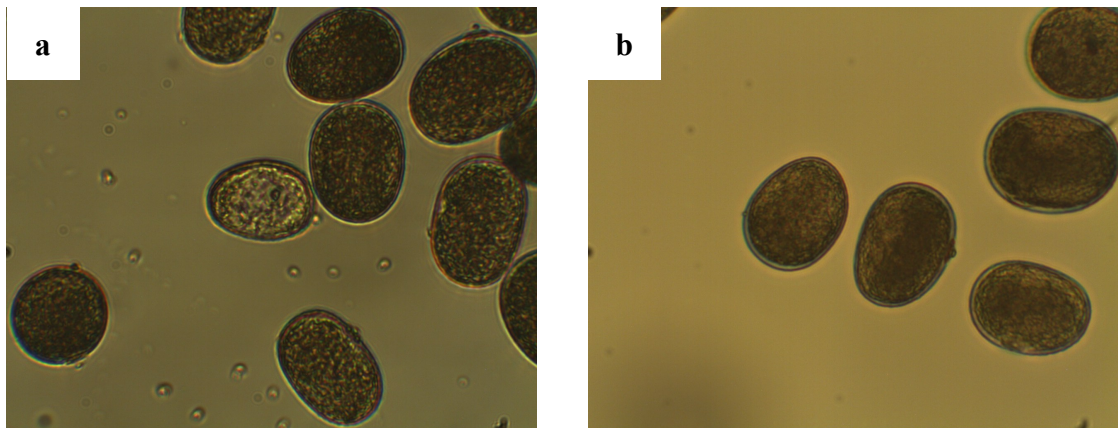


Figure 3.4: Light micrographs of untreated *Secale cereale* pollen ((a) and (b) \times 400 magnification)

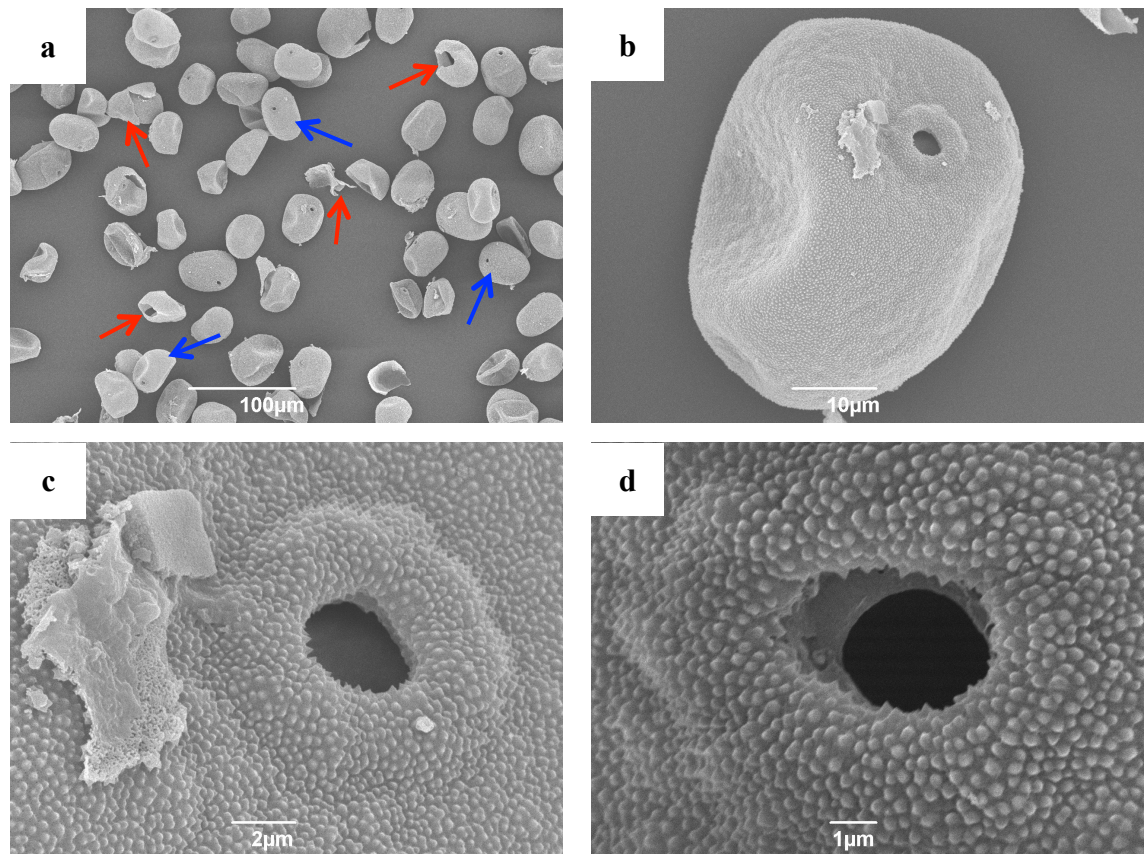


Figure 3.5: Scanning electron micrographs of untreated *Secale cereale* pollen:
 (a) low magnification image demonstrating a range of both intact and cracked grains (highlighted by blue and red arrows respectively); (b) higher magnification image of a slightly collapsed single grain, as indicated by the indents in opposite faces; (c) and (d) high magnification images of the single pores of two different grains, each surrounded by an annulus. *Secale cereale*'s microechinate surface ornamentation is also clear in (c) and (d)

Secale cereale pollen was examined using TEM (Figure 3.6). Transmission electron micrographs show a columellate exine composed of a foot layer, infratectum and tectum with an intine layer also present (Figure 3.6 (a) and (b)).¹¹⁰ The literature claims that the protoplast contains starch grains and polysaccharide vesicles, although these were not identified in the sections here.¹⁰⁸ Nano-channels traverse the entire exine wall (Figure 3.6 (c), (d) and (e)).

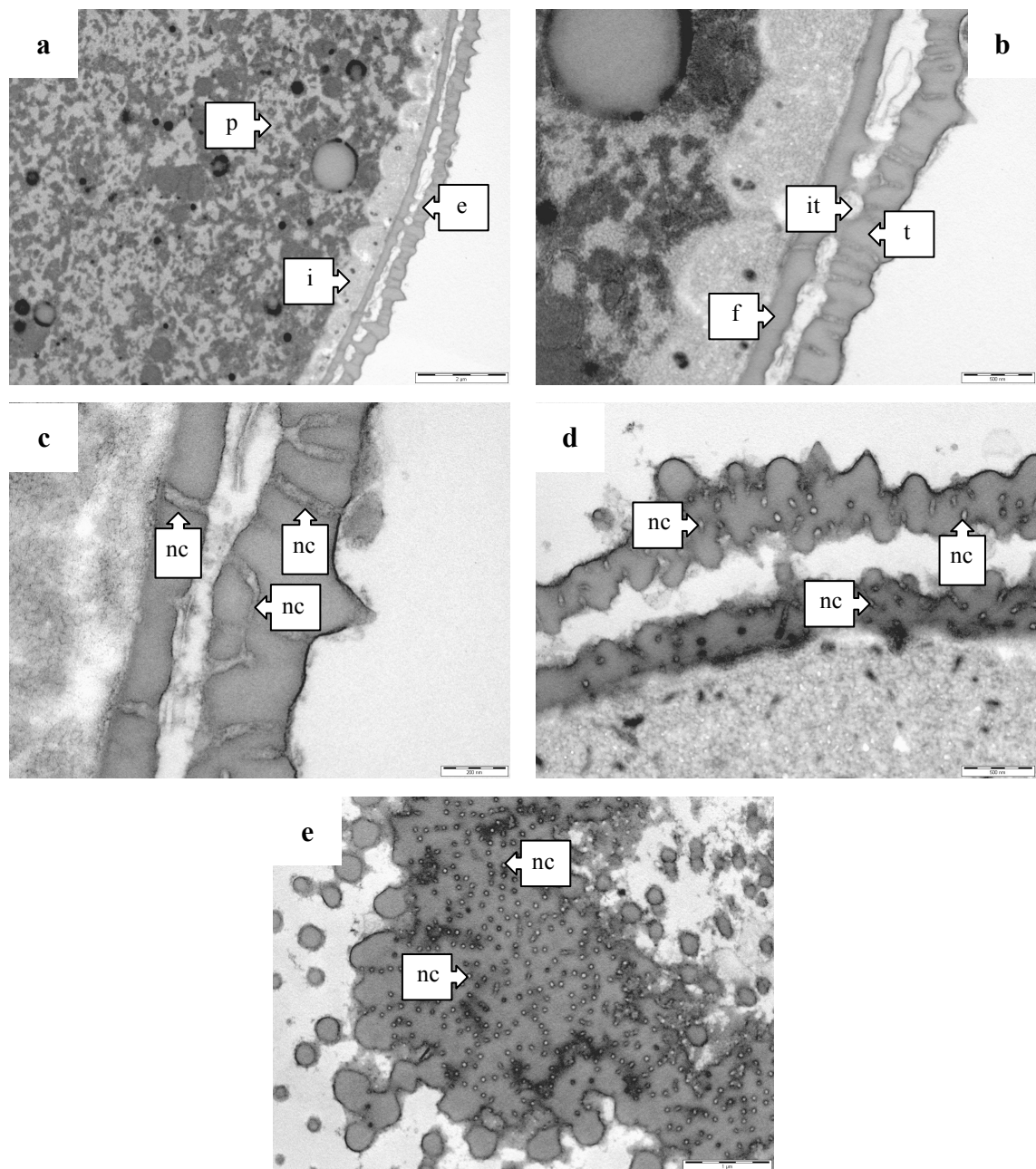


Figure 3.6: Transmission electron micrographs of untreated *Secale cereale* pollen.

Scale bars: (a) = 2 μm ; (b) = 500 nm; (c) = 200 nm; (d) = 500 nm; and (e) = 1 μm

e = exine; f = foot layer i = intine; it = infratectum; nc = nano-channel p = protoplast;
and t = tectum

3.2.3 *Juglans nigra* pollen

Juglans nigra pollen appears translucent under the light microscope (Figure 3.7). Most grains are translucent, but a minority of grains are almost transparent, indicating the lack of a protoplast. These transparent grains enable the many pores of *Juglans nigra* pollen to be easily observed (see Figure 3.7 (b)).

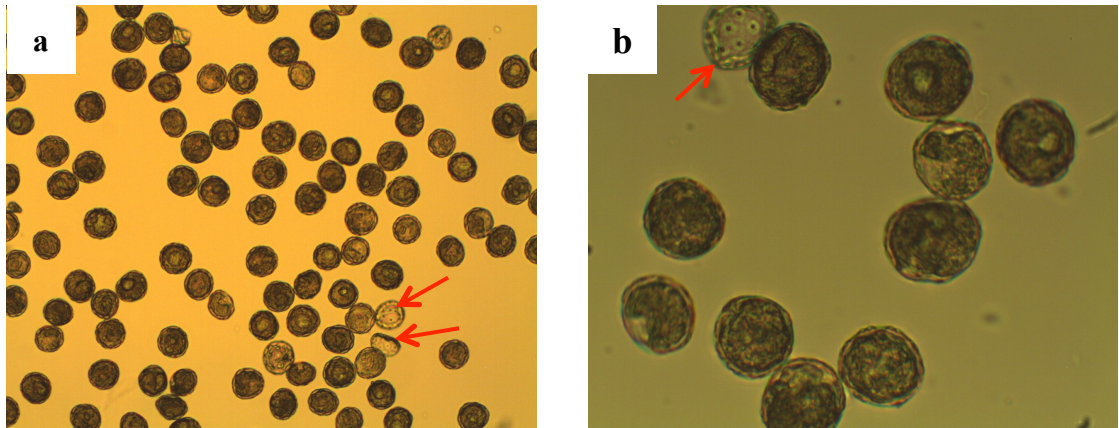


Figure 3.7: Light micrographs of untreated *Juglans nigra* pollen ((a) $\times 100$ and (b) $\times 400$ magnification)

Red arrows = transparent grains that appear to contain no protoplast material

SEM of *Juglans nigra* pollen was carried out to glean further information about its morphology (Figure 3.8). These dehydrated grains largely appear squashed or cup-shaped (Figure 3.8 (a)), and only a few grains are observed in their more hydrated state (Figure 3.8 (b) and (c)). Each grain is approximately 30 μm in diameter. Similarly to *Secale cereale*, *Juglans nigra* pollen possesses a microechinate exine. Each grain has numerous pores, distributed over its entire surface. As a result, pollen from *Juglans nigra* may be described as pantoaperturate.¹⁰⁹ These apertures do not contain opercula, but are covered by a membrane layer (Figure 3.8 (d)).¹¹¹

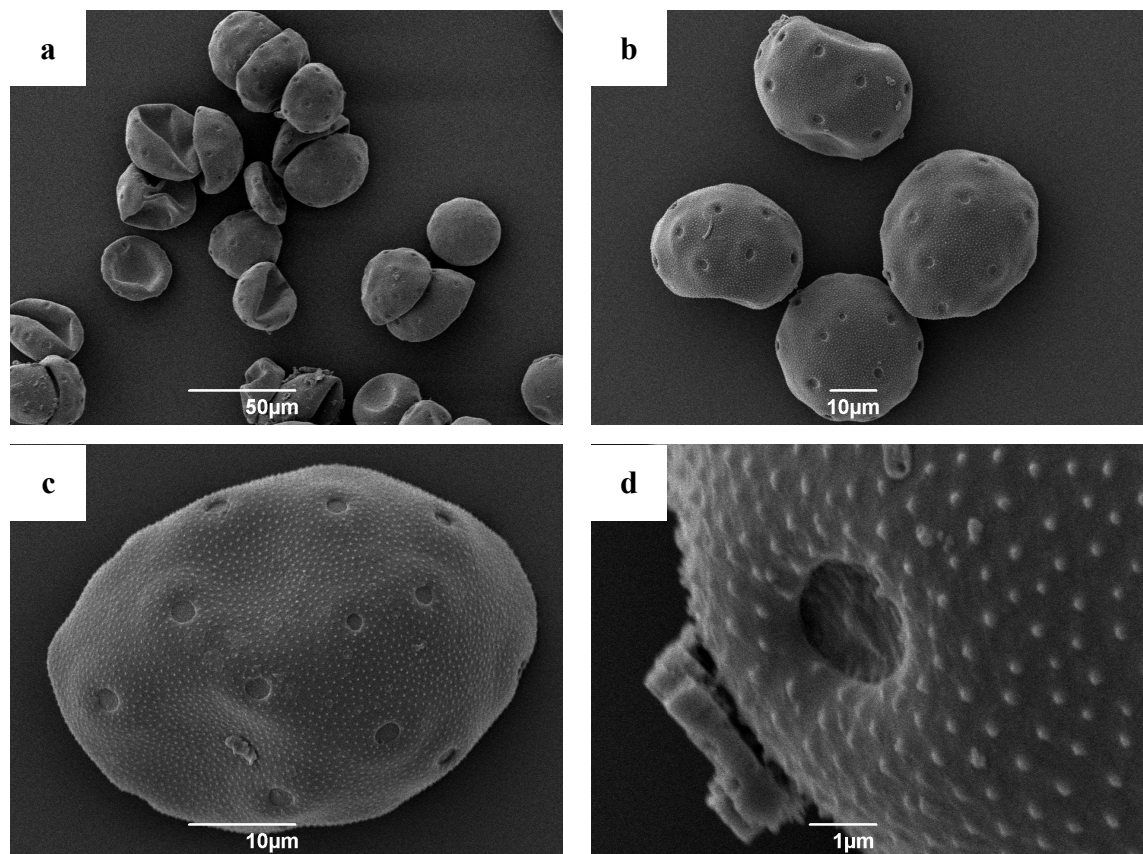


Figure 3.8: Scanning electron micrographs of untreated *Juglans nigra* pollen: (a) low magnification image of intact, but collapsed grains; (b) and (c) more hydrated grains with numerous pores obvious; and (d) high magnification image of a single pore, covered by a membrane layer. *Juglans nigra*'s microechinate surface ornamentation is also clear in (d)

TEM analysis indicates that when hydrated, *Juglans nigra* pollen grains have a circular outline (Figure 3.9 (a)). Published studies indicate that both starch grains and lipid droplets are present in the protoplasts of *Juglans nigra* pollen, although these could not be distinguished in the sections presented in Figure 3.9.¹¹² The exine is made up of a foot layer, infratectum and tectum (Figure 3.9 (b), (c) and (d)). The infratectum of a closely related species (*Juglans regia*) has been described as having a granular texture.¹¹ The infratectum of *Juglans nigra* is similar in appearance, indicating that it is also granular. Calzoni *et al.* described lamellar structures within the infratectum, although these could not be identified in the sections presented in Figure 3.9.¹¹² The intine lies beneath the foot layer, see (Figure 3.9 (a) and (b)). Underneath each aperture is an oncus – a thickened region that is not resistant to acetolysis (Figure 3.9 (a) and (e)).¹⁰⁹ Nano-channels pass through the tectum, but are not seen to traverse the foot layer in the sections presented here.

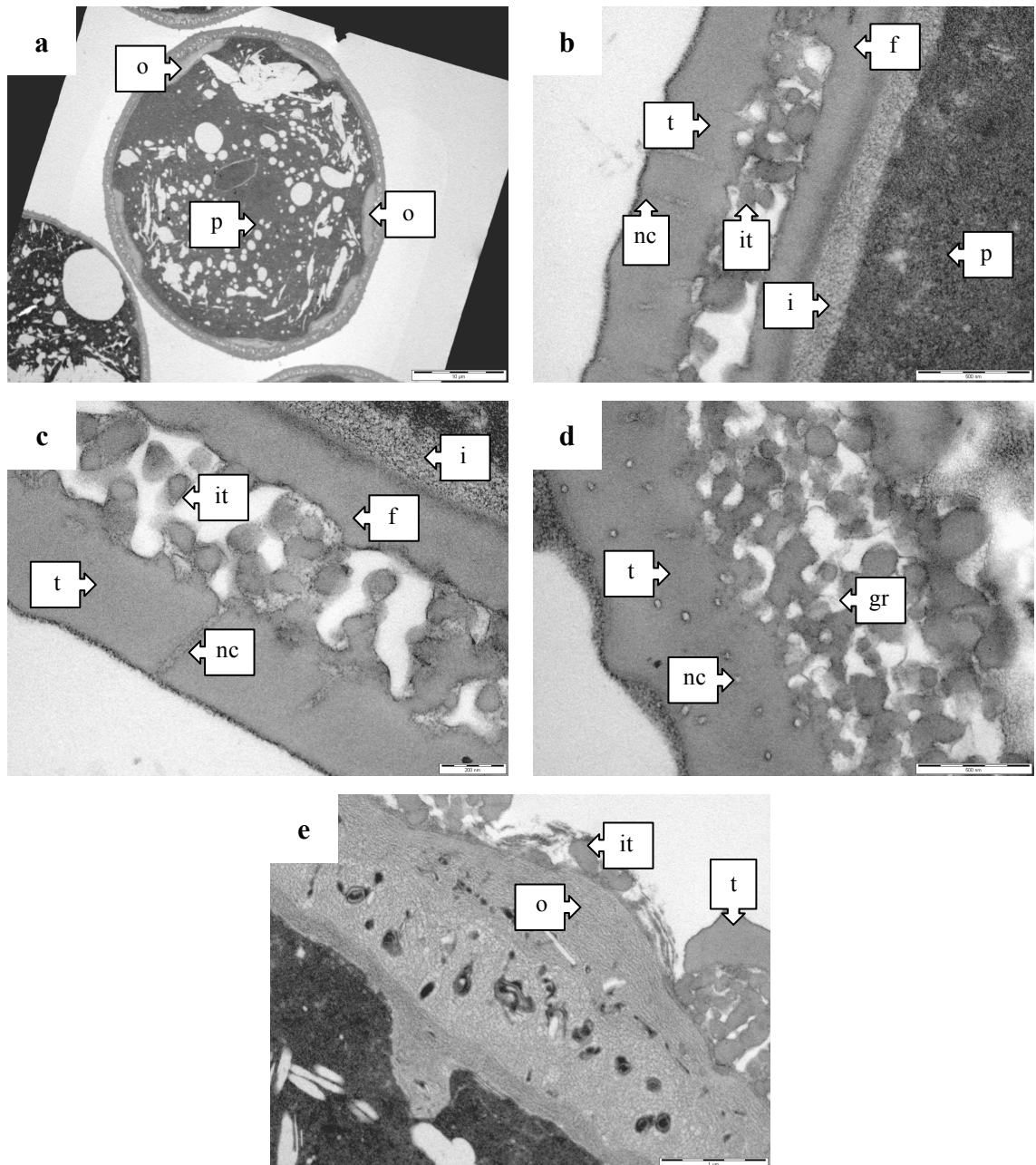


Figure 3.9: Transmission electron micrographs of untreated *Juglans nigra* pollen.

Scale bars: (a) = 10 μm ; (b) = 500 nm; (c) = 200 nm; (d) = 500 nm; and (e) = 1 μm

f = foot layer; gr = granular texture; i = intine; it = infratectum; nc = nano-channel;

o = oncus; p = protoplast; and t = tectum

3.2.4 *Ambrosia artemisiifolia* pollen

Light microscopy was used to inspect untreated *Ambrosia artemisiifolia* pollen (Figure 3.10). Grains have an almost spherical outline, however it is difficult to glean any

further information from these micrographs due to the heavily sculpted exine, making light microscopy challenging.

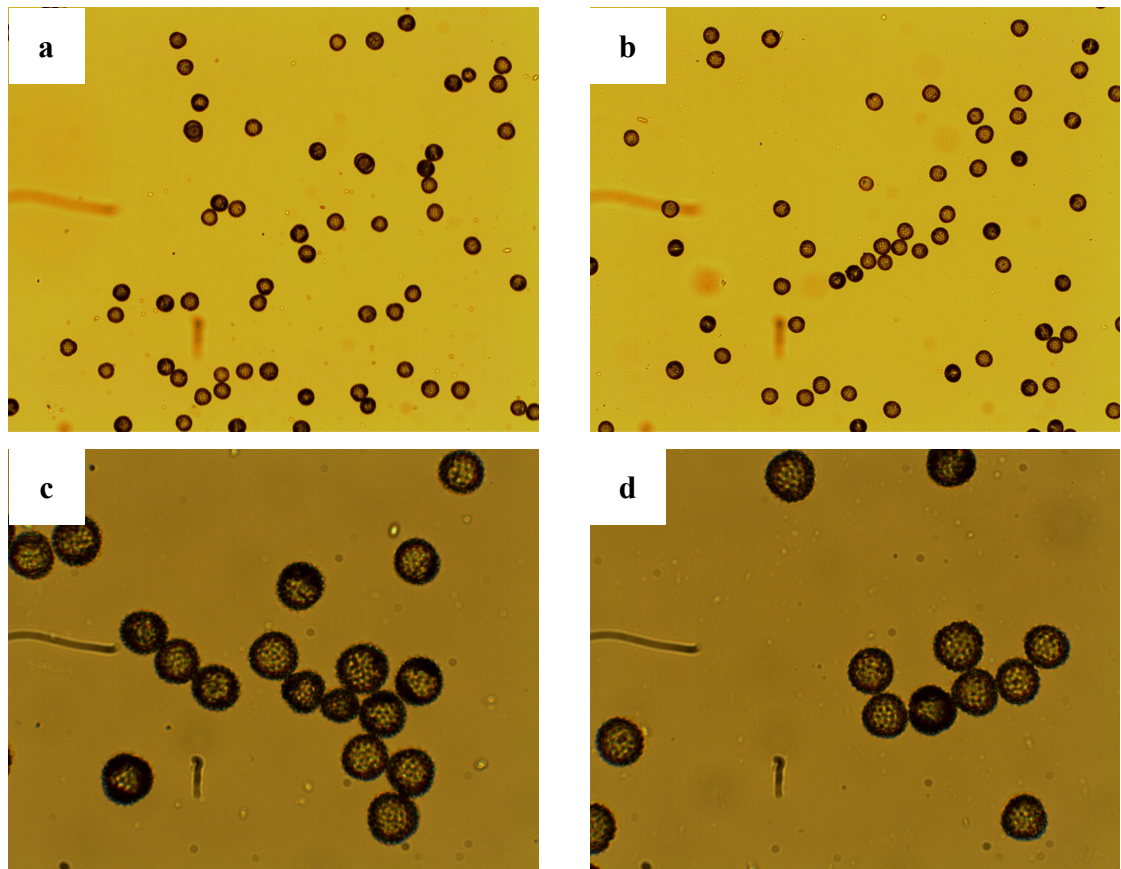


Figure 3.10: Light micrographs of untreated *Ambrosia artemisiifolia* pollen ((a) and (b) $\times 100$ magnification; (c) and (d) $\times 400$ magnification)

Ambrosia artemisiifolia pollen was analysed via SEM (Figure 3.11). Grains are well hydrated with clear, spherical outlines. Each grain is approximately 20 μm in diameter. Although *Ambrosia artemisiifolia* is triporate, only two pores are visible at any one time in these images due to their position within the grains (Figure 3.11 (b) and (c)).¹¹³ These pores are made up of several layers of the pollen wall, and are therefore described as being ‘brevicolporate’. Some pores also appear to be covered by a membrane (Figure 3.11 (d)), although it is not clear from these images what this membrane is formed from. The exine is echinate, meaning that its surface is made up of spines of more than 1 μm in length.¹⁰⁹ The tectum contains holes less than 1 μm in diameter, so is described as ‘perforate’ (Figure 3.11 (d)).

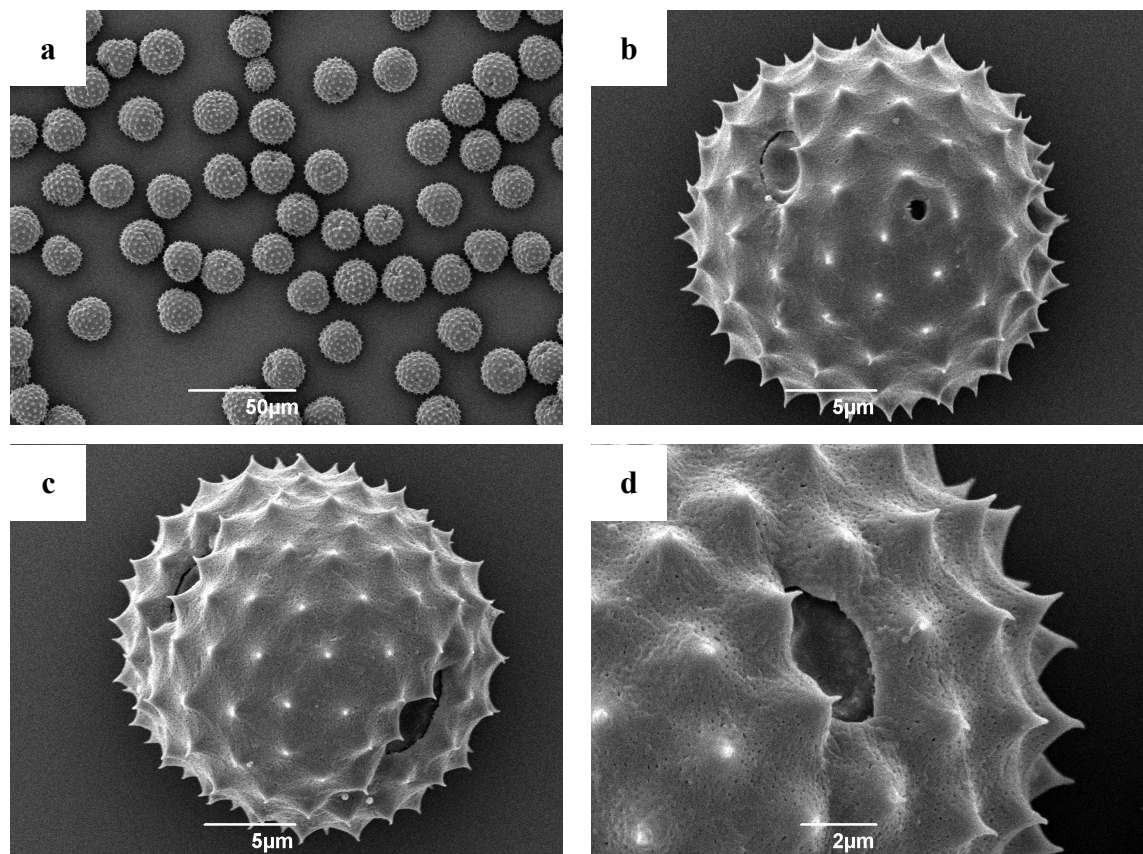


Figure 3.11: Scanning electron micrographs of untreated *Ambrosia artemisiifolia* pollen:

(a) low magnification image of well-hydrated grains; (b) & (c) higher magnification images of single grains, demonstrating their three pores; and (d) a high magnification image of a single pore. The echinate surface ornamentation of the exine is also clear in (b), (c) and (d).

TEM analysis of untreated *Ambrosia artemisiifolia* pollen was performed (Figure 3.12). When hydrated, grains have a spherical outline, and the tectum, infratectum, endexine, intine and protoplast can all be easily identified. *Ambrosia artemisiifolia* has a continuous tectum and a columellate infratectum. In literature, the endexine has been described as lamellar.¹¹³ However, this lamellar structure is not easy to make out in the sections presented in this thesis. In the TEM sections, a single aperture has been sectioned (Figure 3.12 (a) and (d)), and its membrane (as observed in an SEM image (Figure 3.11 (d)) can be made out. However, the composition of this membrane is not clear.

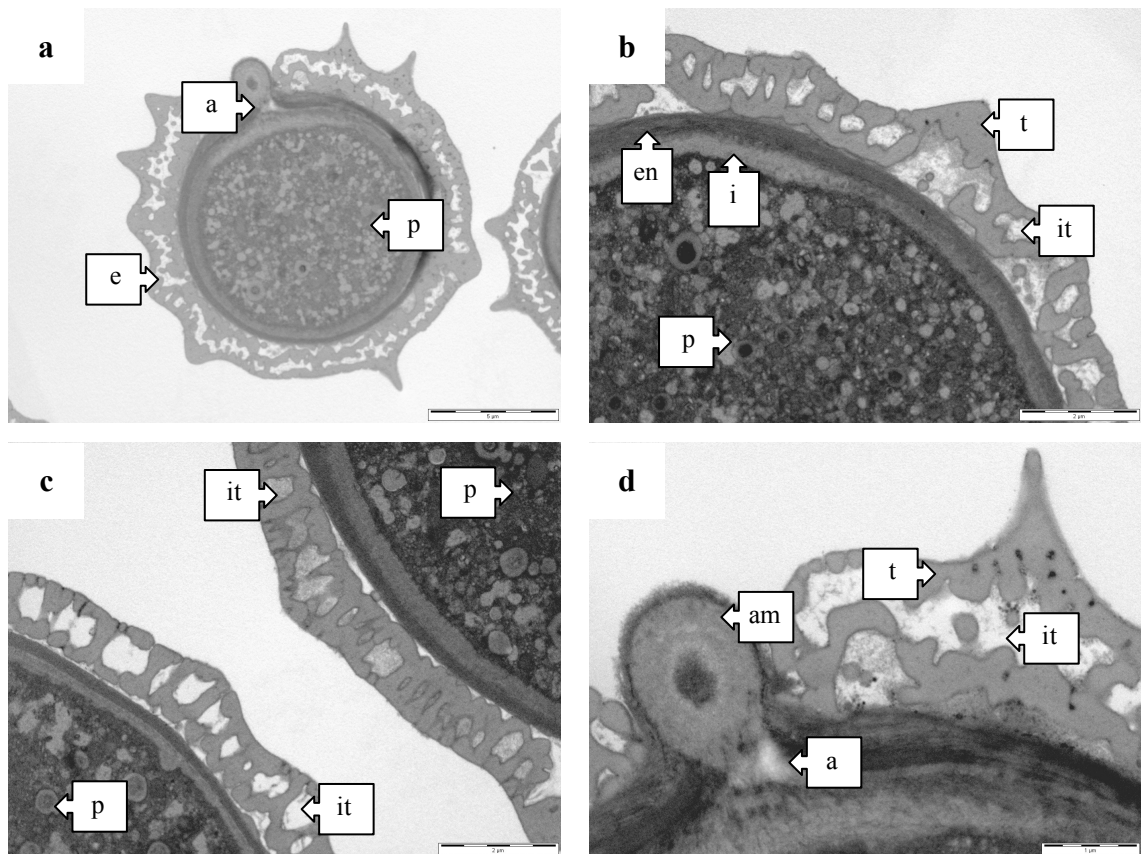


Figure 3.12: Transmission electron micrographs of untreated *Ambrosia artemisiifolia* pollen.

Scale bars: (a) = 5 μm ; (b) & (c) = 2 μm ; and (d) = 1 μm . a = aperture; am = aperture membrane; e = exine; en = endexine; i = intine; it = infratectum; p = protoplast; and t = tectum

3.2.5 *Betula fontinalis* pollen

Betula fontinalis pollen was inspected *via* light microscopy (Figure 3.13). Grains have an almost spherical outline and each grain has three pores, highlighted by red arrows in Figure 3.13 (b). The amount of protoplast within these regions is less than in the remainder of the grain. As grains are almost opaque, SEM and TEM were required to provide more information on structure and morphology.

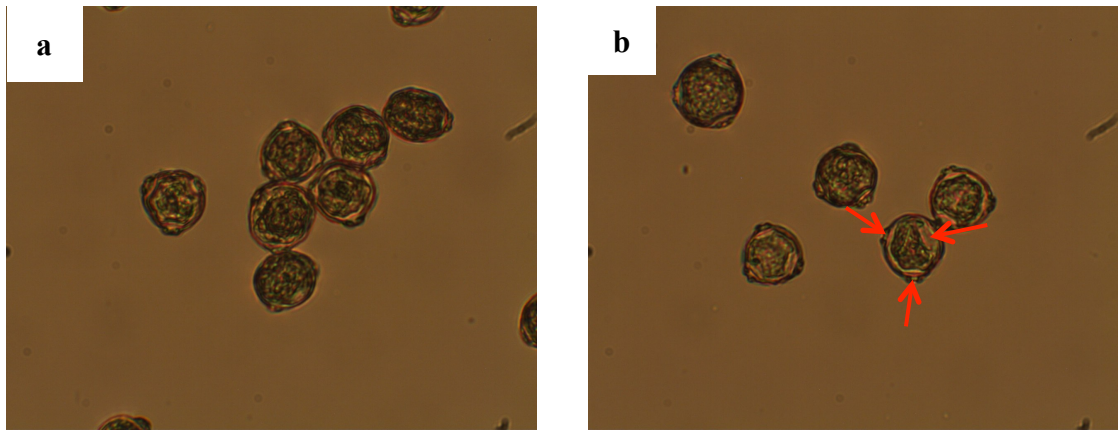


Figure 3.13: Light micrographs of untreated *Betula fontinalis* pollen ((a) and (b) $\times 400$ magnification)

Red arrows = decreased amount of protoplast material in the region of the pores

SEM analysis of dry grains shows that their outline is irregular when not hydrated (Figure 3.14), compared to a spherical outline when hydrated (Figure 3.13). Each grain is approximately 30 μm in diameter. The exine surfaces of closely related species (*Betula pendula* and *Betula humilis*) have been described as granular and rugulate, and are very similar to that of *Betula fontinalis* (Figure 3.14 (c) and (e)).^{114, 115} Each grain is triporate (has three pores) and each pore is surrounded by an annulus, but does not contain an operculum (Figure 3.14 (e)).¹¹⁶ In addition to single grains, tetrads are present (Figure 3.14 (b) and (d)). During pollen development, tetrads are formed from four immature pollen grains. In a tetrad, the exine wall is still being formed, which explains why the surface morphology of the tetrad grains appear different to mature grains within the sample.¹¹

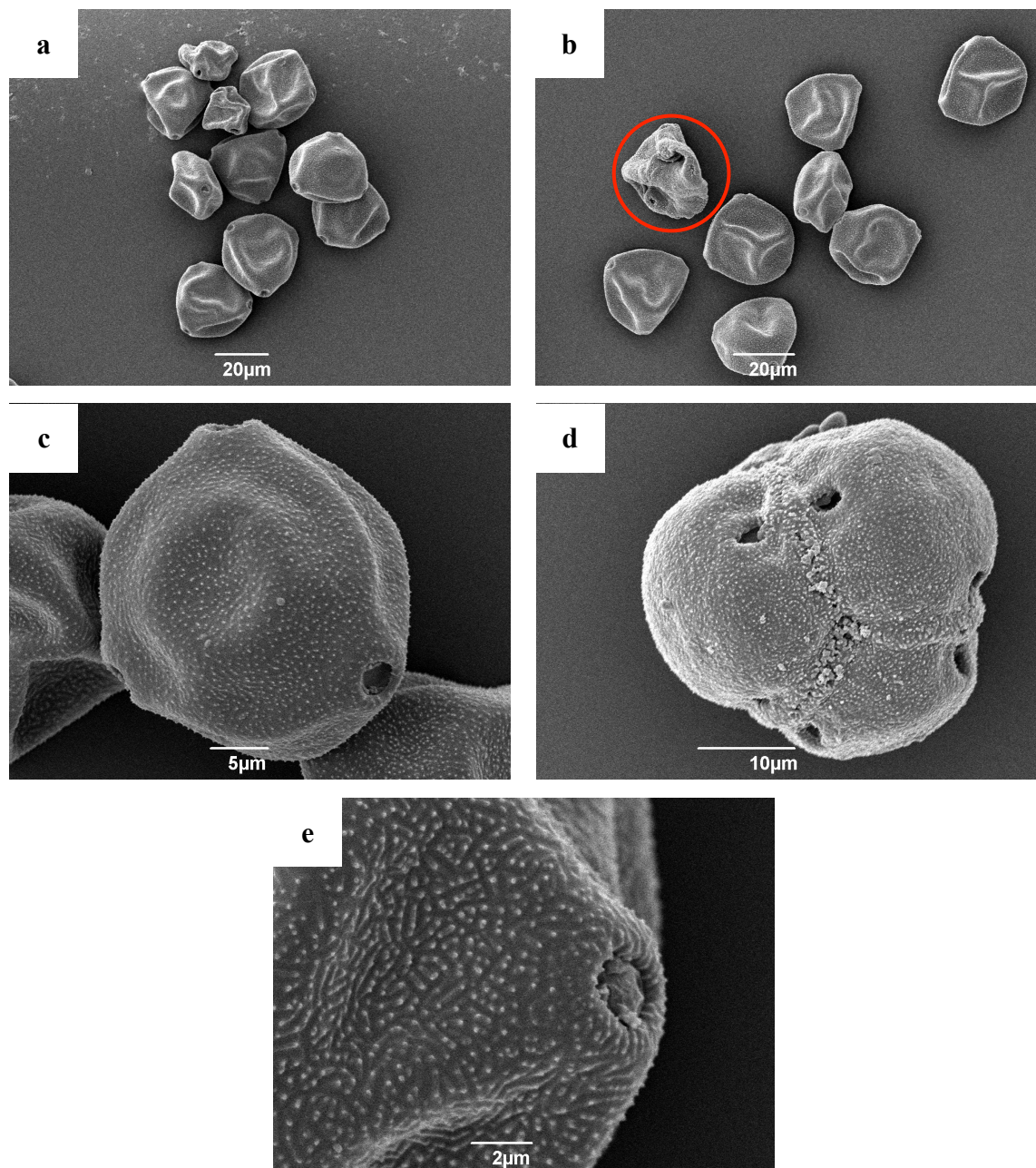


Figure 3.14: Scanning electron micrographs of untreated *Betula fontinalis* pollen: (a) and (b) low magnification images of collapsed grains, with a tetrad highlighted by a red circle; (c) a higher magnification image of a single, hydrated grain, with its three pores visible; (d) a tetrad of immature grains; and (e) a high magnification image of a single pore. *Betula fontinalis*' granular, regulate exine is also clear in (c) and (e).

Palynological analysis of closely-related species (*Betula pendula* and *Betula humilis*) has previously been published, and the TEM analysis of *Betula fontinalis* in this thesis is based on this work.^{114, 115} TEM highlights the pores present within *Betula fontinalis* and the onci that lie beneath each pore (Figure 3.15 (a), (b) and (c)). The protoplasts of *Betula pendula* and *Betula humilis* contain starch grains, and although these are also

likely to be present in *Betula fontinalis*, these grains could not be distinguished in the sections presented here. The exine is composed of the tectum, infratectum and foot layer, with the tectum having a columellate structure (Figure 3.15 (c) and (d)). PalDat (an online palynological database) describes the tectum of *Betula pendula* and *Betula humilis* as being ‘very mighty’ and this also appears to be true of *Betula fontinalis*.¹¹⁴
¹¹⁵ The tectum is particularly thick ($\sim 0.5 \mu\text{m}$) compared to its foot layer ($\sim 0.25 \mu\text{m}$) and also to the tectum of other species studied e.g. *Secale cereale* ($\sim 0.3 \mu\text{m}$) (Figure 3.6) and *Juglans nigra* ($\sim 0.2 \mu\text{m}$) (Figure 3.9). Nano-channels pass through the tectum of *Betula fontinalis* (Figure 3.15 (d)), but in the sections presented here, they do not appear to pass through the foot layer.

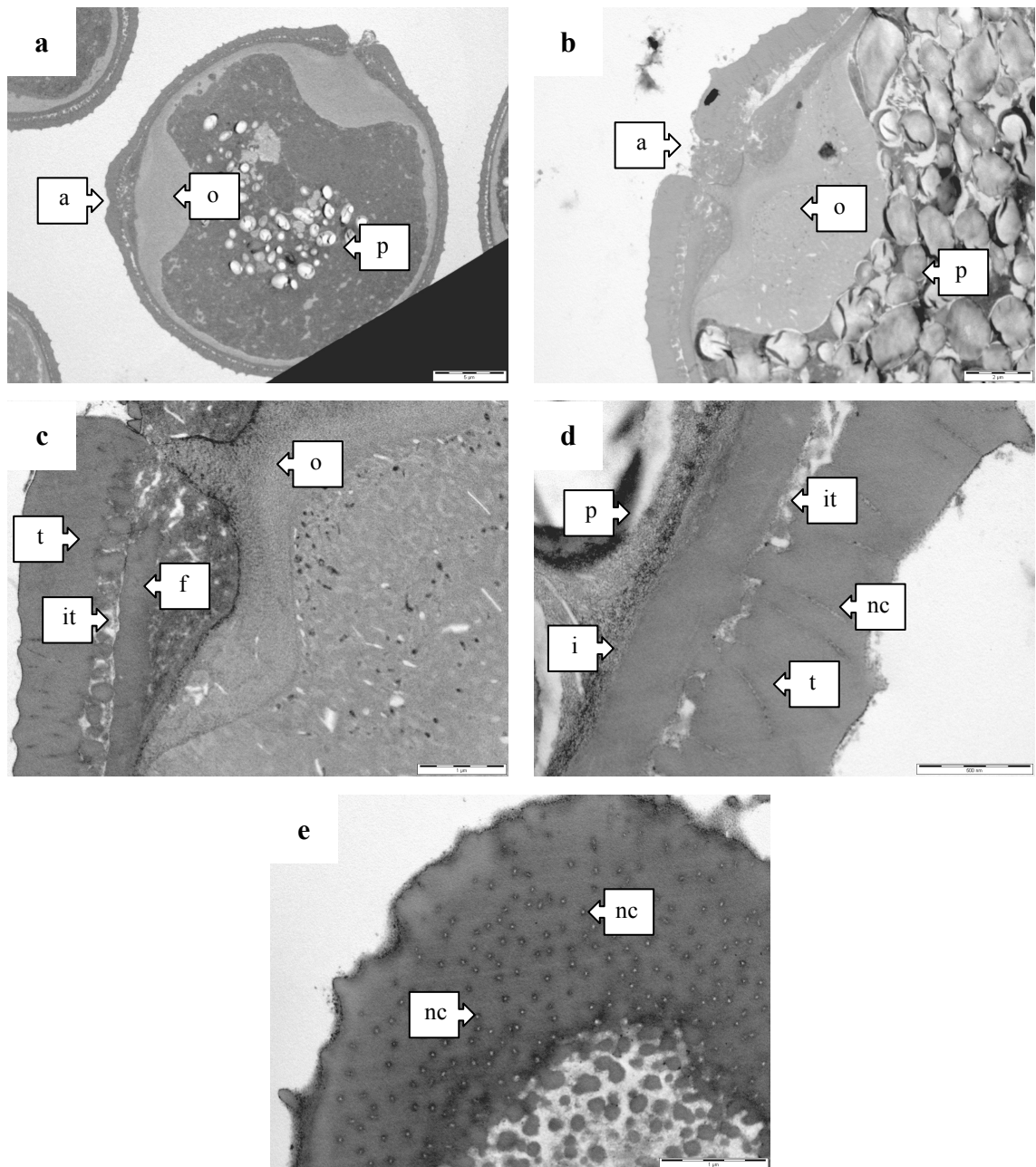


Figure 3.15: Transmission electron micrographs of untreated *Betula fontinalis* pollen.

Scale bars: (a) = 5 μm ; (b) = 2 μm ; (c) = 1 μm ; (d) = 500 nm; and (e) = 1 μm

a = aperture; f = foot layer; i = intine; it = infratectum; nc = nano-channel; o = oncus;

p = protoplast; and t = tectum

3.3 Acetolysis

Acetolysis is one of the most widely used techniques by palynologists to produce pollen and spores for microscopic analysis. It was initially proposed by G. Erdtman whereby pollen and spores are suspended in a 9:1 mixture of acetic anhydride and sulfuric acid

then heated to 70 °C for between one and two minutes.⁵⁴ The suspension is then centrifuged and washed with water.⁸ In this process, acetic anhydride breaks down the cellulose present in pollen and spores, with sulfuric acid acting as a catalyst.⁴⁵ Modifications to the standard method have been published, for example: using glacial acetic acid to wash pollen prior to analysis; changing the temperature used; or changing the time material spends in the acetolysis mixture.⁵⁵ There is no published evidence that acetolysis has been used to prepare microcapsules.

Bleaching is sometimes performed after acetolysis and prior to microscopic analysis. This is carried out in order to whiten pollen and spores, making their morphology easier to evaluate using light microscopy. Sodium hypochlorite, sometimes in the presence of acetic acid and hydrochloric acid, is used to carry out this bleaching.^{45, 117} Bleaching is able to break down the bonds within chromophores (structures within a molecule that make it appear coloured). As sporopollenin contains chromophores, bleaching is likely to alter its highly conjugated structure.¹¹⁸ In addition, other authors have noted that the addition of reagents containing chlorine e.g. hydrochloric acid, can introduce chlorine into sporopollenin's structure.¹³ As bleaching is likely to alter sporopollenin's structure and therefore potentially detrimentally alter its material properties, it will not be further evaluated here.

The acetolysis method followed in this chapter was kindly provided by Carol Furness of the Royal Botanic Gardens, Kew, London.¹¹⁹ Pollen or spores (0.1 g) were suspended in an acetolysis mixture (acetic anhydride and sulfuric acid in a 9:1 ratio (2 ml)). This suspension was heated (90 °C, 2 minutes) and then centrifuged (1500 × g (relative centrifugal force), 5 min). The supernatant fraction was discarded and the pollen or spores re-suspended in deionized water (10 ml) and then re-centrifuged. Washing and centrifugation was carried out a total of three times. This acetolysis procedure was applied as a control experiment to *Lycopodium clavatum* (club moss) spores and *Secale cereale* (rye), *Juglans nigra* (black walnut) and *Betula fontinalis* (water birch) pollen. Analysis of these samples was performed using light microscopy. The resolution of the microscope was sufficient to confirm the presence or absence of protoplast, and pollen or spore wall, but was unable to distinguish between the exine and intine (pollen) or exospore and endospore (spore)

3.3.1 Acetolysis of *Lycopodium clavatum* spores

Light micrographs of untreated and acetolysed *Lycopodium clavatum* spores were compared (Figure 3.16 and Figure 3.17 respectively). Both before and after treatment, spores are opaque, therefore making it difficult to determine the presence or absence of protoplasts. SEM analysis by other authors has indicated that the morphology of *Lycopodium clavatum* spores remains largely unchanged after acetolysis.¹²⁰ However, Wilce suggested that acetolysis causes the proximal face of *Lycopodium* spores to collapse into the spore cavity, thus altering their overall shape.¹²¹ Light micrographs of acetolysed *Lycopodium clavatum* spores prepared for this thesis indicate that no such collapse occurred in this case.

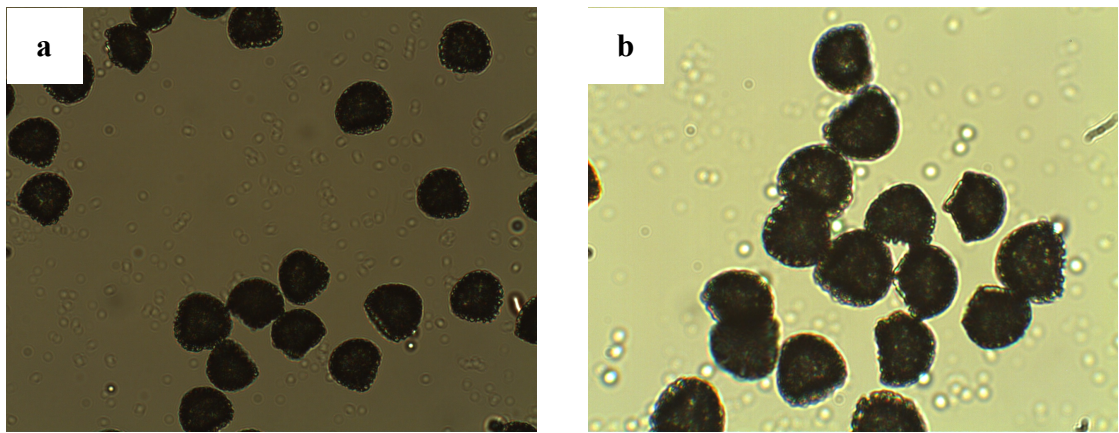


Figure 3.16: Light micrographs of untreated *Lycopodium clavatum* spores ((a) $\times 200$ and (b) $\times 400$ magnification)

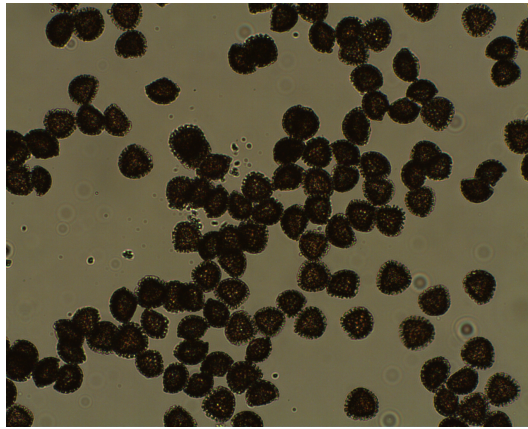


Figure 3.17: Light micrograph of acetolysed *Lycopodium clavatum* spores ($\times 100$ magnification)

3.3.2 Acetolysis of *Secale cereale* pollen

Light micrographs of untreated *Secale cereale* pollen (Figure 3.18) were compared to those of acetolysed pollen from the same species (Figure 3.19). Results show that acetolysis does appear to remove most protoplast material from *Secale cereale* pollen, but some material clearly remains within the grains (Figure 3.19 (b); green arrow). Some residual protoplast material is also seen leaving through the pores (Figure 3.19 (b); red arrows). Increasing the time the pollen spends in the acetolysis solution may remove further protoplast material. However, this is likely to render the grains darker in colour, making them unsuitable as microcapsules, especially where a lighter coloured microcapsule is desirable e.g. in pharmaceutical or display applications. Most grains remain intact, and there appears to be more debris surrounding them after acetolysis, possibly as a result of the degradation of non-sporopollenin components.

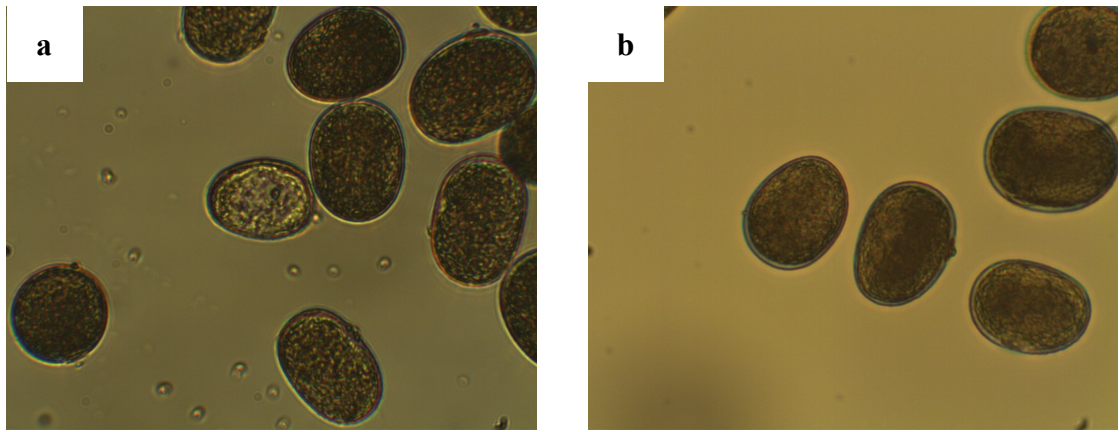


Figure 3.18: Light micrographs of untreated *Secale cereale* pollen ((a) and (b) $\times 400$ magnification)

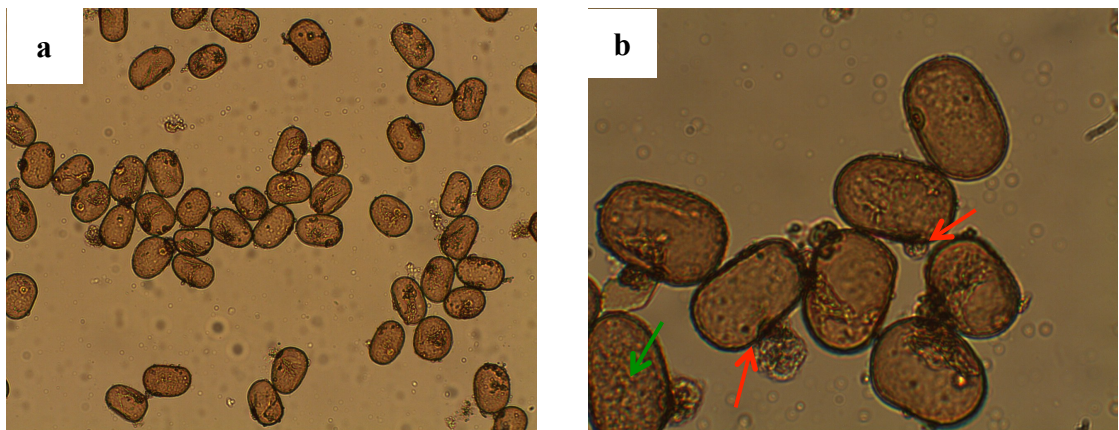


Figure 3.19: Light micrographs of acetolysed *Secale cereale* pollen ((a) $\times 100$ and (b) $\times 400$ magnification)

Red arrows = protoplast material passing through pores of pollen grains; green arrow = protoplast material still within a pollen grain

3.3.3 Acetolysis of *Juglans nigra* pollen

Untreated *Juglans nigra* pollen was compared to acetolysed pollen *via* light microscopy (Figure 3.20 and Figure 3.21 respectively). Higher magnification ($\times 400$) analysis of acetolysed *Juglans nigra* pollen shows that not all protoplast material was successfully removed (Figure 3.21 (b), red arrow). *Juglans nigra* pollen appears darker after acetolysis, indicating that the chemical structure of sporopollenin is likely to have been altered (although the integrity of the pollen grains does not appear to have been affected).

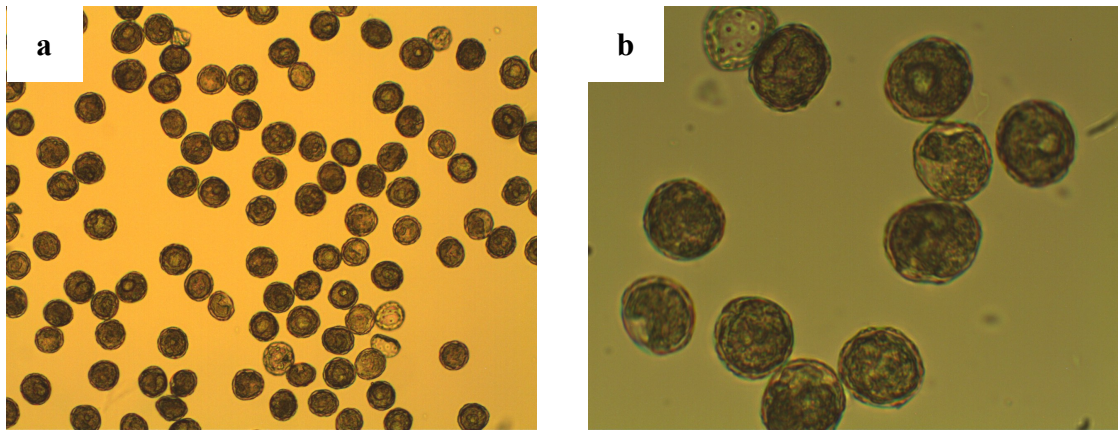


Figure 3.20: Light micrographs of untreated *Juglans nigra* pollen ((a) $\times 100$ and (b) $\times 400$ magnification)

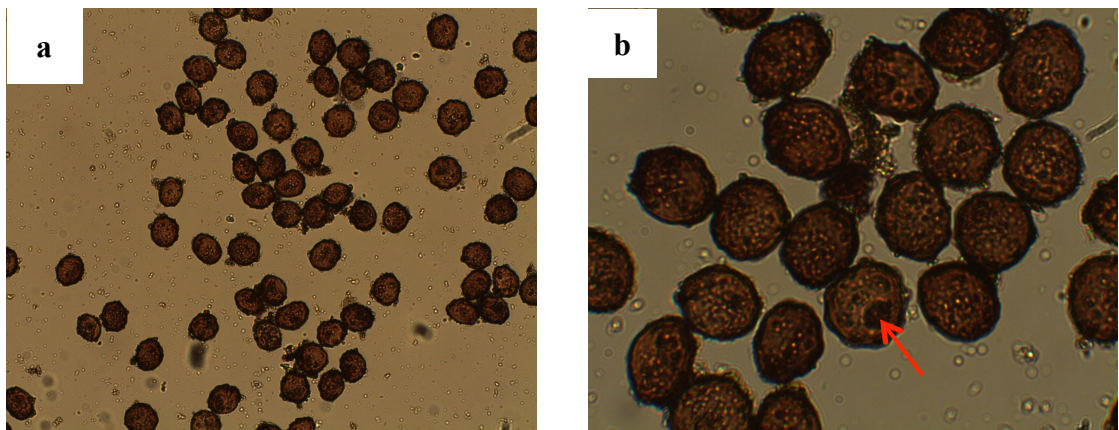


Figure 3.21: Light micrographs of acetolysed *Juglans nigra* pollen ((a) $\times 100$ and (b) $\times 400$ magnification)

Red arrow = protoplast material within grain

3.3.4 Acetolysis of *Betula fontinalis* pollen

Untreated *Betula fontinalis* pollen (Figure 3.22) was compared to acetolysed pollen (Figure 3.23). As observed with *Secale cereale* pollen, acetolysis was successful in removing almost all protoplast material from *Betula fontinalis*. However, acetolysed pollen is darker than untreated pollen, suggesting that acetolysis changes sporopollenin's chemical structure. Similar to untreated pollen, pollen tetrads are observed in the acetolysed sample (Figure 3.23 (a); red arrows), indicating that acetolysis does not appear to break the bonds between individual grains within tetrads.

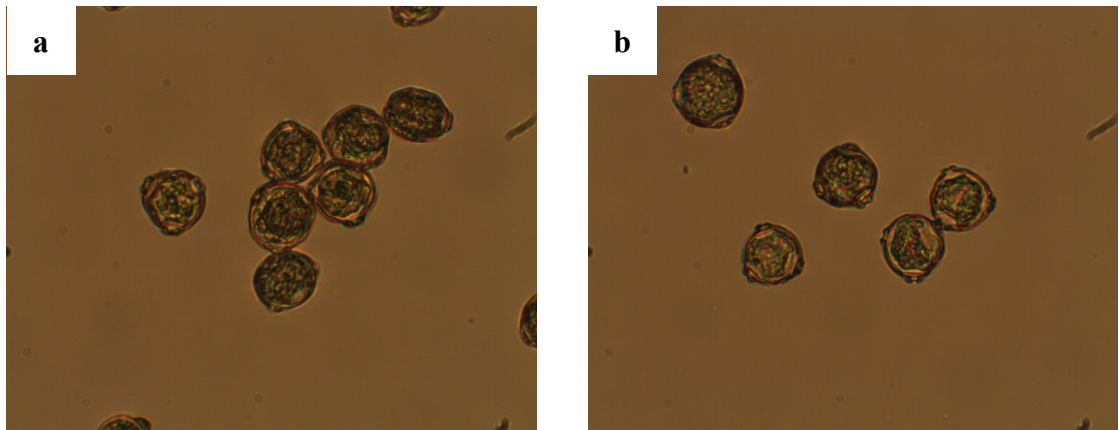


Figure 3.22: Light micrographs of untreated *Betula fontinalis* pollen ((a) and (b) $\times 400$ magnification)

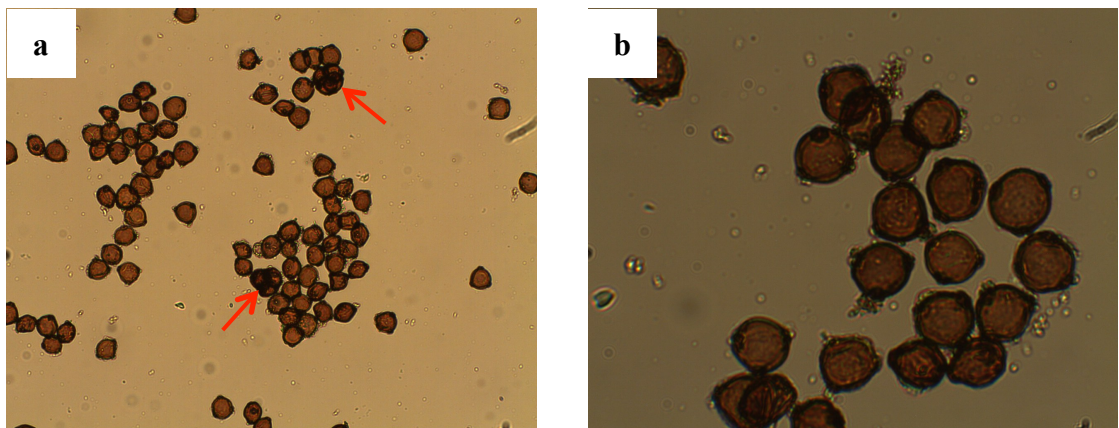


Figure 3.23: Light micrographs of acetolysed *Betula fontinalis* pollen ((a) $\times 100$ and (b) $\times 400$ magnification)

Red arrow = tetrad of pollen grains

3.3.5 Acetolysis: summary of results

1. Acetolysis was confirmed to be a quick and simple method of removing non-sporopollenin material from pollen and spores. However, in all species studied here, not all non-sporopollenin material was successfully removed, indicating that some components with the potential to cause an allergic reaction remained inside pollen and spores. The method left pollen and spores from all species intact.
2. Material produced appeared largely dark brown in colour, meaning that it is unsuitable for use in many applications for which lighter-coloured microcapsules are required, e.g. pharmaceutical, food and display applications. This colour change

indicates that sporopollenin's chemical structure was altered, potentially reducing its desirable material properties e.g. physical and chemical strength, flexibility and ability to absorb ultraviolet (UV) radiation. Bleaching could be used to lighten the colour of the acetolysed pollen and spores studied here; however that would be likely to further alter sporopollenin's structure.

3. No change in the shape of grains was observed post acetolysis. This latter finding is supported by work by Reitsma, who found that although acetolysis does not alter the shape of pollen grains, it does alter their size, depending on the exact acetolysis method used and the time that pollen spends in the acetolysis mixture.¹²²
4. Given that acetolysis produced dark-coloured spores and pollen grains, it was therefore not further considered as a suitable technique for producing microcapsules from pollen or spores.

3.4 Base and acid treatments

Base and acid treatments are the most widely published and patented methods used to produce microcapsules from spores. *Lycopodium clavatum* (club moss) spores were treated with base (commonly potassium hydroxide) followed by acid (usually 85 % (v/v) *ortho*-phosphoric acid) in conjunction with organic solvents. Published data suggests that hollow sporopollenin exine shells were successfully isolated by removal of all the intine and protoplast material. The exact method employed varies slightly between publications.^{57-59, 74, 85, 123} Although microcapsules have been produced from pollen and spores using base and acid, pollen is less well studied. To date, only *Ambrosia trifida* (giant ragweed) pollen appears to have been treated with a modified version of this base and acid protocol (summarised in Figure 3.25), with the aim of producing microcapsules.¹²⁴ Particular modifications to note include: one rather than two base treatments; 1 × 1 h rather than 2 × 6 h reflux in base; using sodium hydroxide rather than potassium hydroxide as the base; the addition of an ethanol reflux; and the reflux in *ortho*-phosphoric acid lasting 1 h rather than 7 days. Fletcher *et al.* did not explain why they varied the conditions, although it is reasonable to speculate that *Ambrosia trifida* was damaged by the method applied to *Lycopodium clavatum*.

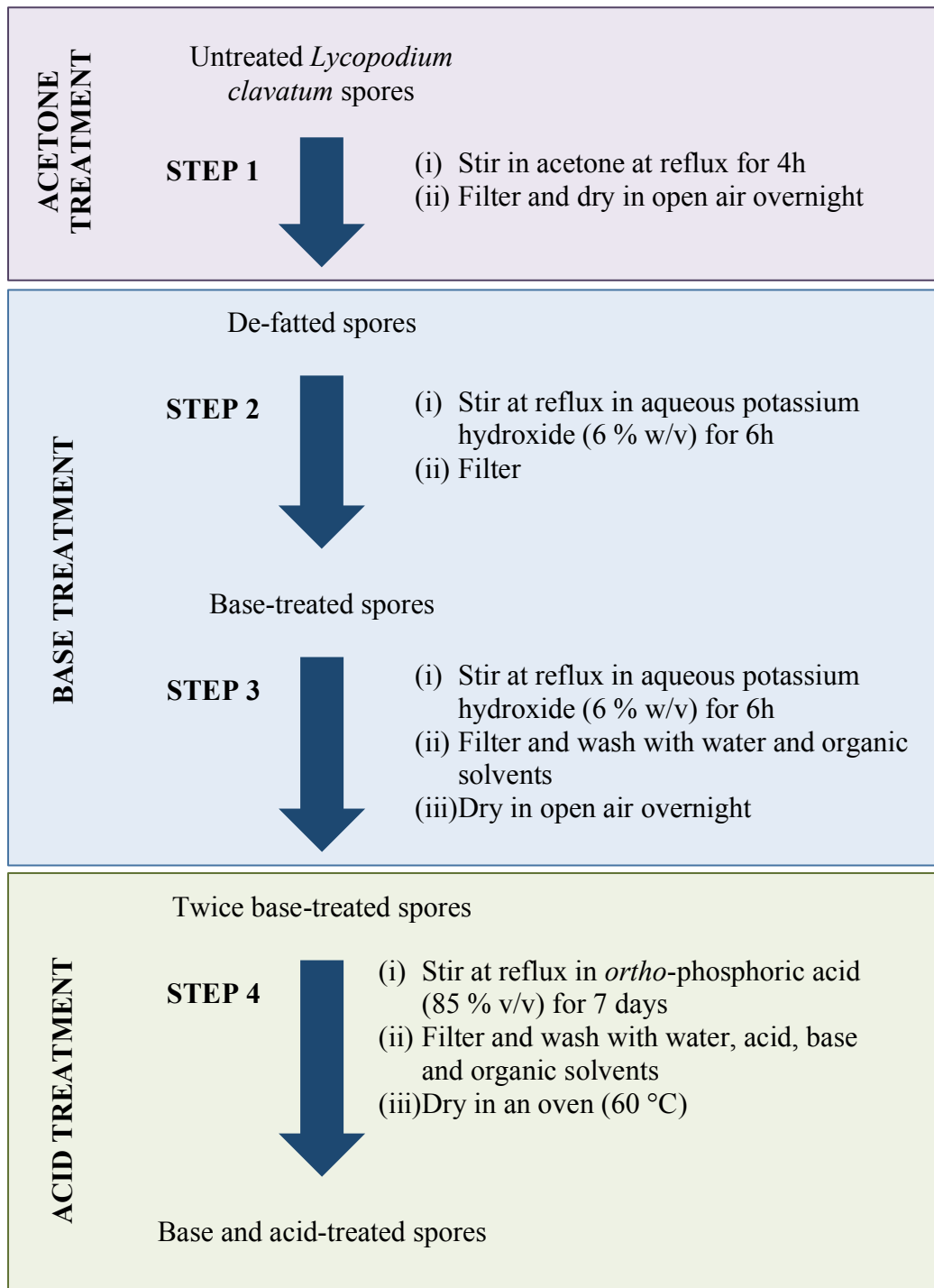


Figure 3.24: Summary of the base and acid treatment protocol applied to *Lycopodium clavatum* spores, published by Atkin *et al.*⁵⁷

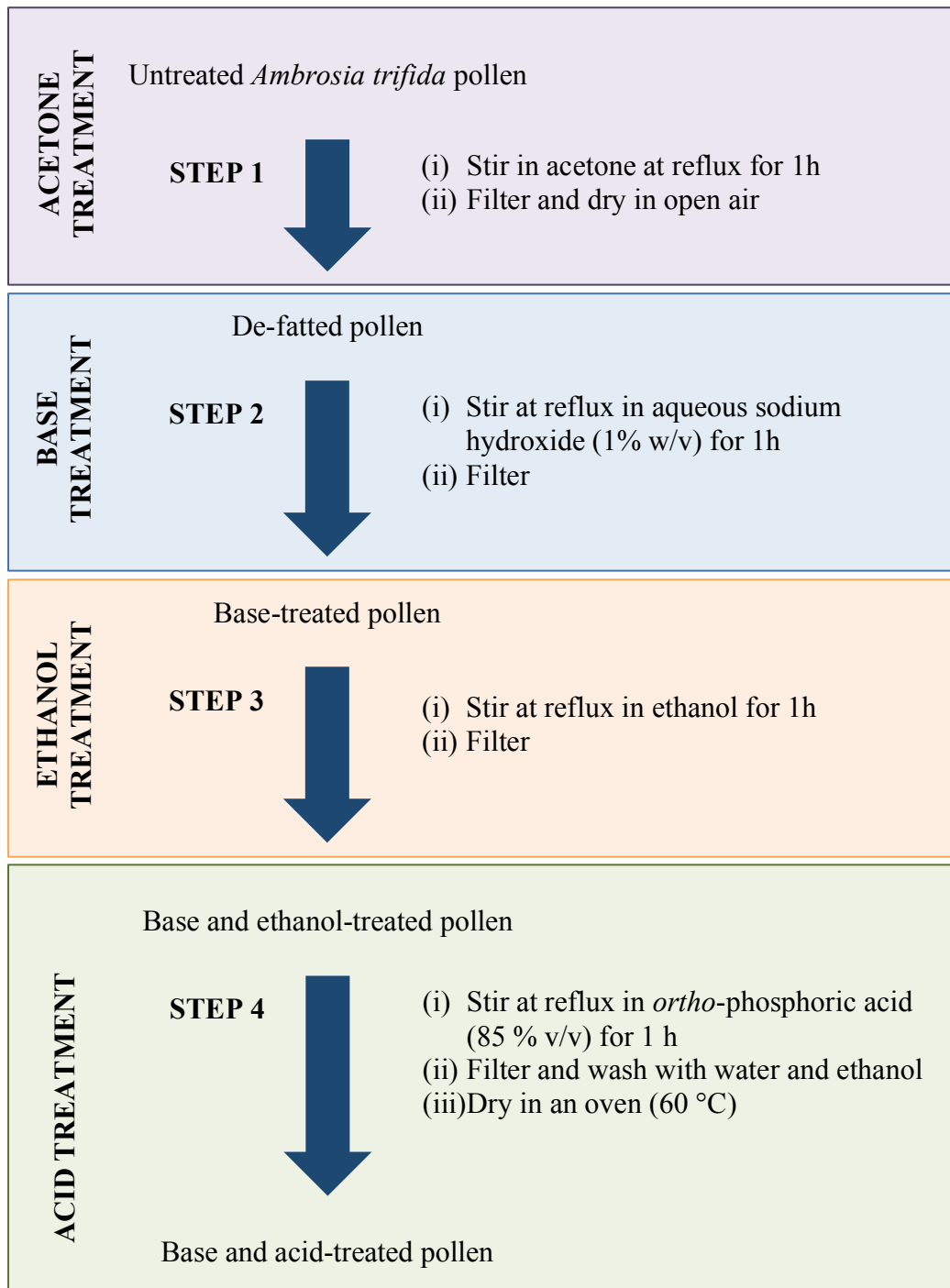


Figure 3.25: Summary of the base and acid treatment protocol applied to *Ambrosia trifida* pollen, published by Fletcher *et al.*¹²⁴

In order to test the suitability of the standard base and acid treatment proposed by Atkin *et al.* (summarised in Figure 3.24) on both pollen and spores, it was applied to *Lycopodium clavatum* spores, and *Secale cereale* (rye) and *Juglans nigra* (black walnut) pollen as a control experiment.⁵⁷ Small modifications were subsequently made to the method applied to the pollen species to both test weaknesses in the method and to determine whether these modifications improved the outcome.

Ambrosia artemisiifolia pollen was treated using the modified version of this protocol, published by Fletcher *et al.* (summarised in Figure 3.25).¹²⁴ *Ambrosia artemisiifolia* pollen was used in place of *Ambrosia trifida* pollen, since the latter could not be purchased. However, the two species are from the same genera and are therefore closely related. It was predicted that they would behave in a similar fashion when exposed to acid and base. Light microscopy, scanning electron microscopy (SEM) and transmission electron microscopy (TEM) were all used to analyse the material produced.

3.4.1 Base and acid treatment applied to *Lycopodium clavatum* spores

Lycopodium clavatum spores were treated according to the protocol outlined in Figure 3.24. Scanning electron micrographs of untreated *Lycopodium clavatum* spores (Figure 3.26) were compared to those taken of spores after step 1 (Figure 3.27). A low-magnification scanning electron micrograph (Figure 3.27 (a)) shows that all grains appear intact after step 1. However, higher magnification images suggest that the muri on the spores' distal faces (Figure 3.27 (b)) may have been damaged by this treatment. The proximal face (Figure 3.27 (c)) of a second spore appears unchanged. Higher magnification images were only taken of two spores. Although it can be concluded that acetone treatment leaves spores intact, further microscopy is required to determine the extent to which this treatment affects the exine.

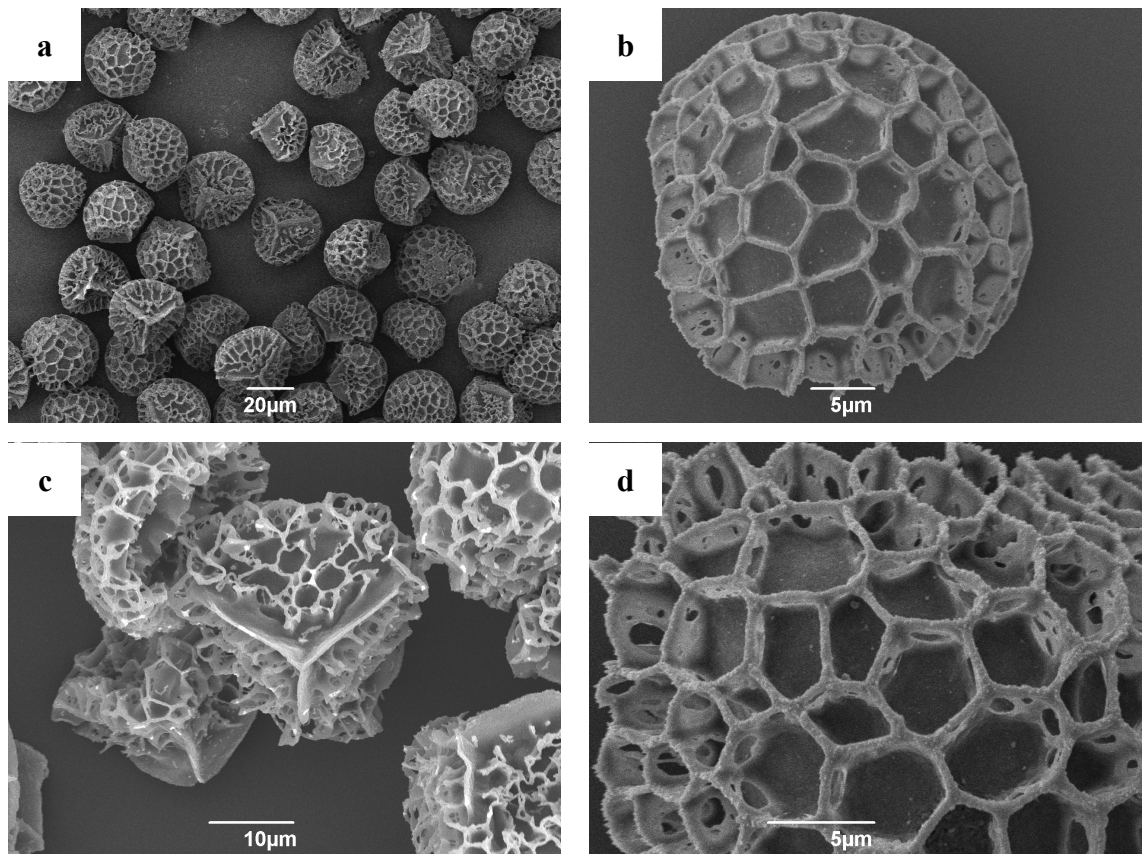


Figure 3.26: Scanning electron micrographs of untreated *Lycopodium clavatum* spores: (a) low magnification image; (b) distal face of spore; (c) proximal face of spore with three laesura forming a trilete scar; and (d) high magnification image

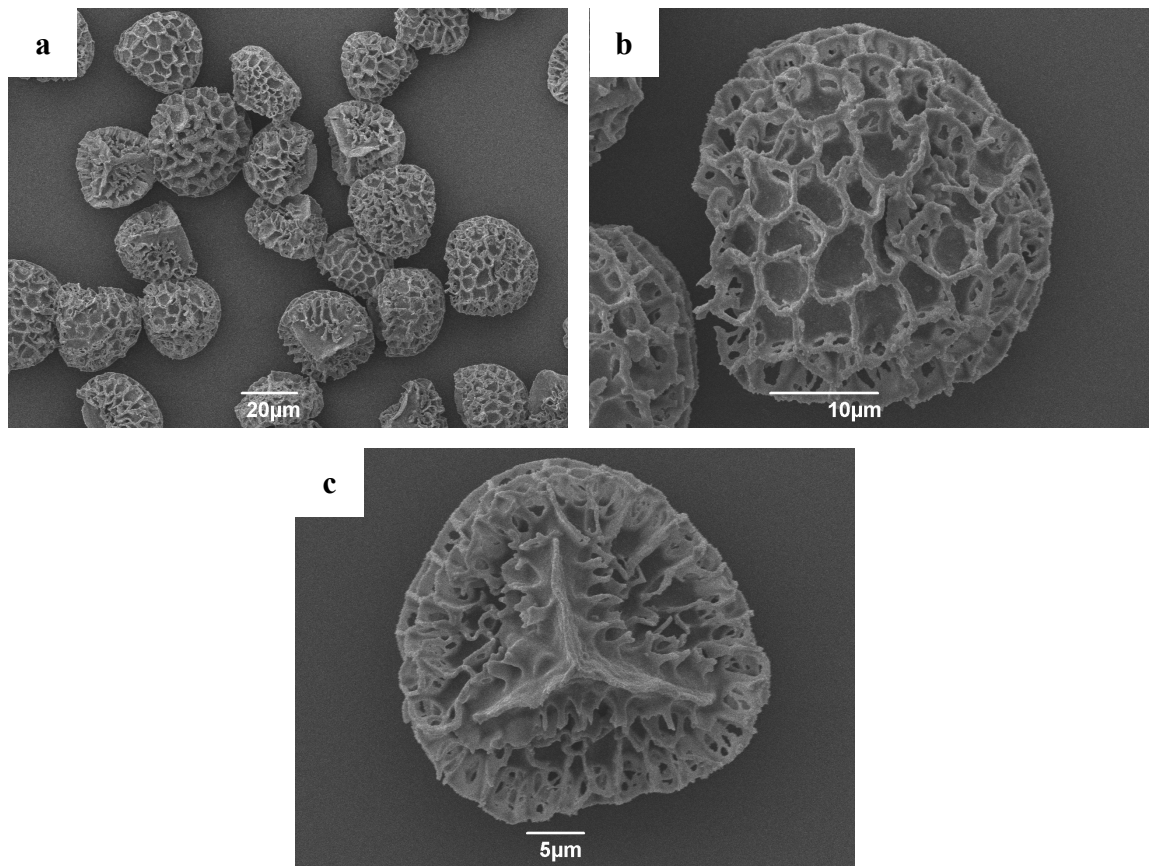


Figure 3.27: Scanning electron micrographs of *Lycopodium clavatum* spores after step 1

After step 2, spores remain intact (Figure 3.28). However, a high magnification image taken of a single spore (Figure 3.28 (b)) highlights possible damage to the distal face. The proximal face seems unchanged (Figure 3.28 (c)). Although the muri appear undamaged, the lumina appear less smooth and possibly more porous. To confirm this damage across the entire sample, further high magnification SEM studies are required. In addition, it is impossible to determine whether this damage was inflicted during step 1, or whether step 2 merely increased damage already present after step 1.

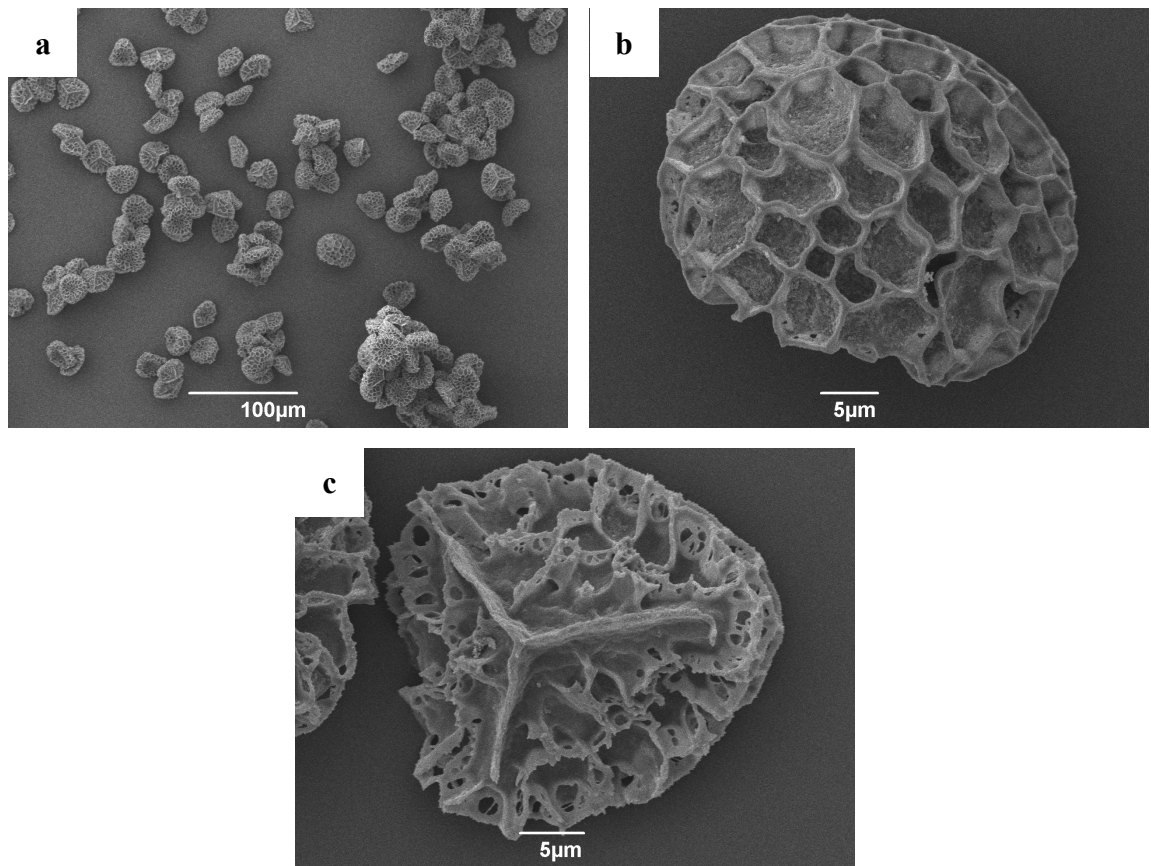


Figure 3.28: Scanning electron micrographs of *Lycopodium clavatum* spores after step 2

After step 3 (i) (second base treatment) (Figure 3.29), spores appear similar to completely untreated spores. A high magnification image of a single spore reveals that its distal and proximal faces are unchanged. This is in contrast to the damaged spores observed after steps 1 and 2 (Figure 3.28 (b)). As these observations are only based on two spores from each sample, more high magnification SEM studies are required to determine whether treatment with base does damage the exine of *Lycopodium clavatum* spores.

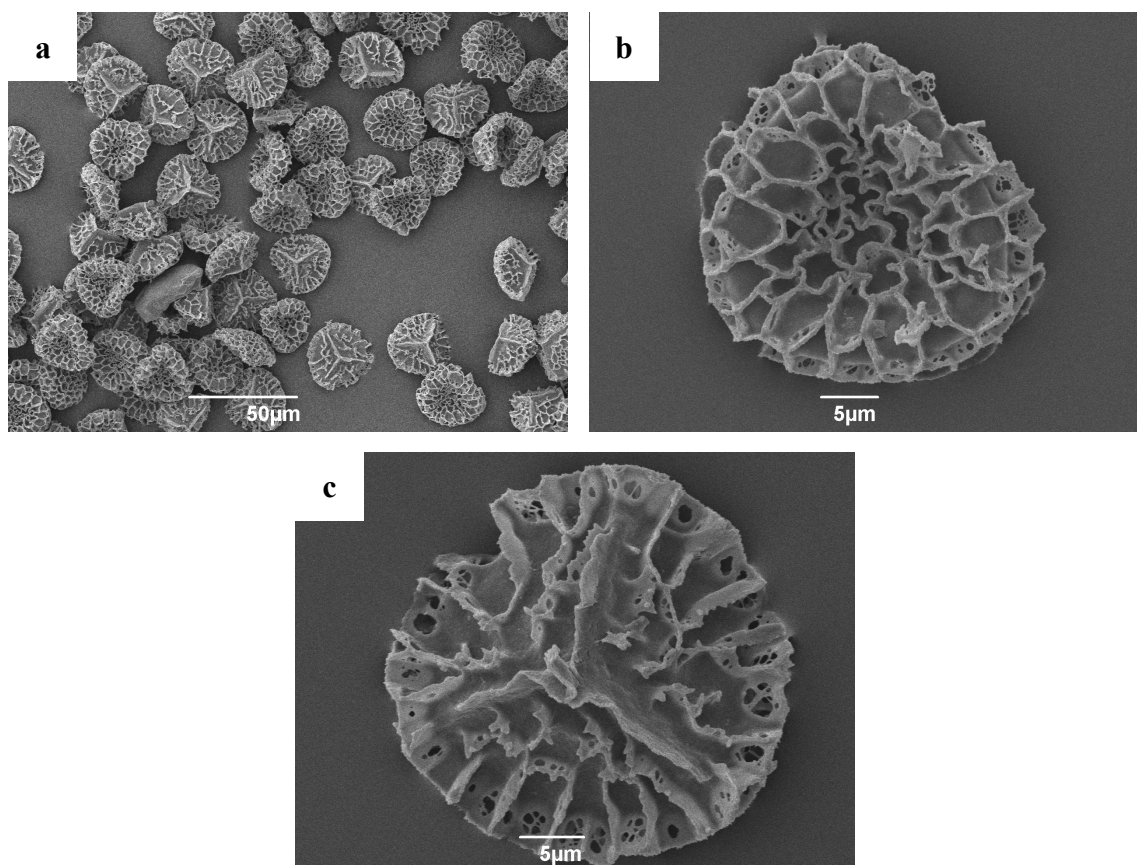


Figure 3.29: Scanning electron micrographs of *Lycopodium clavatum* spores after step 3, part (i)

Scanning electron micrographs were taken after step 3, part (iii) to evaluate the effect of solvents (water, acetone, hydrochloric acid (2 mol dm^{-3}) and sodium hydroxide (2 mol dm^{-3}), and ethanol) on base-treated spores (Figure 3.30). Some spores were observed that appeared different to most in the sample (highlighted by red circles). It was difficult to determine if these spores were damaged, or whether they were part of a standard sample of spores. This variation appears limited to a small number of spores within the sample. *Lycopodium clavatum* spores seem largely undamaged by treatment with base, acid and organic solvents, although some changes to the exine are clear. This is in agreement with the observations reported by Atkin *et al.* Further work is required to understand the nature of the damage caused to the exine and exactly which step(s) in the process contributes to this.

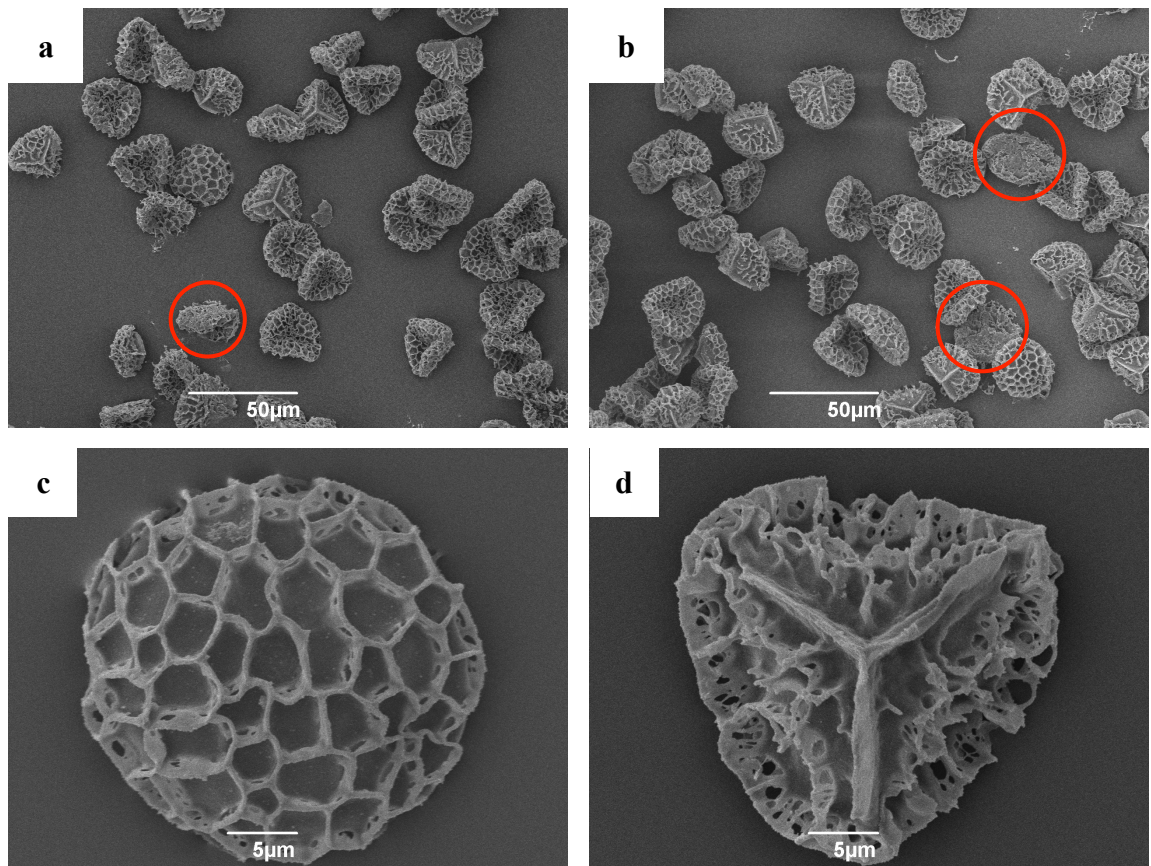


Figure 3.30: Scanning electron micrographs of *Lycopodium clavatum* spores after step 3, part (iii)

Red circles highlight damaged spores

Transmission electron microscopy of base and acid treated *Lycopodium clavatum* spores was carried out. It was challenging to produce sections for TEM analysis as this species was found to be particularly difficult to section and damaged several diamond sectioning knives. Despite this, every effort was made to obtain good quality micrographs that were representative of the samples studied.

Transmission electron micrographs of untreated *Lycopodium clavatum* spores (Figure 3.31) were compared to those taken after step 1 (Figure 3.32). These demonstrate that a large amount of protoplast material was removed during step 1. The exospore and endospore can also be identified and the exospore retains its lamellar structure. In addition to the spores observed, a biological organism of unknown origin (approximate diameter 2 μm) was also seen to be present in spores after step 1 (Figure 3.32 (a)). Although this organism cannot be definitively identified, it does fit within the correct size range for a bacterium (approximately 0.1 - 50 μm) or a fungal spore (approximately 1.5 – 30 μm).^{125, 126}

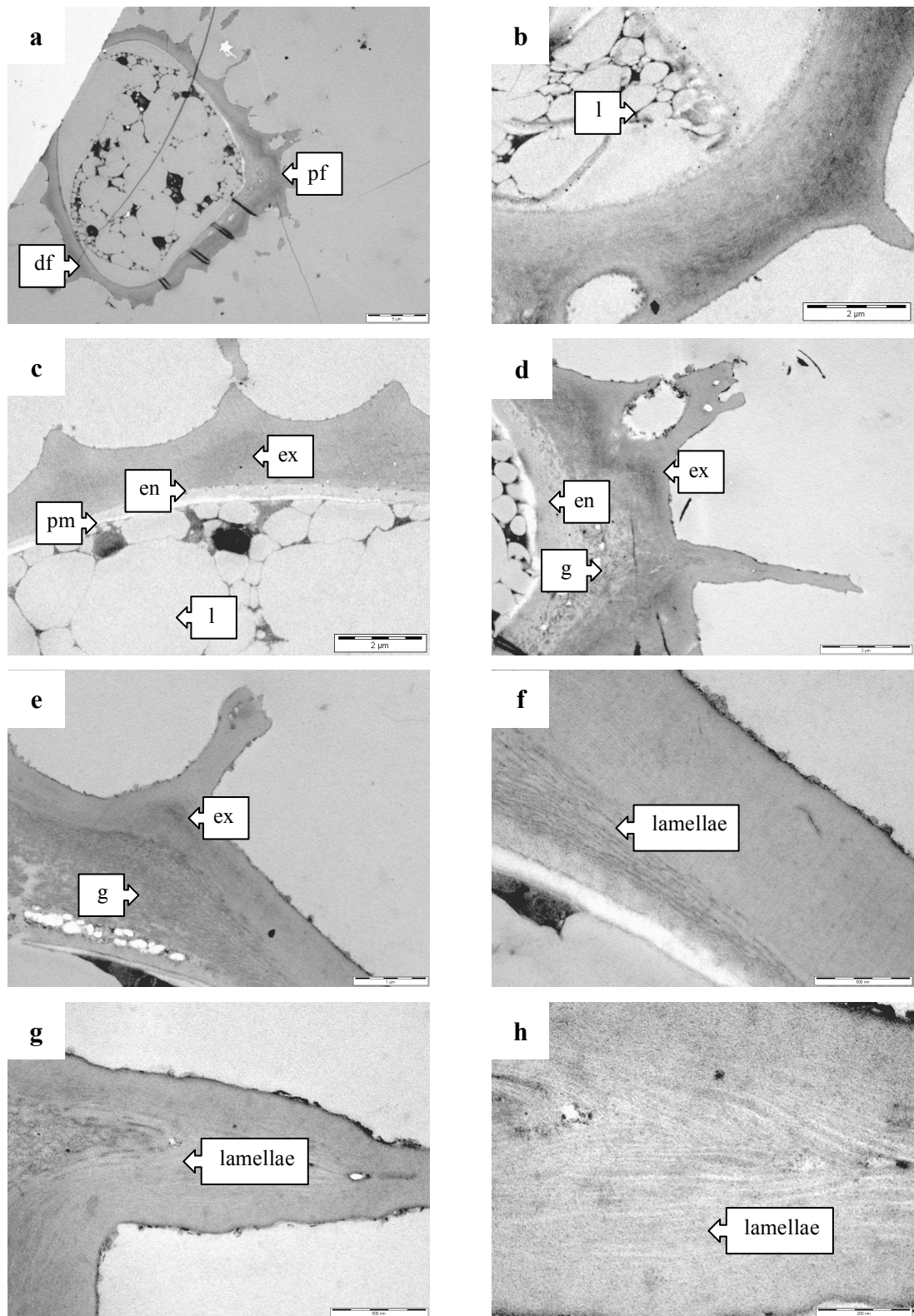


Figure 3.31: Transmission electron micrographs of untreated *Lycopodium clavatum* spores.

Scale bar (a) = 5 μm ; (b) = 2 μm ; (c) = 2 μm ; (d) = 2 μm ; (e) = 1 μm ; (f) = 500 nm;

(g) = 500 nm; and (h) = 200 nm

df = distal face; en = endospore; ex = exospore; g = exospore granular layer;

l = lipid body; pf = proximal face ; and pm = plasma membrane

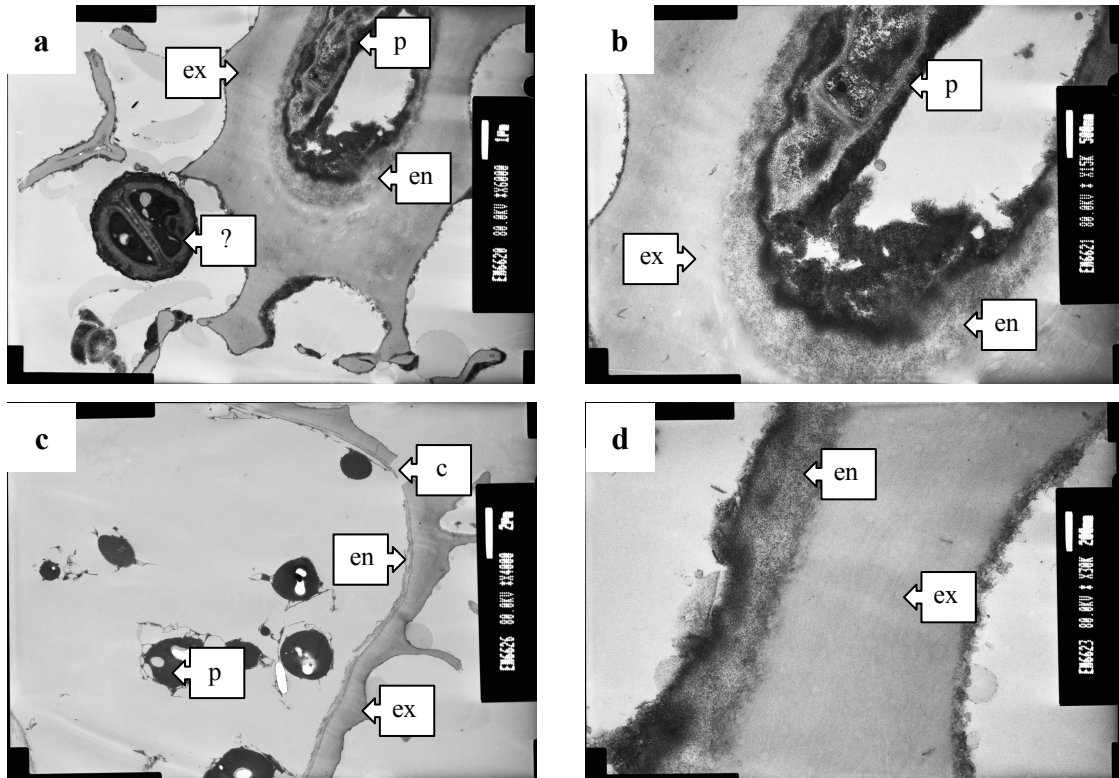


Figure 3.32: Transmission electron micrographs of *Lycopodium clavatum* spores after step 1.

Scale bar (a) = 1 μm ; (b) = 500 nm; (c) = 2 μm ; and (d) = 200 nm

? = biological organism of unknown origin; c = crack; en = endospore; ex = exospore;
p = protoplasm;

TEM shows that after treatment with base (steps 2 and 3), protoplast material appears to have been largely removed (Figure 3.33). The exospore is unchanged compared to untreated spores and is still clearly laminated. There are a series of wall layers that cannot be differentiated between (Figure 3.33 (a), (b) and (c)). These layers are likely to be composed of the endospore and exospore granular layer. However, the potassium hydroxide solution applied is likely to have begun to break down the endospore, making the identification of distinct layers challenging. A blue dashed line highlights these layers in Figure 3.33. A crack is observed in one of the spores (Figure 3.32 (c)). It is difficult to ascertain whether stirring in acetone or preparing spores for TEM caused this damage. However, it is likely to be confined to a minority of spores as SEM (Figure 3.27) indicates that most grains remained intact after step 1.

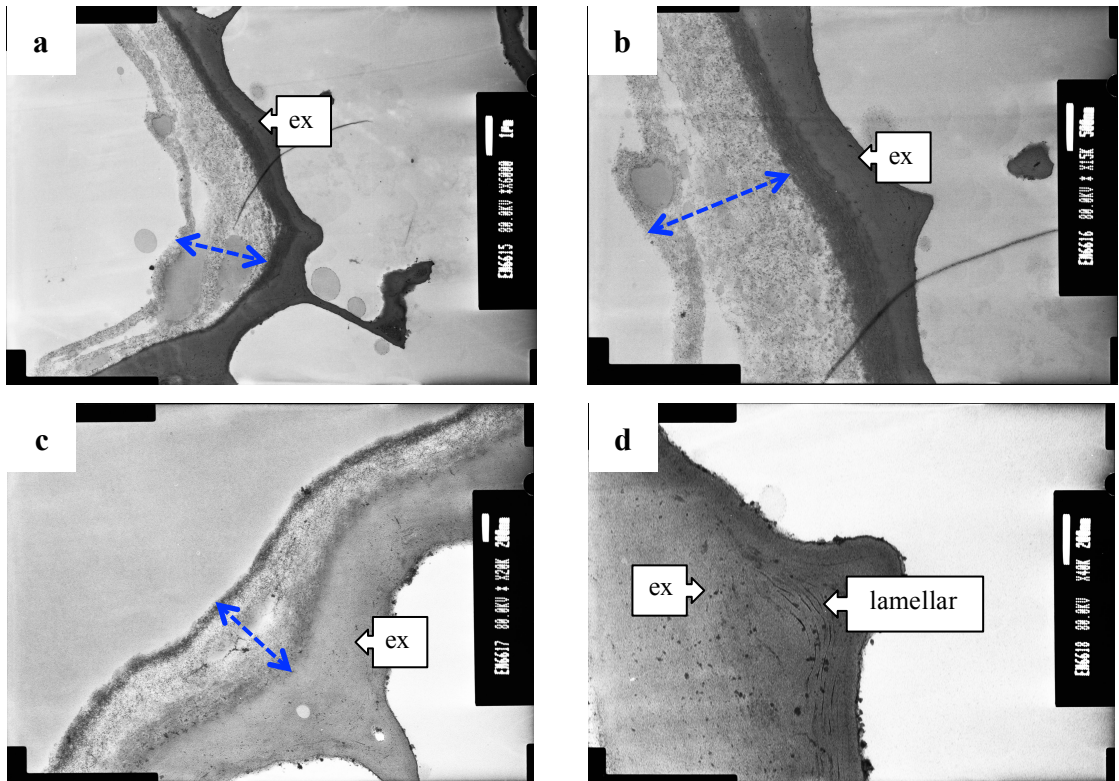


Figure 3.33: Transmission electron micrographs of *Lycopodium clavatum* spores after step 3, part (iii).

Scale bar (a) = 1 μm ; (b) = 500 nm; and (c) and (d) = 200 nm

ex = exospore; blue dashed line = wall layers that cannot be differentiated between

After prolonged treatment with acid (step 4), TEM reveals that the endospore layer no longer seems to be present. The uniform staining of the remaining layer (indicated by dashed yellow lines in Figure 3.34 (c) and (d)) suggests that this is the exospore layer, as the granular layer present prior to step 4 is differently stained (Figure 3.33). In addition, the granular layer is known to only form at the proximal regions of *Lycopodium clavatum* spores, whereas the single layer observed in Figure 3.34 (a) is distributed uniformly over all regions of the spore.¹⁰⁷ The acid and base treatment protocol proposed by Atkin *et al.* does appear to remove all non-sporopollenin components leaving just the exospore remaining. This supports published findings that the protocol is suitable for producing microcapsules from *Lycopodium clavatum* spores.

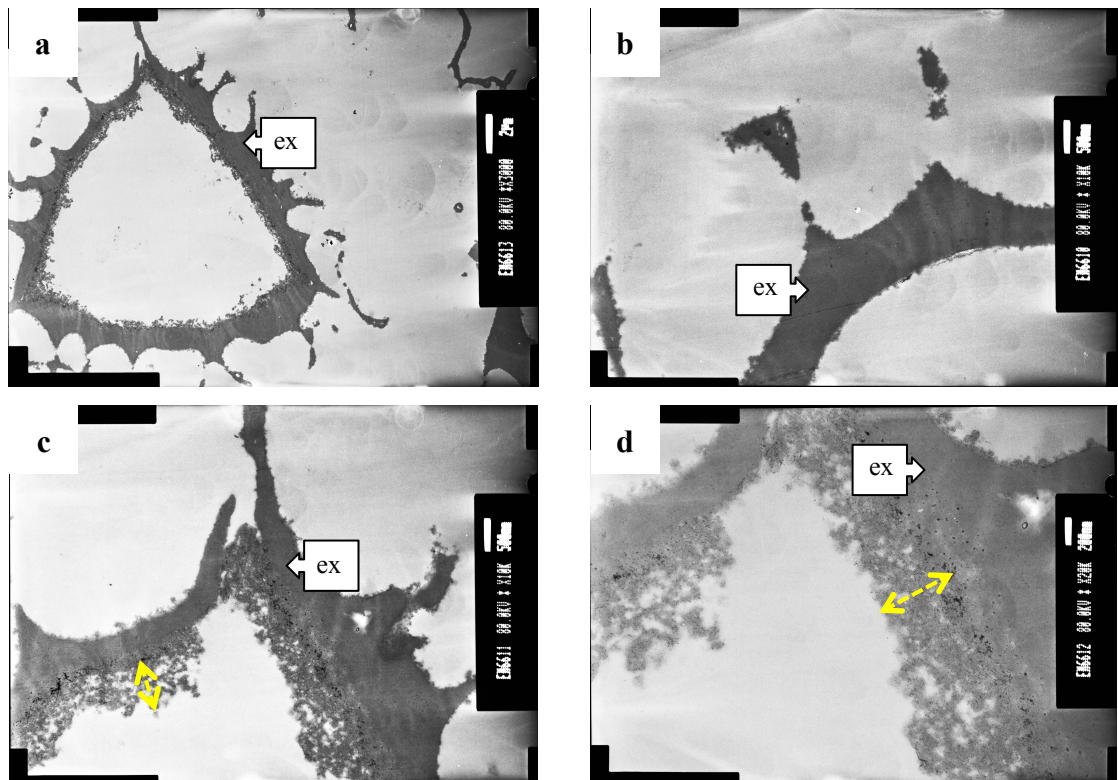


Figure 3.34: Transmission electron micrographs of *Lycopodium clavatum* spores after step 4.

Scale bar (a) = 2 μm ; (b) and (c) = 500 nm; and (d) = 200 nm

ex = exospore; yellow dashed line = non-uniform edge of the exospore

3.4.2 Base and acid treatment applied to *Secale cereale* pollen

The base and acid treatment protocol summarised in Figure 3.24 was applied to *Secale cereale* pollen. Light microscopy was used to compare untreated *Secale cereale* pollen (Figure 3.35) to pollen after step 1 (Figure 3.36). After step 1, pollen appears unchanged compared to untreated pollen. However, step 2 caused notable damage to pollen, and many grains appear cracked and broken (Figure 3.37). Base treatment did, however, produce more transparent grains that appear to have a large quantity of their protoplast material removed. Nevertheless, the damage caused was so great that the method proposed by Atkin *et al.* was deemed unsuitable for producing microcapsules from *Secale cereale* pollen without further modification. Cracked and damaged grains would be unlikely to encapsulate substantial quantities of material without encapsulated material leaking out. The proposed second base treatment (step 3) and the acid step (step 4) were not attempted for this reason.

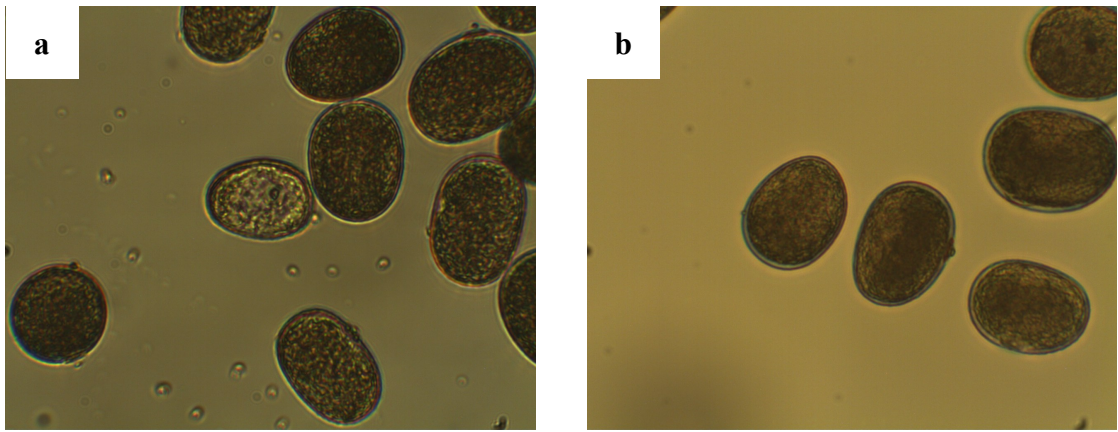


Figure 3.35: Light micrographs of untreated *Secale cereale* pollen ((a) and (b) $\times 400$ magnification)

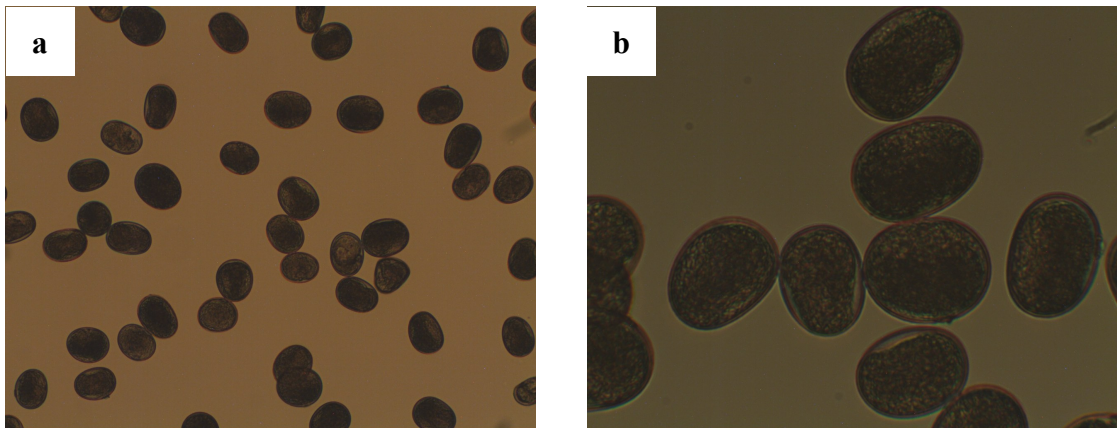


Figure 3.36: Light micrographs of *Secale cereale* pollen after step 1 ((a) $\times 100$ and (b) $\times 400$ magnification)

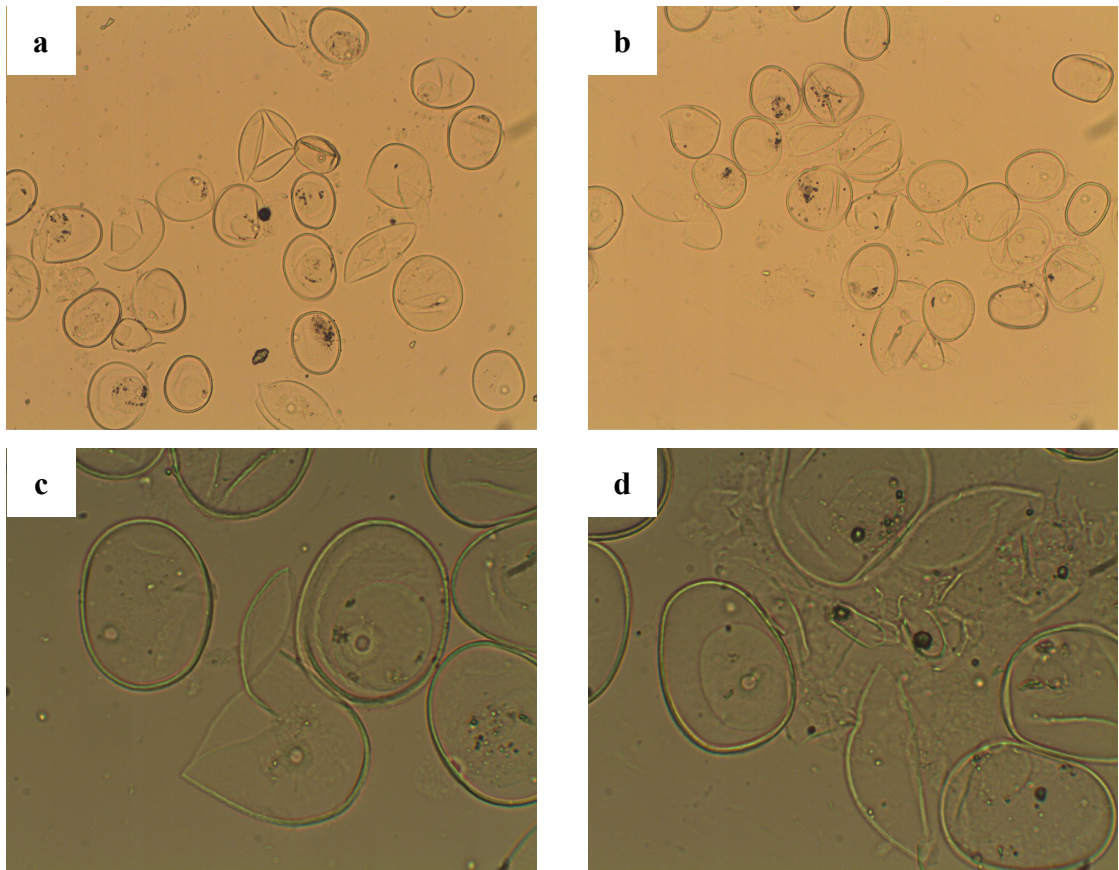


Figure 3.37: Light micrographs of *Secale cereale* pollen after step 2 ((a) & (b) $\times 100$, and (c) and (d) $\times 400$ magnification)

In order to evaluate the effect of temperature on the pollen during step 2, this step was repeated at room temperature, rather than at reflux. After 2 h, a proportion of grains appear damaged (Figure 3.38), similar to samples heated at reflux (Figure 3.37). This indicates that heating is unlikely to be responsible for the damage to *Secale cereale* pollen observed during step 2.

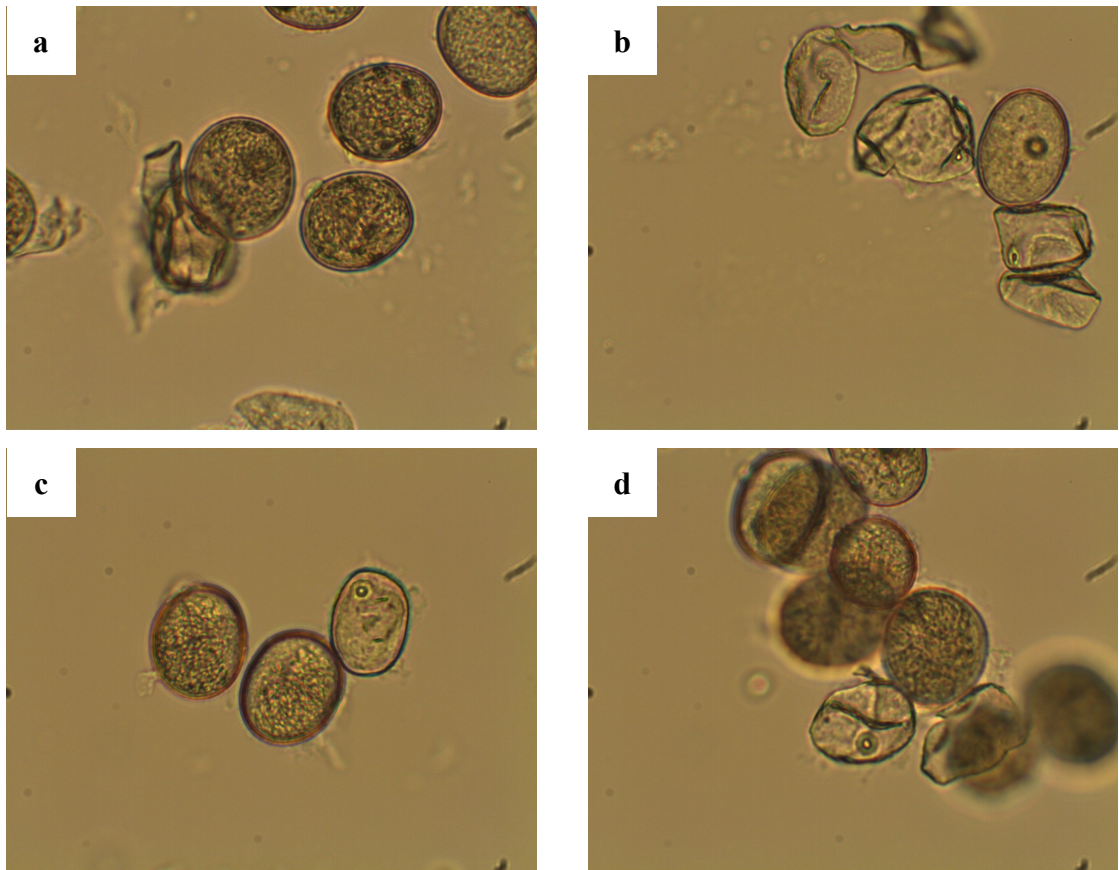


Figure 3.38: Light micrographs of *Secale cereale* pollen after step 2 (2 h, room temperature) ((a), (b), (c) and (d) $\times 400$ magnification)

To determine the effect of agitation, untreated *Secale cereale* pollen was suspended in potassium hydroxide (6 % (w/v)) (step 2) without stirring. After 4 h 30 min, light microscopy shows that a large number of grains are ruptured (Figure 3.39) and that compared to a stirred sample (Figure 3.37), more protoplast material is present. In an attempt to highlight any intine or protoplast material present, grains were stained with an aqueous solution of Ruthenium Red. Ruthenium Red binds to polysaccharides, which are found largely in the intine (and to a more limited extent, the protoplast) of pollen.¹²⁷ Stained pollen appears slightly pink in colour. However, the solution appeared to fail to penetrate a majority of grains. These results indicate that stirring is required to remove protoplast material, but that it is unlikely to cause a majority of the damage to grains observed.

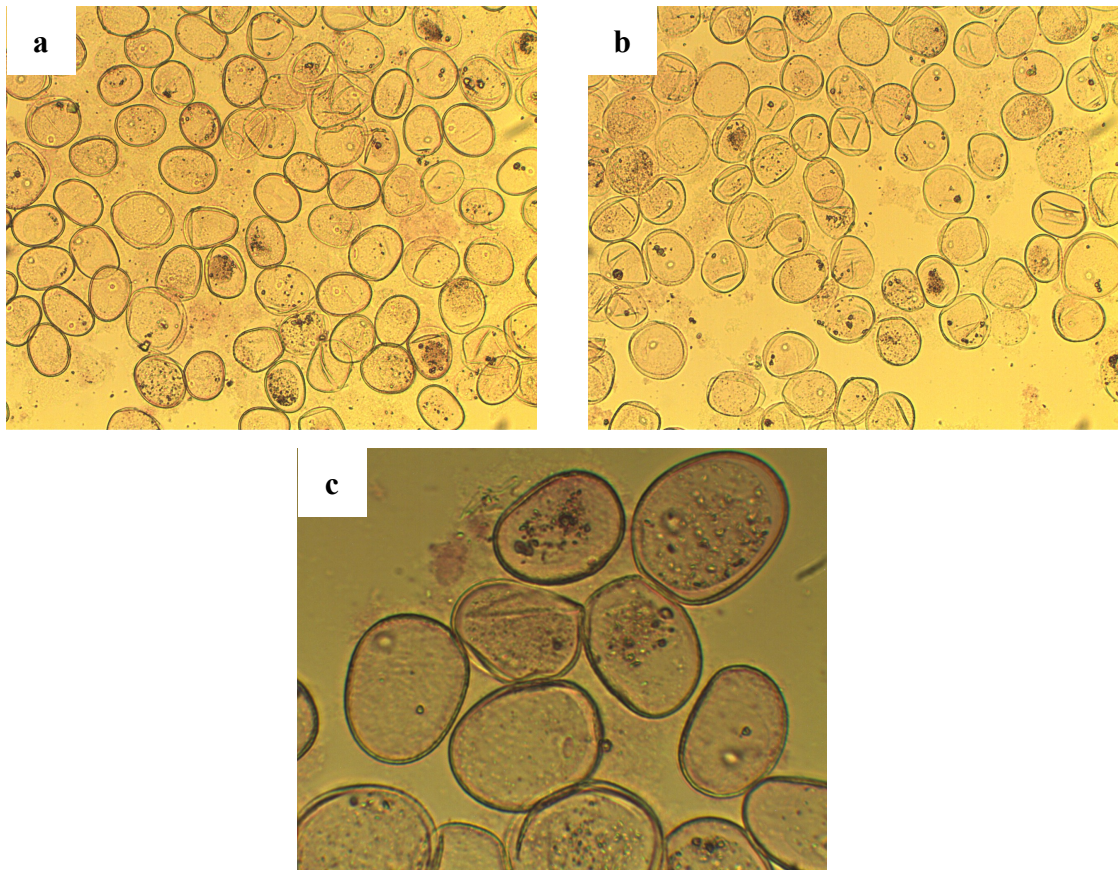


Figure 3.39: Light micrographs of *Secale cereale* pollen after step 2 (4 h 30 min, without stirring). Slide stained with Ruthenium Red. ((a) and (b) $\times 100$, and (c) $\times 400$ magnification)

Repeating step 2 at room temperature (Figure 3.38) and without stirring (Figure 3.39) did not notably reduce damage to the grains. This suggests that potassium hydroxide was likely to be the primary factor in the damage caused to the pollen. It may be the case that base treatment breaks down the intine, leaving the exine structurally weaker and therefore more susceptible to damage.

The combined thickness of the exospore and endospore of *Lycopodium clavatum* spores is approximately 1 – 2 μm , compared to the exine of *Secale cereale* pollen, which is approximately 0.5 μm thick. *Lycopodium clavatum* spores possess a strong, lamellar exospore (Figure 3.40), whereas *Secale cereale*'s infratectum is columellate (Figure 3.41) and therefore may be structurally weaker in comparison (see Figure 3.42 for a schematic of these structures). These factors could explain why the published base and acid protocol is suitable to produce microcapsules from *Lycopodium clavatum* spores but not *Secale cereale* pollen.

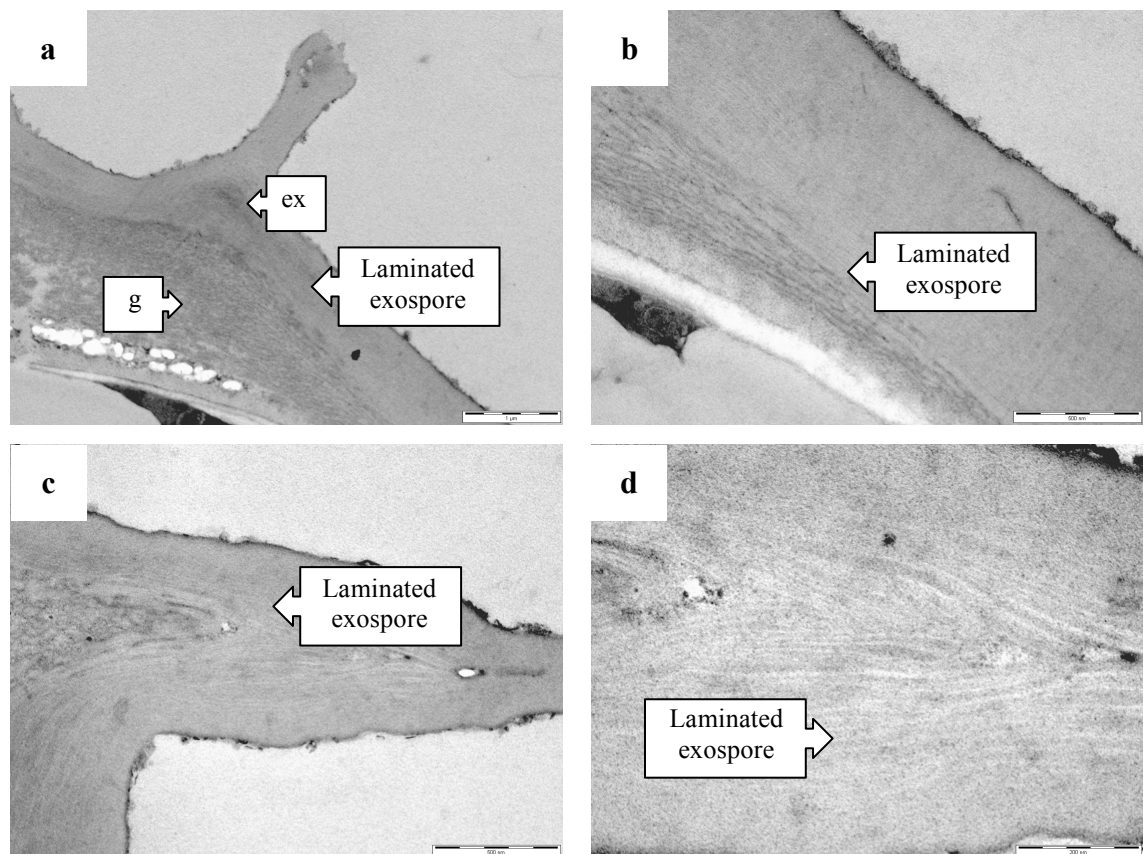


Figure 3.40: Transmission electron micrographs of untreated *Lycopodium clavatum* spores, highlighting their laminated exospore.

Scale bar (a) = 1 μm ; (b) & (c) 500 nm; and (d) 200 nm. ex = exospore; and g = exospore granular layer

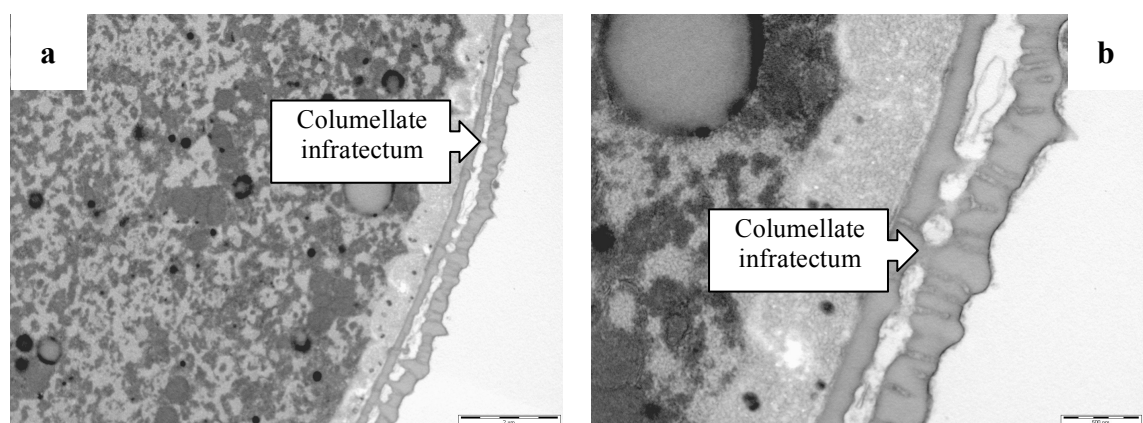


Figure 3.41: Transmission electron micrographs of untreated *Secale cereale* pollen, highlighting its columellate infratectum.

Scale bars: (a) = 2 μm and (b) = 500 nm

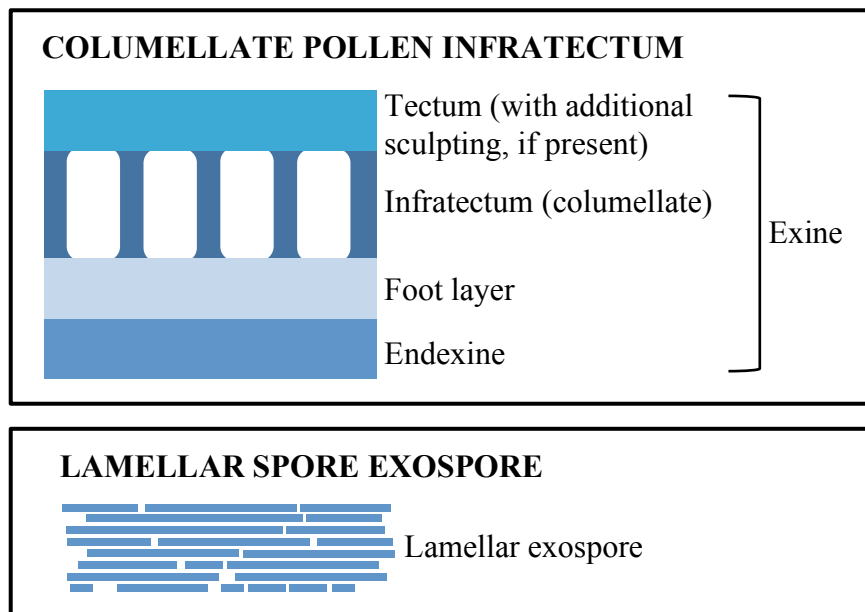


Figure 3.42: Schematic representing the columellate exine of *Secale cereale* pollen and the lamellar exospore of *Lycopodium clavatum* spores

Bolick and Vogel postulate that pollen originating from low humidity environments is exposed to greater dehydration stresses, meaning that grains have stronger exines.¹²⁸ However, that paper did not evaluate how humidity influences the wall strength of spores. *Lycopodium clavatum* requires a humid atmosphere for successful growth, whereas *Secale cereale* is drought-tolerant.¹²⁹ Therefore, according to this theory, *Secale cereale* pollen should have a stronger wall. As this is not the case, Bolick and Vogel's theory does not seem applicable when comparing the wall strength of *Secale cereale* pollen to that of *Lycopodium clavatum* spores.

3.4.3 Base and acid treatment applied to *Juglans nigra* pollen

Untreated *Juglans nigra* pollen (Figure 3.43) was compared to *Juglans nigra* pollen stirred in acetone at reflux for 6 hours (step 1, Figure 3.24) via light microscopy (Figure 3.44). Grains appear unchanged when compared to untreated pollen. After step 2, a majority of the grains are transparent, indicating that protoplast material has been removed, but a large proportion of grains are also cracked (Figure 3.45). In addition, a number of grains seem misshapen and have not retained their outline shape, and it is also evident that some grains still contain protoplast material. The grains are surrounded by debris; possibly the result of the degradation of non-sporopollenin components.

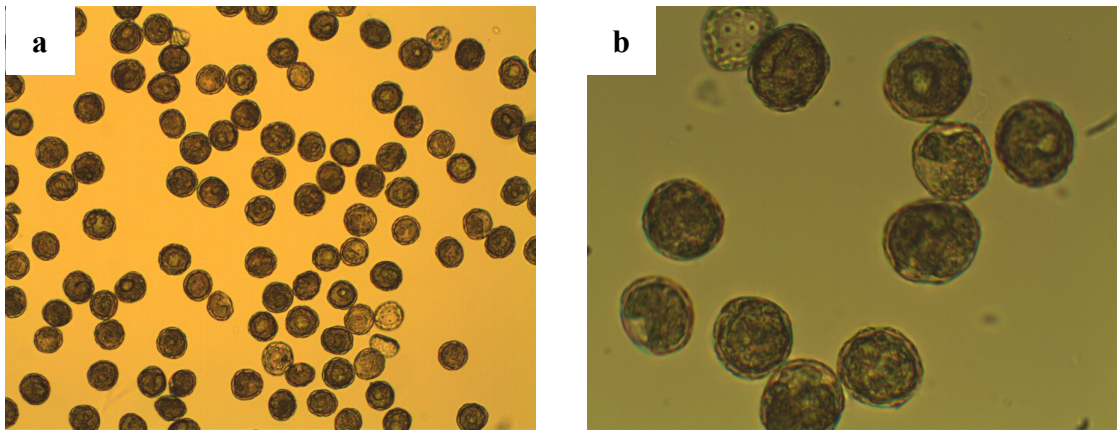


Figure 3.43: Light micrographs of untreated *Juglans nigra* pollen ((a) $\times 100$ and (b) $\times 400$ magnification)

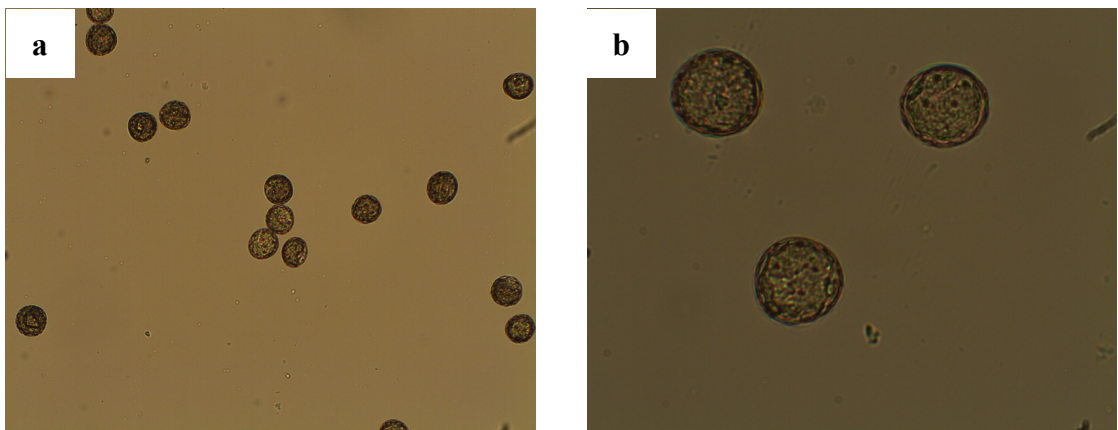


Figure 3.44: Light micrographs of *Juglans nigra* pollen after step 1 ((a) $\times 100$ and (b) $\times 400$ magnification)

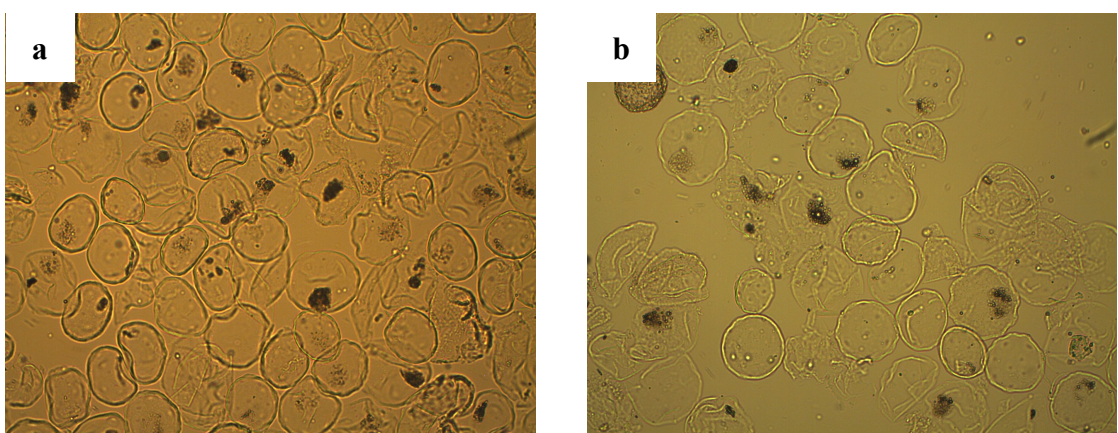


Figure 3.45: Light micrographs of *Juglans nigra* pollen after step 2 ((a) and (b) $\times 100$ magnification)

After step 3, *Juglans nigra* pollen is unrecognisable and the grains have broken down into dark brown ‘sheets’ of material, although it is possible to observe the occasional

ruptured grain in the preparation (Figure 3.46). Step 4 was not attempted, as it was clear that acid treatment would not result in intact pollen microcapsules. As a result, the base and acid treatment protocol proposed by Atkin *et al.* cannot be considered suitable for *Juglans nigra* pollen without further modification.

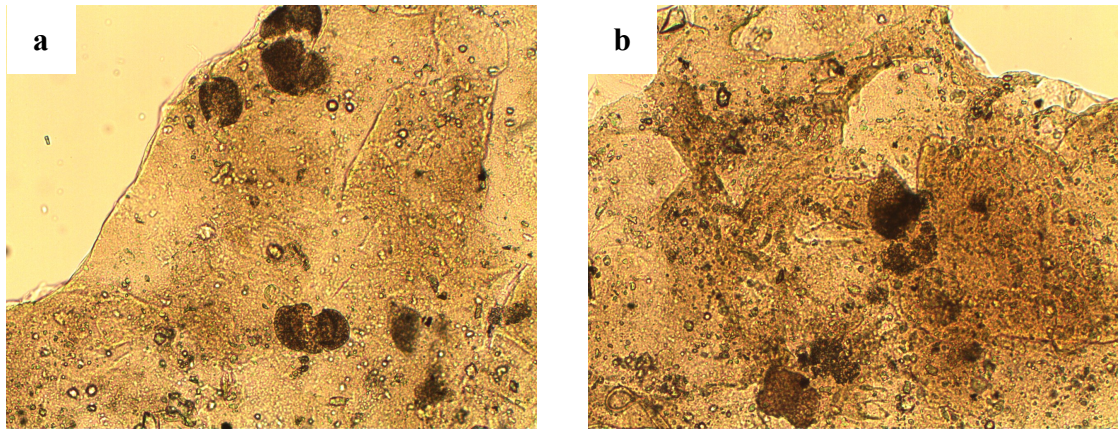


Figure 3.46: Light micrographs of *Juglans nigra* pollen after step 3 ((a) and (b) $\times 100$ magnification)

To determine whether temperature was influential in damaging grains, step 2 was repeated, but at room temperature rather than at reflux. After 4 h 30 min, a sticky brown suspension was observed that was difficult to inspect *via* light microscopy, at least in part because of the aggregation of the grains (Figure 3.47). The sample taken contained a mixture of damaged and intact grains, in a similar manner to pollen heated at reflux (Figure 3.45). This indicates that reflux conditions are unlikely to have contributed to the damage to *Juglans nigra* pollen during base treatment. Without further analysis, it is impossible to determine what caused the ‘stickiness’ of this sample. It may be that base treatment alters the surface of the grains, making them soft and tacky. Alternatively, this treatment may result in an increase in electrostatic attraction between grains.

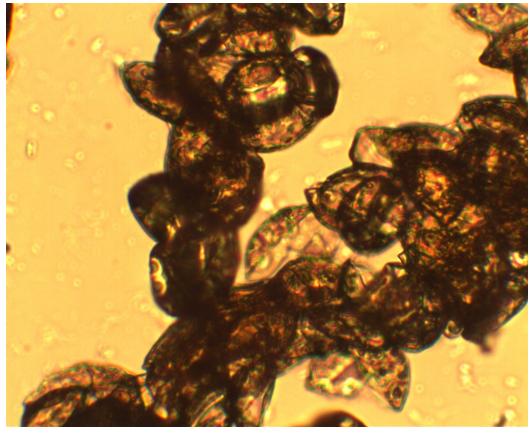


Figure 3.47: Light micrograph of *Juglans nigra* pollen after step 2 (4 h 30 min, room temperature) ($\times 400$ magnification)

Repeating step 2 at reflux but without stirring resulted in pollen grains that contain more protoplast material (Figure 3.48), compared to the same stirred sample (Figure 3.45). In addition, *Juglans nigra* pollen that was not stirred during step 2 is less misshapen compared to the stirred pollen. These results indicate that stirring during step 2 helps to remove protoplast material, but does cause some of the damage to grains. However, potassium hydroxide is probably the factor that causes the most damage to the exine of *Juglans nigra* pollen during base treatment. *Juglans nigra* possesses a granular infratectum (Figure 3.49), which may be structurally weaker in comparison to the lamellar exospore of *Lycopodium clavatum* spores (Figure 3.42). This could explain why *Lycopodium clavatum* is better able to withstand treatment with base, acid and solvent, compared to *Juglans nigra* pollen.

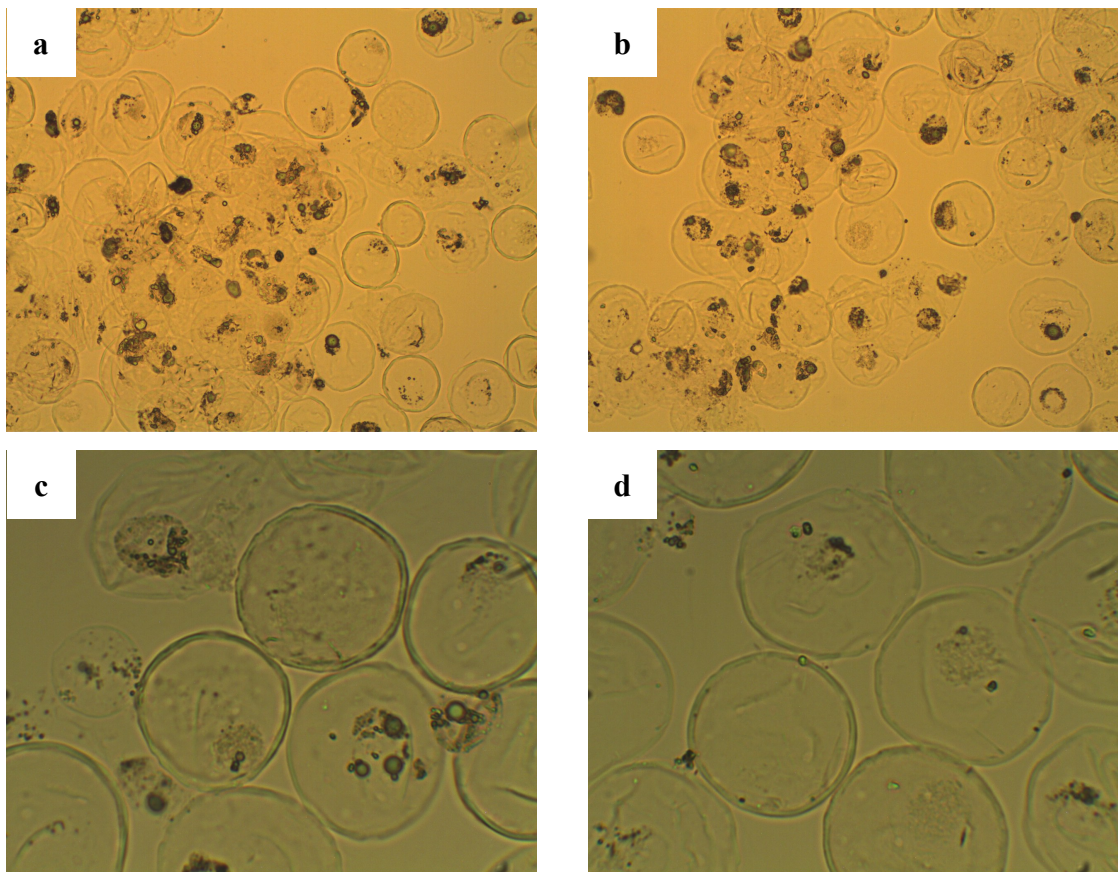


Figure 3.48: Light micrographs of *Juglans nigra* pollen after step 2 (6 h, without stirring). ((a) and (b) $\times 100$ and (c) and (d) $\times 400$ magnification)

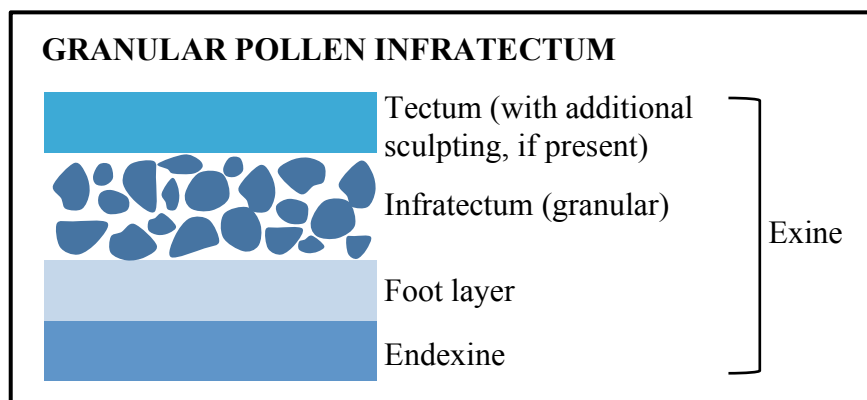


Figure 3.49: Schematic representing the granular infratectum of *Juglans nigra* pollen

3.4.4 Base and acid treatment applied to *Ambrosia artemisiifolia* pollen

The method proposed by Fletcher *et al.* to produce sporopollenin exine shells from *Ambrosia trifida* (giant ragweed) pollen was applied to *Ambrosia artemisiifolia*

(common ragweed) pollen (see Figure 3.25 for an overview of this method).¹²⁴ Light microscopy was used to compare untreated pollen (Figure 3.50) to pollen after step 1 (Figure 3.51). Light microscopy demonstrates that after step 1, pollen is unchanged compared to untreated pollen. After step 3, the products were again examined by light microscopy and not all grains remained intact (Figure 3.52). Some grains appear completely destroyed (Figure 3.52 (a)), whereas others retain some of their structure (Figure 3.52 (b), (c) and (d)). Treatment with acetone, base and ethanol did not appear to remove all protoplast material (Figure 3.52 (d)), suggesting that acid is necessary for such removal. However, the damage caused by steps 1 to 3 was deemed too great to allow the production of microcapsules following this method, so the final acid step (step 4) was not attempted. Fletcher *et al.* did not publish light micrographs, scanning electron micrographs or transmission electron micrographs to report the effects of base and acid treatment on *Ambrosia trifida*. Therefore, it is impossible to evaluate how the results reported in this thesis compare with published results.

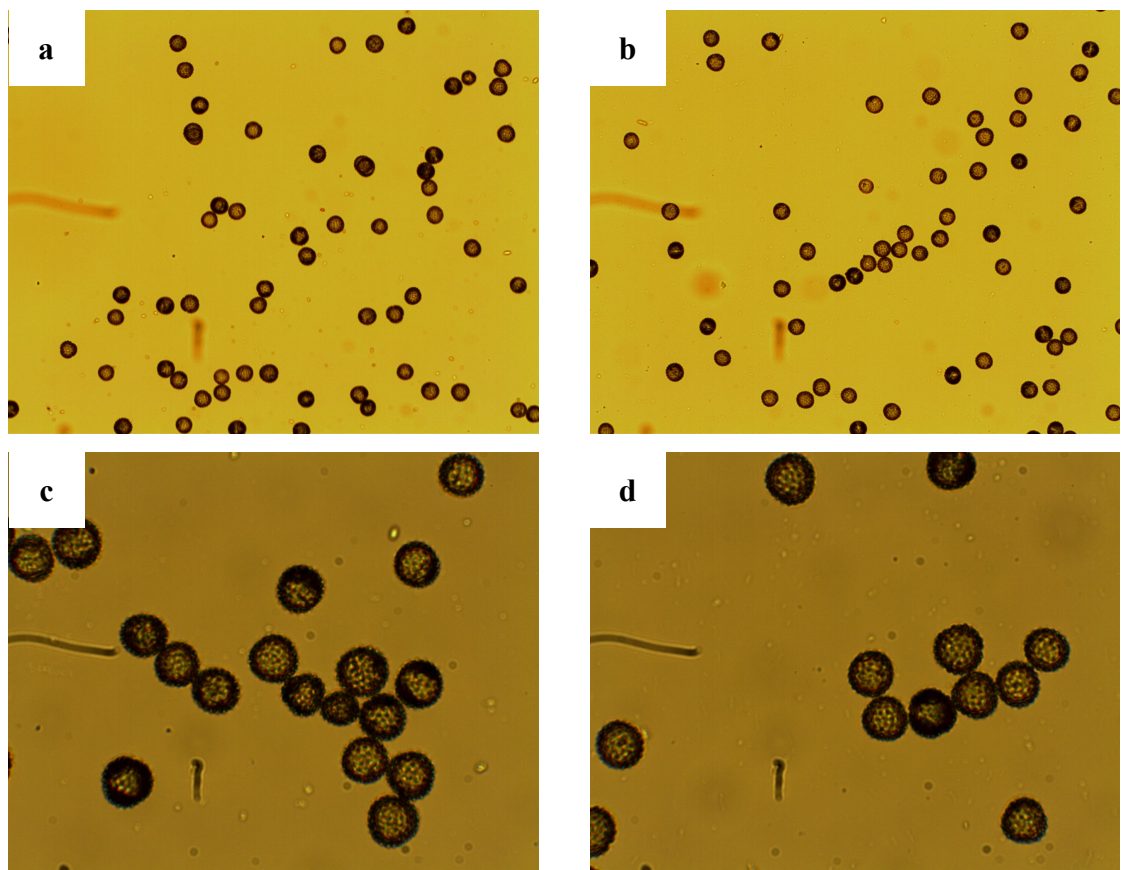


Figure 3.50: Light micrographs of untreated *Ambrosia artemisiifolia* pollen ((a) and (b) $\times 100$ magnification; (c) and (d) $\times 400$ magnification)

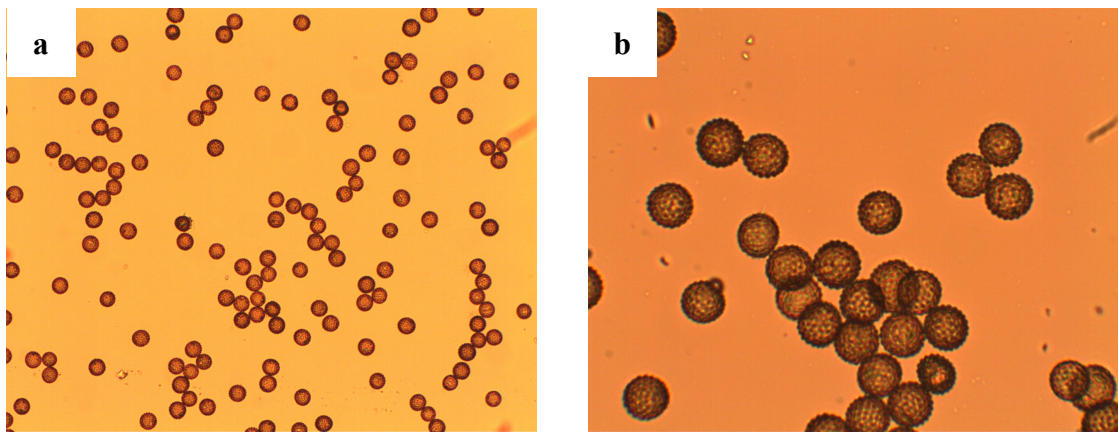


Figure 3.51: Light micrographs of *Ambrosia artemisiifolia* pollen after step 1 ((a) $\times 100$ and (b) $\times 400$ magnification)

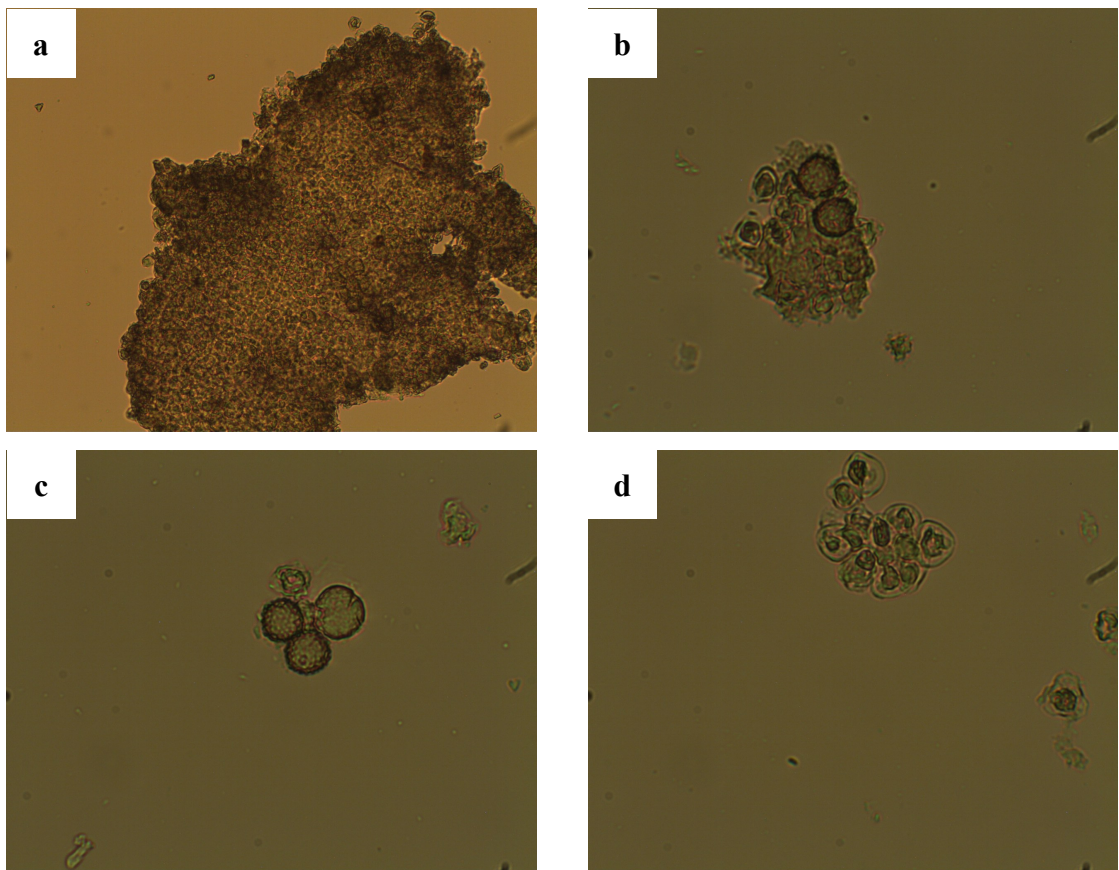


Figure 3.52: Light micrographs of *Ambrosia artemisiifolia* pollen after step 3 ((a) $\times 100$ and (b), (c) and (d) $\times 100$ magnification)

The published method used to produce microcapsules from *Ambrosia trifida* (or in this case, *Ambrosia artemisiifolia*) pollen could be considered more ‘gentle’ than the similar method, also published by Fletcher *et al.*, to produce microcapsules from *Lycopodium clavatum* spores.^{57, 124} Base treatment steps applied to this species of pollen were shorter, so it is intuitive that any chemical damage would be reduced. In addition, as

pollen was stirred for a shorter period, damage caused by the action of stirring could be predicted to be diminished. However, it appears that even these modifications were not sufficient to enable the production of microcapsules from pollen.

Ambrosia artemisiifolia has a columellate infratectum (Figure 3.53). This could be considered weak in comparison to the lamellar exospore of *Lycopodium clavatum* spores, which were able to withstand treatment with base and acid. *Ambrosia artemisiifolia* pollen possesses a laminated endexine (although this was difficult to make out during TEM analysis (see section 3.2.4), which would have been expected to impart strength to the pollen, in a similar way to the lamellar exospore of *Lycopodium clavatum*. However, this does not appear to have been the case. In order to produce microcapsules from *Ambrosia artemisiifolia* pollen, alternative methods need to be developed, or the base and acid treatment proposed here further modified.

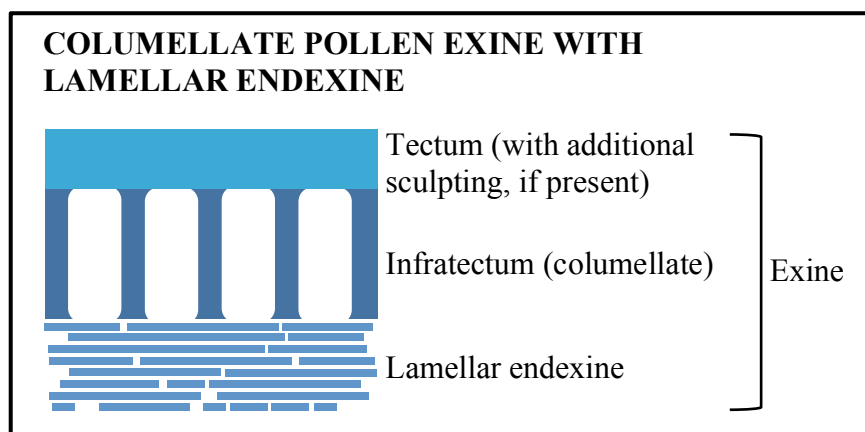


Figure 3.53: Schematic representing the columellate infratectum and lamellar endexine of *Ambrosia artemisiifolia* pollen

3.4.5 Base and acid treatments: summary of results

1. Microcapsules were successfully produced from *Lycopodium clavatum* spores using the method published by Atkin *et al.*⁵⁷ However, the same protocol applied to *Secale cereale* and *Juglans nigra* pollen damaged the pollen so considerably that the acid step was not attempted.
2. Light micrographs indicated that it was the base treatment step rather than treatment with acetone that initiated damage to pollen. Applying the base treatment

(step 2) at room temperature or without stirring did not reduce the amount of damage to *Secale cereale* pollen, suggesting that potassium hydroxide caused the majority of the damage observed. Increased levels of protoplast material were observed inside grains in un-stirred samples. Similar results were observed with *Juglans nigra* pollen.

3. Microcapsules were not successfully produced from any of the pollen species via the method proposed by Atkin *et al.*, despite modifications.¹²⁴ Neither could microcapsules be synthesised from *Ambrosia artemisiifolia* pollen using the method published by Fletcher *et al.*¹²⁴ Base treatment resulted in damaged grains that would be unsuitable for use as microcapsules. Therefore, it may be prudent to evaluate other methods, for example enzyme treatments that may selectively remove all non-sporopollenin material without damaging the exine.

3.5 Treatments involving enzymes

Treatments involving enzymes have been used to remove non-sporopollenin material from pollen to produce sporopollenin for both chemical and microscopic analysis.^{64, 65, 130, 131} A study using light microscopy published by Loewus *et al.* suggests that intact exine shells can be obtained from a range of pollen species using 4-methylmorpholine *N*-oxide (MMNO) and cyclohexylamine (CHA) (Figure 3.54), in combination with enzymes and bovine serum albumin (BSA).⁶⁴ The primary aim of that study was to obtain exine material for structural and chemical analysis, rather than producing intact pollen microcapsules. Up to now, no enzymatic methods have been reported that have the primary aim of producing microcapsules from pollen. In this chapter, the method published by Loewus *et al.* was evaluated for its suitability to produce microcapsules from range of pollen species, belonging to a variety of taxonomic families. *Secale cereale* (rye), *Juglans nigra* (black walnut) and *Betula fontinalis* (water birch) pollen were selected as they come from different families (Poaceae, Juglandaceae and Betulaceae respectively) and are therefore likely to exhibit different chemical and structural properties.

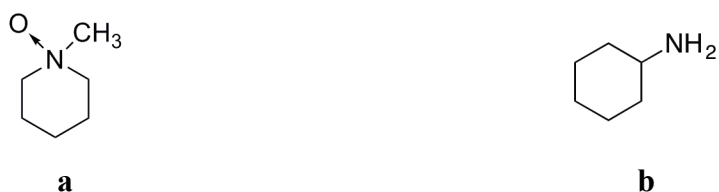


Figure 3.54: Structure of (a) 4-methylmorpholine *N*-oxide (MMNO) and (b) cyclohexylamine (CHA)

The general procedure used is summarised in Figure 3.55. An aqueous solution of MMNO and CHA was used in an attempt to break the bond between the exine and intine.¹⁴ This solution was placed into the glass mortar of a Potter-Elvehjem tissue grinder (Figure 3.56). A polytetrafluoroethylene (PTFE) pestle was cycled up and down past the solution inside the mortar to further facilitate the breaking of exine-intine bonds within the pollen. The pollen was then incubated in solution with Cellulysin, Macerace and (BSA), with the aim of digesting protoplasts. Pollen was washed and centrifuged to obtain exine material. In addition to the published method, after step 5 (washing), pollen was filtered through a glass sinter and dried *in vacuo*. This was carried out to obtain dry samples, which could be stored without the potential for bacterial or fungal growth.

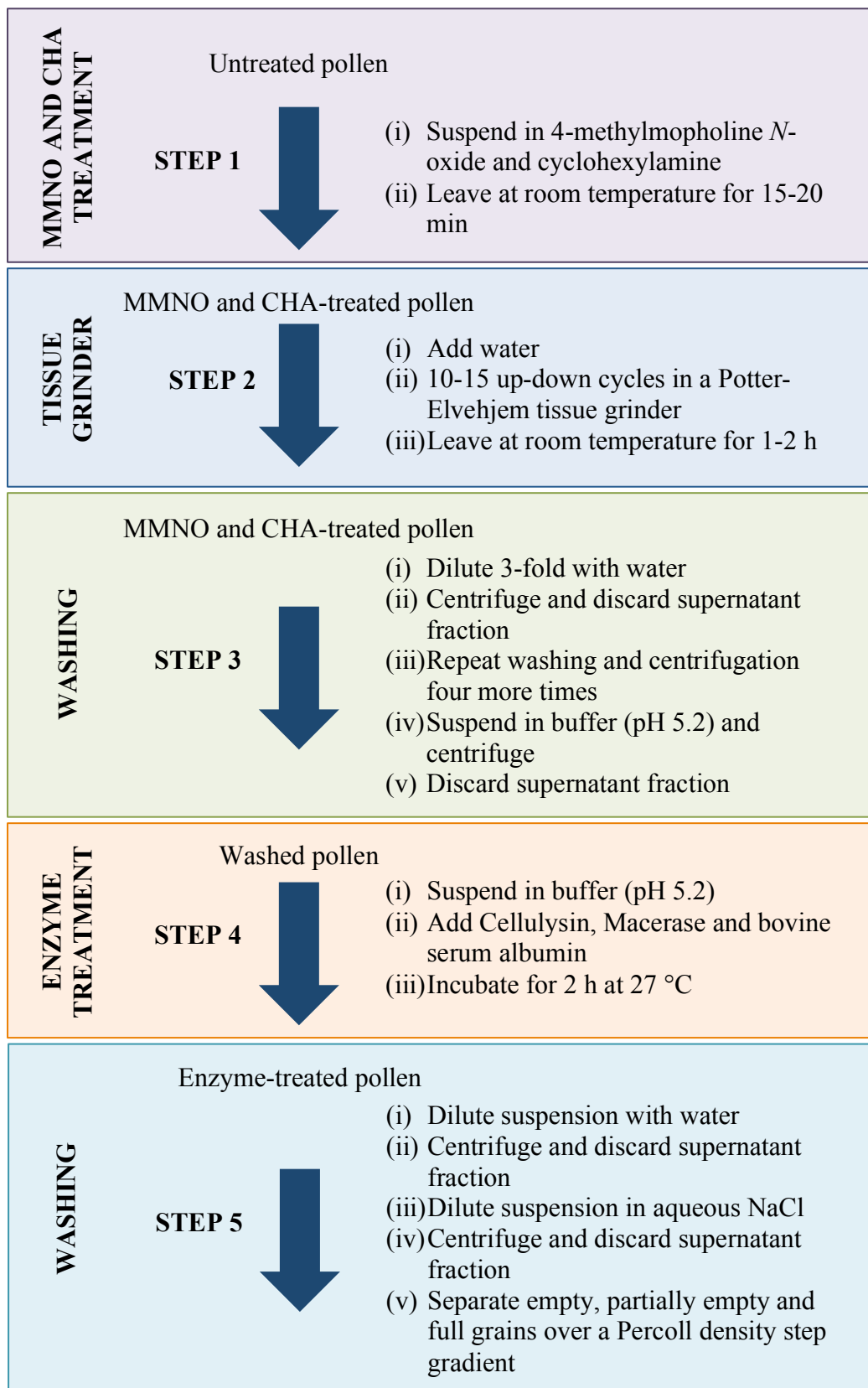








Figure 3.55: Summary of the enzyme method published by Loewus *et al.*⁶⁴



Figure 3.56: Potter-Elvehjem tissue grinder

In an attempt to optimise the published procedure for the species under investigation in this chapter, some of the variables within the published method were altered. The mass of enzymes and (BSA) used, the incubation time in the enzyme solution and the number of pestle cycles performed were all varied. Samples produced were analysed *via* light microscopy. This efficient analytical technique was selected to rapidly screen the large number of samples prepared. Coloured arrows added to the light micrographs highlight features, such as cracked grains, free protoplast material and empty grains. Table 3.1 provides a key to the arrows used. Although Loewus *et al.* claim that the published method is able to remove the intine; the resolution of the light microscope is insufficient to determine whether it is absent or present. As a result, only the pollen wall and protoplast are identifiable in the micrographs. Some samples were analysed in greater detail using transmission electron microscopy (TEM), meaning that sufficient resolution and magnification were achieved in order to evaluate the intine. *Betula fontinalis* was also analysed using laser scanning confocal microscopy (LSCM) to provide information on fluorescent components. Z-stacks were prepared using this technique to provide further information on the location of fluorescent materials within pollen grains.

Table 3.1 Summary of coloured arrows used to highlight features within light micrographs

Arrow colour	Feature identified
	Material ejected through a pore of a pollen grain
	Protoplast detached from pollen wall
	Empty pollen grain
	Partially empty pollen grain
	Cracked or damaged pollen grain
	Free protoplast material

3.5.1 Enzyme treatment applied to *Juglans nigra* pollen

The enzyme method summarised in Figure 3.55 was applied to *Juglans nigra* pollen. Ten pestle cycles were performed. The pollen was incubated in the enzyme suspension for a total of 42 h in an attempt to maximise the amount of protoplast material removed. Light microscopy was used to compare untreated pollen (Figure 3.57) to samples of enzyme-treated pollen taken at 16 h and 42 h (Figure 3.58 and Figure 3.59 respectively). After enzyme treatment, it is clear that some protoplast material has detached from the pollen wall. However, the resolution of the light microscope was insufficient to also determine whether the intine has separated from the exine. Little difference is observed between pollen grains in samples at 16 h and 42 h. However, the amount of motile bacteria observed increased between 16 and 42 h: posing a risk of harming those handling these slides and samples.

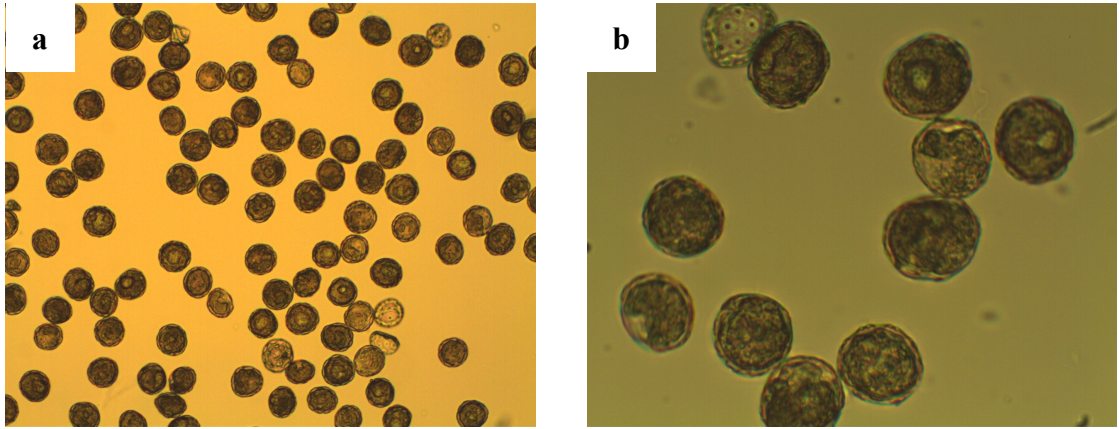


Figure 3.57: Light micrographs of untreated *Juglans nigra* pollen ((a) $\times 100$ and (b) $\times 400$ magnification)

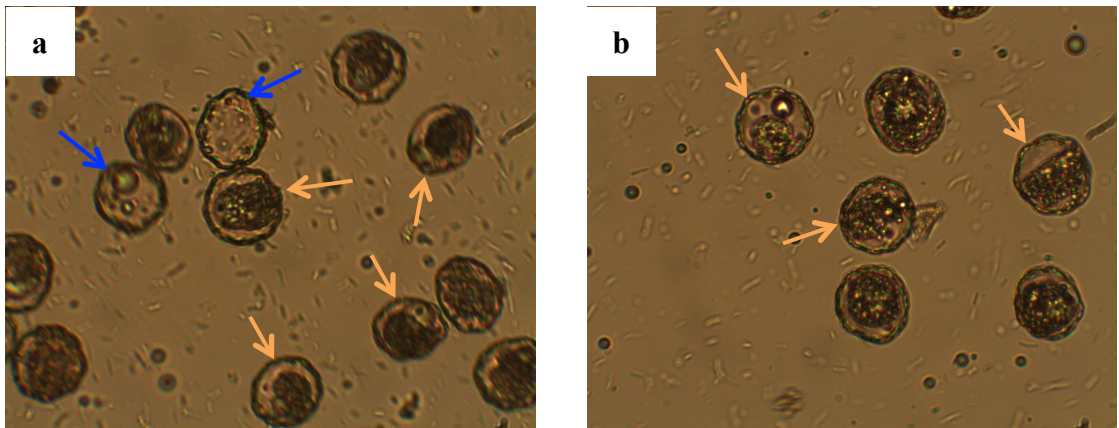


Figure 3.58: Light micrographs of enzyme-treated *Juglans nigra* pollen after step 5 (iv) (ten pestle cycles, 16 h in enzyme suspension) ((a) and (b) $\times 400$ magnification)

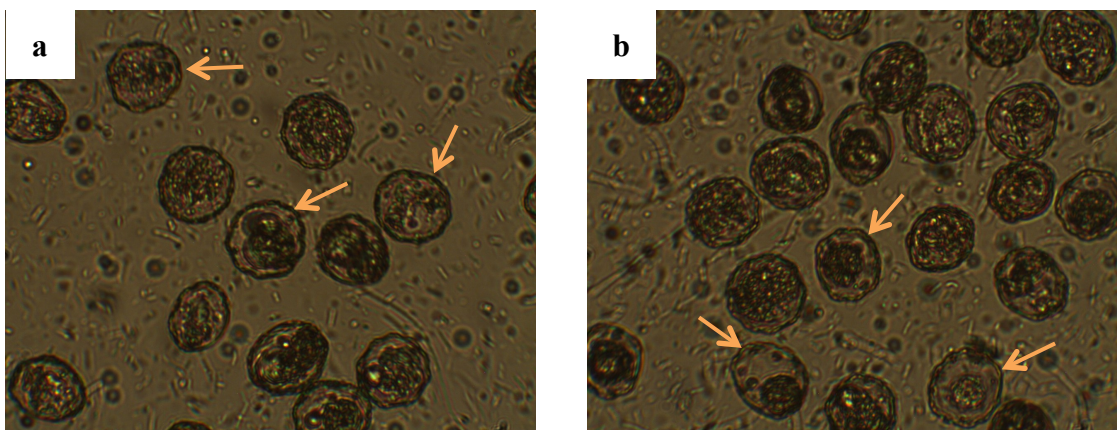


Figure 3.59: Light micrographs of enzyme-treated *Juglans nigra* pollen after step 5 (iv) (ten pestle cycles, 42 h in enzyme suspension) ((a) and (b) $\times 400$ magnification)

Grains were separated over a Percoll density step gradient (step 5 (v)). Loewus *et al.* described that ‘Sporoplasts, free or attached to exine, remained in the first band;

partially emptied tetrads in the second; and completely empty exine walls settled as a pellet together with anther fragments'.⁶⁴ ('Sporoplast' is sometimes used as an alternative to describe the protoplast.) The material recovered as a pellet after centrifugation was examined by light microscopy (Figure 3.60). A majority of grains are transparent and appear empty, and only a small fraction of grains still contain protoplast material. Some cracked grains were identified. However, the amount of material recovered as a pellet was minimal (less than 5 % of the starting material).

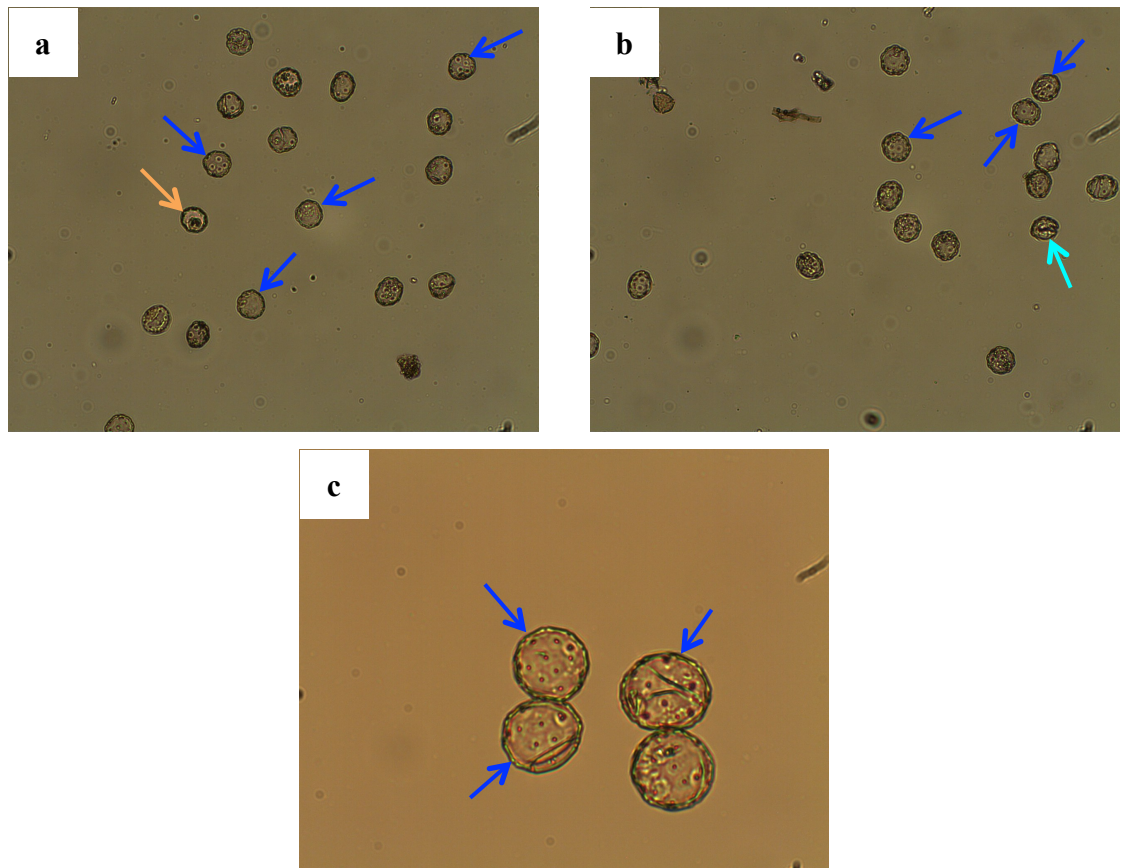


Figure 3.60: Light micrographs of enzyme-treated *Juglans nigra* pollen after step 5 (v) (ten pestle cycles) ((a) and (b) $\times 100$ magnification, and (c) $\times 400$ magnification)

Loewus *et al.* centrifuged samples during step 5 (v) at $3000 \times g$, where the term g represents the relative centrifugal force.¹³² However, the centrifuge (Fisher Scientific accuspinn 400) used during the preparation of samples during the work presented here was only rated to $2590 \times g$ (4000 rpm). In order to ensure its safe operation, the centrifuge was set to 75 % of its maximum rotor speed (3000 rpm, $1459 \times g$). As a result, the forces described by Loewus *et al.* were not achieved. This may have contributed to the low yield. However, Figure 3.59 indicates that a majority of grains were not empty after enzyme treatment, so a high yield was not anticipated.

The Percoll density gradient was difficult and time-consuming to prepare and provided only limited information about the success of the enzyme method; in particular if any empty grains were collected. However, such information could be gleaned without the need for a density gradient. As a result, the density gradient step (step 5 (v)) was omitted from further attempts to replicate the published enzyme method.

To test the effect of the number of pestle cycles performed, the number of cycles applied during step 2 (ii) was increased from ten to thirty. *Juglans nigra* pollen was incubated in the enzyme suspension (step 4 (ii)) for 20 h in an attempt to maximise the effect of the enzymes. Light microscopy (Figure 3.61) indicates no substantial difference in samples to those when only ten pestle cycles were applied (Figure 3.58 and Figure 3.59), suggesting that increasing the number of pestle cycles does not increase the amount of protoplast material removed from this species.

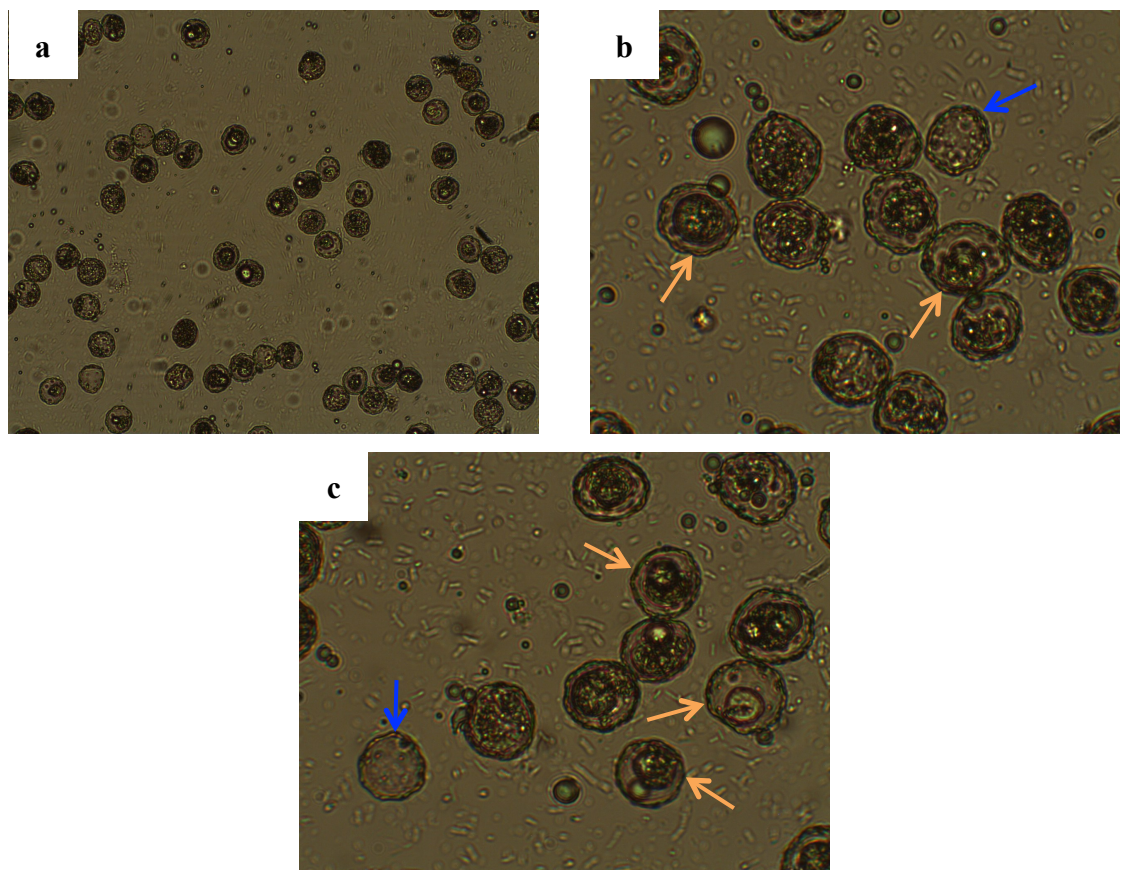


Figure 3.61: Light micrographs of enzyme-treated *Juglans nigra* pollen after step 5 (iv) (thirty pestle cycles, 20 h in enzyme suspension) ((a) $\times 100$ magnification, and (b) and (c) $\times 400$ magnification)

To evaluate the influence of the enzymes and BSA on this species, The mass of both was doubled, and the enzyme method was again applied to *Juglans nigra* pollen. Ten pestle cycles were carried out and pollen was incubated in the enzyme suspension for a total of 48 h. Samples were taken for analysis by light microscopy at 24 h (Figure 3.62) and 48 h (Figure 3.63). After 24 h, most grains still contained protoplast material, but this decreased after 48 h. Despite increasing the mass of enzymes used and the incubation period in the enzyme suspension, not all protoplast material was removed from all grains.

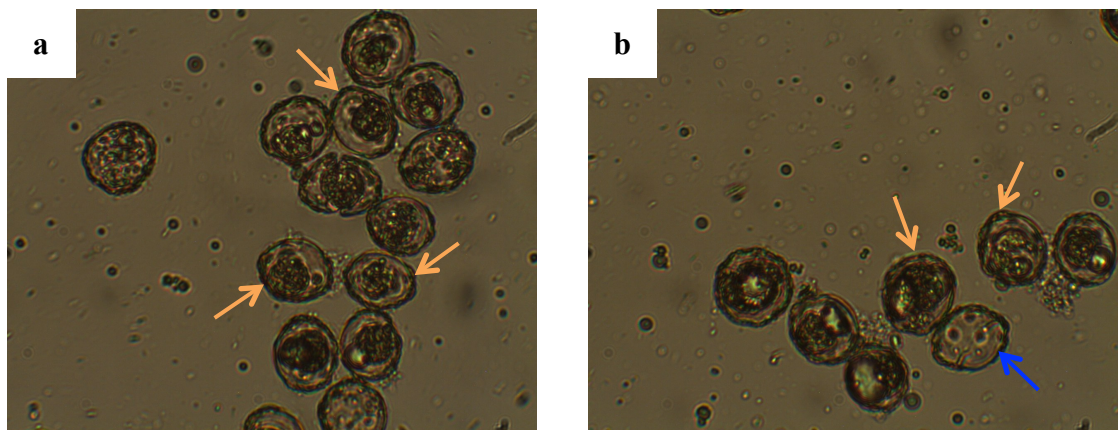


Figure 3.62: Light micrographs of enzyme-treated *Juglans nigra* pollen after step 5 (iv) (ten pestle cycles, 24 h in doubled mass of enzyme suspension) ((a) and (b) $\times 400$ magnification)

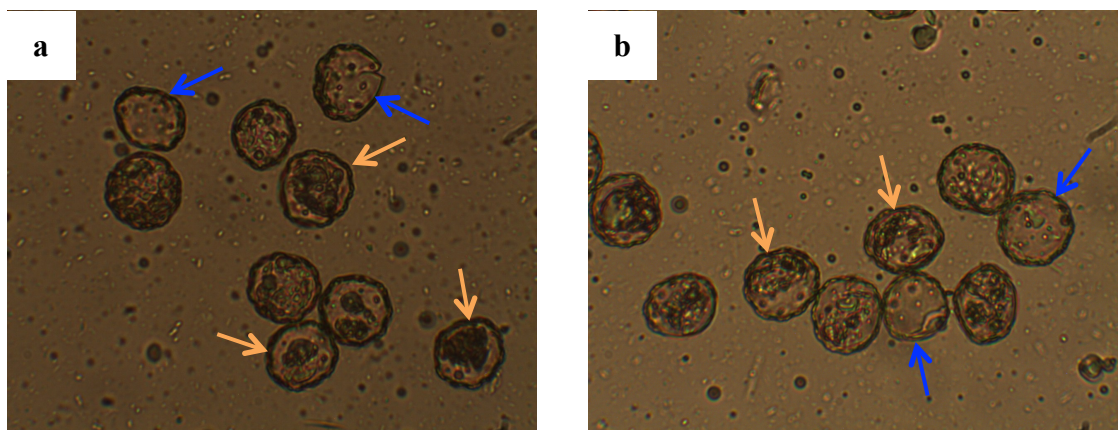


Figure 3.63: Light micrographs of enzyme-treated *Juglans nigra* pollen after step 5 (iv) (ten pestle cycles, 48 h in doubled mass of enzyme suspension) ((a) and (b) $\times 400$ magnification)

The mass of enzymes and (BSA) used, the number of pestle cycles applied and the incubation time were varied. Although all protoplast material was removed from a

limited number of grains, microcapsules could not be successfully produced in large quantities from *Juglans nigra* pollen using the method proposed by Loewus *et al.*, or by applying modified versions of this method.

3.5.2 Enzyme treatment applied to *Betula fontinalis* pollen

Betula fontinalis pollen (Figure 3.64) was treated according to the enzyme protocol summarised in Figure 3.55. Ten pestle cycles were performed and the products examined by light microscopy after step 3 (v) (Figure 3.65). Analysis was carried out at this stage in an attempt to determine the effects of CHA, MMNO and cycles within the tissue grinder on pollen. A small amount of protoplast material can be seen being ejected through the pores of the pollen, but the grains still appear similar to untreated pollen, in that they still contain protoplasts. After treatment with enzymes (step 5 (iv)) grains remain unchanged (Figure 3.66), although no more protoplast material is seen exiting through the pores. Grains still clearly contain non-sporopollenin material.

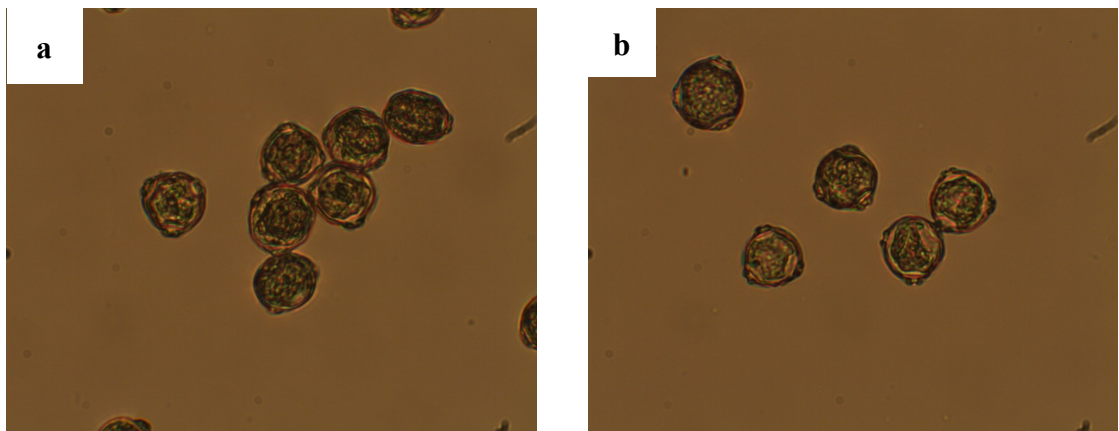


Figure 3.64: Light micrographs of untreated *Betula fontinalis* pollen ((a) and (b) $\times 400$ magnification)

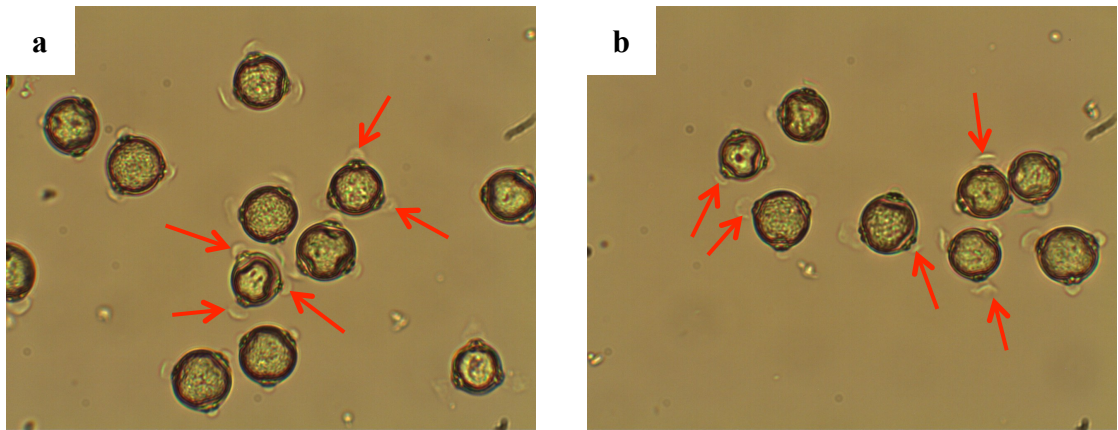


Figure 3.65: Light micrographs of MMNO and CHA-treated *Betula fontinalis* pollen after step 3 (v) (ten pestle cycles) ((a) and (b) $\times 400$ magnification)

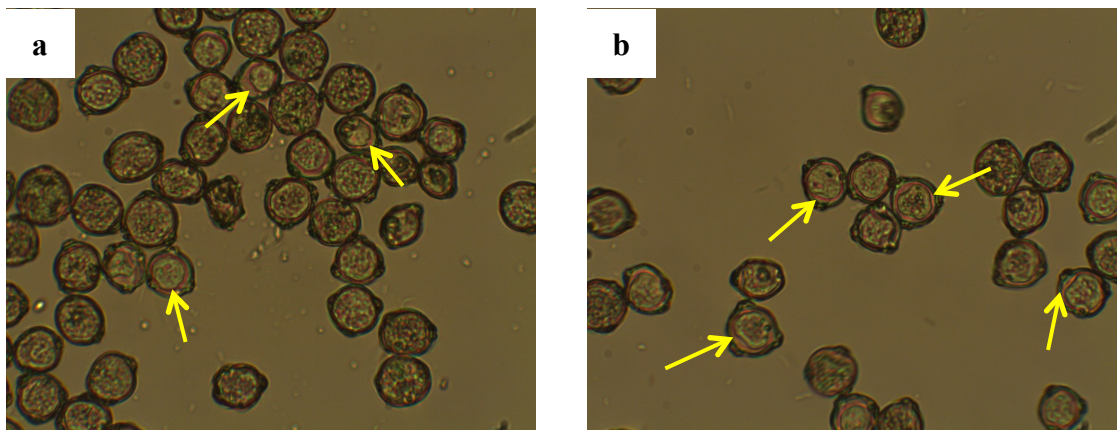


Figure 3.66: Light micrographs of enzyme-treated *Betula fontinalis* pollen after step 5 (iv) (ten pestle cycles) ((a) and (b) $\times 400$ magnification)

The number of pestle cycles performed during step 2 was increased to 30 to try to further detach the exine from the intine, thereby making the release of the protoplast easier. Light microscopy was carried out after step 3 (iv), and although most grains remain intact, a number of cracked grains with associated protoplast material are observed (Figure 3.67) This suggests that increasing the number of pestle cycles increases the probability of damage to grains. After step 5 (iv), almost all grains still seem to contain protoplasts, although most appear detached from the pollen wall (Figure 3.68).

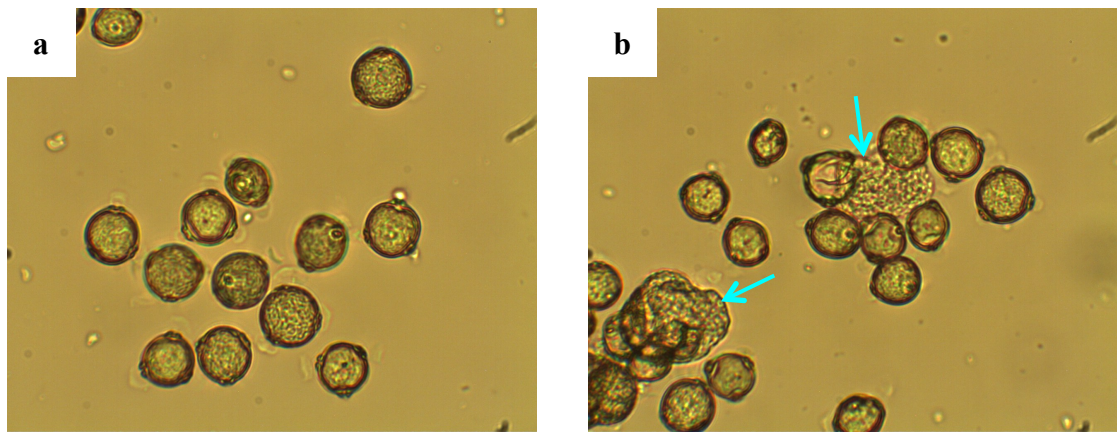


Figure 3.67: Light micrographs of MMNO and CHA-treated *Betula fontinalis* pollen after step 3 (iv) (thirty pestle cycles) ((a) and (b) $\times 400$ magnification)

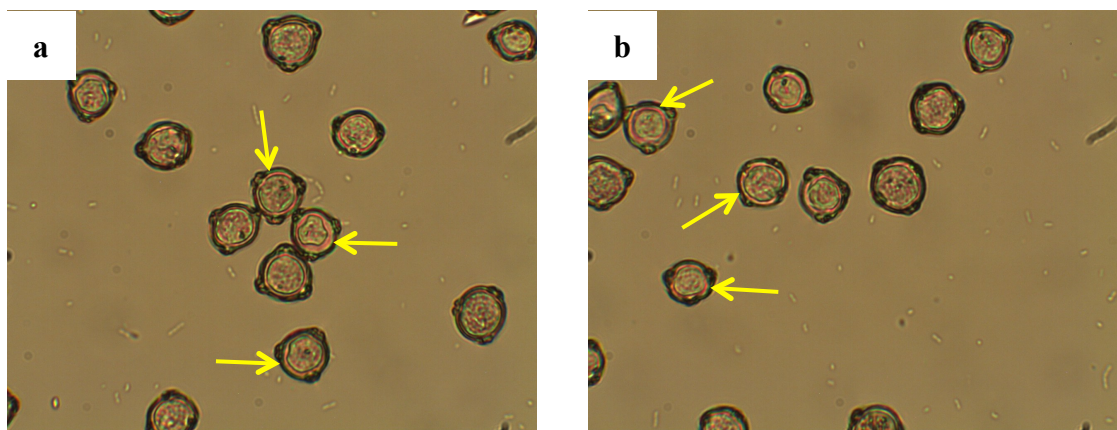


Figure 3.68: Light micrographs of enzyme-treated *Betula fontinalis* pollen after step 5 (iv) (thirty pestle cycles) ((a) and (b) $\times 400$ magnification)

Transmission electron micrographs of untreated *Betula fontinalis* pollen (Figure 3.69) were compared to those taken of pollen after step 5 (iv) (30 pestle cycles) (Figure 3.70). Results indicate that most grains are intact after treatment and contain varying quantities of protoplast material. When comparing untreated pollen with enzyme-treated pollen, some protoplast material appears to have been digested and is detached from the pollen wall. The exine appears unchanged, with the tectum, infratectum and foot layer still present. In some grains, the intine is still present (Figure 3.70, (f)), but in others it seems to have been removed (Figure 3.70, (g)). The onci appear to have been removed by the enzyme treatment. Biological material of unknown origin is present in some grains (Figure 3.70 (c), (d), (e), (g) and (h)). However, it is not clear whether this material was present before enzyme treatment or whether it entered the grains after treatment. However, this biological material fits within the expected size range for a bacterium (approximately 0.1 – 50 μm) or fungal spore (approximately 1.5 – 30 μm).^{125, 126}

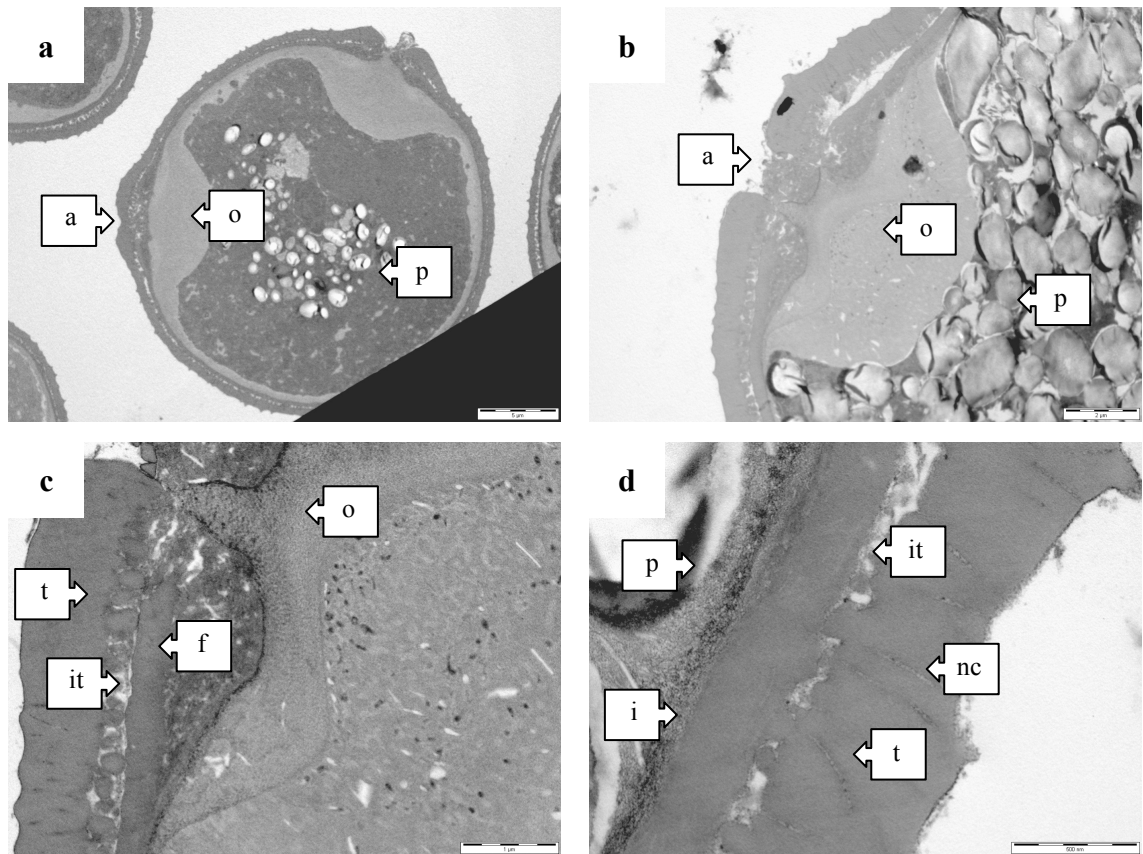


Figure 3.69: Transmission electron micrographs of untreated *Betula fontinalis* pollen.

Scale bars: (a) = 5 μm ; (b) = 2 μm ; (c) = 1 μm ; and (d) = 500 nm

a = aperture; f = foot layer; i = intine; it = infratectum; nc = nano-channel; o = oncus;
p = protoplast; and t = tectum

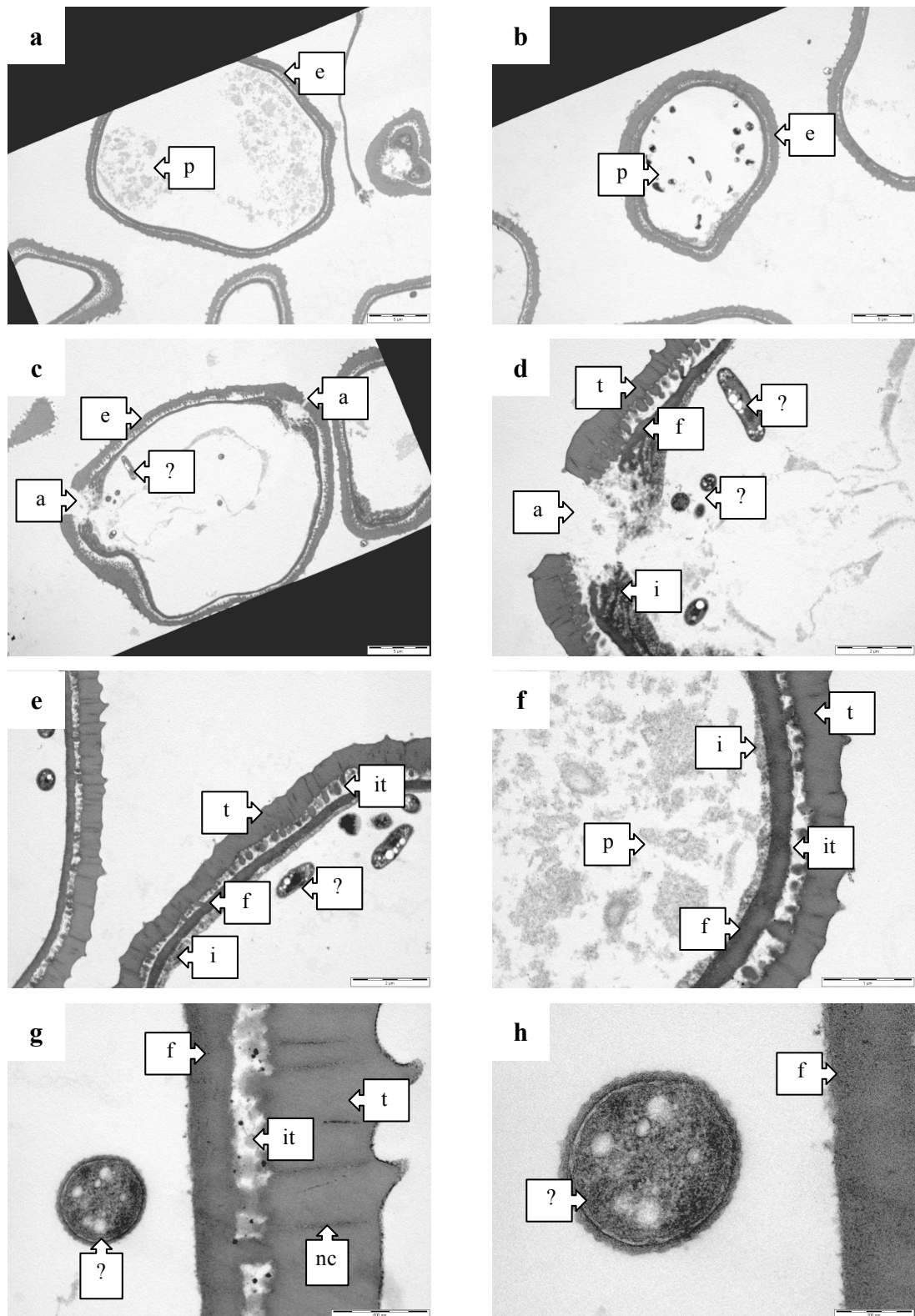


Figure 3.70: Transmission electron micrographs of *Betula fontinalis* pollen after step 5 (iv).

Scale bars: (a), (b) and (c) = 5 μm ; (d) and (e) = 2 μm ; (f) = 1 μm ; (g) = 500 nm; and (h) = 200 nm. ? = biological material of unknown origin; a = aperture; e = exine; f = foot layer; i = intine; it = infratectum; nc = nano-channel; p = protoplast; and t = tectum

Untreated *Betula fontinalis* pollen analysed by LSCM shows grains containing protoplasts (Figure 3.71). Previous palynological analysis of pollen from the same genus (*Betula pendula*) suggests that darker areas observed in the protoplasts of untreated pollen may be starch grains.¹³³ Onco can be clearly distinguished beneath the apertures of grains. LSCM performed after step 5 (iv) provides further evidence that some grains contain protoplast material after enzyme-treatment (Figure 3.72). Excitation at 561 nm clearly shows the pollen wall, and excitation at 405 nm highlights protoplast material detached from this wall. Onco can no longer be distinguished or are not present at all. Directly comparing untreated with enzyme-treated pollen shows that the enzyme treatment appears to remove some protoplast material from *Betula fontinalis* pollen (Figure 3.73).

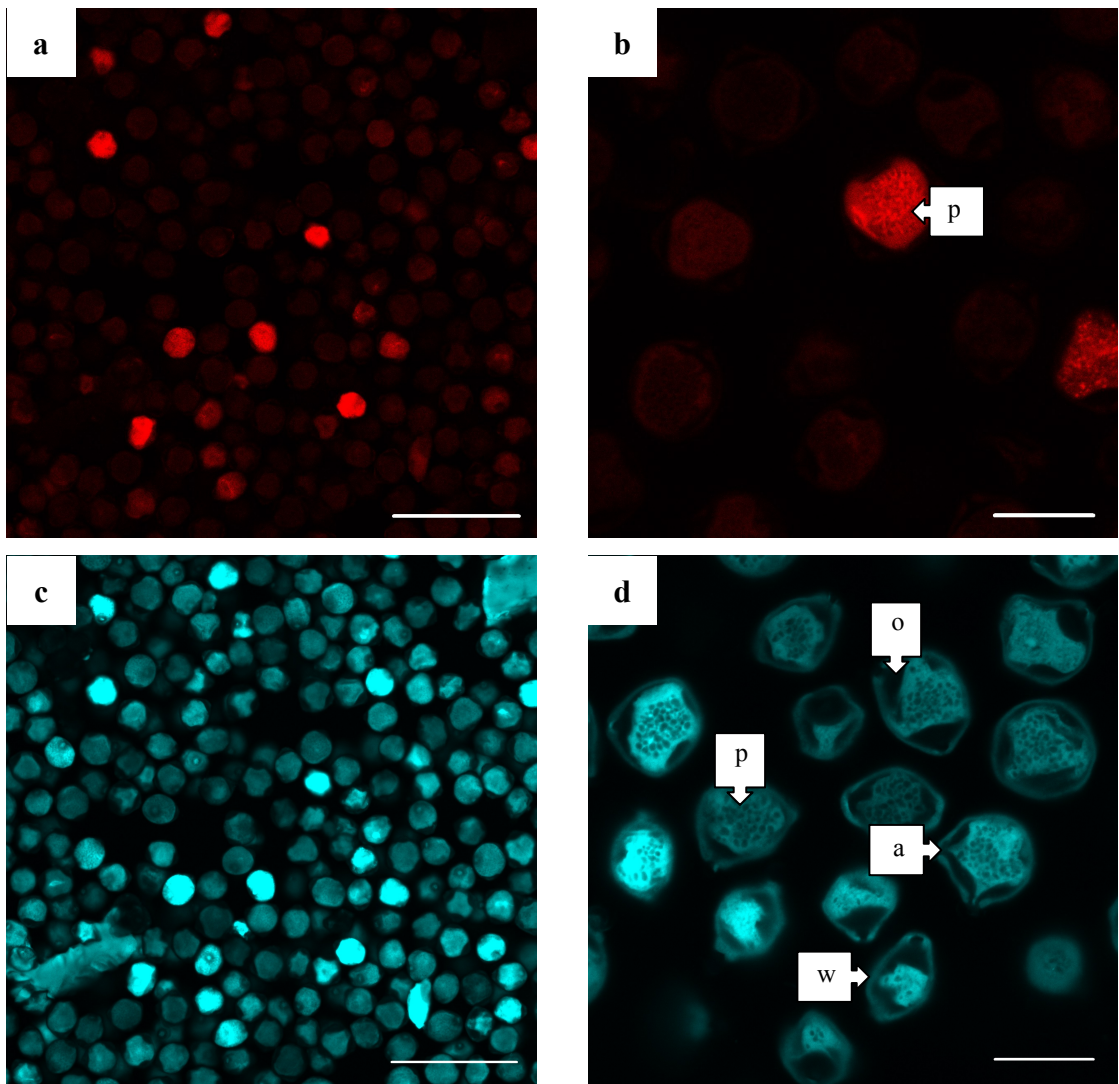


Figure 3.71: LSCM images of untreated *Betula fontinalis* pollen: (a) and (b) excitation wavelength 405 nm; (c) and (d) excitation wavelength 633 nm.

Scale bar: (a) and (c) = 100 μm ; (b) and (d) = 25 μm

a = aperture; o = oncus; p = protoplast; and w = pollen wall

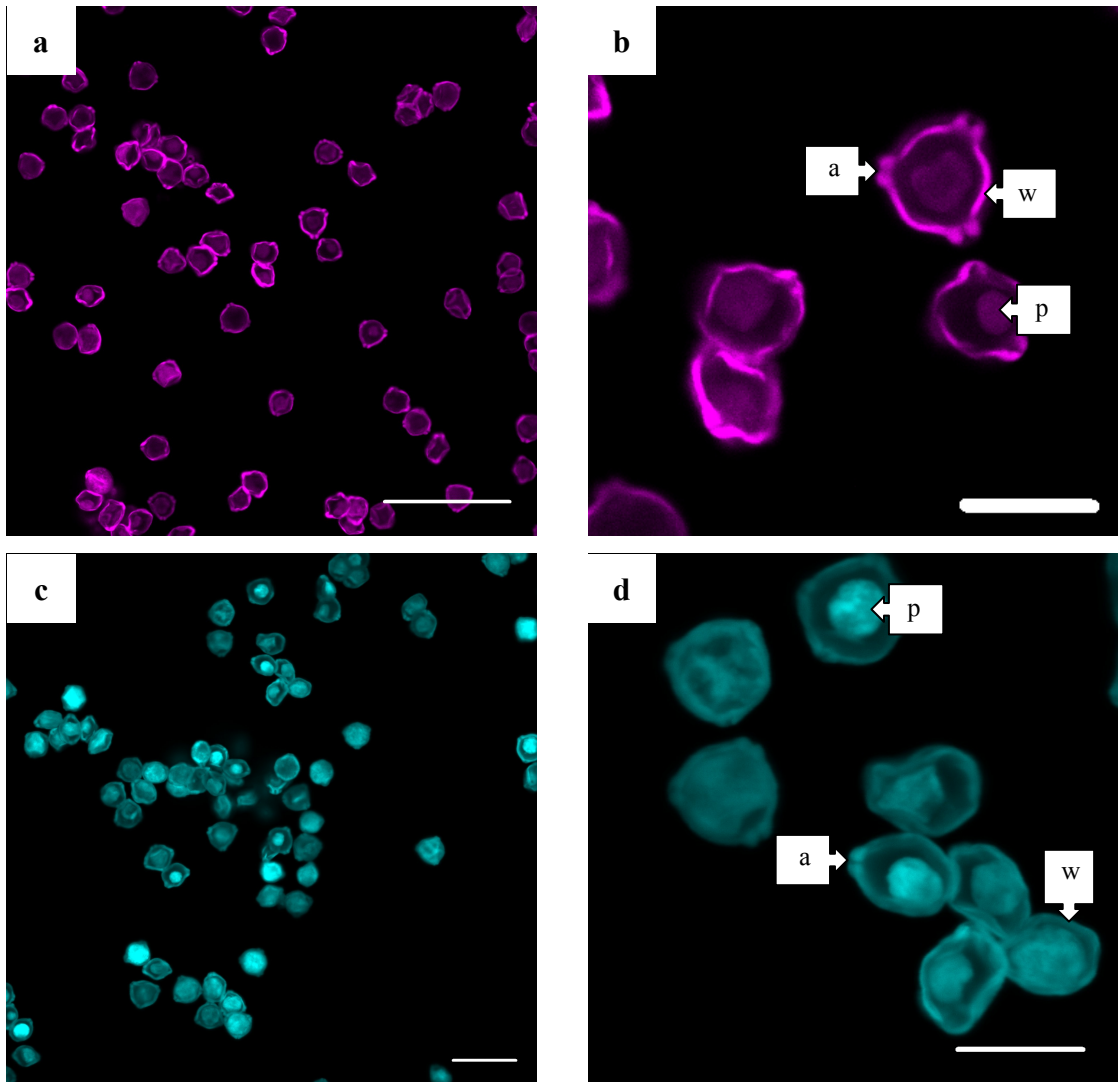


Figure 3.72: LSCM images of *Betula fontinalis* pollen after step 5 (iv): (a) and (b) excitation wavelength 561 nm; (c) and (d) excitation wavelength 405 nm.

Scale bar: (a) = 50 μm ; (b) and (d) = 25 μm ; and (c) = 100 μm

a = aperture; p = protoplast; and w = pollen wall

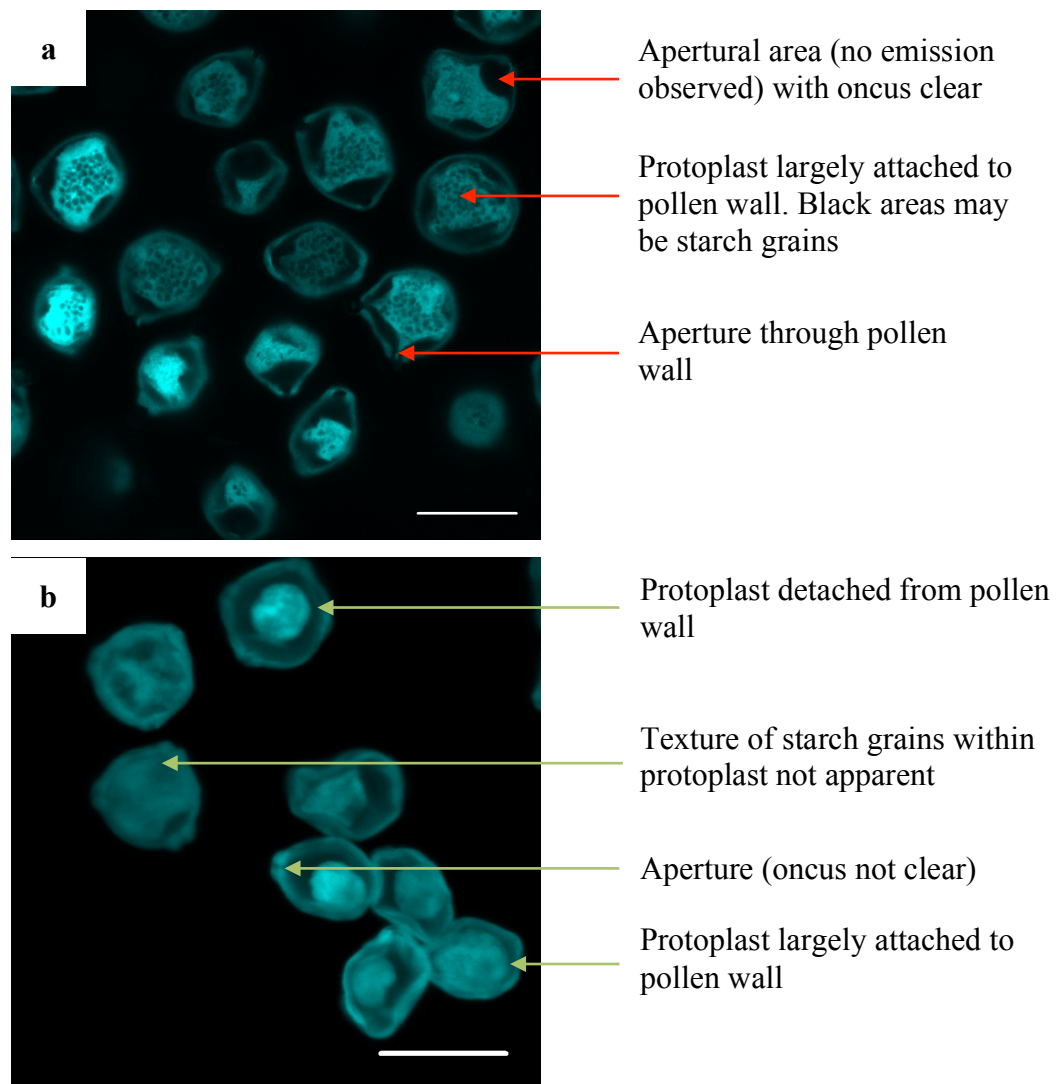


Figure 3.73: LSCM images of *Betula fontinalis* pollen (a) untreated and (b) enzyme-treated, excitation wavelength 405 nm. Scale bars = 25 μm

A z-stack of two pollen grains was taken perpendicularly to the z-axis (Figure 3.74). These images show that throughout the two grains imaged, the protoplasts are no longer bound to the pollen wall. This suggests that the MMNO and CHA treatment was successful in breaking down the pollen wall-intine bond, but the resolution achieved by the LSCM means it is impossible to determine whether or not the exine-intine bond was broken. In addition, a greater number of grains would need to be evaluated to find out whether these conclusions can be applied to the entire sample studied.

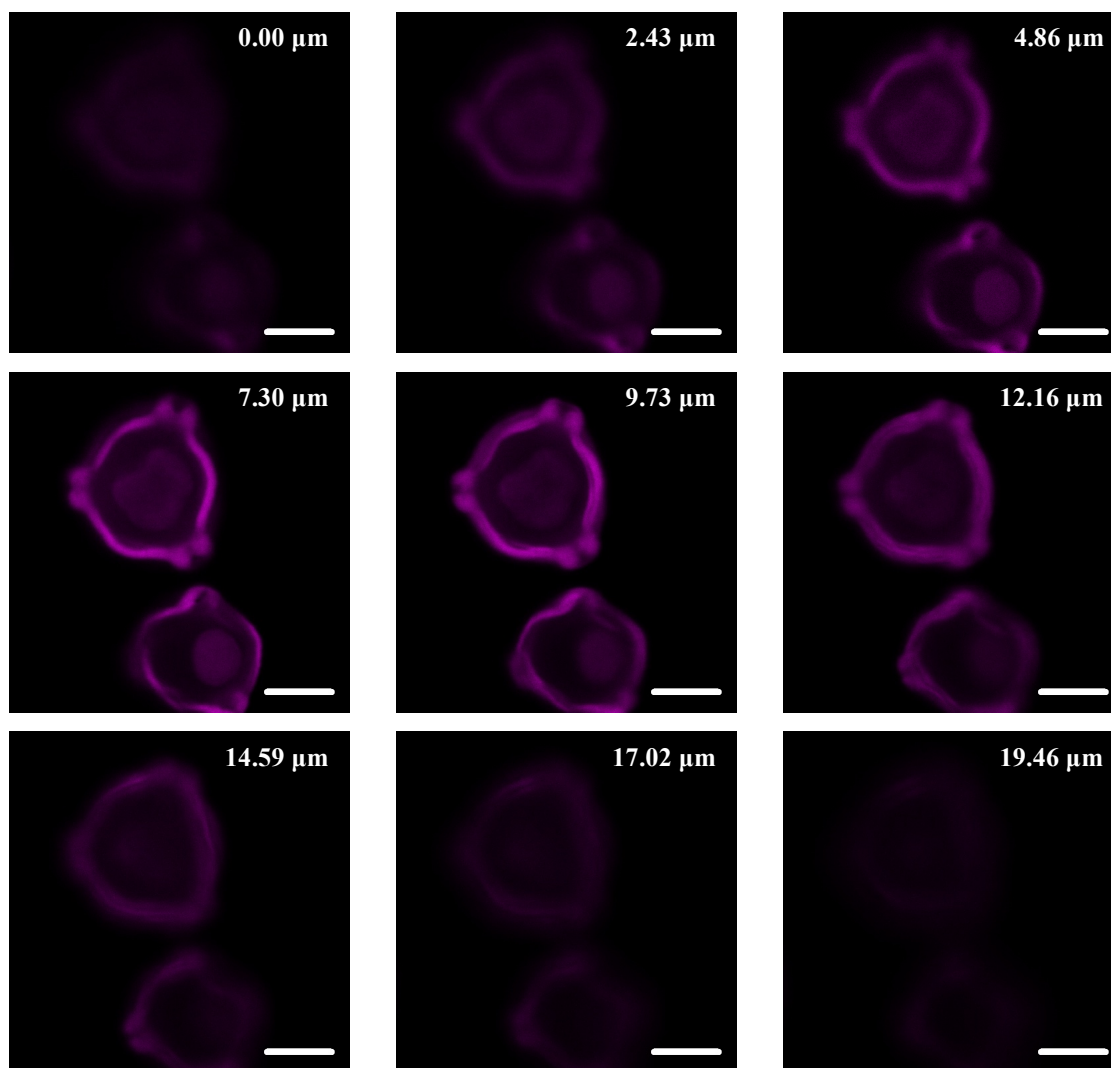


Figure 3.74: LSCM z-stack images of *Betula fontinalis* pollen after step 5 (iv), taken perpendicular to the z-axis.

Excitation wavelength 561 nm. Scale bars = 10 μm . Dimensions indicate position along the z-axis.

Light microscopy, TEM and LSCM demonstrate that some of the protoplast material of *Betula fontinalis* pollen was successfully digested using the enzyme protocol published by Loewus *et al.*⁶⁴ The treatment was sufficiently gentle not to alter the structure of the exine, including the tectum, infratectum and foot layer and is unlikely to have altered the chemistry of the sporopollenin exine. However, clearly all non-sporopollenin material was not removed and most grains continue to contain some protoplast material. Therefore, the method published by Loewus *et al.* cannot be considered suitable for producing microcapsules from *Betula fontinalis* pollen, because components that could elicit a human allergic response still remain.

3.5.3 Enzyme treatment applied to *Secale cereale* pollen

The enzyme treatment proposed by Loewus *et al.* (see Figure 3.55 for summary) was applied to *Secale cereale* pollen and light microscopy was used to compare treated pollen to untreated pollen (Figure 3.75).⁶⁴ During step 2 (ii), 10 pestle cycles were performed and light micrographs were taken of the product after step 3 (v) (Figure 3.76). Although most grains remain intact, a large proportion is cracked. Some grains appear transparent and most of these grains have a visible crack, through which the protoplast is likely to have been released. Protoplast material is observed leaving through the single pore of some grains and free protoplasm material is also present around the grains.

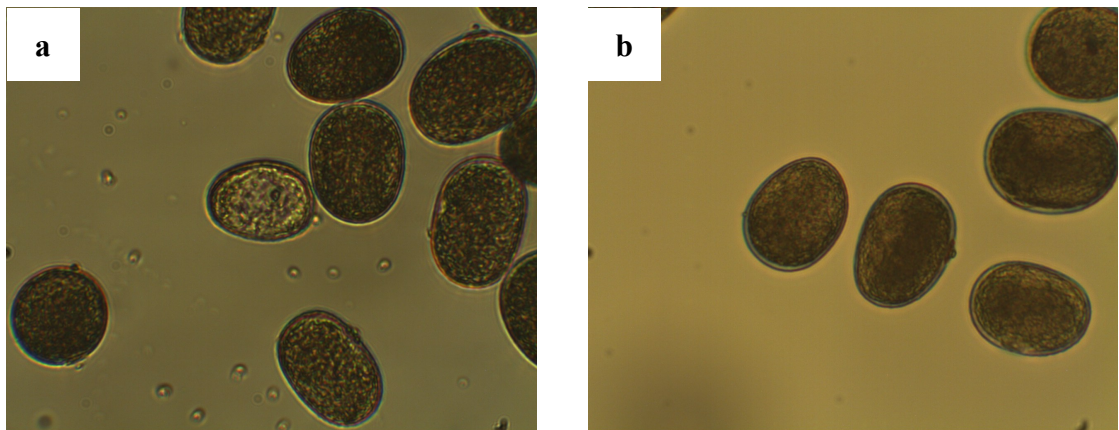


Figure 3.75: Light micrographs of untreated *Secale cereale* pollen ((a) and (b) $\times 400$ magnification)

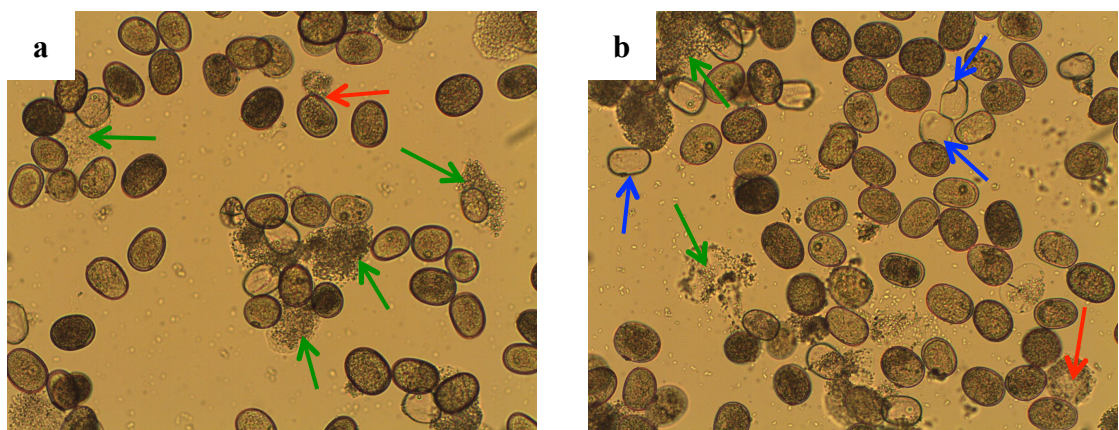


Figure 3.76: Light micrographs of MMNO and CHA-treated *Secale cereale* pollen after step 3 (v) (10 pestle cycles) ((a) and (b) $\times 100$ magnification)

After step 5 (iv), almost all grains still contain their protoplasts (Figure 3.77). Fewer cracked, transparent grains are apparent, possibly because they floated to the top of the centrifuge tube and were removed along with the supernatant fraction during washing steps 5 (i) to (iv). Because almost all grains still contained their protoplasts after applying the published enzyme treatment, this method cannot be considered suitable for the production of microcapsules from *Secale cereale* pollen without further modification.

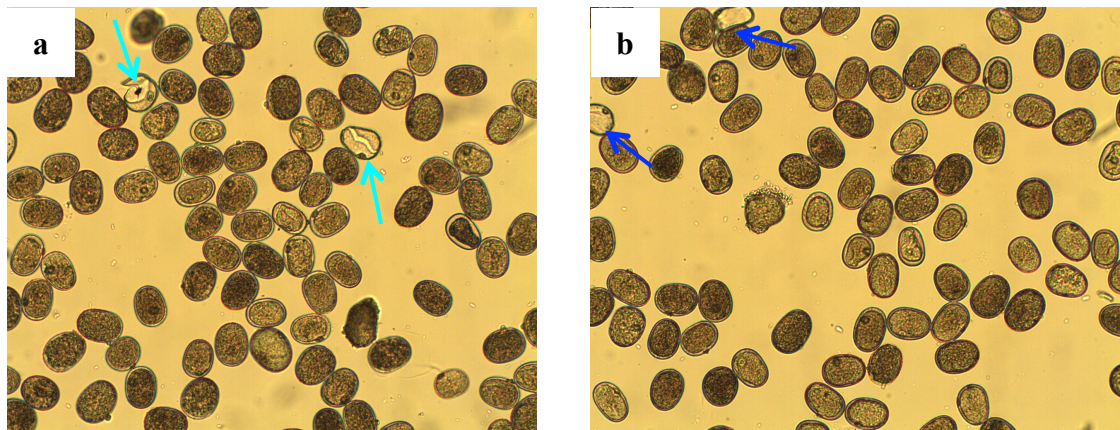


Figure 3.77: Light micrographs of enzyme-treated *Secale cereale* pollen after step 5 (iv) (10 pestle cycles) ((a) and (b) $\times 100$ magnification)

In an attempt to digest more protoplast material, *Secale cereale* pollen was incubated in the enzyme suspension (step 4 (iii)) for 40 h instead of 1 – 2 h. The number of pestle cycles performed was kept at 10. Samples were taken for light microscopy after 18 h and 40 h (Figure 3.78 and Figure 3.79 respectively). After 18 h, most grains appear intact and still contain protoplasts, with some free protoplast material surrounding grains. A very few cracked grains are observed (Figure 3.78 (c)). After 40 h, some partially emptied grains are present. However, these are limited in number and clearly still contain non-sporopollenin material. In addition, motile bacteria were observed on the slide, potentially presenting a health hazard. Despite increasing the incubation time in the enzyme suspension, microcapsules were still not successfully synthesised from *Secale cereale* pollen using the enzyme method published by Loewus *et al.*

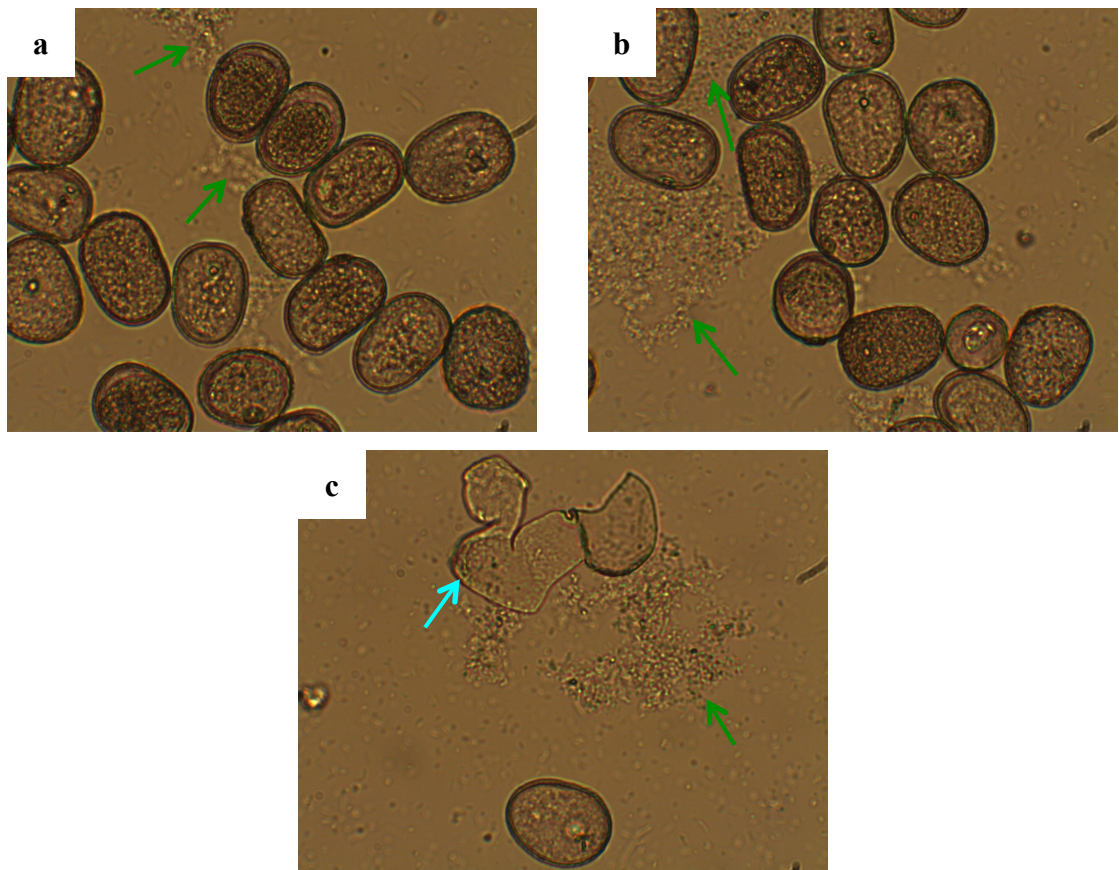


Figure 3.78: Light micrographs of enzyme-treated *Secale cereale* pollen after step 5 (iv) (10 pestle cycles, 18 h in enzyme suspension) ((a), (b) and (c) $\times 400$ magnification)

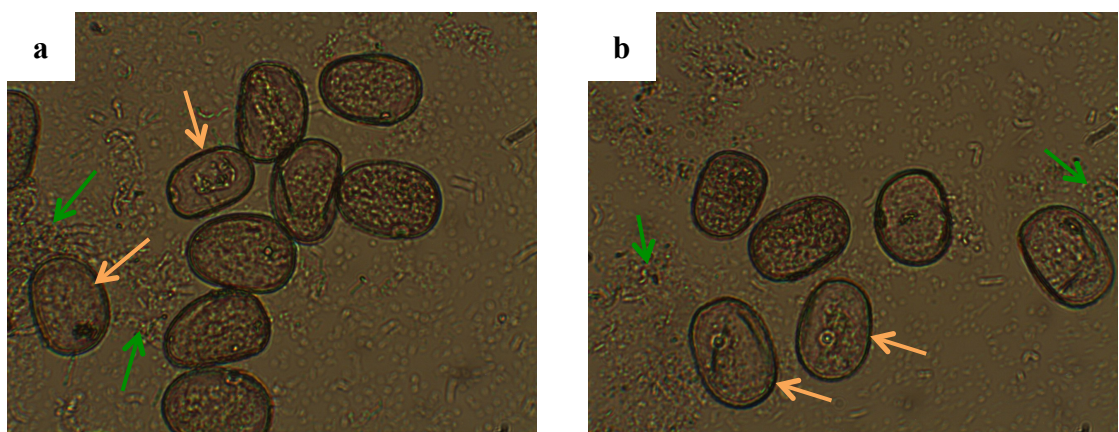


Figure 3.79: Light micrographs of enzyme-treated *Secale cereale* pollen after step 5 (iv) (10 pestle cycles, 40 h in enzyme suspension) ((a) and (b) $\times 400$ magnification)

The number of pestle cycles performed during step 2 (ii) was increased from 10 to 30. Samples were incubated in the enzyme suspension for 20 h. Light microscopy indicates that increasing the number of pestle strokes removes more protoplast material (Figure 3.80), but also produces a greater number of cracked and damaged grains.

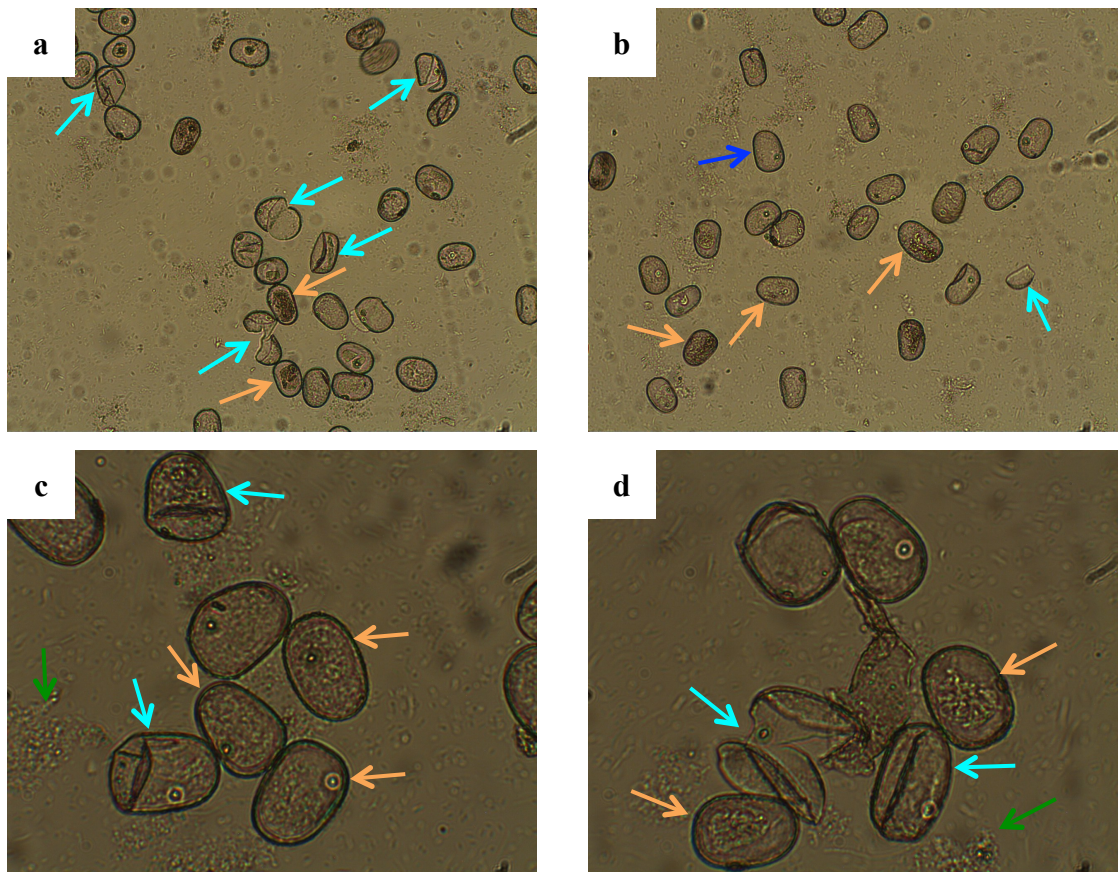


Figure 3.80: Light micrographs of enzyme-treated *Secale cereale* pollen after step 5 (iv) (thirty pestle cycles, 20 h in enzyme suspension) ((a) and (b) $\times 100$, and (c) and (d) $\times 400$ magnification)

The mass of each enzyme and the bovine serum albumin used was doubled. Ten pestle and mortar cycles were performed, and *Secale cereale* pollen was incubated in the enzyme suspension for 48 h in an attempt to remove as much protoplast material as possible. Samples were taken for light microscopy after 24 and 48 h (Figure 3.81 and Figure 3.82 respectively). After 24 h, a considerable amount of protoplast material had been removed, and this further increased after 48 h. However, a high proportion of grains were cracked and damaged, possibly caused by the stirring during the extended incubation period.

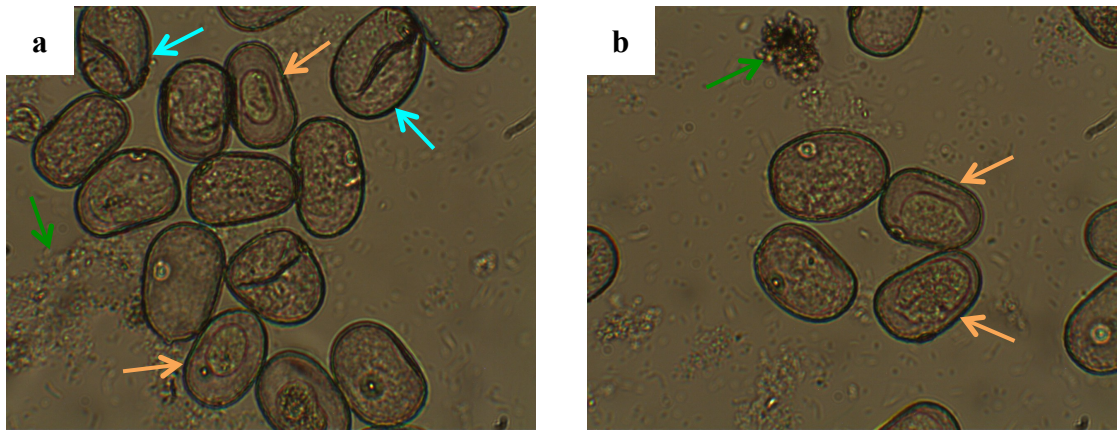


Figure 3.81: Light micrographs of enzyme-treated *Secale cereale* pollen after step 5 (iv) (10 pestle cycles, 24 h in enzyme suspension, double mass of enzymes) ((a) and (b) $\times 400$ magnification)

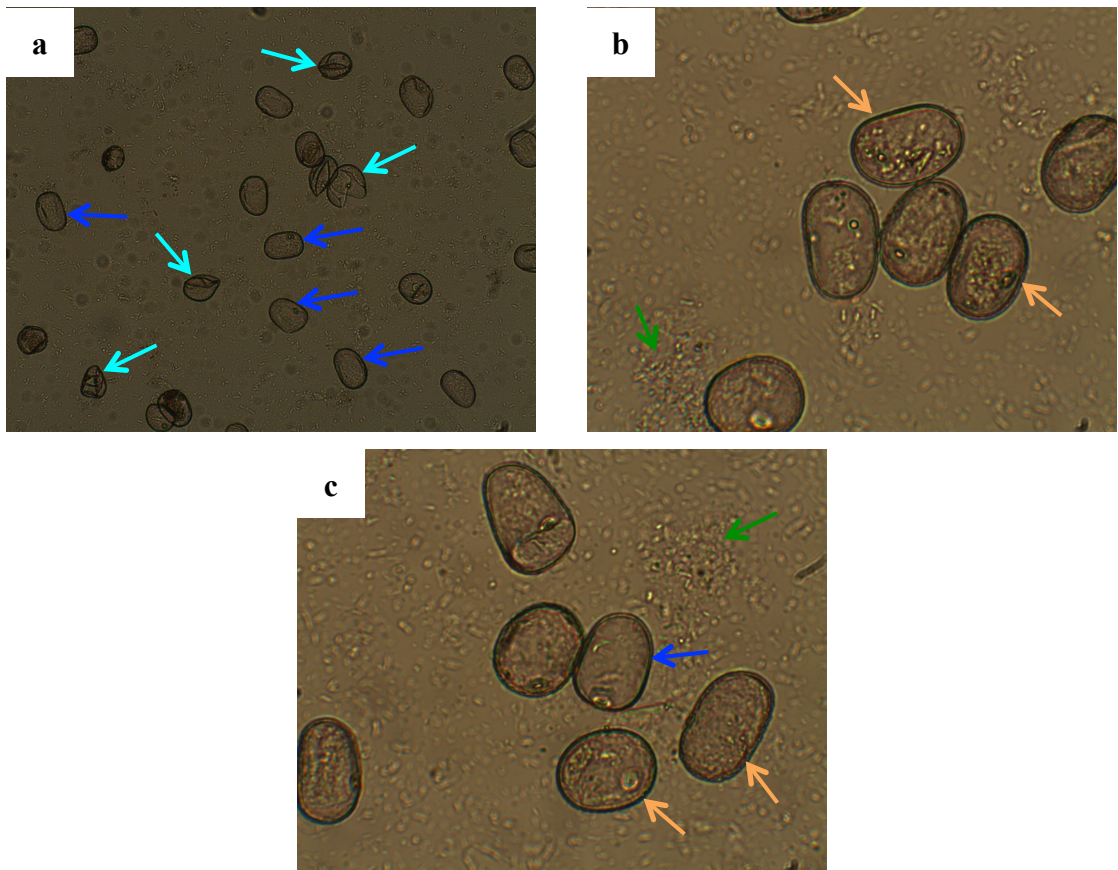


Figure 3.82: Light micrographs of enzyme-treated *Secale cereale* pollen after step 5 (iv) (10 pestle cycles, 48 h in enzyme suspension, double mass of enzymes) ((a) $\times 100$ and (b) and (c) $\times 400$; magnification)

The method published by Loewus *et al.* was found to be unsuitable for producing microcapsules from *Secale cereale* pollen. Modifications were made to this method, but

they were not adequate to the task of producing microcapsules free from non-sporopollenin material from this species.

3.5.4 Treatments involving enzymes: summary of results

1. Microcapsules were not successfully produced from *Juglans nigra*, *Betula fontinalis* and *Secale cereale* pollen using the enzyme treatment proposed by Loewus *et al.*⁶⁴ Although all protoplast material appeared to be removed from some grains within each species, most still contained some of this material. This remaining non-sporopollenin material could elicit an allergic response in humans who come into contact with it.
2. LSCM and TEM showed that the enzyme method was gentle enough to leave the exine of *Betula fontinalis* pollen unaltered and undamaged. *Juglans nigra* pollen grains also remained intact. However, stirring *Secale cereale* pollen in the enzyme suspension resulted in cracked grains, which are obviously unsuitable as microcapsules. Therefore, although the enzyme method used here removed some non-sporopollenin material from all species studied and left most grains structurally intact, it cannot be considered a suitable method to produce microcapsules from pollen without further modification.

3.6 Conclusions

Untreated *Lycopodium clavatum* spores and *Secale cereale*, *Juglans nigra*, *Ambrosia artemisiifolia*, and *Betula fontinalis* pollen were examined using light microscopy, SEM and TEM. These were compared to pollen and spores treated using acetolysis, base and acid treatments, and enzyme treatments.

Acetolysed pollen and spores appeared to be intact and emptied of all non-sporopollenin material. However, material produced was dark brown in colour, meaning that, without bleaching, these pollen grains and spores are not suitable for applications where lighter-coloured microcapsules are needed e.g. food, pharmaceutical and display applications. The colour change observed could also indicate that acetolysis caused a change to

sporopollenin's chemical structure. Bleaching could further alter its structure, possibly resulting in changes to its desirable material properties e.g. permeability, flexibility, and ability to absorb UV radiation. However, it has not been demonstrated experimentally that acetolysis or bleaching does chemically alter sporopollenin's structure. Because of possible changes to the chemistry of sporopollenin and the need for bleaching, acetolysis was not considered a suitable treatment to produce microcapsules from the species under investigation.

The base and acid treatment applied to *Lycopodium clavatum* spores produced microcapsules free of almost all non-sporopollenin material. However, when the base step of this method was applied to *Secale cereale* and *Juglans nigra* pollen, grains produced were so damaged that the subsequent acid step was not attempted. Despite modifications to this base step, microcapsules could not be produced from these pollen species. An alternative base and acid treatment published by Fletcher *et al.* was applied to *Ambrosia artemisiifolia* pollen, but this produced damaged grains that could not be used as microcapsules, as encapsulated material would easily leak out. Results indicate that base and acid treatments may only be suitable for use on spores, as these treatments damaged the pollen species under investigation.

As a gentler alternative to acetolysis and base and acid treatments, a treatment involving enzymes was applied to *Juglans nigra*, *Secale cereale*, and *Betula fontinalis* pollen. This method removed some protoplast material from some grains, but others retained much of their non-sporopollenin material. In addition, although stirring in the enzyme suspension did not damage the exines of *Betula fontinalis* and *Juglans nigra* pollen; the comparatively fragile exine of *Secale cereale* pollen became cracked. As a result, the enzyme method evaluated here cannot be considered suitable to produce microcapsules from the species under investigation. Although modifications to overcome these difficulties were attempted, treatments involving enzymes still failed to remove all non-sporopollenin material (therefore resulting in the possibility of an allergic response) and caused some grains to become cracked.

Despite attempting a range of methods on a variety of pollen species, microcapsules could only successfully produced from *Lycopodium clavatum* spores a using base and acid treatment. One of the primary reasons to treat spores with base and acid is to remove non-sporopollenin material, which may elicit an allergic response if it comes

into contact with human subjects. This is likely if microcapsules are used for food, pharmaceutical, or cosmetic applications. However, subjects are unlikely to come into direct contact with microcapsules in other scenarios, for example, where they are used in displays or self-healing materials.^{134, 135} Alternatively, microcapsules may be encapsulated within a matrix to avoid human contact, for example in pressure measurement films.¹³⁶ It may be possible to use partially emptied pollen grains in such applications.

Chapter 4:
Encapsulation of *Lactobacillus*
bacteria into enzyme-treated *Betula*
***fontinalis* pollen**

4 Encapsulation of *Lactobacillus* bacteria into enzyme-treated *Betula fontinalis* pollen

4.1 Introduction

Paunov *et al.* have published evidence which shows that live yeast cells appeared to be encapsulated inside base and acid treated *Lyopodium clavatum* spores.⁷⁴ They demonstrated that the yeast cells retained some of their biological activity after encapsulation, as shown by the production of carbon dioxide (compared to spores without added *Lactobacilli*). In this thesis, to test whether other biological organisms could be encapsulated, an attempt was made to encapsulate *Lactobacillus* bacteria inside enzyme-treated *Betula fontinalis* pollen. *Betula fontinalis* pollen was used instead of *Lycopodium clavatum* spores to determine whether pollen could be used as a microcapsule.

Lactobacilli (from the genus *Lactobacillus*) are rod-shaped bacteria that are typically 0.5 – 1.2 µm in width by 1.0 – 10.0 µm in length.¹³⁷ Bergey describes these as appearing ‘commonly in short chains’.¹³⁷ They are not usually pathogenic and were therefore selected to use in this work, as they were unlikely to cause harm.

4.2 Materials and methods

Enzyme-treated *Betula fontinalis* pollen was prepared by the method described in section 7.2.3. A freeze-dried yogurt culture containing *Lactobacillus* bacteria was purchased from Ascott Dairy Supplies, UK. This culture was selected as it was unlikely to contain harmful bacteria that could not be used safely in a standard chemical laboratory. The yogurt culture was incubated in MRS broth – a nutrient broth developed by and named after De Man, Rogosa and Sharpe as a medium for the growth of

Lactobacillus bacteria.¹³⁸ The MRS broth containing *Lactobacilli* was stirred with enzyme-treated *Betula fontinalis* pollen at 30 °C for three days. Samples were taken every 24 h for examination by light microscopy.

Aseptic technique would have been desirable during the steps described above to limit the growth of bacteria, other than that found in the yogurt culture. Unfortunately this was not possible using the apparatus available. Every effort was made to ensure glassware and the work area was kept clean. Unused MRS broth (both with and without the addition of *Lactobacillus* bacteria) and all samples produced were treated with a concentrated bleach solution prior to disposal to destroy as much of the bacteria present as possible.

4.3 Results

Samples were taken every 24 h and inspected *via* light microscopy. At 24, 48, and 72 h (Figure 4.1 to Figure 4.3) no encapsulation is immediately obvious *via* the light micrographs taken. After 72 h, motion was observed that appeared to be within the confines of a limited number of grains. This movement could not be captured as distinct bacteria were difficult to observe through the walls of the pollen grains, and the motion was too fast to be recorded using the video-capture software available. Although the bacteria may have been encapsulated, it is also possible that bacteria could have been trapped between the slide and the pollen grain, or the pollen grain and the coverslip, thereby giving the impression of encapsulation. However, some bacteria were observed to move only within the cross-sectional area of the pollen grains, thus supporting the view that some bacteria were successfully encapsulated.

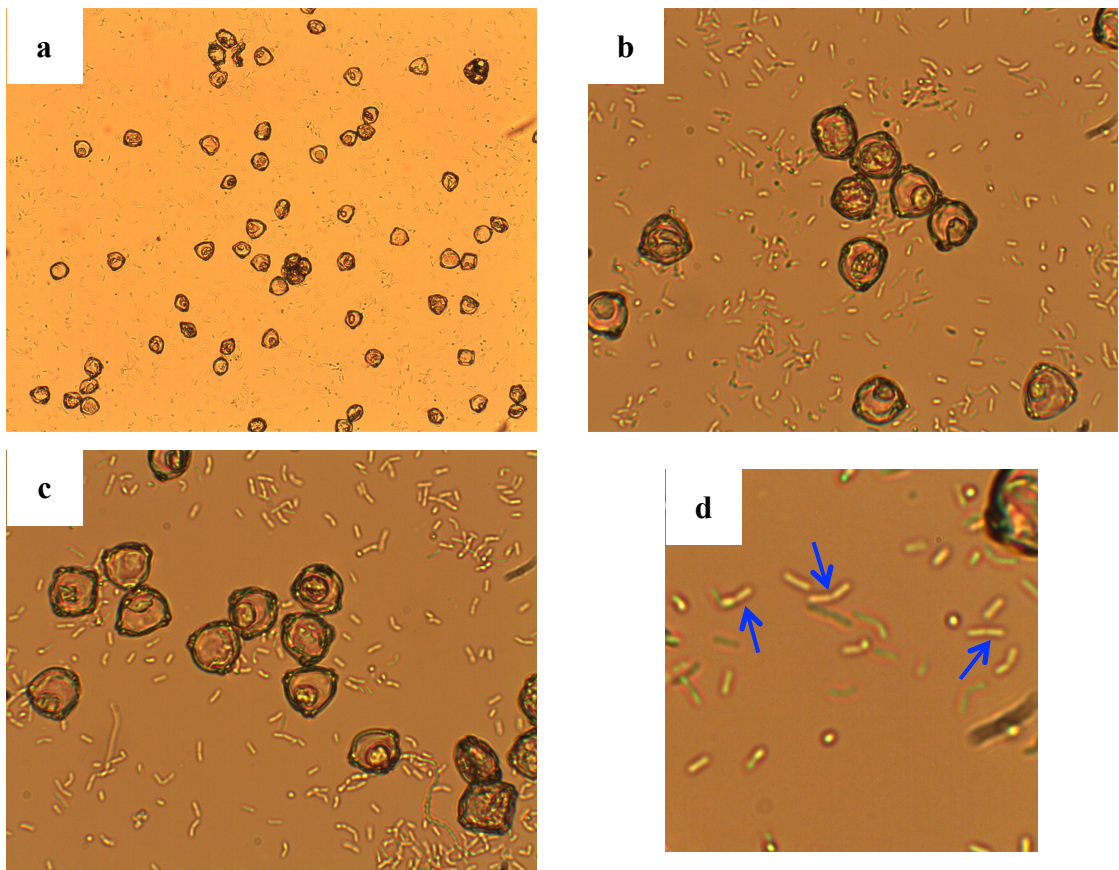


Figure 4.1: Light micrographs of enzyme-treated *Betula fontinalis* pollen stirred with yogurt culture in MRS broth (24 h)
(a) $\times 100$; and (b) and (c) $\times 400$ magnification; and (d) a digitally enlarged region of (b).
Blue arrows highlight dividing bacteria

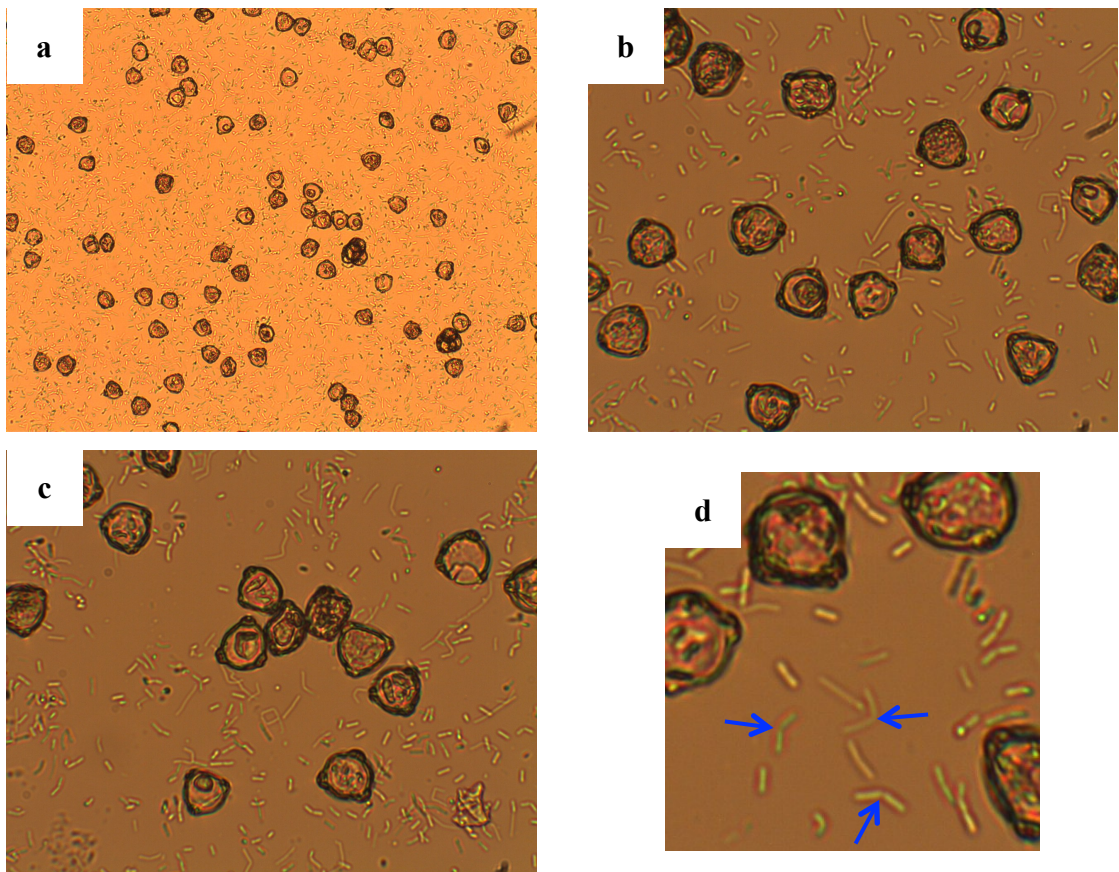


Figure 4.2: Light micrographs of enzyme-treated *Betula fontinalis* pollen stirred with yogurt culture in MRS broth (48 h)
(a) $\times 100$; and (b) & (c) $\times 400$ magnification; and (d) a digitally enlarged region of (b).
Blue arrows highlight dividing bacteria

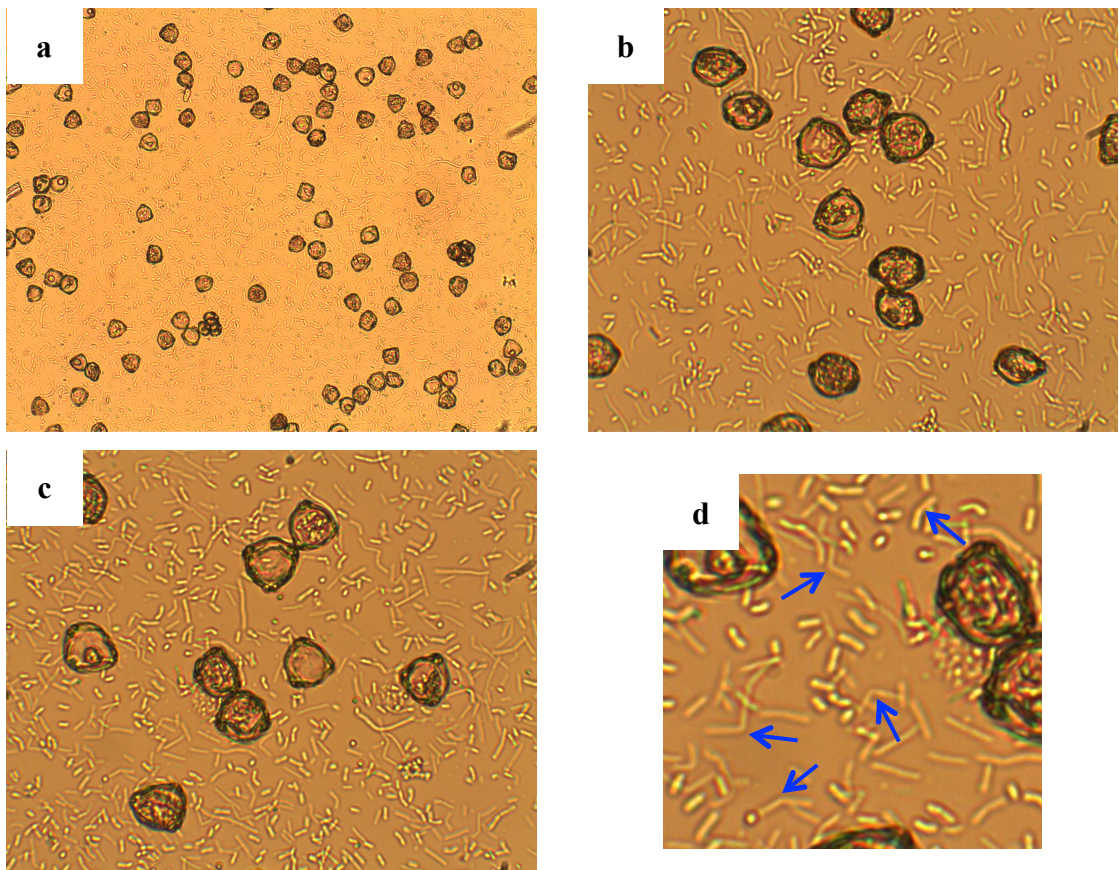


Figure 4.3: Light micrographs of enzyme-treated *Betula fontinalis* pollen stirred with yogurt culture in MRS broth (72 h)
 (a) $\times 100$ and (b) & (c) $\times 400$ magnification; and (d) a digitally enlarged region of (c)
 Blue arrows highlight dividing bacteria

As expected, bacteria appear rod-shaped, and the arrows in Figure 4.1 to Figure 4.3 highlight a number of these. The amount of bacteria present in each sample appears to increase over each 24 h period. Binary fission is the process by which most bacteria reproduce, and a number of digitally enlarged images (light micrograph (d) shown in in Figure 4.1 to Figure 4.3) highlight bacteria undergoing the cell separation phase of this process.¹³⁹ Multiplying bacteria appear as two, joined, rod-shaped cells, separated by a narrow spindle region. No bacterial cells were observed to actively separate during the short periods of microscopy. However, bacteria increased in number of the duration of the experiment, which suggests that binary fission and therefore bacterial multiplication did take place. This indicates that the conditions selected for bacterial growth, i.e. temperature and growth medium, were suitable.

Surprisingly, biological organisms of unknown origin were observed during TEM analysis of enzyme-treated *Betula fontinalis* pollen without the addition of *Lactobacilli*

(Figure 4.4). These organisms could be a single species; cut along different axis, thereby giving the impression of differently shaped organisms. Alternatively, they could be from different species. The longest recorded dimension of these organisms is approximately $2.5\ \mu\text{m}$ (Figure 4.4 (c)), and the shortest approximately $0.4\ \mu\text{m}$ (Figure 4.4 (e)). This size range indicates that the unknown organisms are most likely to be bacteria (typically $0.1 - 50\ \mu\text{m}$) or fungal spores (typically $1.5 - 30\ \mu\text{m}$).^{125, 126}

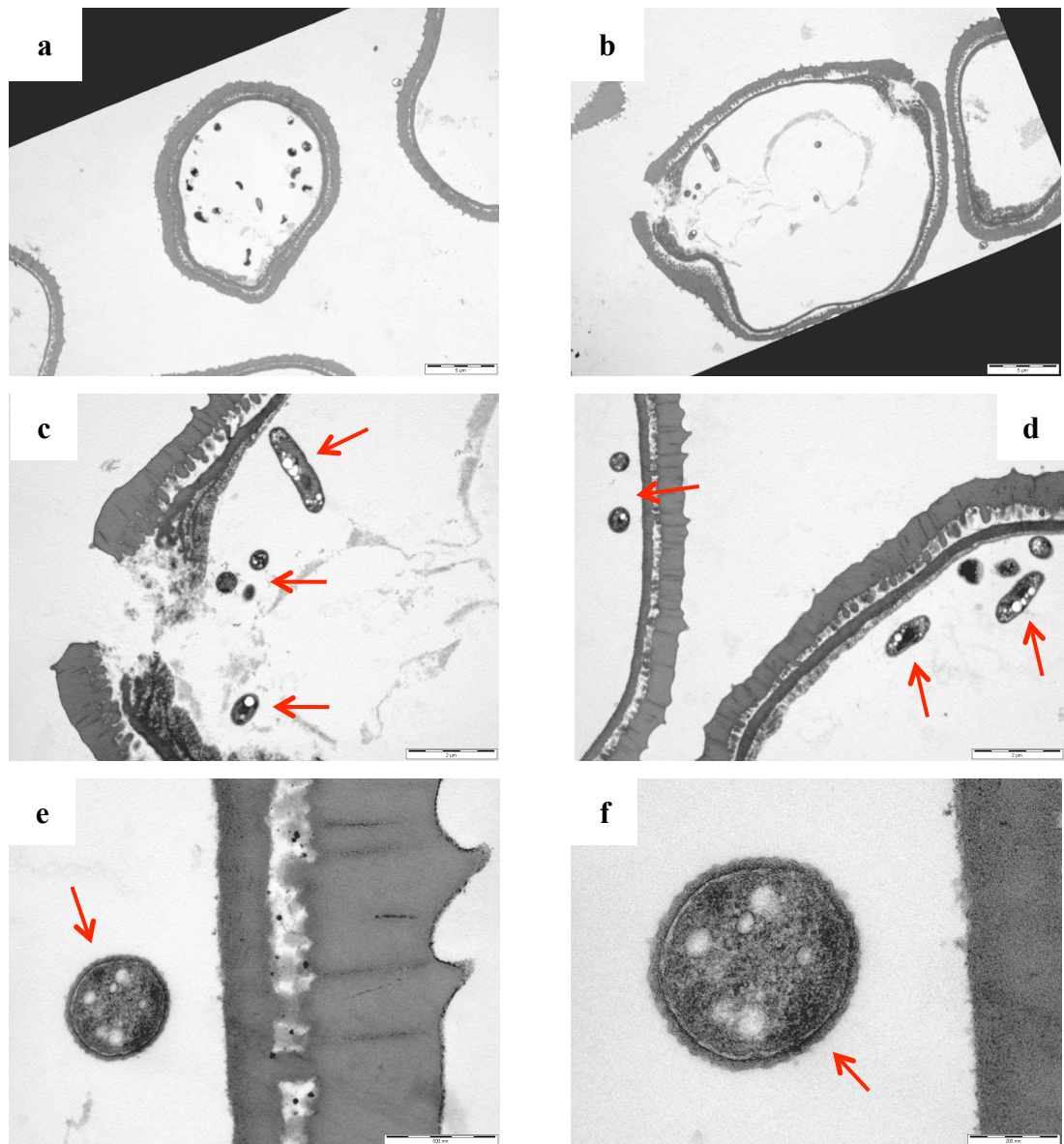


Figure 4.4: Transmission electron micrographs of enzyme-treated *Betula fontinalis* pollen containing unidentified organisms.

Scale bars: (a) and (b) = $5\ \mu\text{m}$; (c) and (d) = $2\ \mu\text{m}$; (e) = $500\ \text{nm}$; and (f) = $200\ \text{nm}$.

Biological material of unknown origin highlighted with red arrows

Appezato-da-Glória *et al.* were able to inoculate pollen from *Citrus sinensis* (sweet orange) with *Collectotrichum acutatum* spores *in vitro*.¹⁴⁰ (*Collectotrichum acutatum* is a plant pathogen that causes fungal growth.) Light micrographs from this paper demonstrate that fungal hyphae (a filamentous component of the fungus) were able to enter the pollen grains directly through the grains' walls as well as through their pores. Similar fungal growth was observed inside alfalfa pollen inoculated with *Verticillium albo-atrum*, *Sclerotinia sclerotiorum*, *Botrytis cinerea*, *Coniothyrium minitans* Campbell and *Gliocladium cantenulatum* Gilman and Abbott spores.¹⁴¹⁻¹⁴⁴ This research illustrates that biological organisms can enter pollen grains. One factor that may drive the growth of spores inside the pollen grains is the nutrient-rich environment that the protoplast provides.

4.4 Conclusions

Lactobacillus bacteria were not definitively encapsulated inside enzyme-treated *Betula fontinalis* pollen. However, previously published work suggests that encapsulation of biological organisms within pollen grains is possible. It could be that the bacteria in the freeze-dried yogurt culture used were too large to enter the pores of enzyme-treated *Betula fontinalis* pollen and that selecting a smaller species of bacteria may facilitate encapsulation. An alternative approach could be to encapsulate the spores of bacteria (typically 0.8 – 1.2 μm in diameter).¹⁴⁵ Bacterial spores have been engineered for the delivery of vaccines.¹⁴⁶⁻¹⁴⁸ If encapsulated inside enzyme-treated pollen, it is possible that encapsulation could prolong the life of these vaccines, potentially making them easier to handle and store.

Chapter 5:
Fluorescent microcapsules produced
from pollen and spores

5 Fluorescent microcapsules produced from pollen and spores

5.1 Introduction

Fluorescence takes place when a fluorochrome (a fluorescent molecule), absorbs a photon and then re-emits a photon at a lower energy. A wide variety of synthetic materials fluoresce, as well as substances found in nature, for example vitamin B2.¹⁴⁹ Although these materials vary widely in structure, they almost always possess a high degree of conjugation.¹⁵⁰ Each fluorochrome shows both absorption and emission spectra, which depend on its molecular structure. These emission and absorption profiles can be influenced by factors such as solvent, pH, concentration and crystal structure, as well as interactions with other fluorochromes. Techniques including spectrofluorometry and laser scanning confocal microscopy (LSCM) are used to measure absorption and emission and are able to probe molecular structure and interactions.

Pollen and spores autofluoresce i.e. they fluoresce without the addition of fluorescent dyes.⁹⁹ Different species of pollen and spore have distinct absorption and emission spectra, which demonstrates their differing chemical compositions.⁹⁹ See section 1.7.2 for a discussion of fluorescent materials found within pollen and spores. The analysis of untreated, base, and acid-treated and enzyme-treated pollen and spores by visual inspection, light microscopy, spectrofluorometry and laser scanning confocal microscopy (LSCM) are described in this chapter. In addition, untreated and enzyme-treated pollen was treated with solutions of Rhodamine B (RhB) (Figure 5.1), in order to synthesise fluorescent microcapsules.

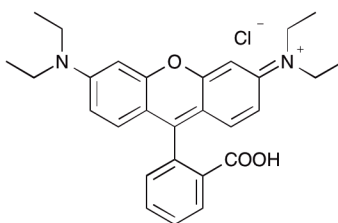


Figure 5.1: Structure of Rhodamine B

Published work only describes the production and use of *Lycopodium clavatum* (club moss) spores as microcapsules; therefore pollen microcapsules are novel.^{57-59, 80} It was expected that pollen and spores treated to remove non-sporopollenin material would exhibit different emission to untreated pollen and spores due to their differing chemical compositions. Indeed, pollen and spores have been dyed with fluorochromes for structural and chemical analyses.¹⁵¹⁻¹⁵³ However, microcapsules synthesised from pollen have not been combined with fluorochromes with the primary aim of producing fluorescent microcapsules.

Work to synthesise microcapsules from spores has focussed on using base and acid treatments to remove non-sporopollenin material from *Lycopodium clavatum* spores.⁵⁷ However, as this method changes the colour of the spores from pale yellow to dark brown, it is highly likely to alter the chemical composition of sporopollenin, and therefore its fluorescence.⁵⁸ Loewus *et al.* applied an enzyme-treatment to *Betula alba verrucosa* and *Betula pendula* (both white birch) pollen to produce exine material for analysis (though their primary aim was not to produce microcapsules).⁶⁴ Loewus *et al.* used this approach in order to minimise any chemical and structural changes to the sporopollenin exine. Therefore, emission arising from sporopollenin would not be expected to be altered. As pollen from these exact species could not be purchased, *Betula fontinalis* (water birch) pollen was selected as a suitable alternative. Being from the same genera, it was considered likely to exhibit similar properties. Untreated pollen and spores from other genera (*Juglans nigra* (black walnut) and *Lycopodium clavatum*) were also combined with RhB to investigate whether altering the genera influenced the observed fluorescence.

Untreated, base, and acid-treated and enzyme-treated pollen and spores from a range of species were mixed with solutions of RhB. The concentrations of these solutions ranged from 1×10^{-3} to 1×10^{-6} mol dm⁻³ of RhB, and both water and ethanol were used as solvents. The species used and treatments applied to each are summarised in Table 5.1.

The emission spectra of RhB in water and ethanol show peak emission wavelengths of approximately 596 nm and 597 nm respectively (Figure 5.2). These emission spectra only partly overlap the emission spectrum of *Betula fontinalis* pollen (Figure 5.2), meaning that when physically combined, the spectra of the pollen or spores and RhB should be distinguishable. Both ethanol and water were used in order to determine the effect of changing the solvent on the emission from pollen, spores and RhB.

Table 5.1: Summary of treatments applied to pollen and spores

Species	Untreated	Treatment applied	
		Enzyme	Base and acid
<i>Lycopodium clavatum</i> (club moss)	● ○ ◇		●
<i>Betula fontinalis</i> (water birch)	● ○ ◇	● ○ ◇	●
<i>Taraxacum officinale</i> (dandelion)	●	●	
<i>Ambrosia artemisiifolia</i> (common ragweed)	●	●	
<i>Juglans nigra</i> (black walnut)	●		
<i>Secale cereale</i> (rye)	●		

● Analysed without addition of RhB solutions

○ Analysed after treatment with aqueous solutions of Rhodamine B

◇ Analysed after treatment with ethanolic solutions of Rhodamine B

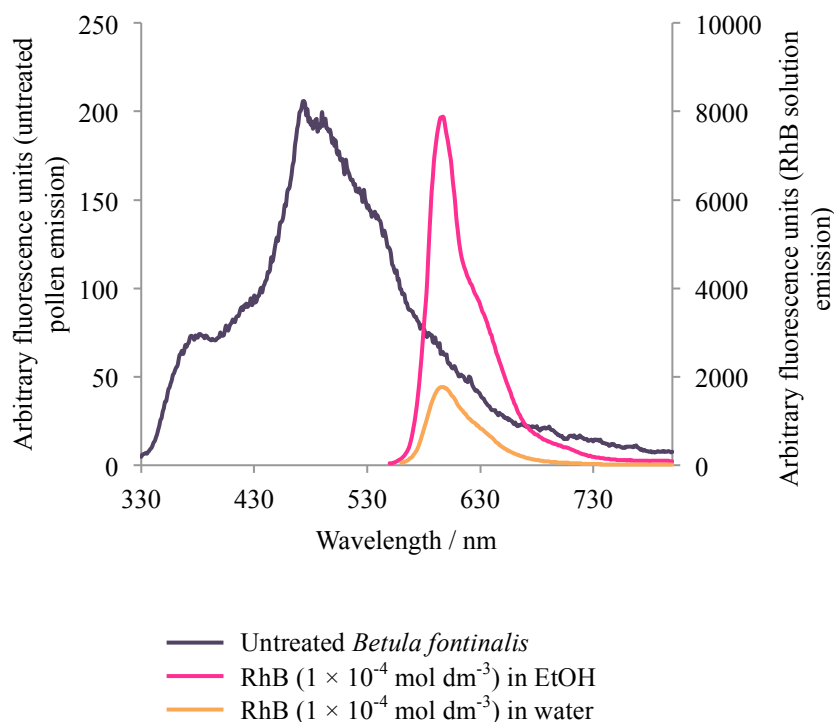


Figure 5.2: Emission spectra of untreated *Betula fontinalis* pollen (excitation λ 300 nm, 350 nm longpass filter), Rhodamine B (1×10^{-4} mol dm⁻³ in EtOH, excitation λ 543 nm) and Rhodamine B (1×10^{-4} mol dm⁻³ in water, excitation λ 548 nm)

In recent work to evaluate historic ultraviolet-B (UV-B) radiation, *p*-coumaric acid and ferulic acid have been described as possible models for sporopollenin.^{38, 39, 154, 155} Saturated solutions of these acids were prepared and their emission compared with that of both untreated and enzyme-treated *Betula fontinalis* pollen. The acid solutions were combined with RhB and their fluorescence compared to that of RhB encapsulated *Betula fontinalis* pollen (untreated and enzyme-treated). The similarities and differences of these spectra were evaluated in order to assess the suitability of these acids as sporopollenin models.

5.2 Materials and methods

Pollen and spores were used as purchased without any pre-treatment such as sieving or washing. Rhodamine B (RhB) was used without additional purification. The base and acid treatment applied was published by Atkin *et al.*, and the enzyme-treatment by Loewus *et al.* (for further discussion see chapter 3). Solutions of RhB were prepared at concentrations of 1×10^{-3} , 10^{-4} , 10^{-5} and 10^{-6} mol dm⁻³ in both water and ethanol. Pollen

and spores (see Table 5.1 for species used) were stirred in these solutions of RhB for 2h, then filtered and washed with the same solvent used to dissolve RhB. Solutions of RhB (without the addition of pollen and spores) were also analysed independently. In addition, saturated solutions of *p*-coumaric acid and ferulic acid (both with and without added RhB) were prepared for analysis.

Spectrofluorometry of the solid pollen and spore samples was carried out using a front-face excitation geometry. Solutions of RhB and saturated solutions of *p*-coumaric acid and ferulic acid were analysed in quartz cuvettes with a 90° excitation geometry. LSCM was performed in single-track mode, unless multi-track mode was specified.

5.3 Visual observations

Photographs were taken of all samples produced in order to observe any colour differences by eye. Untreated pollen from the genera studied was observed to be pale yellow to yellow in colour (Figure 5.3). These photographs demonstrate that species cannot be differentiated on the basis of colour merely by eye.

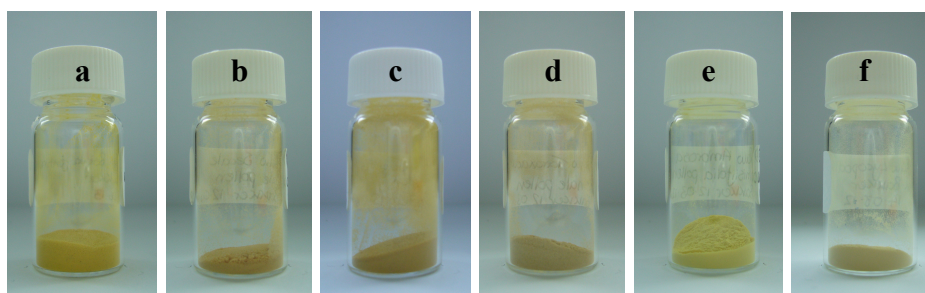


Figure 5.3: Photographs of untreated pollen from (a) *Betula fontinalis*; (b) *Secale cereale*; (c) *Juglans nigra*; (d) *Taraxacum officinale*; (e) *Ambrosia artemisiifolia*; and spores from (f) *Lycopodium clavatum*

Following the enzyme-treatment protocol described by Loewus *et al.*, *Betula fontinalis* and *Ambrosia artemisiifolia* pollen do not visibly change colour and remain yellow (Figure 5.4). In contrast, when *Lycopodium clavatum* spores were treated with base and acid, they changed from a pale yellow to dark brown in colour (Figure 5.5), meaning that both untreated and base and acid-treated *Lycopodium clavatum* spores can be readily differentiated by eye.

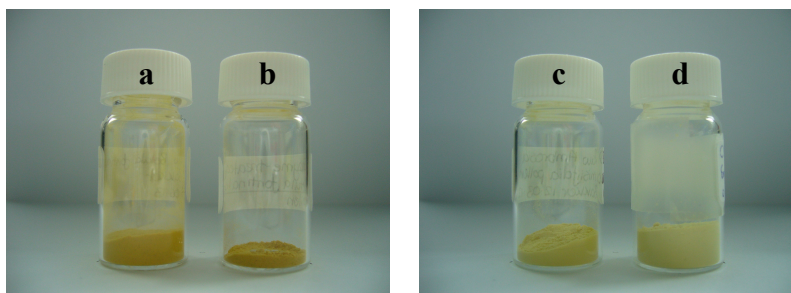


Figure 5.4: Photographs of *Betula fontinalis* pollen (a) untreated and (b) after enzyme treatment; *Ambrosia artemisiifolia* pollen (c) untreated and (d) after enzyme-treatment

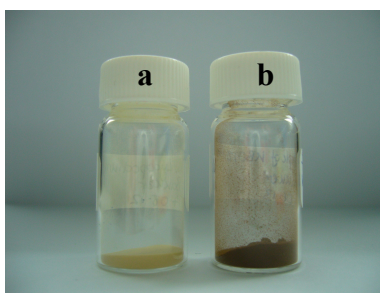


Figure 5.5: Photograph of *Lycopodium clavatum* spores (a) untreated and (b) after base and acid treatment

Enzyme-treated *Betula fontinalis* pollen was treated using solutions of RhB in ethanol. At the highest solution concentration ($1 \times 10^{-3} \text{ mol dm}^{-3}$), the colour of the bright pink fluorochrome is easy to observe through the yellow pollen (Figure 5.7 (a)). However, at lower concentrations ($1 \times 10^{-4} \text{ mol dm}^{-3}$ and $1 \times 10^{-5} \text{ mol dm}^{-3}$), the pink colour is less obvious, and the pollen is more orange than pink (Figure 5.7 (b) and (c)). At the lowest RhB concentration ($1 \times 10^{-6} \text{ mol dm}^{-3}$, Figure 5.7 (d)), the pollen is yellow, and appears the same colour as enzyme-treated pollen without the addition of RhB (Figure 5.4). Similar observations were made when the solvent used to dissolve RhB was replaced with water (Figure 5.6). This suggests that the colour change observed by eye when the concentration of RhB was changed is independent of the solvent used.

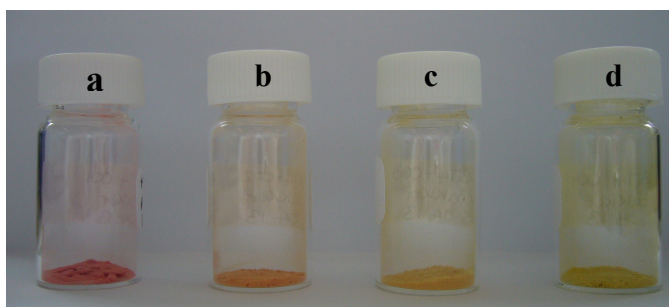


Figure 5.6: Photograph of enzyme-treated *Betula fontinalis* pollen treated with ethanolic solutions of RhB.

RhB solution concentrations: (a) $1 \times 10^{-3} \text{ mol dm}^{-3}$; (b) $1 \times 10^{-4} \text{ mol dm}^{-3}$; (c) $1 \times 10^{-5} \text{ mol dm}^{-3}$; and (d) $1 \times 10^{-6} \text{ mol dm}^{-3}$

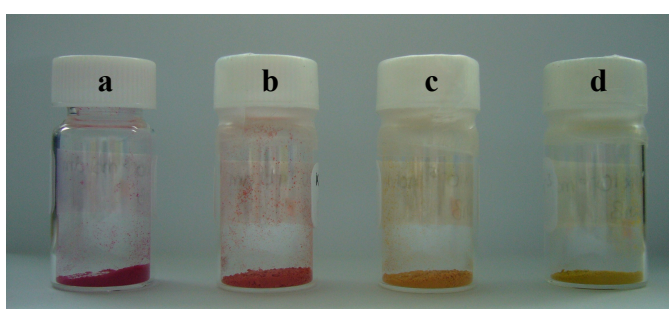


Figure 5.7: Photograph of enzyme-treated *Betula fontinalis* pollen treated with aqueous solutions of RhB.

RhB solution concentrations: (a) $1 \times 10^{-3} \text{ mol dm}^{-3}$; (b) $1 \times 10^{-4} \text{ mol dm}^{-3}$; (c) $1 \times 10^{-5} \text{ mol dm}^{-3}$; and (d) $1 \times 10^{-6} \text{ mol dm}^{-3}$

In order to determine whether enzyme-treatment was necessary to facilitate the encapsulation of RhB, both untreated *Betula fontinalis* and *Juglans nigra* pollen were combined with RhB dissolved in water (Figure 5.8 and Figure 5.9) and in ethanol (Figure 5.10 and Figure 5.11). Even without any treatment to remove the intine or protoplast, brightly coloured products were observed. As with enzyme-treated pollen, higher concentrations of RhB ($1 \times 10^{-3} \text{ mol dm}^{-3}$) produced brighter pink samples, whereas lower concentrations (1×10^{-4} and $10^{-5} \text{ mol dm}^{-3}$) produced orange-yellow samples. Pollen treated with the lowest concentration RhB solution ($1 \times 10^{-6} \text{ mol dm}^{-3}$) appears almost identical to pollen without the addition of RhB (Figure 5.3) These results indicate that enzyme-treatment is not required to produce fluorescent microcapsules, as the results from untreated *Betula fontinalis* are indistinguishable by eye from enzyme-treated *Betula fontinalis* pollen combined with RhB (Figure 5.7 and

Figure 5.6). It was impossible to determine *via* visual inspection whether RhB was successfully encapsulated inside the pollen or merely bound to its surface.

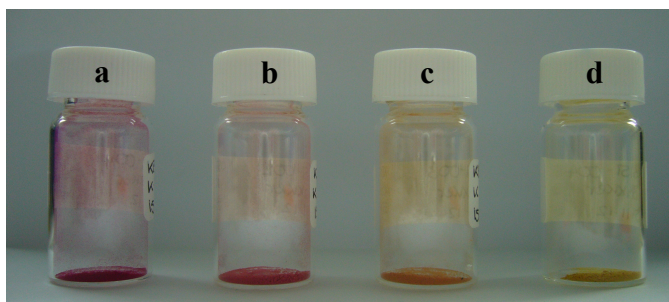


Figure 5.8: Photograph of untreated *Betula fontinalis* pollen treated with aqueous solutions of RhB.

RhB solution concentrations: (a) $1 \times 10^{-3} \text{ mol dm}^{-3}$; (b) $1 \times 10^{-4} \text{ mol dm}^{-3}$; (c) $1 \times 10^{-5} \text{ mol dm}^{-3}$; and (d) $1 \times 10^{-6} \text{ mol dm}^{-3}$

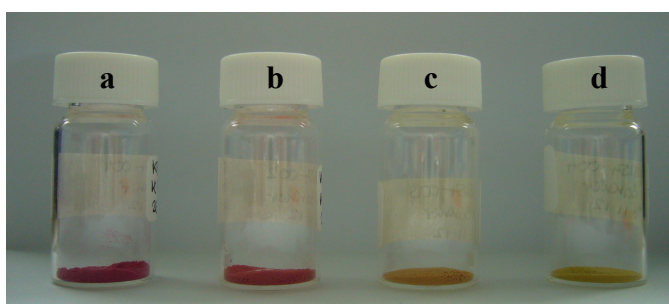


Figure 5.9: Photograph of untreated *Juglans nigra* pollen treated with aqueous solutions of RhB.

RhB solution concentrations: (a) $1 \times 10^{-3} \text{ mol dm}^{-3}$; (b) $1 \times 10^{-4} \text{ mol dm}^{-3}$; (c) $1 \times 10^{-5} \text{ mol dm}^{-3}$; and (d) $1 \times 10^{-6} \text{ mol dm}^{-3}$

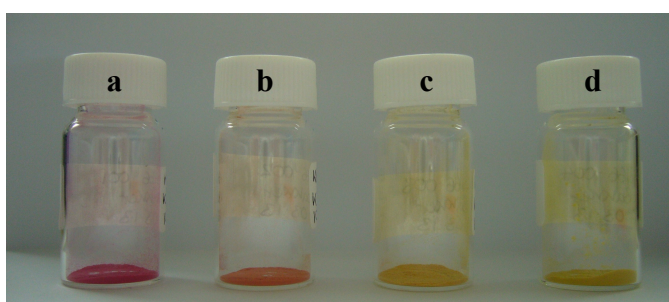


Figure 5.10: Photograph of untreated *Betula fontinalis* pollen treated with ethanolic solutions of RhB.

RhB solution concentrations: (a) $1 \times 10^{-3} \text{ mol dm}^{-3}$; (b) $1 \times 10^{-4} \text{ mol dm}^{-3}$; (c) $1 \times 10^{-5} \text{ mol dm}^{-3}$; and (d) $1 \times 10^{-6} \text{ mol dm}^{-3}$

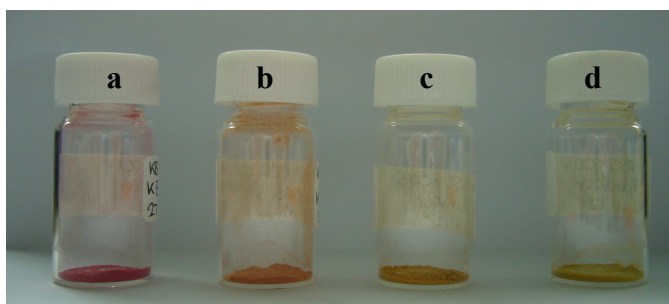


Figure 5.11: Photograph of untreated *Juglans nigra* pollen treated with ethanolic solutions of RhB.

RhB solution concentrations: (a) $1 \times 10^{-3} \text{ mol dm}^{-3}$; (b) $1 \times 10^{-4} \text{ mol dm}^{-3}$; (c) $1 \times 10^{-5} \text{ mol dm}^{-3}$; and (d) $1 \times 10^{-6} \text{ mol dm}^{-3}$

Untreated *Lycopodium clavatum* spores were combined with RhB in ethanol at varying concentrations and, as with pollen, higher RhB concentrations produced pinker samples (Figure 5.12). However, when base and acid-treated spores were treated with ethanolic RhB solutions, a colour change was much harder to distinguish by eye (Figure 5.13). Base and acid-treated *Lycopodium clavatum* spores are dark brown (Figure 5.5 (b)). The pink colour of RhB is therefore less visible when combined with the already darkly coloured base and acid-treated spores. In contrast, the pink RhB is easy to see when combined with untreated *Lycopodium clavatum* spores, which are pale yellow in colour (Figure 5.5 (a)). These results suggest that base and acid-treated spores are not suitable candidates as microcapsules where it is desirable for the presence of a fluorochrome to be detected by eye. Base and acid-treated spores can be bleached to produce whiter exine microcapsules.¹⁵⁶ However, as bleaching results in a colour change, it is possible that this may further alter sporopollenin's structure (even more so than base and acid treatment), thus potentially reducing some of its desirable properties e.g. chemical and physical resilience.

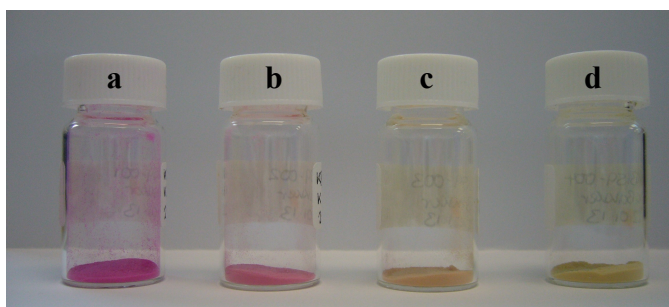


Figure 5.12: Photograph of untreated *Lycopodium clavatum* spores treated with ethanolic solutions of RhB.

RhB solution concentrations: (a) $1 \times 10^{-3} \text{ mol dm}^{-3}$; (b) $1 \times 10^{-4} \text{ mol dm}^{-3}$; (c) $1 \times 10^{-5} \text{ mol dm}^{-3}$; and (d) $1 \times 10^{-6} \text{ mol dm}^{-3}$

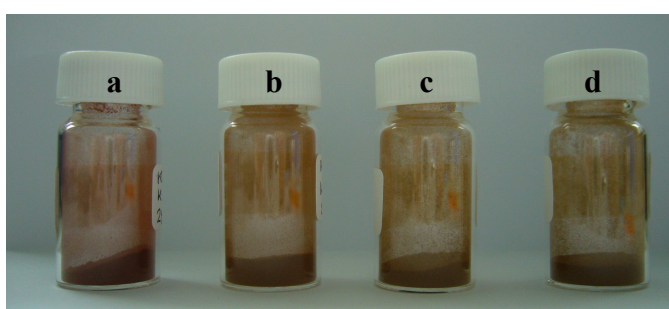


Figure 5.13: Photograph of base and acid-treated *Lycopodium clavatum* spores treated with ethanolic solutions of RhB.

RhB solution concentrations: (a) $1 \times 10^{-3} \text{ mol dm}^{-3}$; (b) $1 \times 10^{-4} \text{ mol dm}^{-3}$; (c) $1 \times 10^{-5} \text{ mol dm}^{-3}$; and (d) $1 \times 10^{-6} \text{ mol dm}^{-3}$

5.3.1 Visual observations: summary of results

1. Untreated pollen and spores could not be differentiated by eye. After treatment with the enzyme method published by Loewus *et al.*, treated pollen could not be distinguished from untreated pollen of the same species.⁶⁴ In contrast, base and acid treatment rendered *Lycopodium clavatum* spores much darker in appearance compared to untreated spores.
2. Higher concentrations (1×10^{-3} and $10^{-4} \text{ mol dm}^{-3}$) of RhB solution applied to enzyme-treated *Betula fontinalis* pollen produced intensely pink-coloured pollen. Lower concentrations (1×10^{-5} and $10^{-6} \text{ mol dm}^{-3}$) rendered the pollen more orange or yellow respectively. The solvent used to dissolve RhB did not produce a visually

identifiable difference. Similar results were observed when the same RhB solutions were applied to untreated pollen (*Betula fontinalis* and *Juglans nigra*) and spores (*Lycopodium clavatum*), indicating that RhB binds to both untreated and enzyme-treated pollen and to untreated spores.

3. Similar results were not observed after ethanolic solutions of RhB were applied to base and acid-treated *Lycopodium clavatum* spores. The dark appearance of base and acid-treated spores masked the colour of RhB, so no difference was observed as the concentration of the RhB solution applied was varied. Therefore, encapsulation or binding of RhB could not, in this instance, be determined by visual inspection alone. This lack of differentiation could be overcome by bleaching of base and acid-treated spores, prior to the application of RhB solutions.

5.4 Analysis by Spectrofluorometry

Spectrofluorometry of solid pollen and spore samples was carried out using a front-surface excitation geometry. The experimental setup required for this geometry meant that the total quantity of solid material analysed and the amount of material that lay within the incident beam could not be maintained between samples. As a result, the variation in emission intensity between samples could not be quantified, although the emission wavelengths and relative ratios of peak heights could be. Raw data was presented and it was not normalised. Solutions were analysed using a standard 90° geometry. Each sample was analysed once. On occasions where untreated pollen and spores were analysed several times, emission spectra for each species were the same, suggesting that repeated analyses of samples would not have influenced the results collected. Where peak ratios were presented as scatter plots, error bars were not included, as the error could not be quantified. Therefore, only qualitative conclusions were drawn from these plots.

5.4.1 Spectrofluorometry of untreated pollen and spores

The emission spectra of untreated pollen (*Betula fontinalis* (water birch), *Juglans nigra* (black walnut), *Secale cereale* (rye), *Taraxacum officinale* (dandelion) and *Ambrosia*

artemisiifolia (common ragweed)) and spores (*Lycopodium clavatum* (club moss)) were collected (Figure 5.14). An excitation wavelength (λ) of 300 nm was utilised in order to maximise the emission from the pollen and spores. As predicted, the spectra highlight the differences in emission profiles between species, even before any additional fluorochromes were added. This variation has been previously reported in the literature.⁹⁹ In addition to an intense emission peak around 470 nm, most species also show distinct emission peaks between 360 – 390 nm, 400 – 430 nm and possess a broader band from 650 – 750 nm. Due to the complex chemical structure of pollen and spores, assigning the source of these peaks and bands is challenging.

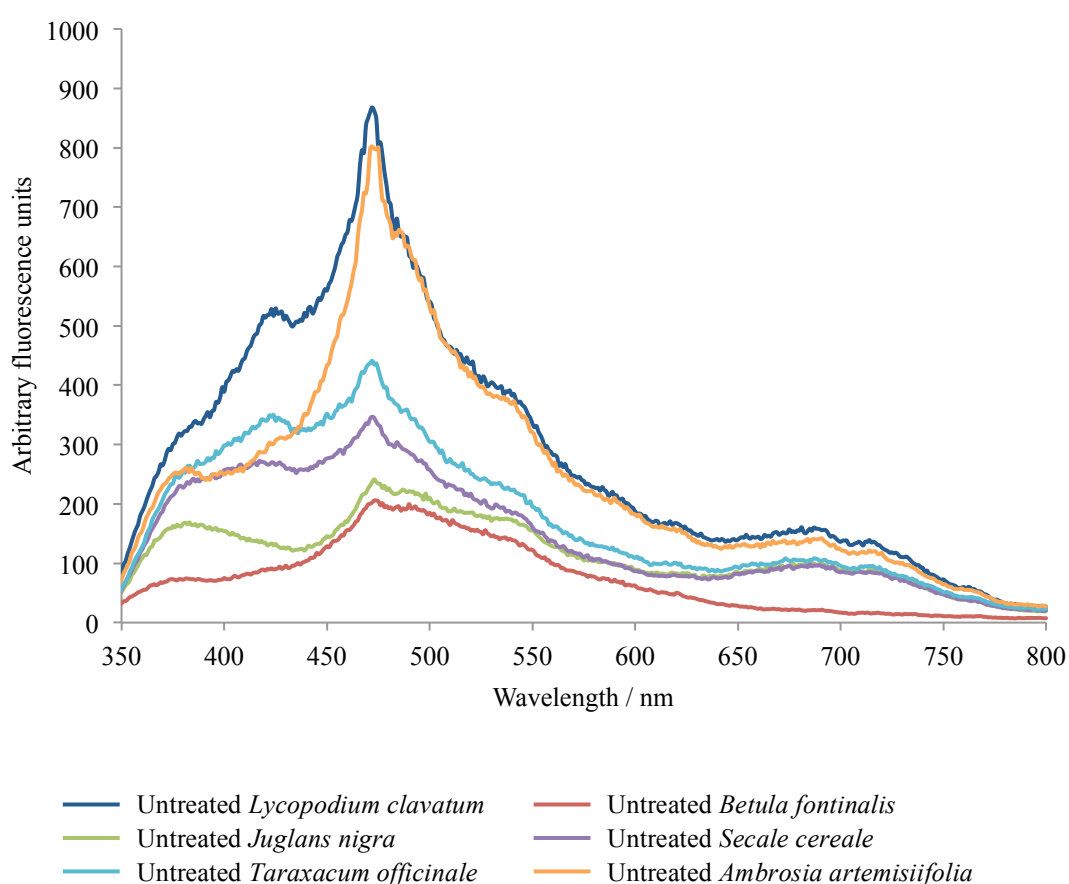


Figure 5.14: Fluorescence emission spectra of untreated *Lycopodium clavatum* spores and untreated *Betula fontinalis*, *Juglans nigra*, *Secale cereale*, *Taraxacum officinale* and *Ambrosia artemisiifolia* pollen (excitation λ 300 nm, 350 nm longpass filter applied)

The complex and largely unknown chemical structure of sporopollenin makes assigning its emission peaks difficult. Sporopollenin is known to autofluoresce more strongly compared to other pollen or spore components, suggesting that emission at around 470 nm arises from sporopollenin.¹⁵⁷ Sporopollenin has a phenolic component, and intense

peaks at around 470 nm are probably due to this.¹⁵⁷ Published work suggests that *p*-coumaric acid and ferulic acid (Figure 5.15) could be major moieties of sporopollenin.³⁹ As these acids fluoresce in the region $\sim 350 - 400$ nm in solution (Figure 5.16), the relatively weak emission observed in all genera in this range may also be attributed to sporopollenin.¹⁵⁵ It is possible that other structures within pollen and spores, namely the intine, endospore and protoplast, emit in the regions described here, but their relatively weak emission is probably masked by sporopollenin's comparatively intense emission.⁹⁵

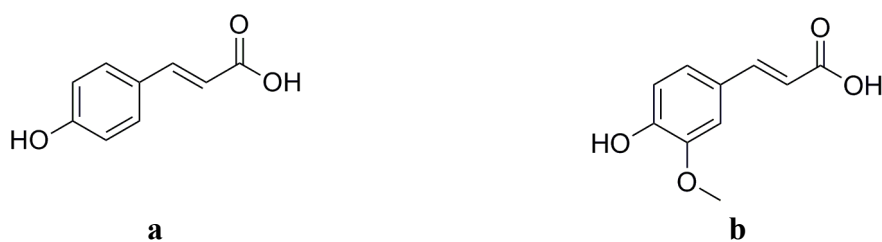


Figure 5.15: Structure of (a) *p*-coumaric acid and (b) ferulic acid

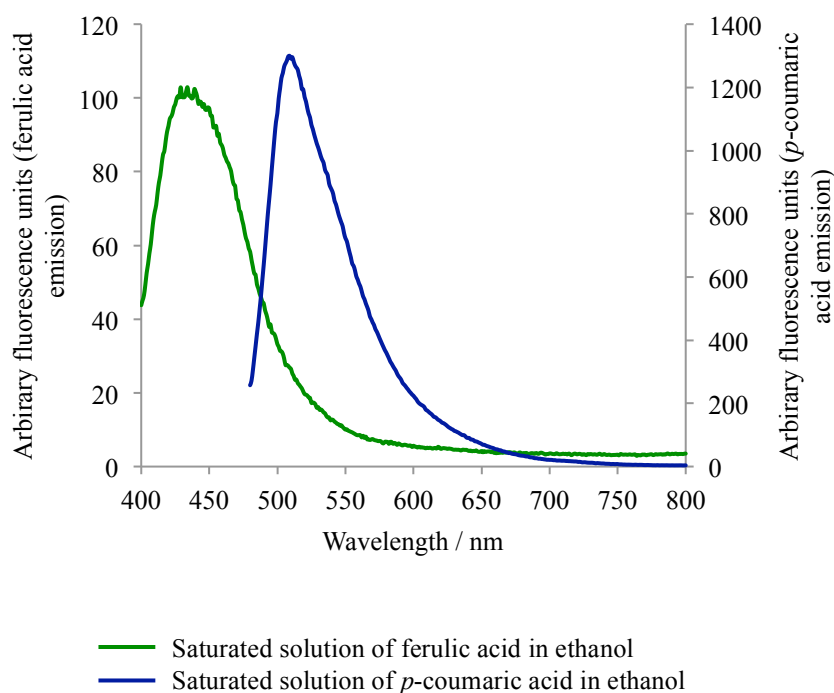


Figure 5.16: Emission spectra of saturated ethanolic solutions of ferulic acid (excitation λ 385 nm) and *p*-coumaric acid (excitation λ 450 nm)

Flavonoids (derived from flavone) and carotenoids (derived from lycopene) (Figure 5.17) are often found in or on the pollen grain or spore wall, and are thought to be partly responsible for the characteristic colours of pollen and spores.¹⁵⁸ These molecules

fluoresce weakly in the region 500 – 600 nm.^{159, 160} Therefore, emission bands observed in almost all species between 650 – 750 nm could originate from the pollen and spore walls.

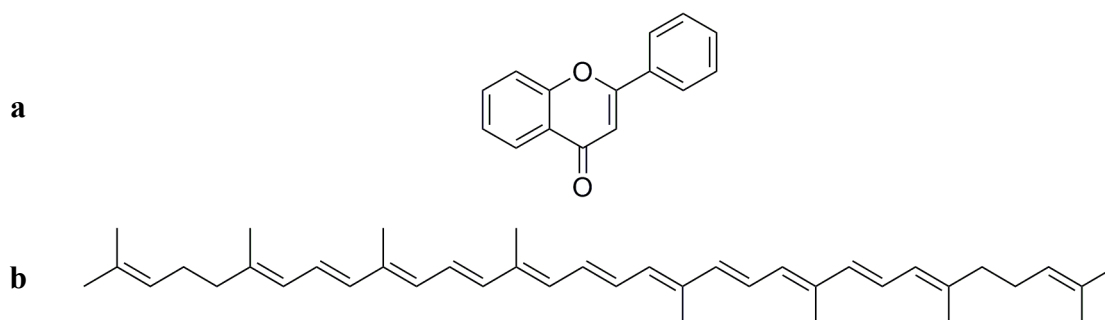


Figure 5.17: Structure of (a) flavone and (b) lycopene

Deoxyribonucleic acid (DNA) is found in the nuclei of pollen and spores. DNA is known to fluoresce in the region 415 – 420 nm, but has a low quantum yield, meaning it only fluoresces weakly, especially in comparison to the intense emission of sporopollenin.^{95, 161, 162} In addition, DNA has an absorption maximum at around 260 nm, so the excitation wavelength of 300 nm used in this experiment is insufficient to efficiently promote it to its excited state, therefore resulting in only weak emission. Due to these factors, emission from DNA is probably not present in the spectra presented in Figure 5.14.

Peaks seen in all genera at around 450 - 470 nm have been attributed to a variety of sources, including cellulose, terpenoids, flavonoids and the co-enzymes nicotinamide adenine dinucleotide phosphate (NADPH) and nicotinamide adenine dinucleotide (NADH).^{95, 163, 164} The intine of pollen and spores is thought to be primarily composed of polysaccharides, including cellulose, so is likely to contribute to emission observed around 470 nm. However, autofluorescence of the intine has been described as weak when compared to that of the exine; therefore its emission in Figure 5.14 is probably masked by that of sporopollenin.¹⁵⁷

Sodeau *et al.* suggested that species from the same botanical order might display similar fluorescence characteristics.⁹⁵ The taxonomy of the species investigated in this thesis is summarised in Figure 5.18. *Betula fontinalis* and *Juglans nigra* (order: Fagales) display similar fluorescence at around 470 nm. However, *Betula fontinalis* shows much weaker emission at around 360 – 390 nm and lacks the emission between 650 – 750 nm that

Juglans nigra has. *Taraxacum officinale* and *Ambrosia artemisiifolia* (both from the Asterales order and the Asteraceae family) show similar emission at 470 nm and between 650 – 750 nm. However, *Ambrosia artemisiifolia* shows much weaker emission in the 400 – 430 nm region compared to *Taraxacum officinale*. Therefore, this limited sample suggests that although pollen from the same family or order displays some similarities in their fluorescence characteristics, their emission profiles are far from identical. In addition, pollen and spores from different orders display similar emission; for example, *Lycopodium clavatum* (order: Lycopodiales) and *Ambrosia artemisiifolia* (order: Asterales) have very similar emission profiles between 650 – 750 nm.

ORDER	FAMILY	GENUS AND SPECIES
Lycopodiales	Lycopodiaceae	<i>Lycopodium clavatum</i> (club moss)
Poales	Poaceae	<i>Secale cereale</i> (rye)
Fagales	Betulaceae	<i>Betula fontinalis</i> (water birch)
	Juglandaceae	<i>Juglans nigra</i> (black walnut)
Asterales	Asteraceae	<i>Taraxacum officinale</i> (dandelion)
		<i>Ambrosia artemisiifolia</i> (common ragweed)

Figure 5.18: Summary of the orders, genera and species under investigation.
Genera and species in italics with their common names in brackets

5.4.1.1 Spectrofluorometry of untreated pollen and spores: summary of results

1. Fluorescence emission spectra from each species studied (*Betula fontinalis*, *Juglans nigra*, *Secale cereale*, *Taraxacum officinale* and *Ambrosia artemisiifolia* pollen, and *Lycopodium clavatum* spores) were distinct. However, all possessed a strong peak at around 470 nm with a weaker band between 350 – 450 nm, both attributable to sporopollenin. The complex structure of pollen and spores made assigning emission peaks to other individual components challenging.

2. Sodeau *et al.* suggested that similar fluorescence might be expected from species of the same botanical order.⁹⁵ Results from this thesis could not support their hypothesis.

5.4.2 Spectrofluorometry of untreated, enzyme-treated and base & acid-treated pollen and spores

Pollen from *Betula fontinalis*, *Ambrosia artemisiifolia* and *Taraxacum officinale* were treated according to the enzyme protocol described by Loewus *et al.*, and their emission was measured *via* spectrofluorometry.⁶⁴ The enzyme method aims to detach the protoplast from the intine and subsequently release the protoplast from the remaining exine shell and break down the intine. The emission of enzyme-treated pollen was compared to that of untreated pollen (Figure 5.19, Figure 5.21 and Figure 5.20). After enzyme-treatment, it would be reasonable to predict that signals relating to the protoplast and intine should decrease or disappear altogether. The enzymes used in this method (cellulysin and macerage), as well as bovine serum albumin (BSA), do not digest sporopollenin, therefore its chemical structure should remain unaltered. The chemical environment in which sporopollenin exists may be altered by the digestion of neighbouring components, namely the intine and protoplast. Although this may influence sporopollenin's emission, any effect is likely to be small and therefore possibly difficult to discern.

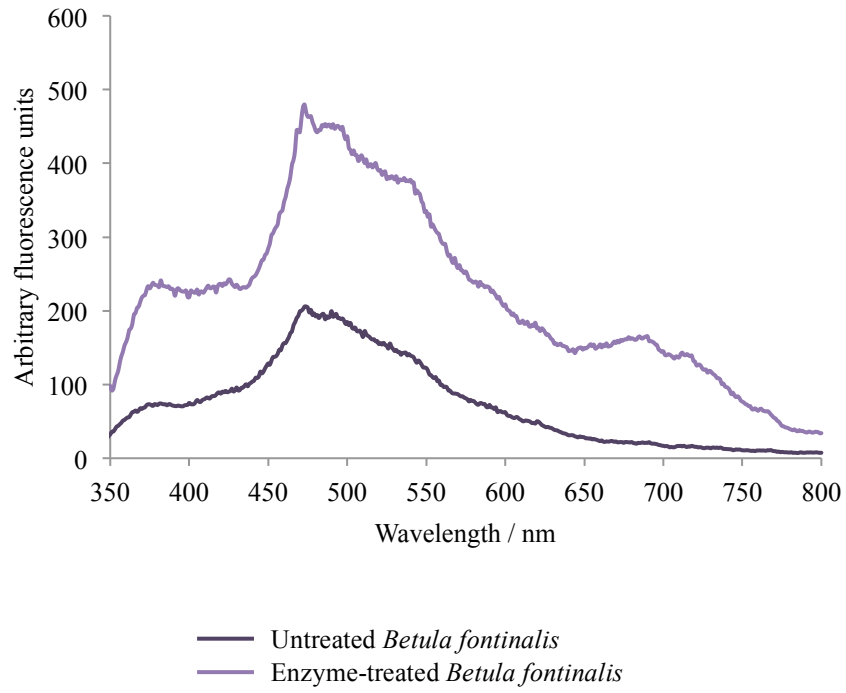


Figure 5.19: Fluorescence emission spectra of untreated and enzyme-treated *Betula fontinalis* pollen (excitation λ 300 nm, 350 nm longpass filter)

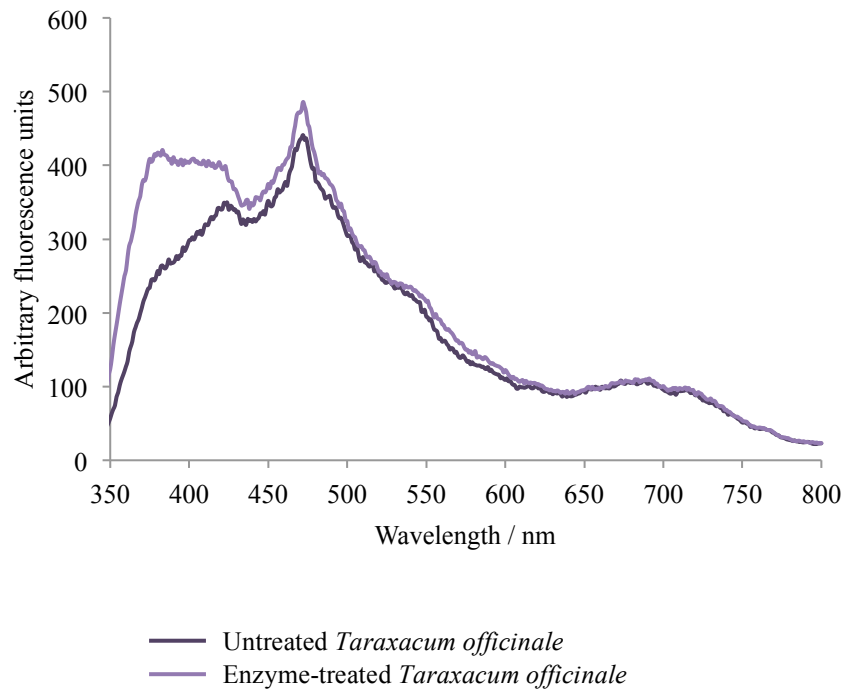


Figure 5.20: Fluorescence emission spectra of untreated and enzyme-treated *Taraxacum officinale* pollen (excitation λ 300 nm, 350 nm longpass filter)

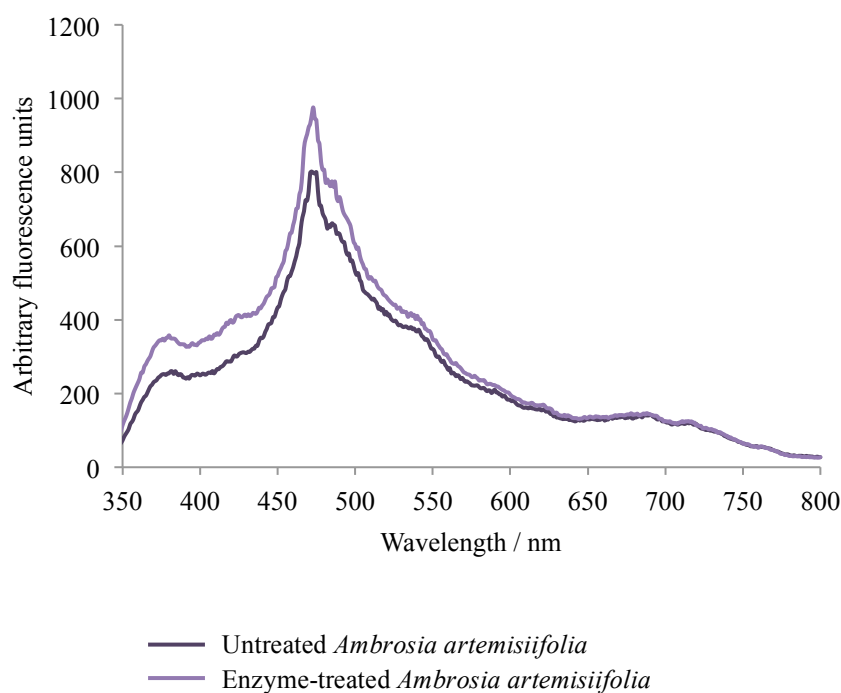


Figure 5.21: Fluorescence emission spectra of untreated and enzyme-treated *Ambrosia artemisiifolia* pollen (excitation λ 300 nm, 350 nm longpass filter)

Peaks at 350 – 370 nm, 470 nm and 650 – 750 nm are thought to be attributable to sporopollenin's autofluorescence (see section 5.4.1).^{155, 157, 159, 160} The most intense sporopollenin peak appears at 470 nm, and all species retain this peak after enzyme treatment. This provides further evidence to suggest that sporopollenin is unaffected by the enzyme treatment applied.

Ambrosia artemisiifolia and *Taraxacum officinale* both maintain emission peaks between 650 – 750 nm after enzyme treatment. *Betula fontinalis* appears to develop a peak in this region after enzyme treatment. However, as the overall intensity of untreated *Betula fontinalis*'s emission is particularly low, emission in the 650 – 750 nm region may simply be too weak to be observed. These results further indicate that the enzyme treatment did not change the sporopollenin exine of *Ambrosia artemisiifolia* and *Taraxacum officinale*, but may have modified that of *Betula fontinalis*.

The three species examined all emit in the region 350 – 370 nm (thought to be attributed to sporopollenin emission), both before and after enzyme treatment. However, the relative intensity of these peaks compared to the strong peak at 470 nm does not remain consistent. Peak intensities and ratios are summarised in Table 5.2. For example, *Taraxacum officinale* has a peak ratio of 0.5 before treatment but 0.8 after treatment,

indicating that the peak in the 350 – 370 nm region has grown after enzyme treatment. It is unclear why these peak ratios change, as there is no reason to think that the chemistry of sporopollenin is altered by the enzyme protocol employed. Structures that lie in close proximity to sporopollenin, namely the intine and protoplast, are likely to be chemically changed by the enzyme treatment. As a result, sporopollenin's interaction with these structures will change, thus altering sporopollenin's local chemical environment and therefore possibly its emission profile. The uncertainty within the ratios plotted is difficult to quantify due to noise within the data and varying peak intensities. Normalisation of the data was not considered possible, as baselines could not be determined for all samples due to the variation in emission intensity. This, in turn, could not be maintained due to the experimental setup.

Table 5.2: Emission intensities at 370 nm and 470 nm and calculated peak ratios of untreated and enzyme-treated *Betula fontinalis*, *Ambrosia artemisiifolia* and *Taraxacum officinale* pollen. Data taken from Figure 5.19 - Figure 5.20

	Before enzyme treatment			After enzyme treatment		
	Peak emission intensity in the region of:		Ratio of intensities	Peak emission intensity in the region of:		Ratio of intensities
	370 nm	470 nm		370 nm	470 nm	
<i>Betula fontinalis</i>	66.85	199.2	0.3	217.9	442.5	0.5
<i>Ambrosia artemisiifolia</i>	250.1	802.4	0.3	357.8	922.1	0.4
<i>Taraxacum officinale</i>	206.9	434.5	0.5	373.1	471.6	0.8

The intine of pollen is likely to fluoresce weakly in the 450 – 470 nm region (see section 5.4.1). Published results suggest that the enzyme treatment is likely to break down the intine of pollen.⁶⁴ Therefore, a decrease in emission in the 450 – 470 nm region would be anticipated for enzyme-treated pollen. Although this decrease is not observed, the intense sporopollenin peak at 470 nm may mask it. From these results, we

cannot be certain what effect the enzyme treatment has on the intine. (see section 5.5 for further discussion).

Overall, the enzyme treatment proposed by Loewus *et al.* altered the fluorescence emission profiles of the pollen species under investigation so that they can be distinguished from their untreated counterparts. This is in contrast to the results of visual inspection (see section 5.3) where untreated and enzyme-treated pollen could not be distinguished by eye. Sporopollenin's emission was not greatly altered by the enzyme treatment, but it is impossible to determine from these complex emission spectra alone whether the intine and protoplast were modified.

Lycopodium clavatum spores and *Betula fontinalis* pollen were treated by applying the base and acid protocol described by Barrier *et al.*⁵⁷ This was carried out in order to determine how this treatment contrasts with the enzyme-treatment in terms of the fluorescence emission observed. Emission spectra of these untreated and base and acid-treated pollen and spores are presented in Figure 5.22 and Figure 5.23. The spectrum of enzyme-treated *Betula fontinalis* was added to Figure 5.23 in order to facilitate comparisons.

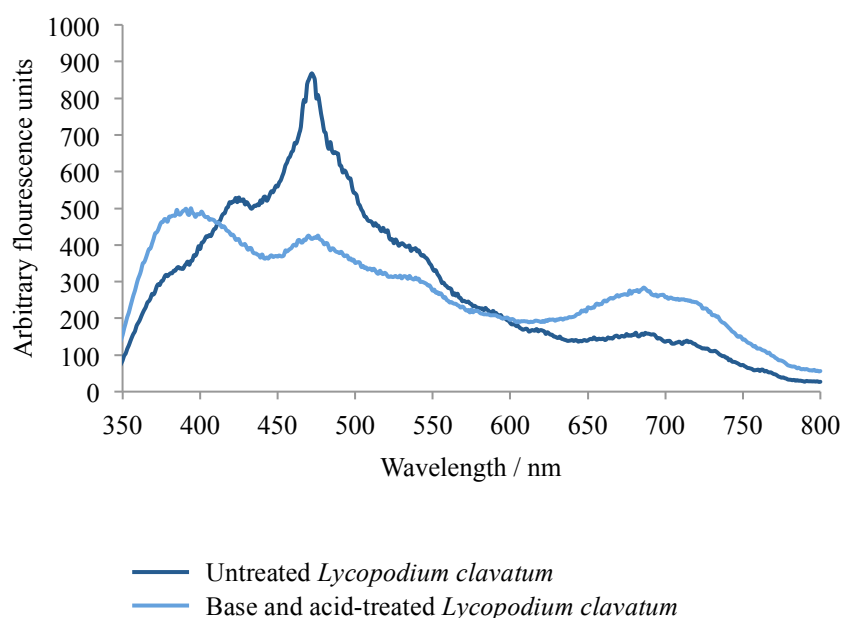


Figure 5.22: Fluorescence emission spectra of untreated and base and acid treated *Lycopodium clavatum* spores (excitation λ 300 nm, 350 nm longpass filter)

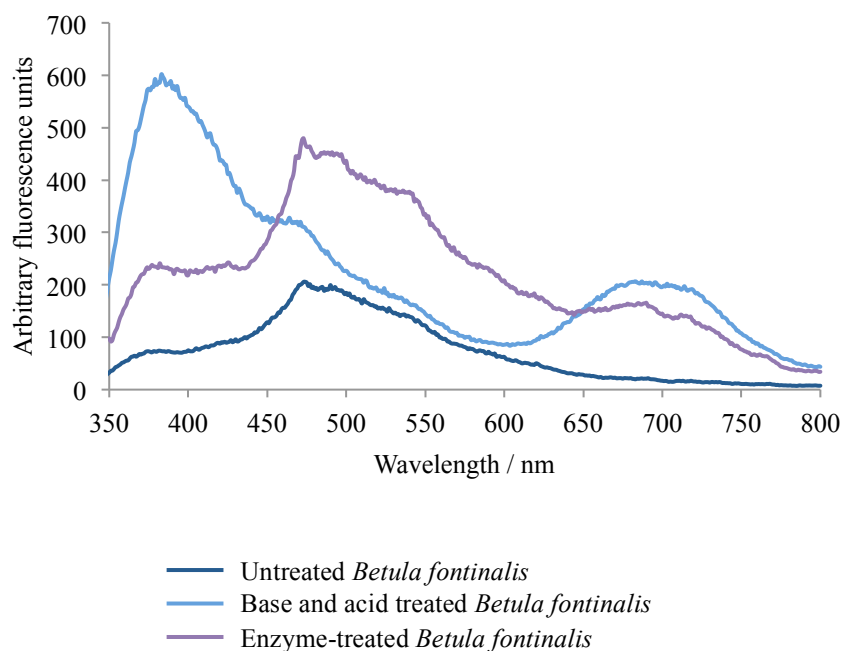


Figure 5.23: Fluorescence emission spectra of untreated and base and acid treated *Betula fontinalis* pollen (excitation λ 300 nm, 350 nm longpass filter)

Both before and after base and acid treatment, both species exhibit peaks at around 470 nm, probably due to sporopollenin emission. However, the intensity of this peak varies relative to the peak at 370 nm observed both before and after treatment. These ratios are summarised in Table 5.3. It is particularly noticeable that after base and acid treatment, *Betula fontinalis*' emission at 370 nm is much more intense than before treatment, with a ratio of 1.6, compared to 0.3 before treatment. A similar change in ratios was observed in enzyme-treated pollen (Table 5.2).

Table 5.3: Emission intensities at 370 nm and 470 nm and calculated peak ratios of untreated and base and acid-treated *Lycopodium clavatum* spores and *Betula fontinalis* pollen. Data taken from Figure 5.22 and Figure 5.23

	Before base and acid treatment			After base and acid treatment		
	Peak emission intensity in the region of:		Ratio of intensities	Peak emission intensity in the region of:		Ratio of intensities
	370 nm	470 nm		370 nm	470 nm	
<i>Lycopodium clavatum</i>	264.8	849.6	0.3	416.5	425.5	1.0
<i>Betula fontinalis</i>	66.85	199.2	0.3	515.1	313.6	1.6

Visual inspection of base and acid-treated *Lycopodium clavatum* spores (see section 5.3) shows that this treatment greatly alters the colour of the spores, turning them from pale yellow to dark brown. Previous research suggests that this method removes all of the intine and protoplast, leaving just the sporopollenin exine remaining.⁵⁷ This colour change therefore suggests that the chemical structure of sporopollenin has probably been altered. Such a structural change could explain the increase in the relative peak intensities of peaks at 370 nm.

An emission band between 650 – 750 nm is observed in all spectra, apart from that for untreated *Betula fontinalis*. In *Lycopodium clavatum*, the intensity decreases relative to the peak at 470 nm. In contrast, for *Betula fontinalis*, after base and acid treatment a band emerges in this region. If this band is due to sporopollenin, this tends to provide further evidence that base and acid treatment alters sporopollenin's chemical structure, although exactly how remains unknown.

5.4.2.1 Spectrofluorometry of untreated, enzyme-treated and base and acid-treated pollen and spores: summary of results

1. Pollen from *Betula fontinalis*, *Ambrosia artemisiifolia* and *Taraxacum officinale* was treated according to the enzyme protocol described by Loewus *et al.*⁶⁴ Emission from each species was distinct. After enzyme treatment, each species retained intense emission peaks at 370 and 470 nm, both attributable to sporopollenin. However, the ratio of these peaks varied when untreated and enzyme-treated pollen were compared.
2. *Lycopodium clavatum* spores and *Betula fontinalis* pollen were treated according to the base and acid protocol published by Barrier *et al.*⁵⁷ Emission spectra were different compared to the same untreated pollen and spores and, as with enzyme-treated pollen, the ratio of peaks at 370 and 470 nm varied. This change in peak ratios may indicate that base and acid-treatment affects sporopollenin's structure.
3. Spectrofluorometry of enzyme and base and acid-treated pollen and spores is a rapid method to differentiate between species. It is able to detect differences that visual inspection alone cannot. However, it is not a suitable method to determine the effect these treatments have on individual components of pollen and spores.

5.4.3 Spectrofluorometry of untreated, enzyme-treated, and base and acid-treated pollen and spores, treated with Rhodamine B

Pollen and spores (untreated, enzyme-treated, and base and acid-treated) from a range of species were treated with aqueous or ethanolic solutions of RhB at concentrations of 1×10^{-3} , 10^{-4} , 10^{-5} and 10^{-6} mol dm⁻³ (see Table 5.1 for a summary of samples prepared). After the application of RhB solutions, pollen and spores were filtered and washed and the resultant samples analysed *via* spectrofluorometry using a front-face excitation geometry. Samples were excited at 300 nm to evaluate sporopollenin emission. When water was used to dissolve RhB, samples were excited at 543 nm, but when ethanol was used, an excitation wavelength of 548 nm was selected. These wavelengths were chosen on the basis of RhB's optimum excitation wavelengths in water and ethanol.⁸³

There are a large number of variables when preparing and analysing pollen and spores treated with RhB for spectrofluorometry. These variables include the species under investigation, treatments used to remove biological material, the fluorochrome applied, the solvents used, and the excitation wavelength selected. In order to reduce these variables and therefore simplify analysis, a majority of the work was carried out on one species of pollen: *Betula fontinalis*. Figure 5.24 summarises the samples prepared from this species and the subsequent excitation wavelengths used, which produced a total of eight emission spectra. These spectra are presented in Figure 5.25 to Figure 5.32.

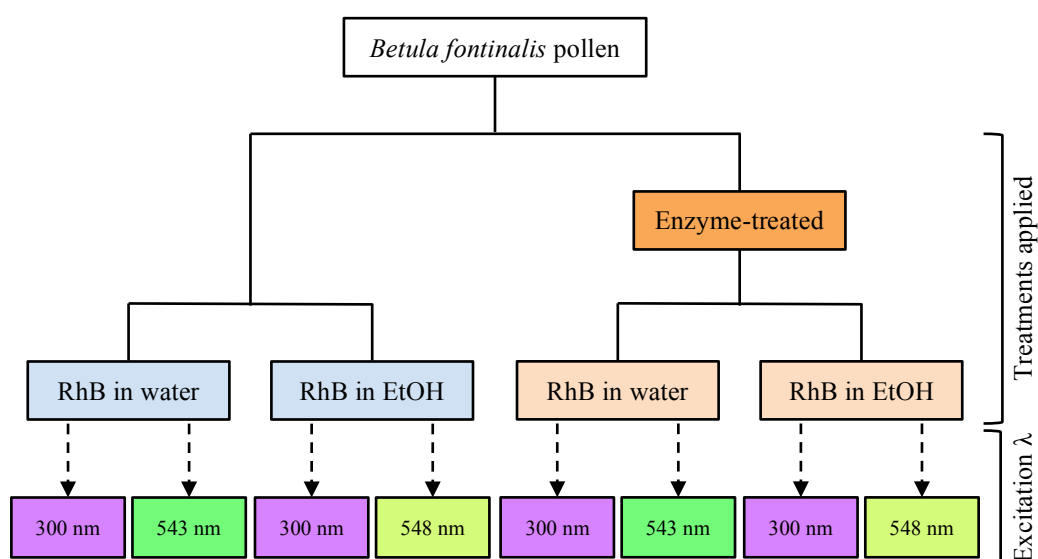


Figure 5.24: Diagram to demonstrate the samples prepared from *Betula fontinalis* pollen for spectrofluorometry and the excitation wavelengths used to produce spectra

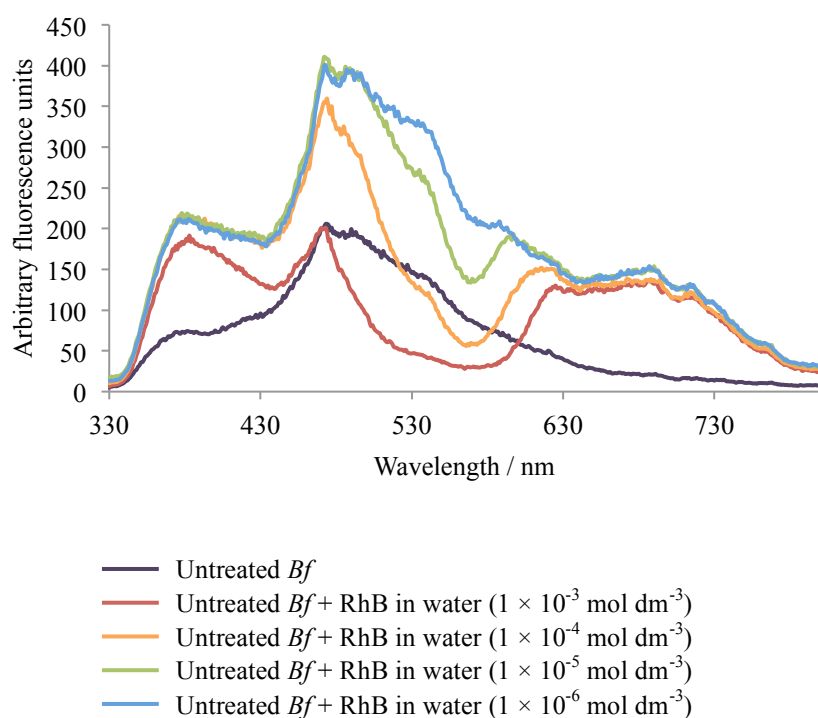


Figure 5.25: Emission spectra of untreated *Betula fontinalis* (*Bf*) pollen, treated with aqueous solutions of RhB of varying concentrations (excitation λ 300 nm, 350 nm longpass filter)

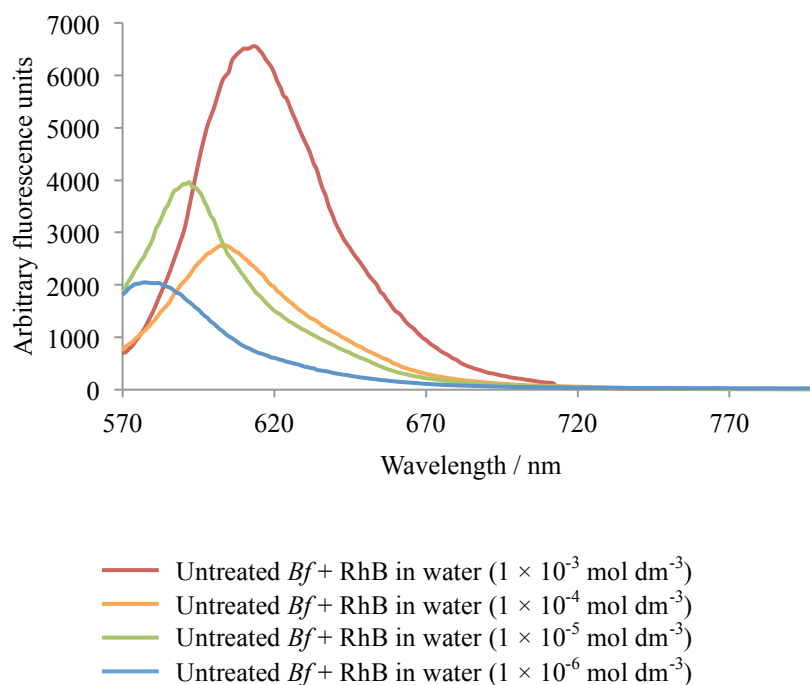


Figure 5.26: Emission spectra of untreated *Betula fontinalis* (*Bf*) pollen, treated with aqueous solutions of RhB of varying concentrations (excitation λ 543 nm)

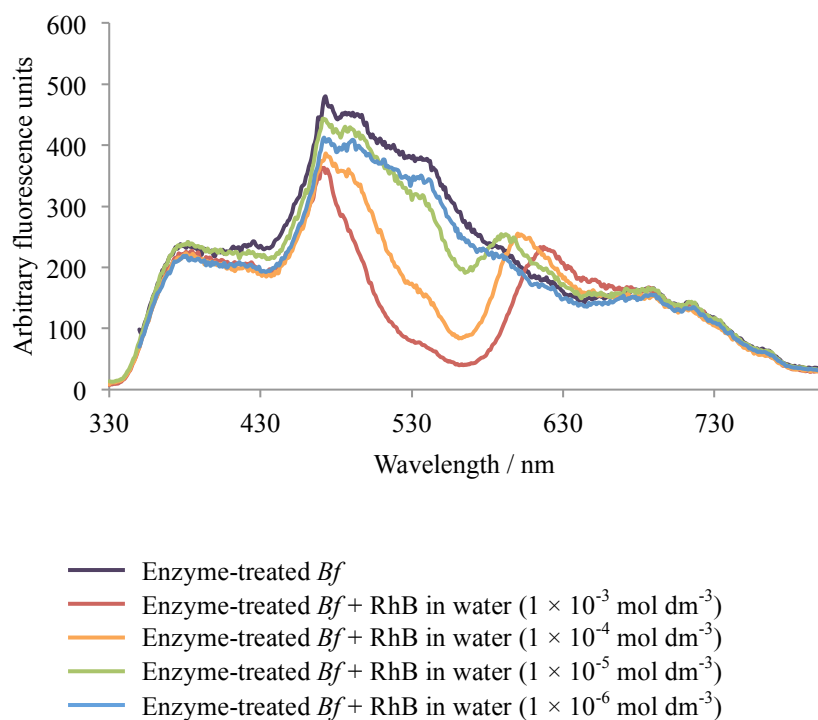


Figure 5.27: Emission spectra of enzyme-treated *Betula fontinalis* (*Bf*) pollen, treated with aqueous solutions of RhB of varying concentrations (excitation λ 300 nm, 350 nm longpass filter)

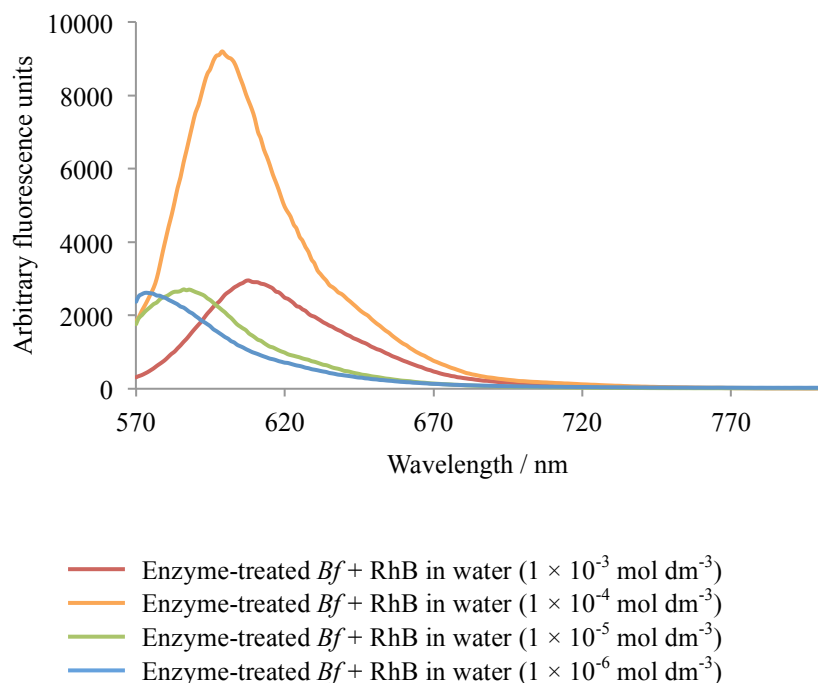


Figure 5.28: Emission spectra of enzyme-treated *Betula fontinalis* (*Bf*) pollen, treated with aqueous solutions of RhB of varying concentrations (excitation λ 543 nm)

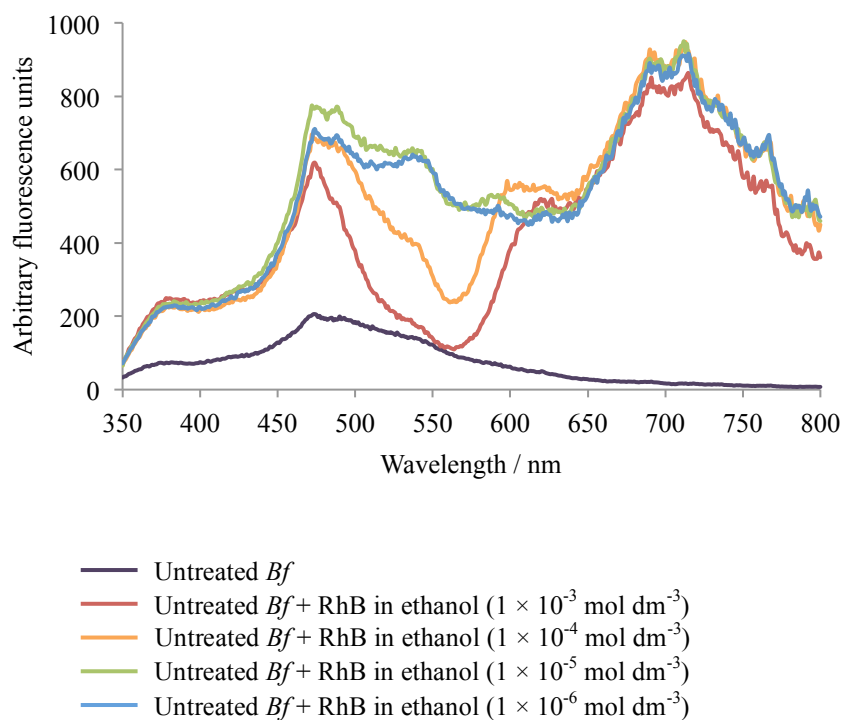


Figure 5.29: Emission spectra of untreated *Betula fontinalis* (*Bf*) pollen, treated with ethanolic solutions of RhB of varying concentrations (excitation λ 300 nm, 350 nm longpass filter)

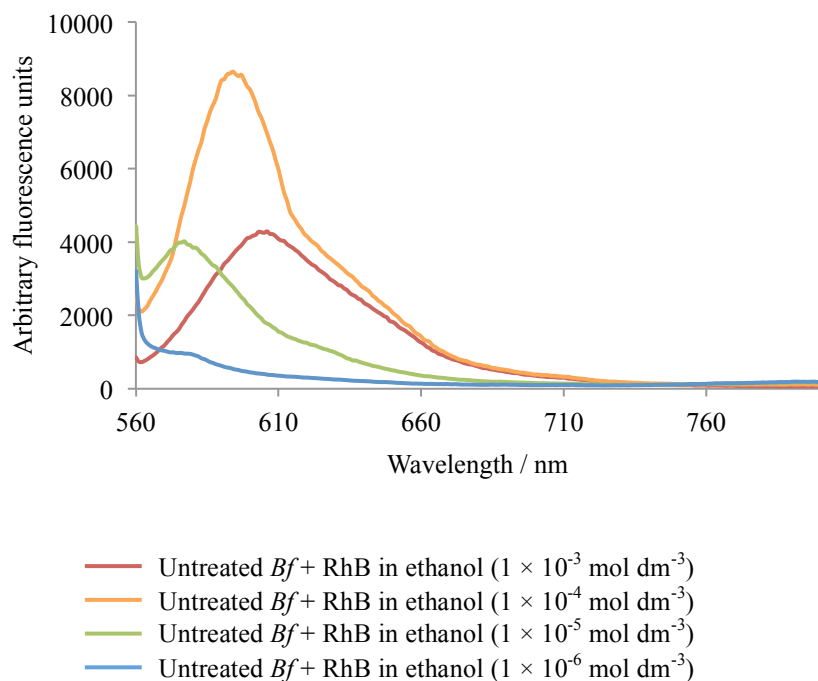


Figure 5.30: Emission spectra of untreated *Betula fontinalis* (*Bf*) pollen, treated with ethanolic solutions of RhB of varying concentrations (excitation λ 548 nm)

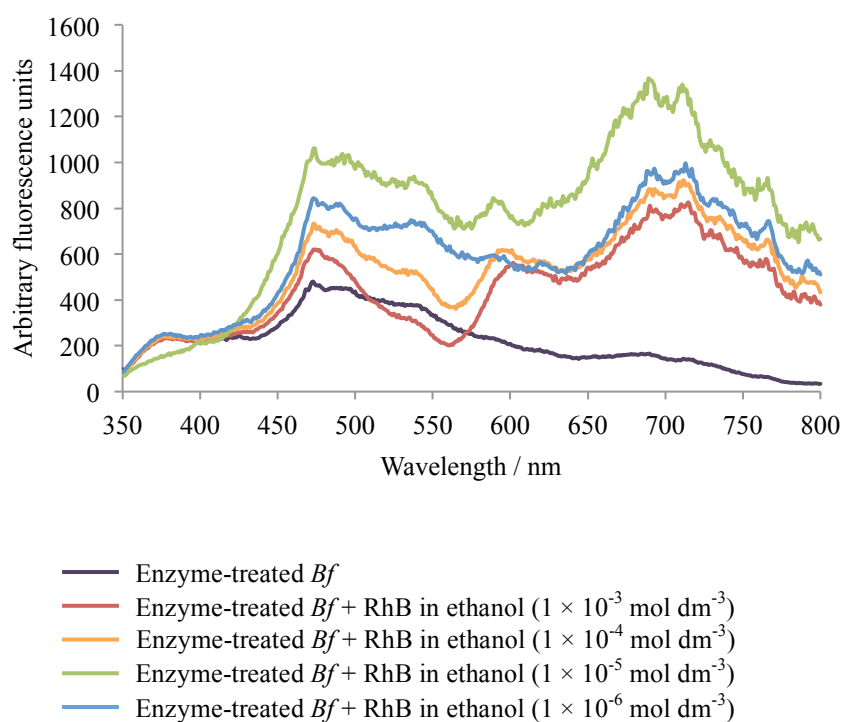


Figure 5.31: Emission spectra of enzyme-treated *Betula fontinalis* (*Bf*) pollen, treated with ethanolic solutions of RhB of varying concentrations (excitation λ 300 nm, 350 nm longpass filter)

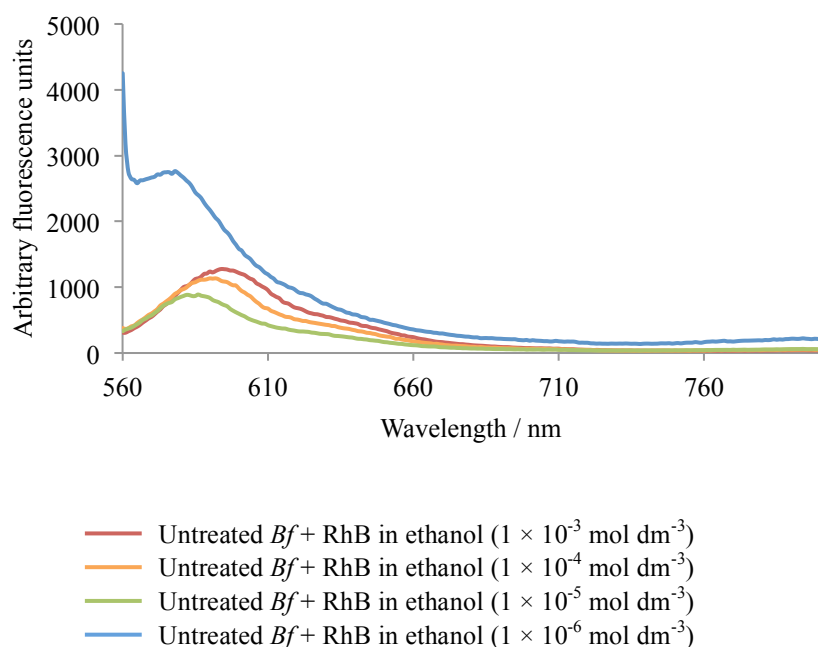


Figure 5.32: Emission spectra of untreated *Betula fontinalis* (*Bf*) pollen, treated with ethanolic solutions of RhB of varying concentrations (excitation λ 548 nm)

All samples possess some similarities in their spectra; however there are differences observed depending on the solvent used; whether the pollen was enzyme-treated; and the concentration of RhB solution applied. All samples excited at 300 nm (Figure 5.25, Figure 5.27, Figure 5.29 and Figure 5.31) show broad peaks around 370 nm, and intense peaks at 470 nm, likely to be due to sporopollenin emission. They also have broad bands around 580 – 640 nm, which are primarily due to RhB emission. Samples excited at 543 or 548 nm (Figure 5.26, Figure 5.28, Figure 5.30 and Figure 5.32) primarily show emission from RhB, as emission from pollen largely occurs at wavelengths below 550 nm, and therefore cannot be seen in these spectra. The key peaks from each spectrum are summarised in Table 5.4 to Table 5.7.

Table 5.4: Summary of peak emission wavelengths of untreated *Betula fontinalis* pollen, treated with aqueous solutions of RhB at varying concentrations. Data taken from Figure 5.25 and Figure 5.26

Concentration of RhB solution applied / mol dm ⁻³	Peak emission at 300 nm excitation λ / nm		Emission at 543 nm excitation λ / nm
	Pollen	Rhodamine B	Rhodamine B
0	382 and *	-	-
1×10^{-3}	383 and 470	625	613
1×10^{-4}	383 and 474	616	604
1×10^{-5}	382 and 472	597	592
1×10^{-6}	383 and 473	588	577

* Only a single peak observed

Table 5.5: Summary of peak emission wavelengths of enzyme-treated *Betula fontinalis* pollen, treated with aqueous solutions of RhB at varying concentrations. Data taken from Figure 5.27 and Figure 5.28

Concentration of RhB solution applied / mol dm ⁻³	Peak emission at 300 nm excitation λ / nm		Emission at 543 nm excitation λ / nm
	Pollen	Rhodamine B	Rhodamine B
0	377 and 473	-	-
1×10^{-3}	384 and 472	617	608
1×10^{-4}	381 and 473	600	599
1×10^{-5}	382 and 471	592	586
1×10^{-6}	381 and 472	*	572

* Emission peak too weak to identify

Table 5.6: Summary of peak emission wavelengths of untreated *Betula fontinalis* pollen, treated with ethanolic solutions of RhB at varying concentrations. Data taken from Figure 5.29 and Figure 5.30

Concentration of RhB solution applied / mol dm ⁻³	Peak emission at 300 nm excitation λ / nm		Emission at 548 nm excitation λ / nm
	Pollen	Rhodamine B	Rhodamine B
0	*	-	-
1×10^{-3}	380 and 474	620	606
1×10^{-4}	385 and 472	598	594
1×10^{-5}	383 and 472	588	577
1×10^{-6}	383 and 474	*	†

* Emission peak too weak to identify

† Peak off scale

Table 5.7: Summary of peak emission wavelengths of enzyme-treated *Betula fontinalis* pollen, treated with ethanolic solutions of RhB at varying concentrations. Data taken from Figure 5.31 and Figure 5.32

Concentration of RhB solution applied / mol dm ⁻³	Peak emission at 300 nm excitation λ / nm		Emission at 548 nm excitation λ / nm
	Pollen	Rhodamine B	Rhodamine B
0	377 and 473	-	-
1×10^{-3}	381 and 475	602	594
1×10^{-4}	378 and 473	595	590
1×10^{-5}	* and 474	589	586
1×10^{-6}	377 and 473	*	578

* Emission peak too weak to identify

5.4.3.1 The effect of changing the solvent used to dissolve Rhodamine B

Samples excited at 300 nm show peaks at 470 nm and 370 nm whether aqueous or ethanolic solutions of RhB were applied. These peaks are likely to be due to sporopollenin's emission. In both solvents, peaks at 370 nm are weaker than those at 470 nm. However when water was used, the ratio between these peaks is greater than when ethanol was used (Table 5.8 and Table 5.9). This observation is independent of whether the pollen was untreated or enzyme-treated, indicating that the ratio of the peaks at 470 nm and 370 nm is probably due to the solvent. The precise reason for this difference is impossible to infer, but several suggestions can be made. For example, this result could indicate that although the pollen appeared dry prior to analysis, some residual solvent may have remained trapped within the pollen, influencing sporopollenin's emission. Alternatively, the water and ethanol may each facilitate the encapsulation or binding of different amounts of RhB. Therefore, one solvent may lead to a higher quantity of RhB being encapsulated or bound, causing a greater change in sporopollenin's local environment. This could lead to a change in sporopollenin's emission profile, potentially altering the ratio of peaks at 370 and 470 nm.

Table 5.8: Emission intensities at 370 nm and 470 nm and calculated peak ratios of untreated *Betula fontinalis* pollen treated with aqueous and ethanolic solutions of RhB at varying concentrations. Data taken from Figure 5.25 and Figure 5.29; peak emission wavelengths used taken from Table 5.4 and Table 5.6

RhB / mol dm ⁻³	Water solvent			Ethanol solvent		
	Peak emission intensity in the region of:		Ratio of intensities	Peak emission intensity in the region of:		Ratio of intensities
	370 nm	470 nm		370 nm	470 nm	
1×10^{-3}	191.6	200.8	1.0	249.0	619.2	0.4
1×10^{-4}	216.1	359.5	0.6	228.6	695.3	0.3
1×10^{-5}	218.1	410.6	0.5	241.0	774.4	0.3
1×10^{-6}	211.5	400.8	0.5	229.8	711.0	0.3

Table 5.9: Emission intensities at 370 nm and 470 nm and calculated peak ratios of enzyme-treated *Betula fontinalis* pollen treated with aqueous and ethanolic solutions of RhB at varying concentrations. Intensity data taken from Figure 5.27 and Figure 5.31; peak emission wavelengths used taken from Table 5.5 and Table 5.7

RhB / mol dm ⁻³	Water solvent			Ethanol solvent		
	Peak emission intensity in the region of:		Ratio of intensities	Peak emission intensity in the region of:		Ratio of intensities
	370 nm	470 nm		370 nm	470 nm	
1×10^{-3}	226.5	362.7	0.6	236.1	619.9	0.4
1×10^{-4}	222.8	386.4	0.6	240.7	731.7	0.3
1×10^{-5}	241.6	443.1	0.6	*	1061.0	-
1×10^{-6}	219.0	412.4	0.5	252.4	843.6	0.3

* Peak too weak to identify

RhB emission also changes when the solvent is altered, independent of the concentration of RhB solution used. This is best observed at excitation wavelengths of 543 and 548 nm. When water was used as a solvent, the peak emission wavelength of RhB is typically longer than when ethanol is used. For example, in untreated pollen

treated with $1 \times 10^{-3} \text{ mol dm}^{-3}$ RhB, peak emission is 613 nm when water was the solvent (Table 5.4), but 606 nm when ethanol was the solvent (Table 5.6). This is consistent with the emission of RhB in solution, with ethanolic solutions emitting at shorter wavelengths than aqueous solutions (Figure 5.33, Figure 5.34 and Table 5.10). This could again suggest that there is residual solvent left within the pollen after filtration and drying, or that each solvent successfully encapsulated different quantities of RhB.

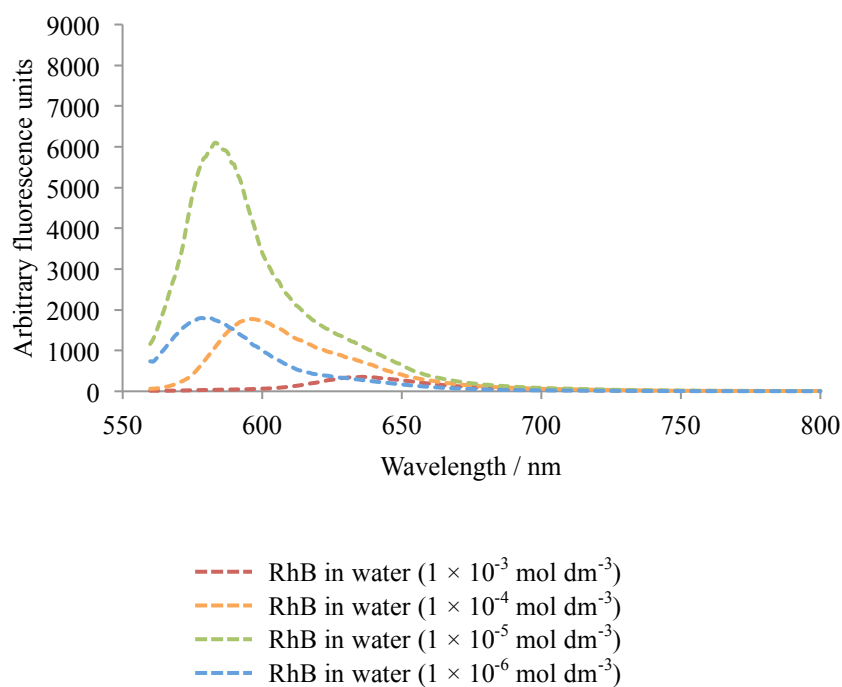


Figure 5.33: Emission spectra of RhB in solution with water at a range of concentrations. (Excitation λ 548 nm)

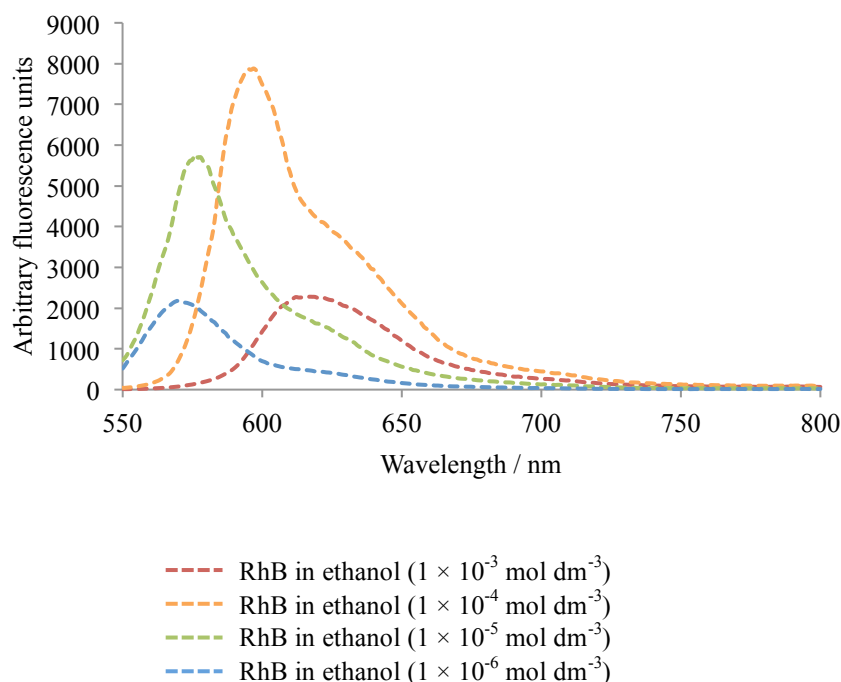


Figure 5.34: Emission spectra of RhB in solution with EtOH at a range of concentrations. (Excitation λ 543 nm)

Table 5.10: Summary of peak emission wavelengths in solutions of RhB at varying concentrations with water (excitation λ 548 nm), or ethanol (excitation λ 543 nm) as the solvent

Concentration RhB / mol dm^{-3}	Peak emission λ / nm	
	Water solvent	Ethanol solvent
1×10^{-3}	636	617
1×10^{-4}	596	597
1×10^{-5}	583	576
1×10^{-6}	581	570

5.4.3.2 The effect of changing the concentration of Rhodamine B applied

The relationship between the concentration of the RhB solution applied to pollen and the intensity of the emission observed is not consistent. For example, Figure 5.32 illustrates that emission at $1 \times 10^{-6} \text{ mol dm}^{-3}$ RhB is approximately twice as intense as that observed at $1 \times 10^{-3} \text{ mol dm}^{-3}$ RhB. However, in Figure 5.26 the lowest concentration of RhB ($1 \times 10^{-6} \text{ mol dm}^{-3}$) emits with less than half the intensity of the highest concentration of RhB ($1 \times 10^{-3} \text{ mol dm}^{-3}$). Here, we propose two possible

explanations for the differences in emission intensities observed. Firstly, as the concentration of RhB is increased, there are more RhB molecules available to absorb incident light. These RhB molecules absorb a large proportion of incident light at the surface of the sample meaning that less light reaches the bulk of the sample (Figure 5.35 (a)). Therefore, fewer fluorochrome molecules are able to fluoresce, leading to weaker emission overall. At lower RhB concentrations, there are fewer fluorochrome molecules, so light is better able to penetrate the sample (Figure 5.35 (b)). As a result, fluorescence is observed from a greater proportion of the fluorochromes, meaning that more intense emission is observed overall. This is known as one of the ‘inner filter’ effects (the other being reabsorption). Spectrofluorometry is usually carried out in dilute solutions to minimise this effect.

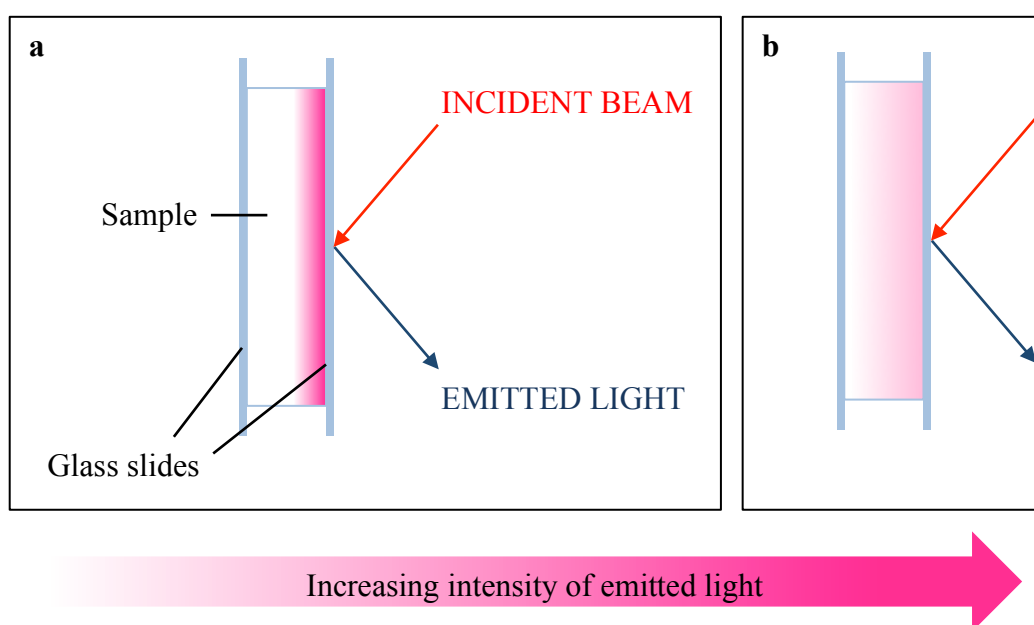


Figure 5.35: The intensity of fluorescence emission related to the concentration of RhB within a sample. (a) High concentration and (b) low concentration of RhB

The second reason for varying emission intensities is likely to be due to the sample preparation. The surface area of the solid samples between the glass slides used cannot be maintained between samples. As a result, the surface area of samples within the incident beam is not always the same, so varying emission intensities are likely to be observed.

As well as the concentration of RhB affecting the intensity of emission observed, it also influences the peak emission wavelength. When excited at 543 or 548 nm, it is clear that higher concentrations of RhB emit at longer peak wavelengths compared to lower

concentrations (Table 5.5 and Table 5.7). For example, *Betula fontinalis* pollen (enzyme-treated), treated with ethanolic solutions of RhB, shows peak emission at 594 nm when treated with the highest concentration of RhB (1×10^{-3} mol dm⁻³), but at 578 nm when treated with the lowest concentration (1×10^{-6} mol dm⁻³).

At the higher RhB concentrations, there is a greater probability of reabsorption (the second of the two inner filter effects) occurring after initial emission from a fluorochrome. Reabsorption takes place when a fluorochrome emits light and this light is then immediately reabsorbed by another fluorochrome (whether of the same or a different type) (Figure 5.36). This second fluorochrome then emits light at a longer wavelength (lower energy) than the initial fluorochrome. This causes a shift in the emission spectrum to longer wavelengths, as shorter wavelength (higher energy) components are lost to reabsorption. However, not all of the light initially emitted is reabsorbed, meaning that a proportion of the fluorochrome's initial emission may still be observed in the emission spectrum. For reabsorption to occur, the absorption and emission bands of a fluorochrome must show good overlap, such as in RhB.¹⁶⁵ RhB is known to exhibit reabsorption in solution over the range of concentrations studied here.¹⁶⁶ The high concentration of RhB molecules in pollen treated with RhB indicates that reabsorption could be possible in these solid samples.

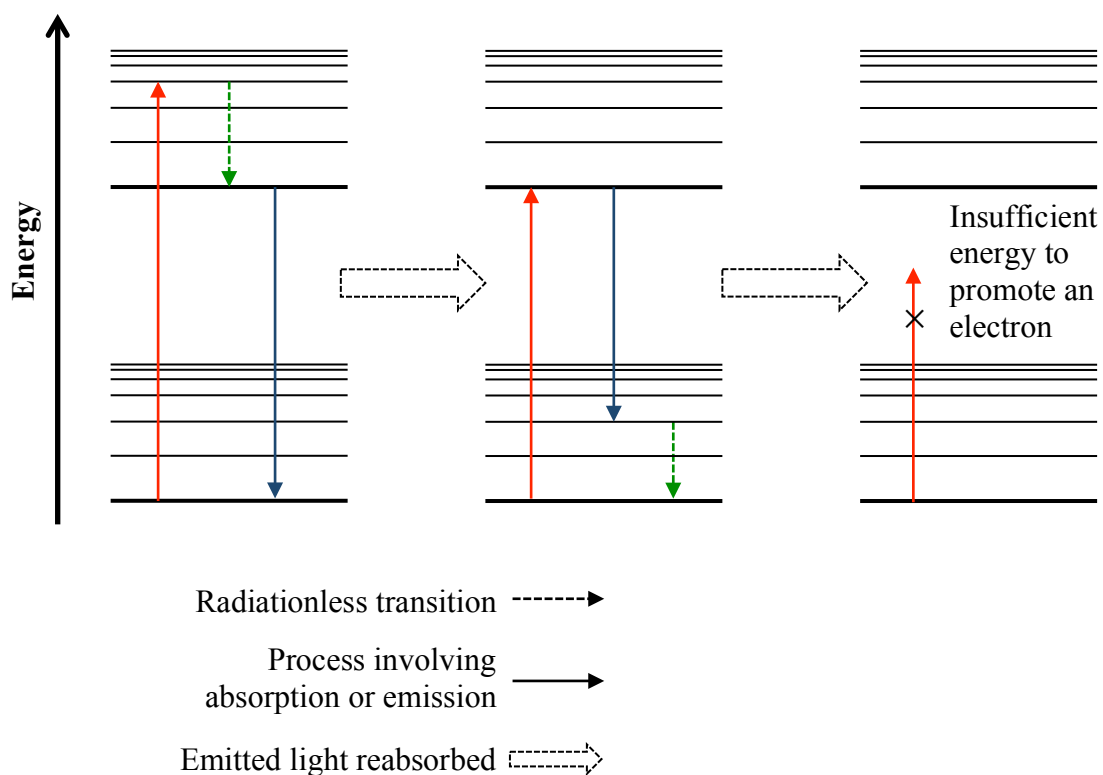


Figure 5.36: Simplified Jablonski diagram illustrating the process of reabsorption

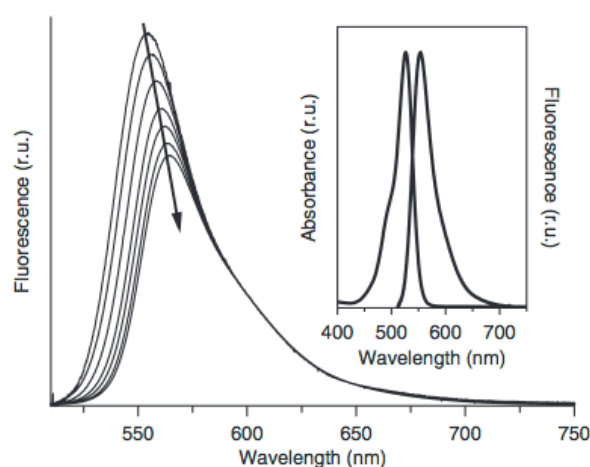


Figure 5.37: Emission spectrum of a fluorochrome demonstrating reabsorption at increasing fluorochrome concentrations (indicated by the arrow). Inset: Absorption and emission spectra of the same fluorochrome, demonstrating that a good overlap between the two is required for reabsorption to take place¹⁶⁵

r.u. = relative units

Spectrofluorometry is usually performed in dilute solutions, meaning that solute molecules are almost always in their monomeric form and therefore a majority of emission comes from monomers. In more concentrated solutions, solute molecules are

more likely to encounter each other, potentially enabling them to form dimers, trimers, tetramers or even polymeric aggregates. These molecular assemblies absorb and emit at different wavelengths compared to their monomeric forms. At higher solute concentrations there will be less of the monomer and more of the aggregate forms, so emission from the monomer form of the solute may no longer be so strongly observed, whereas emission from the aggregate form will begin to appear more strongly (Figure 5.38).⁹⁷ Emission from an aggregate species usually initially appears as a ‘shoulder’ to the monomer peak. The propensity for fluorochromes to form aggregates depends on their structure, as well as the solvent used and the concentration of the fluorochrome. RhB is known to exhibit aggregation in solution, and its conjugated ring system facilitates good packing of molecules.^{167, 168}

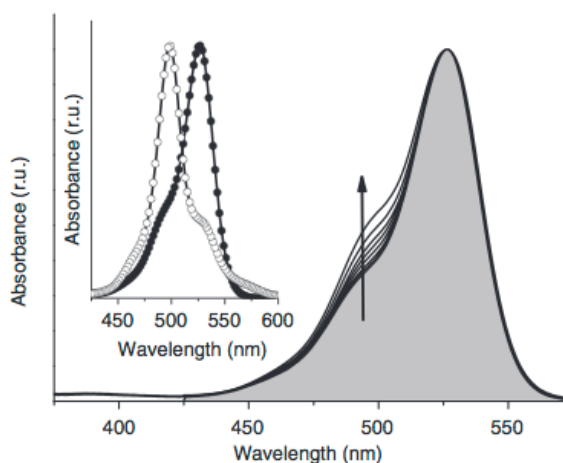


Figure 5.38: Absorption spectrum of a fluorochrome, demonstrating the increased absorption of aggregates (indicated by the arrow) compared to monomer fluorochromes as the concentration of the fluorochrome is increased. Inset: Absorption of monomer (●) and of aggregate (○) fluorochromes¹⁶⁵

r.u. = relative units

Analysis of a fluorochrome similar to RhB, Rhodamine 6G, suggests that dimers form in water, but not in methanol over the range of concentrations studied here.¹⁶⁹⁻¹⁷¹ Other authors have suggested that laser dyes (of which RhB is one) do not aggregate well in polar, organic solvents such as ethanol.¹⁷² Although no shoulder peak is observed as the concentration of RhB was increased, its peak emission does shift to longer wavelengths. Similar behaviour has been observed in monomeric and dimeric forms of RhB.¹⁷³ In pollen treated with RhB, RhB appears bound to and/or encapsulated inside the pollen (see section 5.5 for further discussion of laser scanning confocal microscopy results).

Encapsulation may mimic the high concentration solution environment required for aggregation, although this is impossible to directly evaluate without further investigation.

To compare solid samples with solutions, RhB was dissolved in both water and ethanol and its emission measured (Figure 5.33 and Figure 5.34 respectively). When RhB solutions were excited at 543 or 548 nm, at higher RhB concentrations peak emission shifts to longer wavelengths (Table 5.10). When the peak emission of these solutions is compared with that of pollen treated with RhB, peak emission wavelengths show similar but not identical trends (Figure 5.39 and Figure 5.40). This difference could be explained in several ways. Firstly it indicates that RhB may not have been in solution inside the RhB-treated pollen, but that ethanol and water were probably largely removed *via* vacuum filtration during sample preparation. Secondly, possible interactions between RhB and sporopollenin, not present in solutions without pollen, could also cause shifts in RhB's peak emission. It is impossible to infer from these results which of the two scenarios is the most likely.

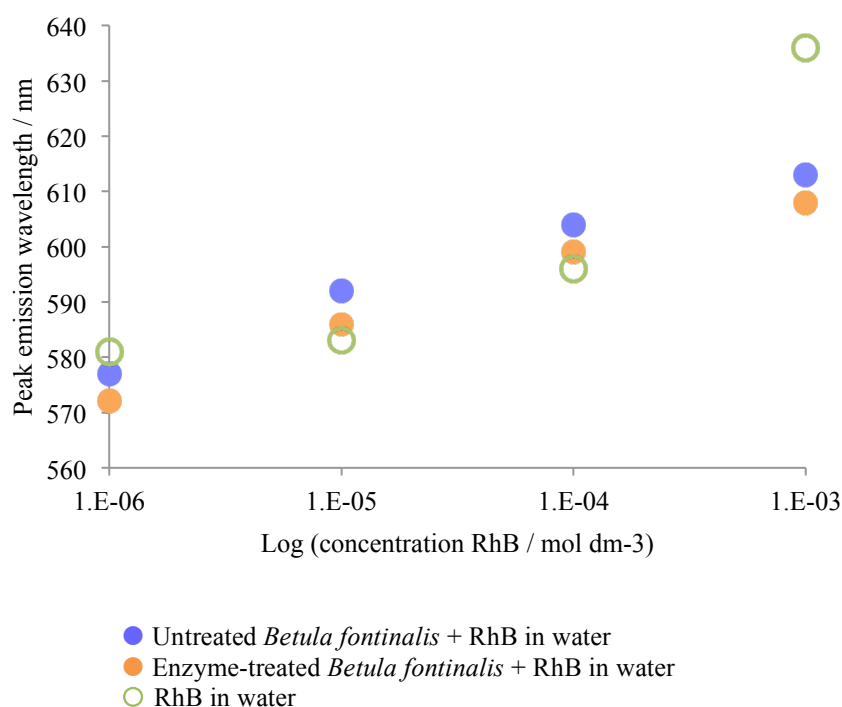


Figure 5.39: Comparison of the peak emission wavelengths of aqueous solutions of RhB and untreated & enzyme-treated *Betula fontinalis* pollen, treated with aqueous solutions of RhB. Concentrations of RhB range from 1×10^{-3} to 1×10^{-6} mol dm⁻³

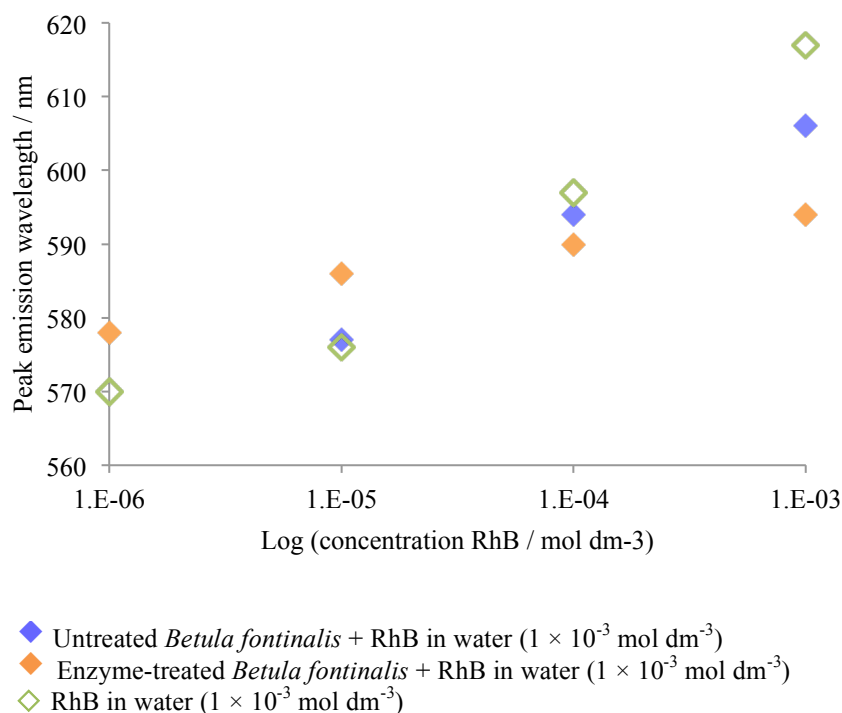


Figure 5.40: Comparison of the peak emission wavelengths of ethanolic solutions of RhB and untreated & enzyme-treated *Betula fontinalis* pollen, treated with ethanolic solutions of RhB. Concentrations of RhB range from 1×10^{-3} to 1×10^{-6} mol dm⁻³. [Peak for untreated *Betula fontinalis* treated with RhB (1×10^{-6} mol dm⁻³) missing as peak too weak to identify on spectrum]

The data point representing a solution of RhB in water (1×10^{-3} mol dm⁻³) in Figure 5.39 could be anomalous, as it does not appear to follow the trend of the other points within this plot. Alternatively, the exceptionally high concentration of RhB may cause a much greater level of reabsorption, compared to the RhB treated pollen. This would lead to the RhB in solution having a longer peak emission wavelength of RhB. Repeat measurement of all samples within this plot would need to be made to determine which scenario is most likely.

Pollen samples treated with RhB and excited at 300 nm all have intense peaks around 470 nm, indicative of sporopollenin emission. These peak emission wavelengths remain fairly consistent between samples, not varying by more than 7 nm, and are summarised in the red columns of Table 5.4 to Table 5.7. However, in samples without added RhB, the peaks are broader and extend towards 580 nm. The addition of RhB causes narrowing of the peaks at around 470 nm, with longer wavelength components (~500 – 580 nm) becoming quenched. Higher concentrations of RhB (i.e. 1×10^{-3} and 1×10^{-4}

mol dm⁻³ RhB) initiated the greatest quenching. This observation indicates that energy emitted by sporopollenin is either being absorbed by, or transferred to, other components within the system. As the effect is only observed in the presence of RhB, it is highly likely that that absorption or transfer involves RhB.

The quenching of sporopollenin's emission may be due to the absorption of light emitted from sporopollenin by RhB. This is possible, as sporopollenin emits light in the region of RhB's peak absorption wavelength (around 550 nm).⁸³ Other quenching mechanisms exist, including energy and electron transfer processes and excimer formation. As pollen treated with RhB was examined in the form of solid samples, fluorochromes could not diffuse throughout the structure, therefore ruling out mechanisms that involve diffusion. These include excimer formation and the exchange or Dexter mechanism.^{97, 174} Resonance or Förster transfer as well as exciton migration do not require a fluid system, so could therefore act as possible quenching mechanisms.⁹⁷ However, all of these mechanisms would generate an additional peak elsewhere in a spectrum in addition to the emission already observed. As such an additional peak is not seen, it is more likely that the quenching observed is due to the absorption of sporopollenin's emission by RhB.

5.4.3.3 The effect of changing the genus of pollen and spores

In order to compare the effects of varying the genus of pollen or spore on fluorescence, untreated *Juglans nigra* pollen and *Lycopodium clavatum* spores were treated with aqueous solutions of RhB. Emission spectra for *Juglans nigra* are presented in Figure 5.41 and Figure 5.42, and those for *Lycopodium clavatum* in Figure 5.43 and Figure 5.44.

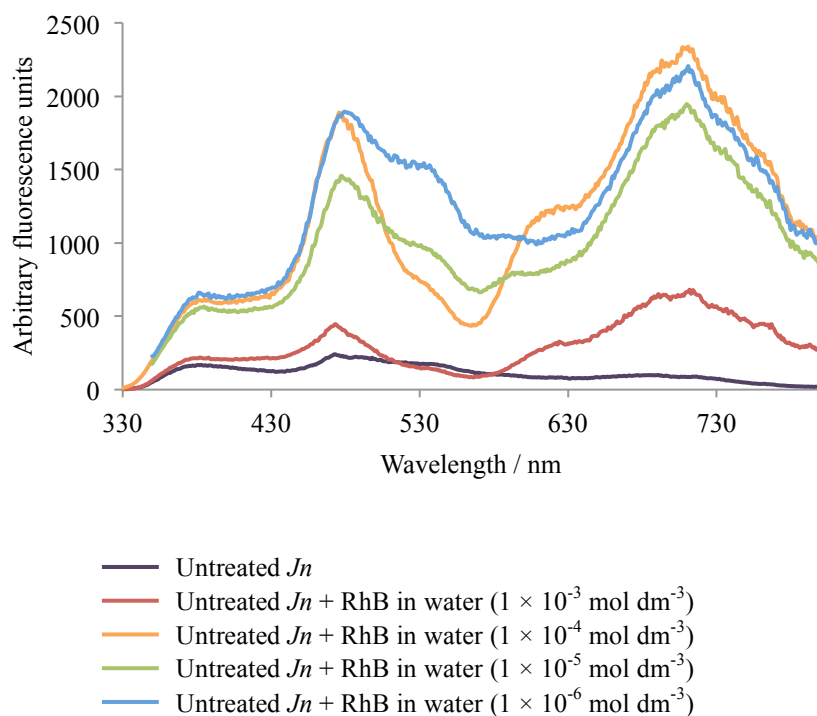


Figure 5.41: Emission spectra of untreated *Juglans nigra* (*Jn*) pollen, treated with aqueous solutions of RhB of varying concentrations (excitation λ 300 nm, 350 nm longpass filter)

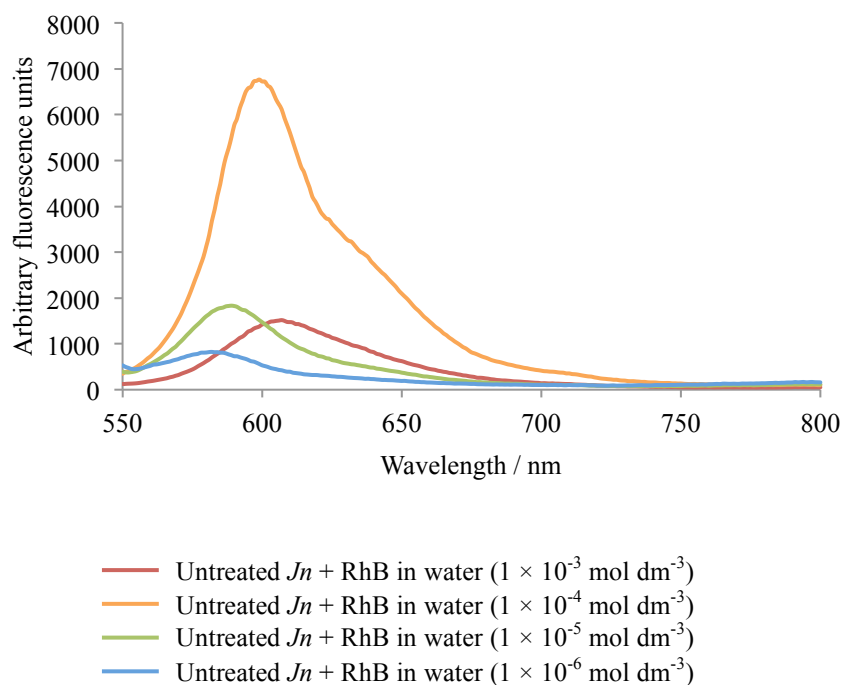


Figure 5.42: Emission spectra of untreated *Juglans nigra* (*Jn*) pollen, treated with aqueous solutions of RhB of varying concentrations (excitation λ 530 nm)

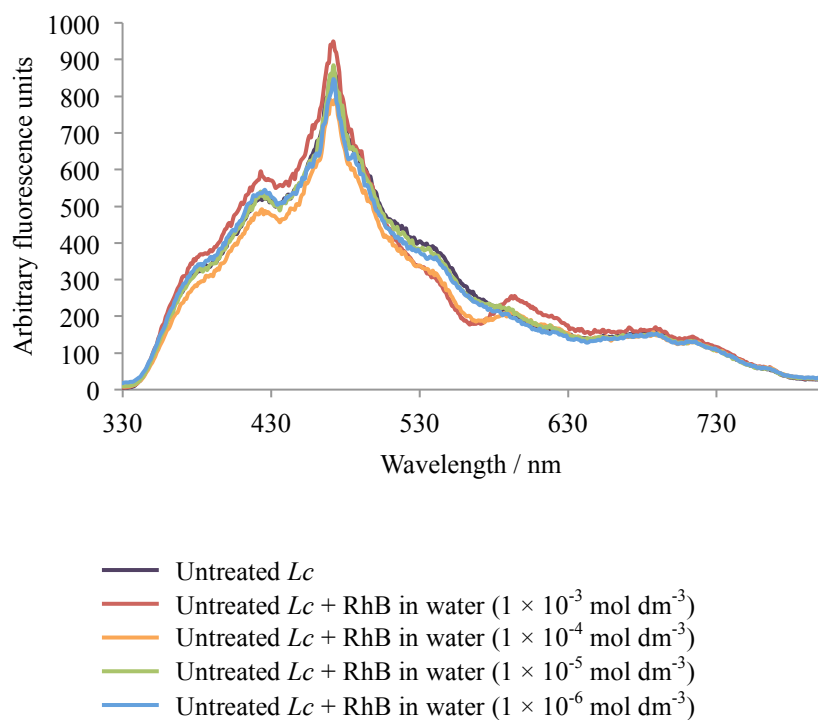


Figure 5.43: Emission spectra of untreated *Lycopodium clavatum* (*Lc*) spores, treated with aqueous solutions of RhB of varying concentrations (excitation λ 300 nm, 350 nm longpass filter)

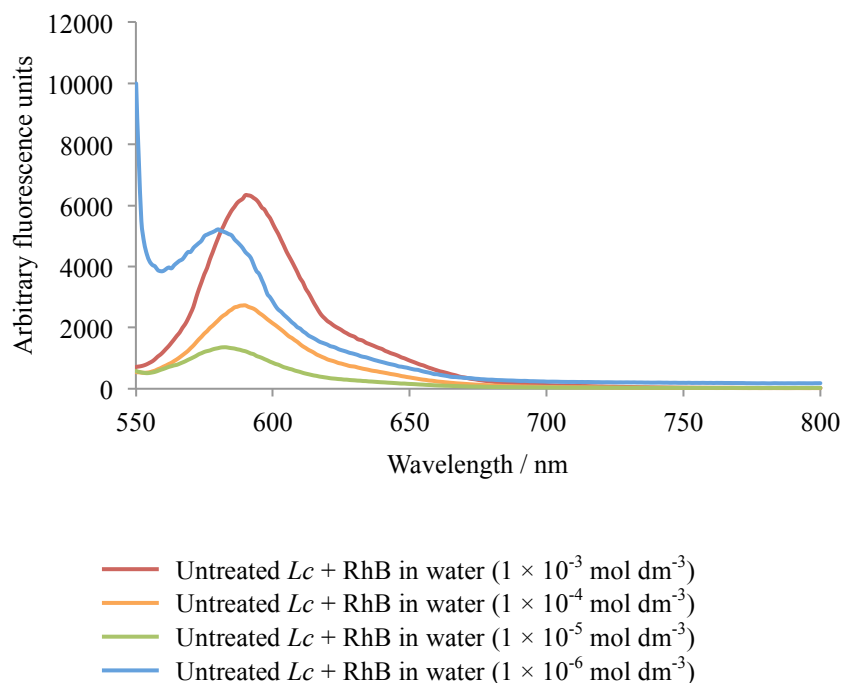


Figure 5.44: Emission spectra of untreated *Lycopodium clavatum* (*Lc*) spores, treated with aqueous solutions of RhB of varying concentrations (excitation λ 530 nm)

RhB emission for all species investigated (*Betula fontinalis*, *Juglans nigra* and *Lycopodium clavatum*), shifts to longer wavelengths as the concentration of the RhB solution applied to the pollen or spores was increased. This shift in emission is summarised in Table 5.11 and Figure 5.45. Results show that although the pattern of RhB emission is the same among all species examined, the exact emission wavelength at each concentration of RhB differs between species, sometimes by as much as 23 nm. Each species may have absorbed different levels of RhB from the aqueous solutions applied, leading to different levels of reabsorption between RhB molecules, and therefore different peak emission. These results may also indicate that RhB lies in close proximity to components within the pollen or spores, allowing these to influence RhB's emission by processes such as reabsorption. LSCM was therefore applied to further probe the proximity of RhB to pollen and spore components, such as the exine, intine and protoplast (see section 5.5).

Table 5.11: Summary of peak emission wavelengths of untreated *Betula fontinalis* and *Juglans nigra* pollen and *Lycopodium clavatum* spores, all treated with aqueous solutions of RhB of varying concentrations

	Peak emission wavelength / nm at varying concentrations of RhB applied / mol dm ⁻³			
	1 × 10 ⁻³	1 × 10 ⁻⁴	1 × 10 ⁻⁵	1 × 10 ⁻⁶
<i>Betula fontinalis</i> *	613	604	592	577
<i>Juglans nigra</i> †	607	599	589	582
<i>Lycopodium clavatum</i> †	590	590	582	580

* Collected by excitation at 543 nm

† Collected by excitation at 530 nm

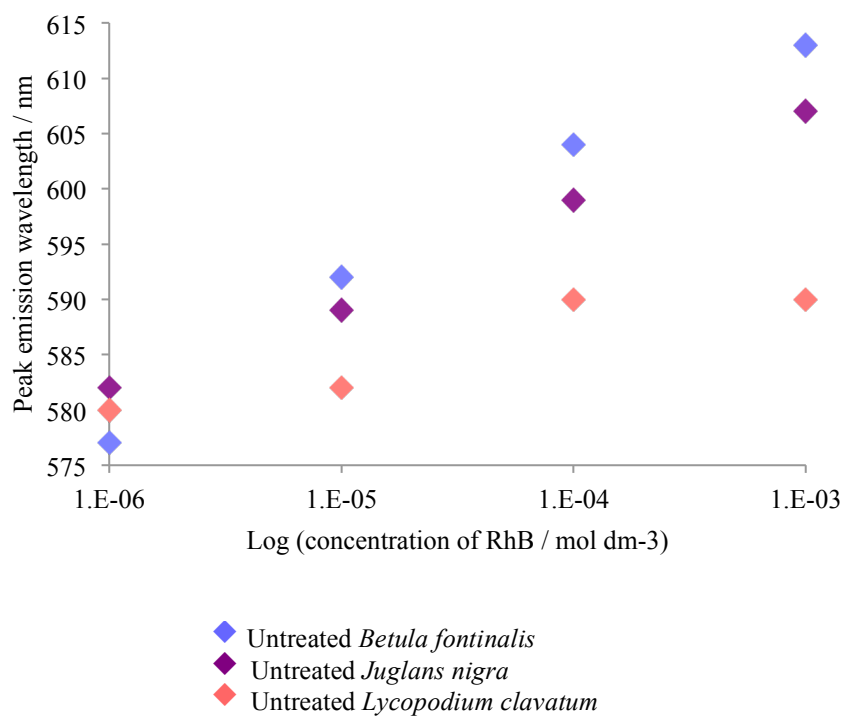


Figure 5.45: Comparison of peak emission wavelengths of untreated *Betula fontinalis* and *Juglans nigra* pollen and *Lycopodium clavatum* spores, treated with aqueous solutions of RhB at various concentrations

5.4.3.4 Spectrofluorometry of untreated, enzyme-treated, and base and acid-treated pollen and spores, treated with Rhodamine B: summary of results

1. Aqueous and ethanolic solutions of RhB of varying concentrations were applied to both untreated and enzyme-treated *Betula fontinalis* pollen. Emission from both the pollen and RhB was observed. The ratio between peaks at 370 and 470 nm (attributed to sporopollenin) was greater when water was used as the solvent, compared to ethanol. This finding was observed in both untreated and enzyme-treated pollen and indicates that different solvents may elicit different degrees of binding or encapsulation of RhB.
2. Higher concentrations of RhB quenched emission from the pollen wall. In addition, RhB's peak emission wavelength shifted to longer wavelengths when the concentration of RhB in the solutions applied to pollen was higher. Reabsorption of RhB's emission or the aggregation of RhB monomers may explain this shift, although it is impossible to infer from these results which effect is most likely.

3. Untreated *Juglans nigra* pollen and *Lycopodium clavatum* spores were treated with aqueous and ethanolic solutions of RhB. The pattern of emission was found to be similar to that observed from untreated *Betula fontinalis* pollen, although the exact emission spectra varied between these species. This indicates that different species may encapsulate or bind different quantities of RhB.

5.4.4 Spectrofluorometry of models for sporopollenin: *p*-coumaric acid and ferulic acid.

p-Coumaric acid and ferulic acid have been proposed as models for sporopollenin when attempting to determine historic levels of UV-B radiation within our atmosphere.¹⁵⁵ A recent review by de Leeuw *et al.* highlighted the presence of *p*-coumaric acid within sporopollenin, with ferulic acid also forming part of this complex biopolymer.³⁷ These acids were combined in solution with RhB and the fluorescence of these solutions measured. The emission of *p*-coumaric acid and ferulic acid (around 510 and 430 nm respectively) is removed from that of RhB (around 590 nm) (Figure 5.46). Therefore, when RhB is combined with each of the acids, it is possible to evaluate their fluorescence independently. However, their spectra lie sufficiently close for interactions (e.g. reabsorption and energy transfer processes) between the acids and RhB to be possible. By comparing spectra of these acids in solution with RhB to untreated pollen and spores, treated with RhB, it may be possible to determine whether *p*-coumaric acid and ferulic acid do act as effective models for sporopollenin.

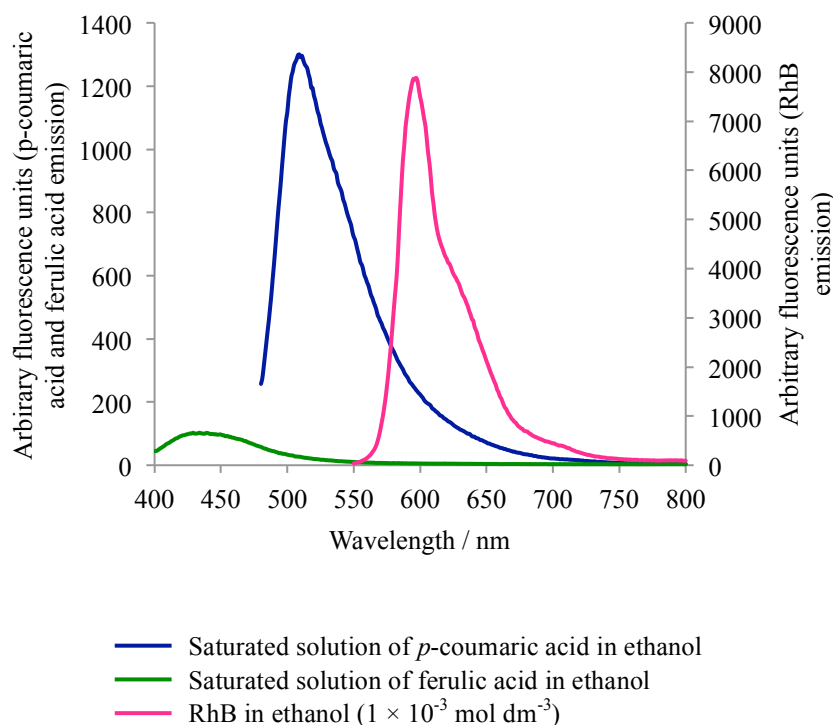


Figure 5.46: Emission spectra of saturated ethanolic solutions of *p*-coumaric acid (excitation λ 450 nm) and ferulic acid (excitation λ 385 nm); and RhB in ethanol ($1 \times 10^{-3} \text{ mol dm}^{-3}$) (excitation λ 543 nm)

Equal volumes of RhB solutions and a saturated solution of *p*-coumaric acid and (both in ethanol) were mixed and the fluorescence emission of the solutions produced measured. The concentration of the RhB solutions added varied between 1×10^{-3} and $10^{-6} \text{ mol dm}^{-3}$ in order to observe how altering the concentration of RhB influenced its own fluorescence emission as well as that of *p*-coumaric acid. Excitation wavelengths of 450 nm (Figure 5.47) and 540 nm (Figure 5.48) were selected in order to promote optimal excitation of *p*-coumaric acid and RhB respectively. The emission maxima for *p*-coumaric acid and RhB at excitation at 450 nm, and for RhB at excitation at 540 nm are summarised in Table 5.12. The data shows that as the concentration of RhB was increased, there is a shift in its peak emission to longer wavelengths. By comparison, the peak emission of *p*-coumaric acid remains fairly constant between 503 and 509 nm. However, the longer wavelength components ($> \sim 520 \text{ nm}$) of *p*-coumaric acid's emission disappear as the concentration of RhB was elevated above $1 \times 10^{-4} \text{ mol dm}^{-3}$. This behaviour is similar to that observed in untreated pollen and spores, treated with solutions of RhB (see section 5.4.3).

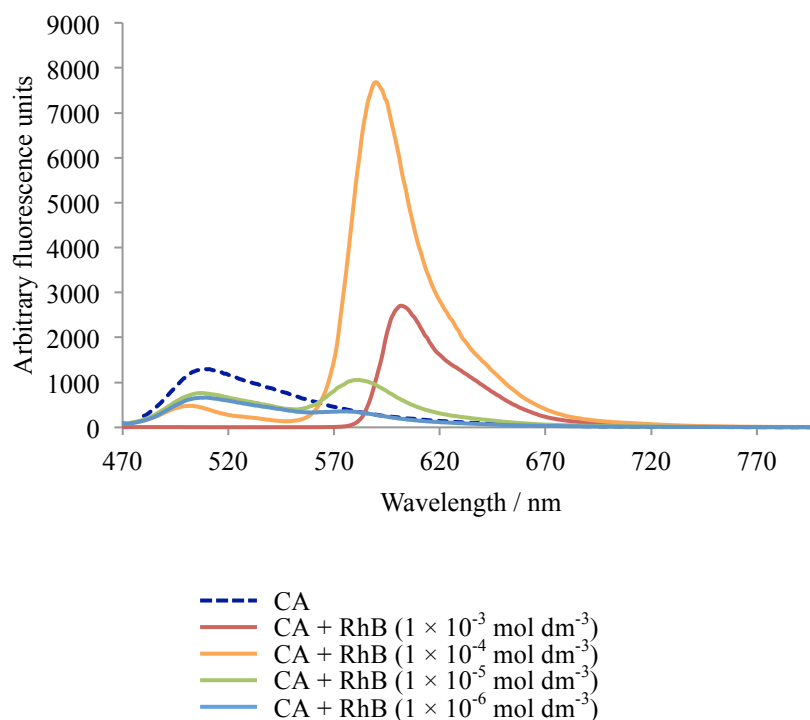


Figure 5.47: Emission spectra of saturated ethanolic solutions of *p*-coumaric acid (CA) mixed with equal volumes of ethanolic solutions of RhB of varying concentrations (excitation λ 450 nm)

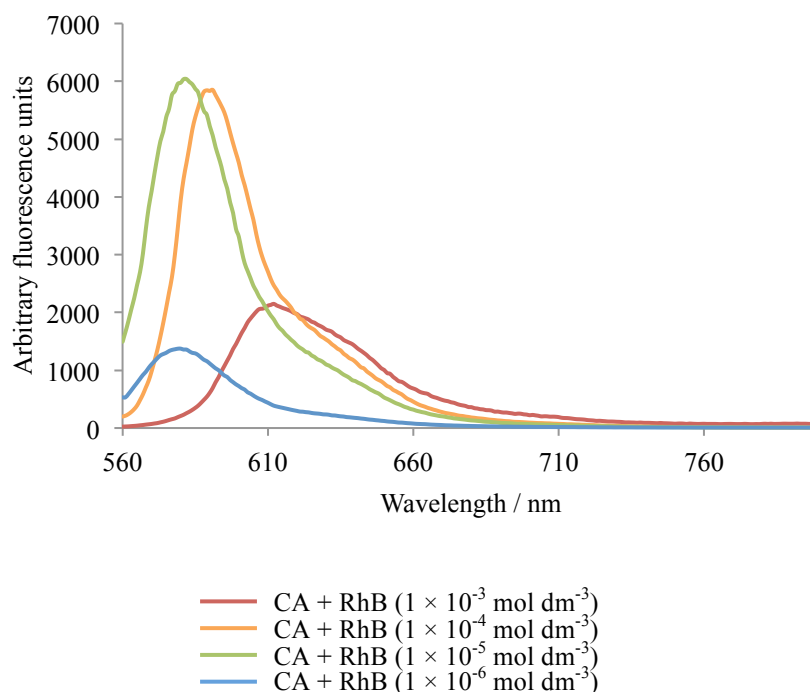


Figure 5.48: Emission spectra of saturated ethanolic solutions of *p*-coumaric acid (CA) mixed with equal volumes of ethanolic solutions of RhB of varying concentrations (excitation λ 540 nm)

Table 5.12: Summary of peak emission wavelengths for the fluorescence of a saturated solution of *p*-coumaric acid with Rhodamine B. All solutions prepared in ethanol

Concentration of RhB solution / mol dm ⁻³	Peak emission at 450 nm excitation λ / nm		Peak emission at 540 nm excitation λ / nm
	<i>p</i> -Coumaric acid	Rhodamine B	Rhodamine B
0	509	-	-
1×10^{-3}	*	602	612
1×10^{-4}	503	590	591
1×10^{-5}	507	582	582
1×10^{-6}	509	576	580

* Peak too weak to identify

The experiment was repeated, but a saturated solution of ferulic acid was used in place of *p*-coumaric acid. Excitation wavelengths of 385 nm and 540 nm were selected to optimally excite ferulic acid and RhB respectively. The fluorescence emission spectra are presented in Figure 5.49 and Figure 5.50 respectively, and peak emission data is summarised in Table 5.13. Similarly to spectra of solutions of *p*-coumaric acid plus RhB, as the concentration of the RhB solution was decreased, its peak emission shifts to shorter wavelengths. The peak emission of ferulic acid remains fairly constant at around 435 nm, but at the highest concentration of RhB (1×10^{-3} mol dm⁻³), the longer wavelength components ($> \sim 480$ nm) diminish. These trends are similar to those observed for *p*-coumaric acid combined with RhB, and to untreated pollen and spores, to which solutions of RhB has been applied.

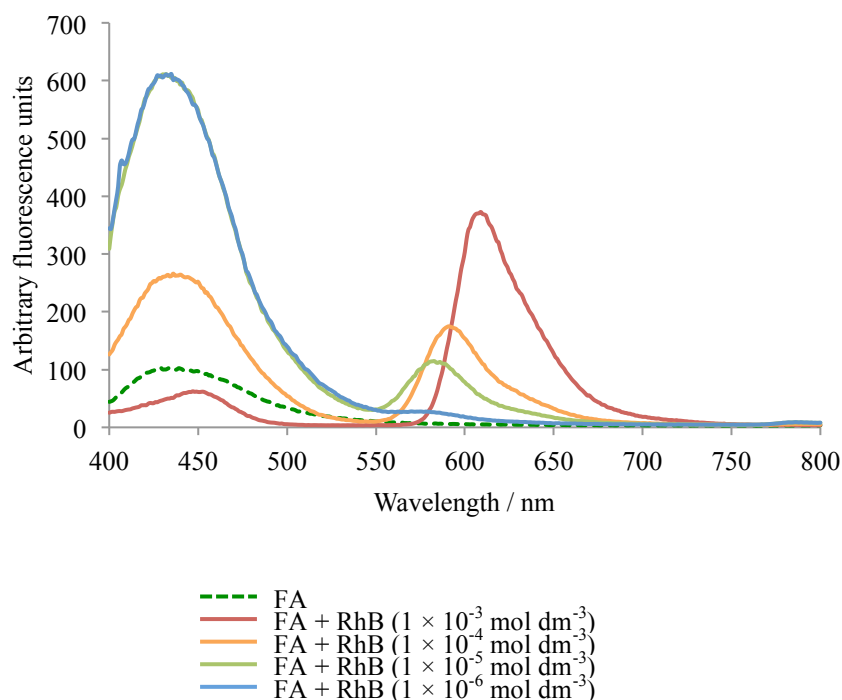


Figure 5.49: Emission spectra of saturated ethanolic solutions of ferulic acid (FA) mixed with equal volumes of ethanolic solutions of RhB of varying concentrations (excitation λ 385 nm)

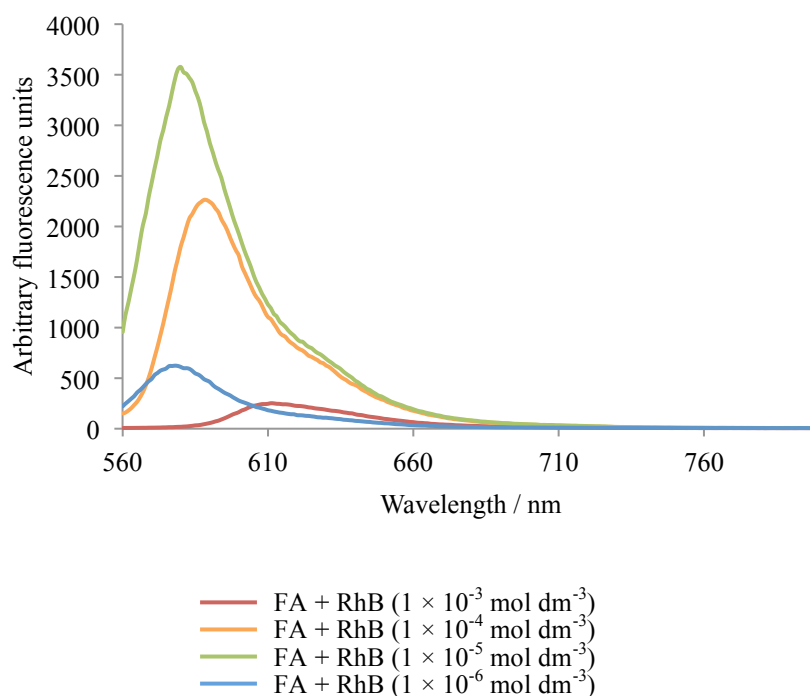


Figure 5.50: Emission spectra of saturated ethanolic solutions of ferulic acid (FA) mixed with equal volumes of ethanolic solutions of RhB of varying concentrations (excitation λ 540 nm)

Table 5.13: Summary of peak emission wavelengths for the fluorescence of a saturated solution of ferulic acid with Rhodamine B. All solutions prepared in ethanol

Concentration of RhB solution / mol dm ⁻³	Peak emission at 385 nm excitation λ / nm		Peak emission at 540 nm excitation λ / nm
	Ferulic acid	Rhodamine B	Rhodamine B
0	434		
1×10^{-3}	447	609	611
1×10^{-4}	436	591	588
1×10^{-5}	432	583	580
1×10^{-6}	435	*	578

* Peak too weak to identify

Solutions of *p*-coumaric acid and ferulic acid, plus RhB, display similar emission behaviour to untreated pollen and spores, treated with RhB. Therefore, peak RhB emission wavelengths from the following samples was compared in Figure 5.51 to more closely evaluate any trends:

- Untreated *Betula fontinalis* pollen, treated with ethanolic solutions of RhB, (Figure 5.30, excitation λ 548 nm)
- Saturated, ethanolic solution of *p*-coumaric acid combined with ethanolic solutions of RhB, (Figure 5.48, excitation λ 540 nm)
- Saturated, ethanolic solution of ferulic acid combined with ethanolic solutions of RhB (Figure 5.50 excitation λ 540 nm).

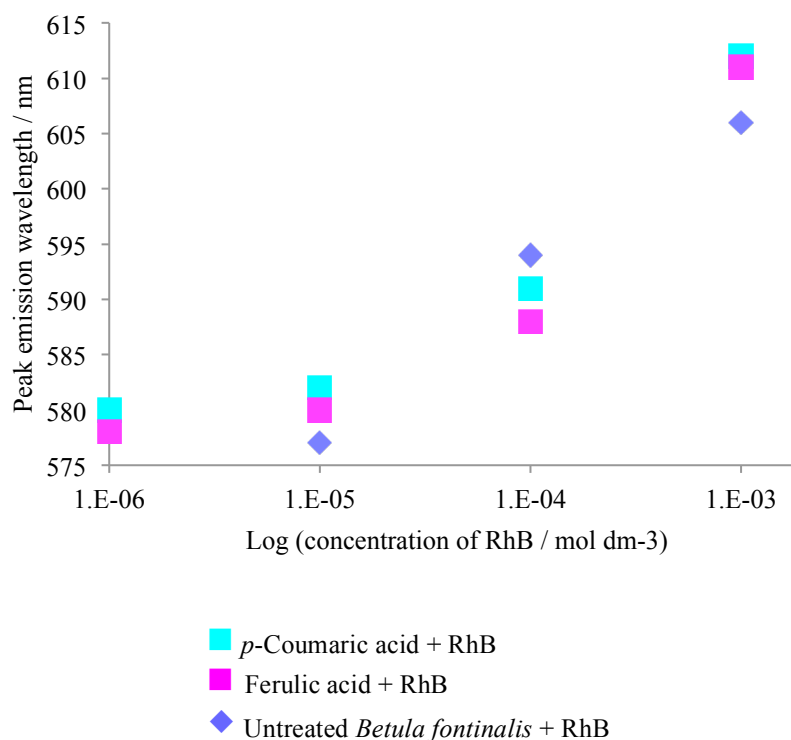


Figure 5.51: Peak emission wavelengths of RhB in ethanol at varying concentrations when combined with saturated, ethanolic solutions of *p*-coumaric acid (excitation λ 450 nm), ferulic acid (excitation λ 540 nm) or untreated *Betula fontinalis* pollen. Data taken from Figure 5.30, Figure 5.48 and Figure 5.50

[Peak for untreated *Betula fontinalis*, treated with RhB (1×10^{-6} mol dm⁻³) missing as too weak to identify on spectrum]

Although patterns observed in spectra of pollen and *p*-coumaric and ferulic acid are similar, this does not conclusively demonstrate that these acids behave in a similar fashion to sporopollenin itself. It is possible that other molecules with entirely different structures to sporopollenin that emit in the same region could demonstrate similar reabsorption of RhB. For example, riboflavin (Figure 5.52) has a peak emission of 531 nm in water and 523 nm in ethanol.^{175, 176} These emission peaks overlap well with the absorption peak of RhB, and could therefore mimic the behaviour observed for both *p*-coumaric and ferulic acids. A RhB–riboflavin conjugate was prepared by Swaan *et al.* When in conjugate form, RhB's emission was quenched (Figure 5.53), indicating that other molecules are capable of quenching RhB's emission in a similar fashion to sporopollenin, *p*-coumaric acid and ferulic acid.¹⁷⁷ Thus, it cannot be conclusively demonstrated that derivative of *p*-coumaric acid or ferulic acid are present in sporopollenin of either pollen or spores.

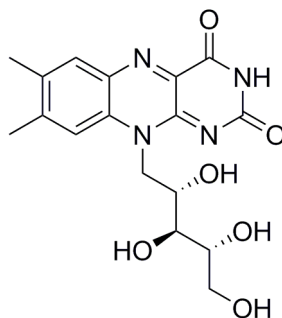


Figure 5.52: Structure of riboflavin

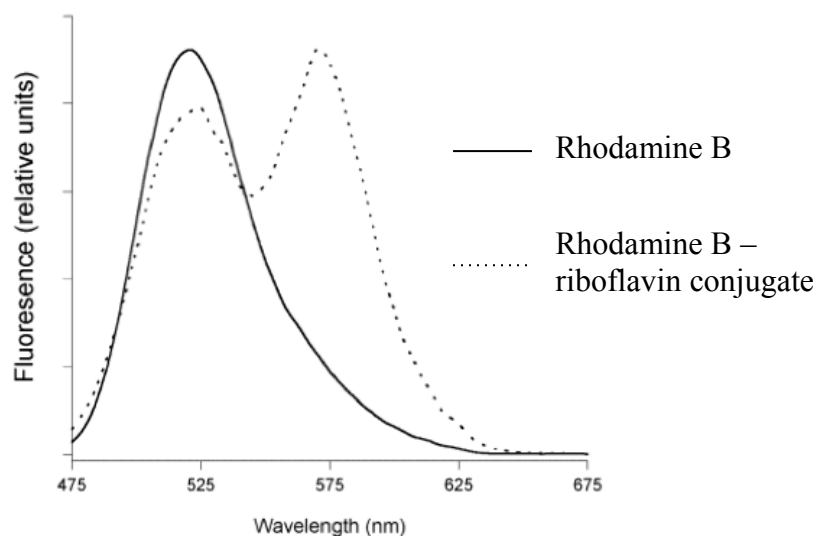


Figure 5.53: Emission spectra of Rhodamine B and a Rhodamine B – riboflavin conjugate (excitation λ 445 nm)¹⁷⁷
r.u. = relative units

5.4.4.1 Spectrofluorometry of models for sporopollenin: summary of results

1. Ethanolic solutions of *p*-coumaric acid and ferulic acid were mixed with ethanolic solutions of RhB. The patterns of emission among untreated *Betula fontinalis* pollen and these proposed sporopollenin models were similar. RhB's peak emission shifted to longer wavelengths at higher RhB concentrations. In all samples, this is likely to be due to the reabsorption of fluorescence emitted from RhB by other RhB molecules in the system. This effect was concentration dependent (see section 5.4.3 for a discussion of this effect).
2. Similar to sporopollenin, emission from *p*-coumaric acid and ferulic acid was quenched by higher concentrations of RhB. This was likely to be due to RhB

molecules reabsorbing emitted light from sporopollenin, or *p*-coumaric or ferulic acid (see section 5.4.3 for an explanation of this effect).

5.5 Analysis by laser scanning confocal microscopy (LSCM)

To identify the location of fluorochromes within both pollen and spores, samples were examined using LSCM. Quenching effects were also investigated. Pollen and spores were suspended in water before being examined using the LSCM.

5.5.1 Single track LSCM

5.5.1.1 LSCM of untreated pollen and spores

Laser scanning confocal micrographs of untreated *Betula fontinalis* (Figure 5.54), *Juglans nigra* (Figure 5.55), *Secale cereale* (Figure 5.56) and *Ambrosia artemisiifolia* pollen (Figure 5.57) and *Lycopodium clavatum* spores (Figure 5.58) were collected. These micrographs demonstrate that for the species under investigation, fluorescence emission is not consistent throughout the sample, or within each spore or pollen grain. Each sample has some pollen grains or spores that show more intense emission than others e.g. Figure 5.54 (c). The reason for this difference is unclear, although it is possible that some grains within each sample are at a different stage in their lifecycle to that of others. At different stages of their lifecycles, pollen and spores are known to possess different chemical compositions.¹⁷⁸ As a result, the quantity of fluorescent material present may differ, giving rise to different levels of emission. This conclusion is supported by work carried out by Roshchina, who observed that fluorescence from pollen differs over the course of its development.⁴⁰ Although individual grains show differing emission, these are indistinguishable in the bulk sample due to the small size of pollen and spores.

For most species, overall emission is more intense when samples were excited at the lower end of the spectrum (405 nm). This correlates well with the observations made

using spectrofluorometry (see section 5.4.3). At longer excitation wavelengths (561 and 633 nm), emission is still observed from the pollen wall, but emission from the protoplast is much less intense in comparison. The location within pollen and spores from which fluorescence is observed is not consistent. In *Lycopodium clavatum* spores, emission predominantly arises from the spore walls, whereas in the pollen species studied, emission is usually equally intense from both the protoplast and the pollen wall.

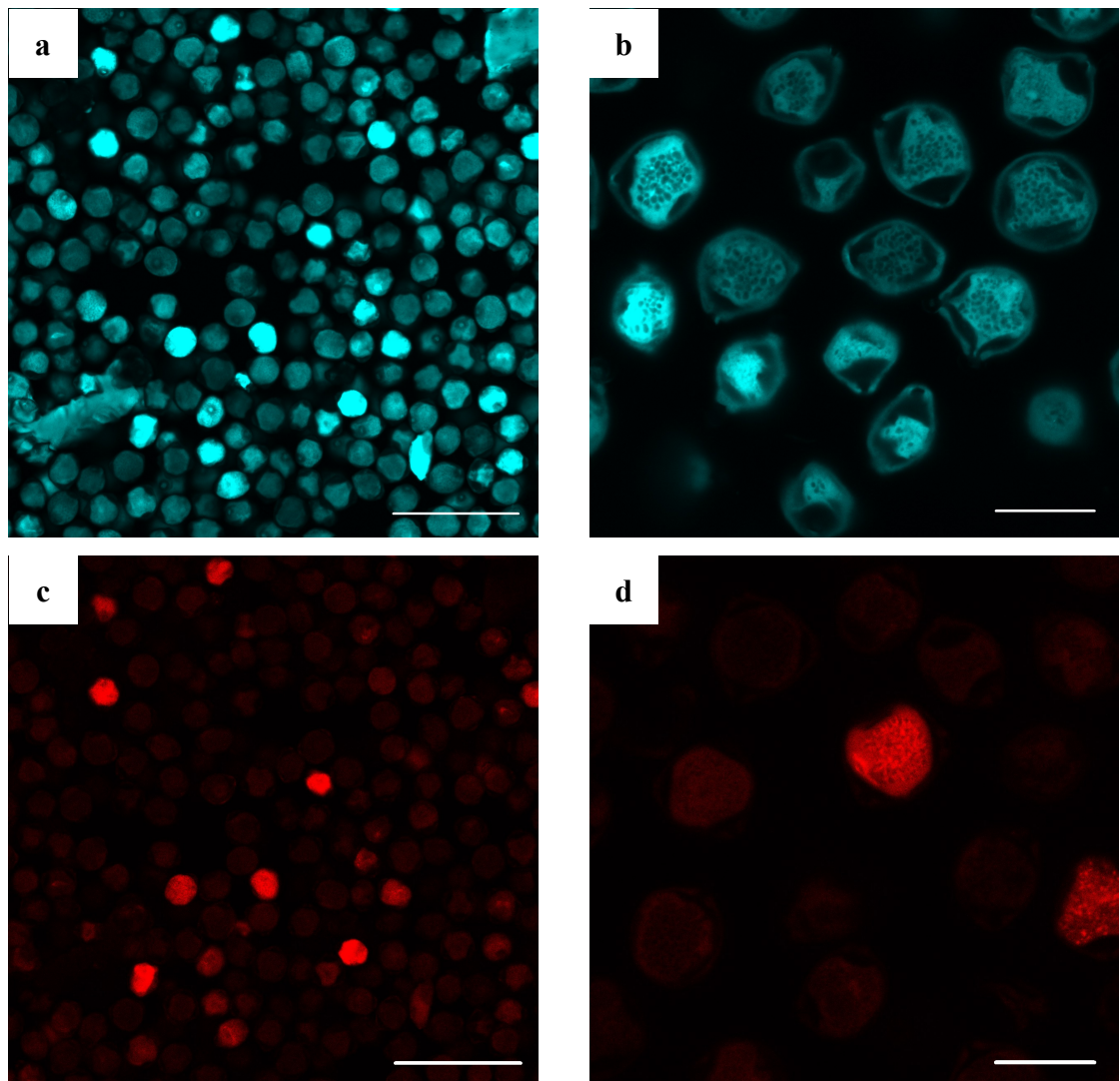


Figure 5.54: LSCM images of untreated *Betula fontinalis* pollen: (a) and (b) excitation wavelength 405 nm; (c) and (d) excitation wavelength 633 nm.

Scale bar: (a) and (c) = 100 μm ; (b) and (d) = 25 μm

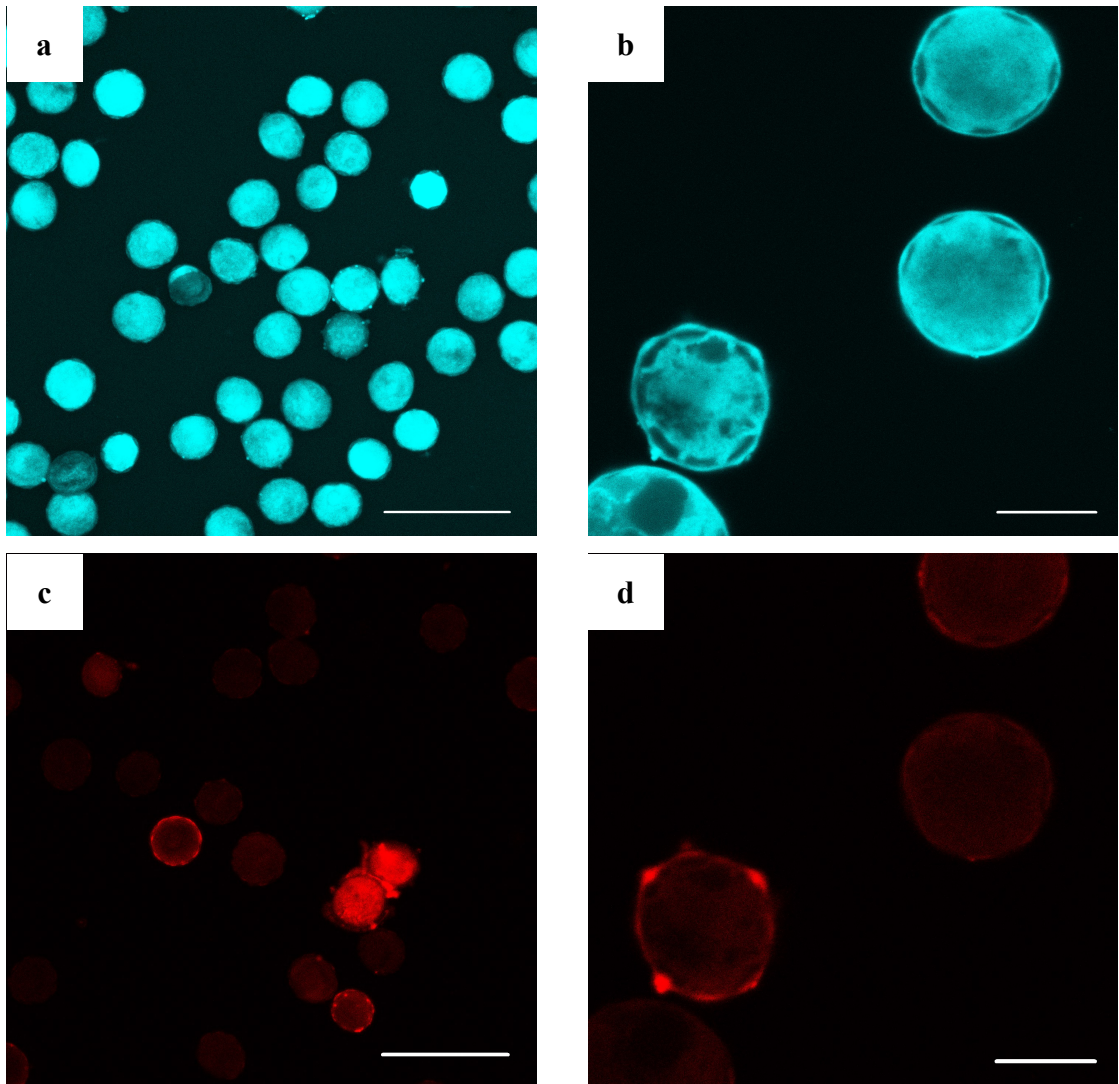


Figure 5.55: LSCM images of untreated *Juglans nigra* pollen: (a) and (b) excitation wavelength 405 nm; (c) and (d) excitation wavelength 633 nm.
Scale bar: (a) and (c) = 100 μm ; (b) and (d) = 25 μm

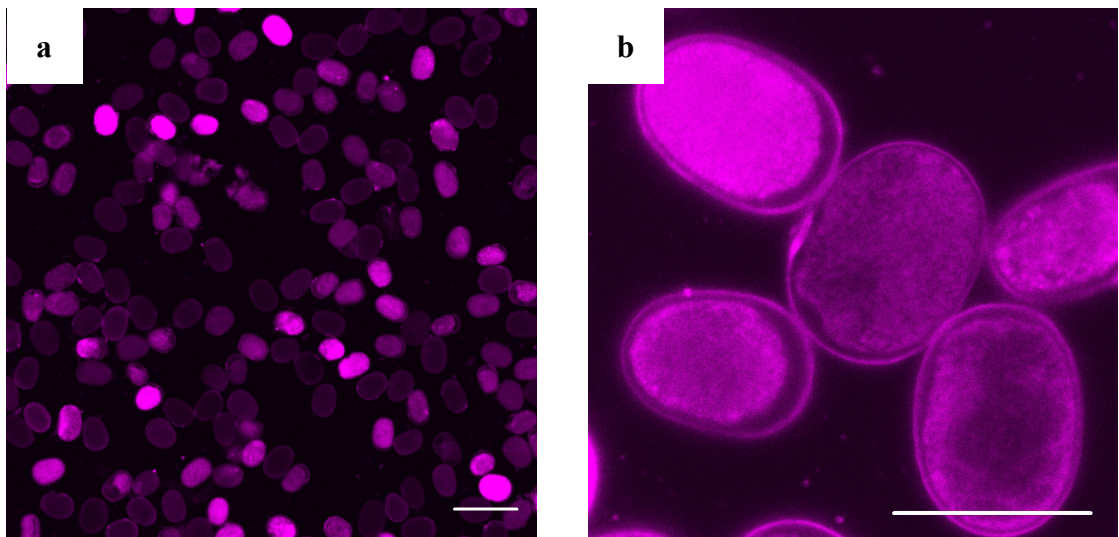


Figure 5.56: LSCM images of untreated *Secale cereale* pollen: (a) and (b) excitation wavelength 561 nm.

Scale bar: (a) = 100 μm ; (b) = 50 μm

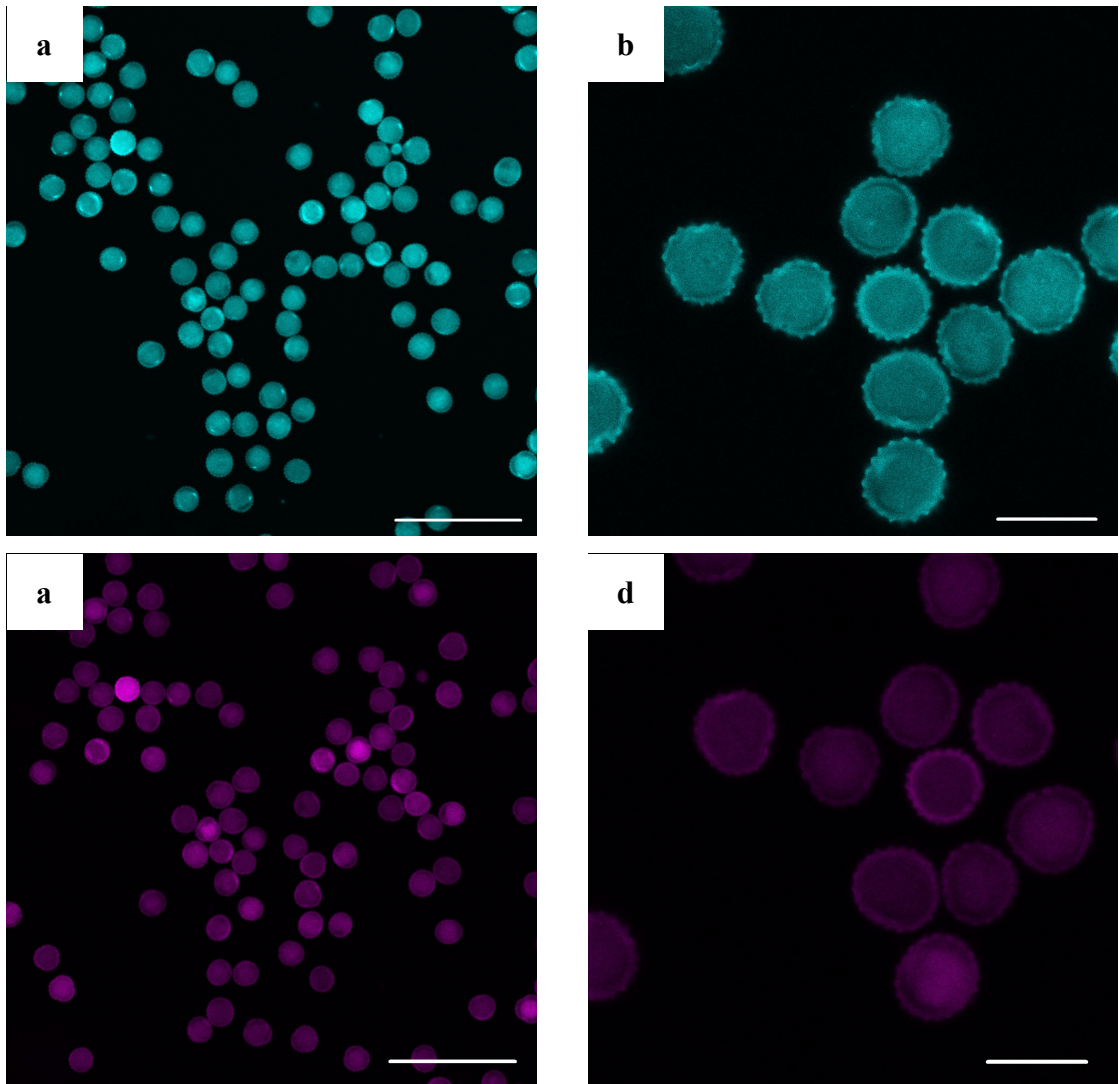


Figure 5.57: LSCM images of untreated *Ambrosia artemisiifolia* pollen: (a) and (b) excitation wavelength 405 nm; (c) and (d) excitation wavelength 561 nm.

Scale bar: (a) and (c) = 100 µm; (b) and (d) = 25 µm

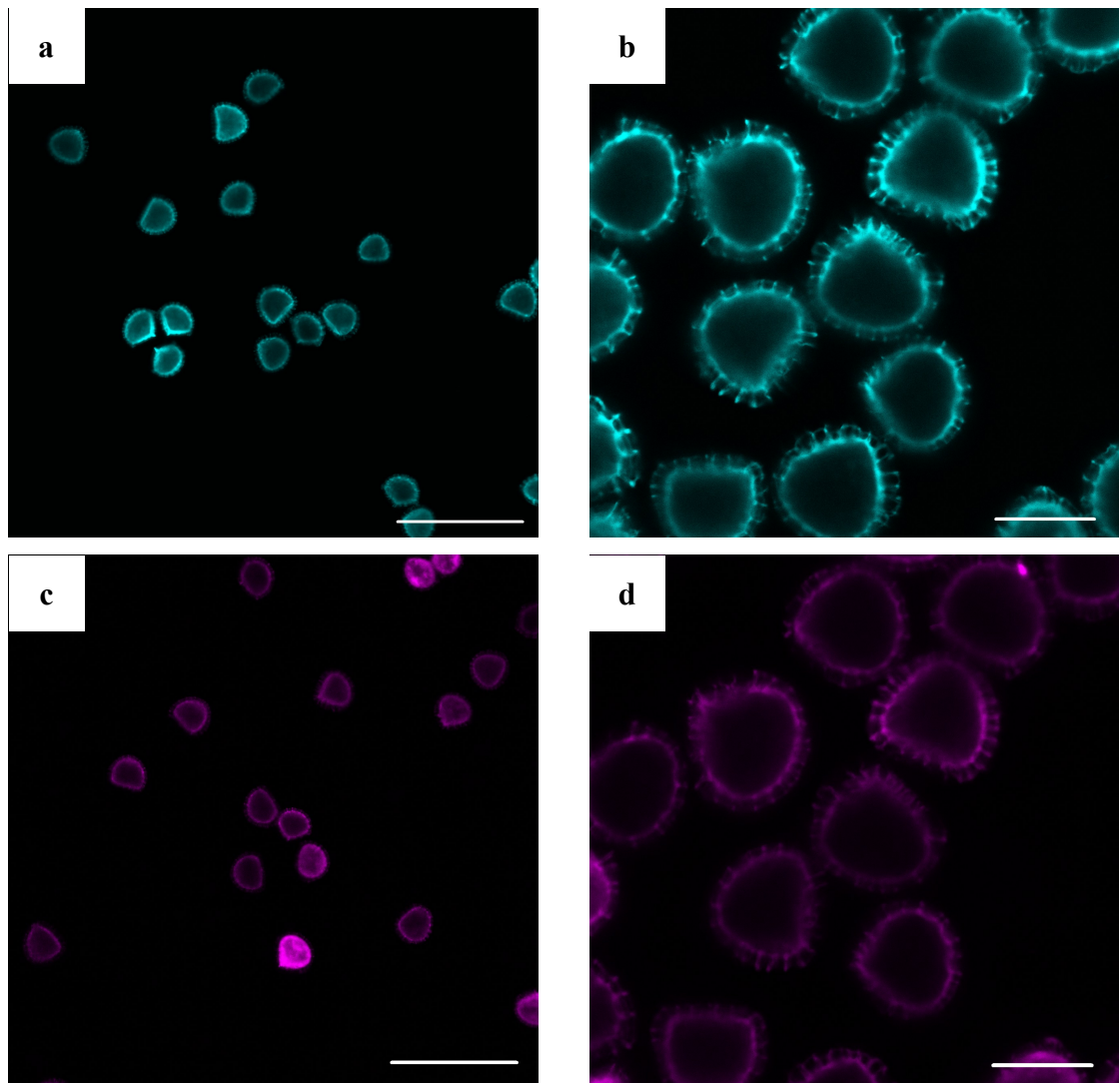


Figure 5.58: LSCM images of untreated *Lycopodium clavatum* spores: (a) and (b) excitation wavelength 405 nm; (c) and (d) excitation wavelength 561 nm.

Scale bar: (a) and (c) = 100 μm ; (b) and (d) = 25 μm

5.5.1.2 LSCM of enzyme-treated pollen

The enzyme treatment published by Loewus *et al.* was applied to *Betula fontinalis* pollen, and the treated pollen analysed by LSCM (Figure 5.59).⁶⁴ The confocal micrographs taken were compared to those for untreated *Betula fontinalis* pollen (Figure 5.54). It is clear that this enzyme treatment does not remove all material from all grains. Some grains still appear full of protoplast material, whereas in others the protoplast appears shrunken and detached from the pollen wall. The level of resolution of the LSCM means that it is impossible to determine whether or not the intine was removed.

Directly comparing untreated and enzyme-treated pollen, the treatment applied appears to remove some of the structure present in the protoplast of *Betula fontinalis* (Figure 5.60). Previous palynological analysis of pollen from the same genus (*Betula pendula*) suggests that these darker areas observed in the protoplast of untreated pollen may be starch grains.¹³³

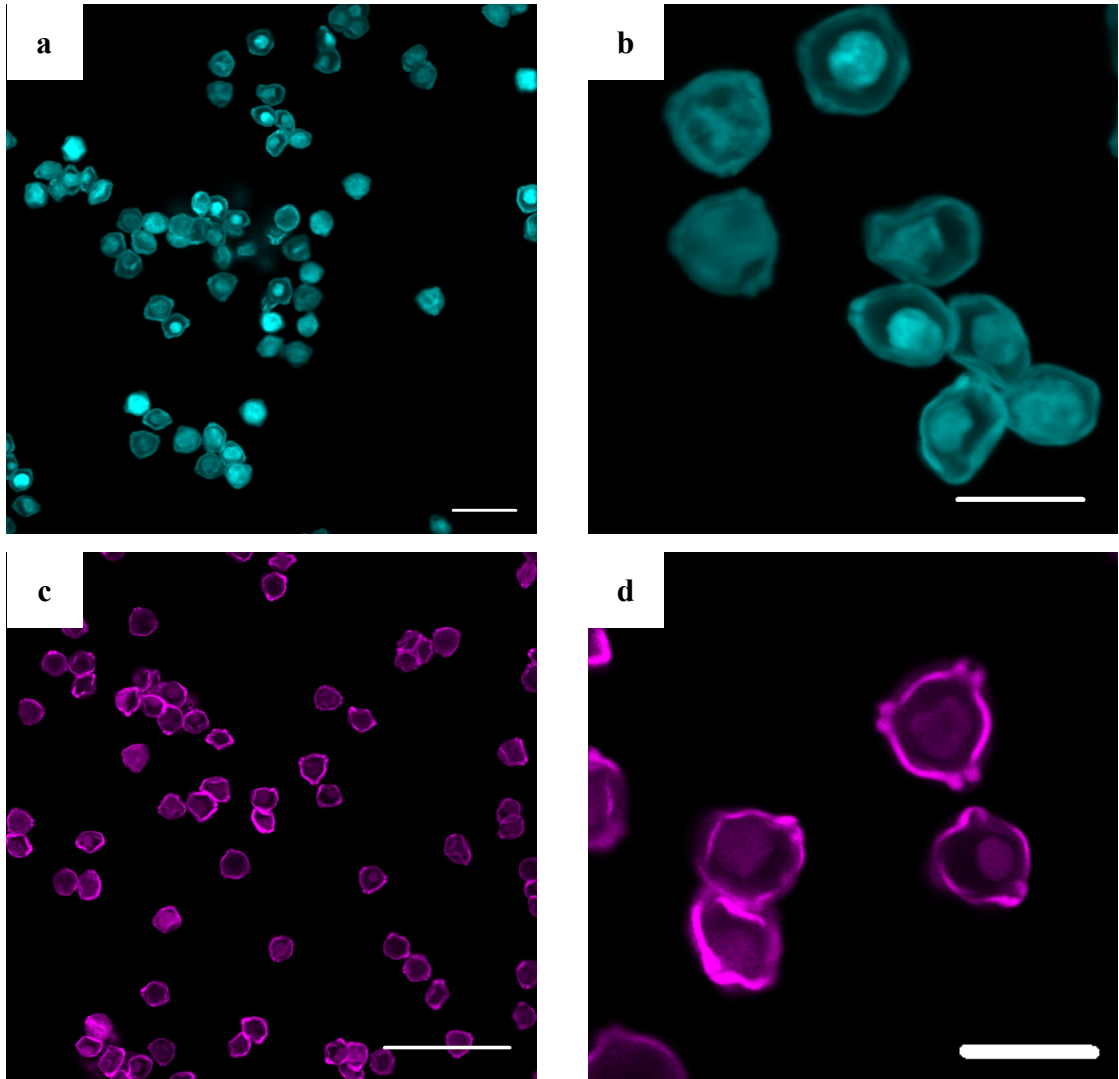


Figure 5.59: LSCM images of enzyme-treated *Betula fontinalis* pollen: (a) and (b) excitation wavelength 405 nm; (c) and (d) excitation wavelength 561 nm.

Scale bar: (a) = 50 μm ; (b) and (d) = 25 μm ; and (c) = 100 μm

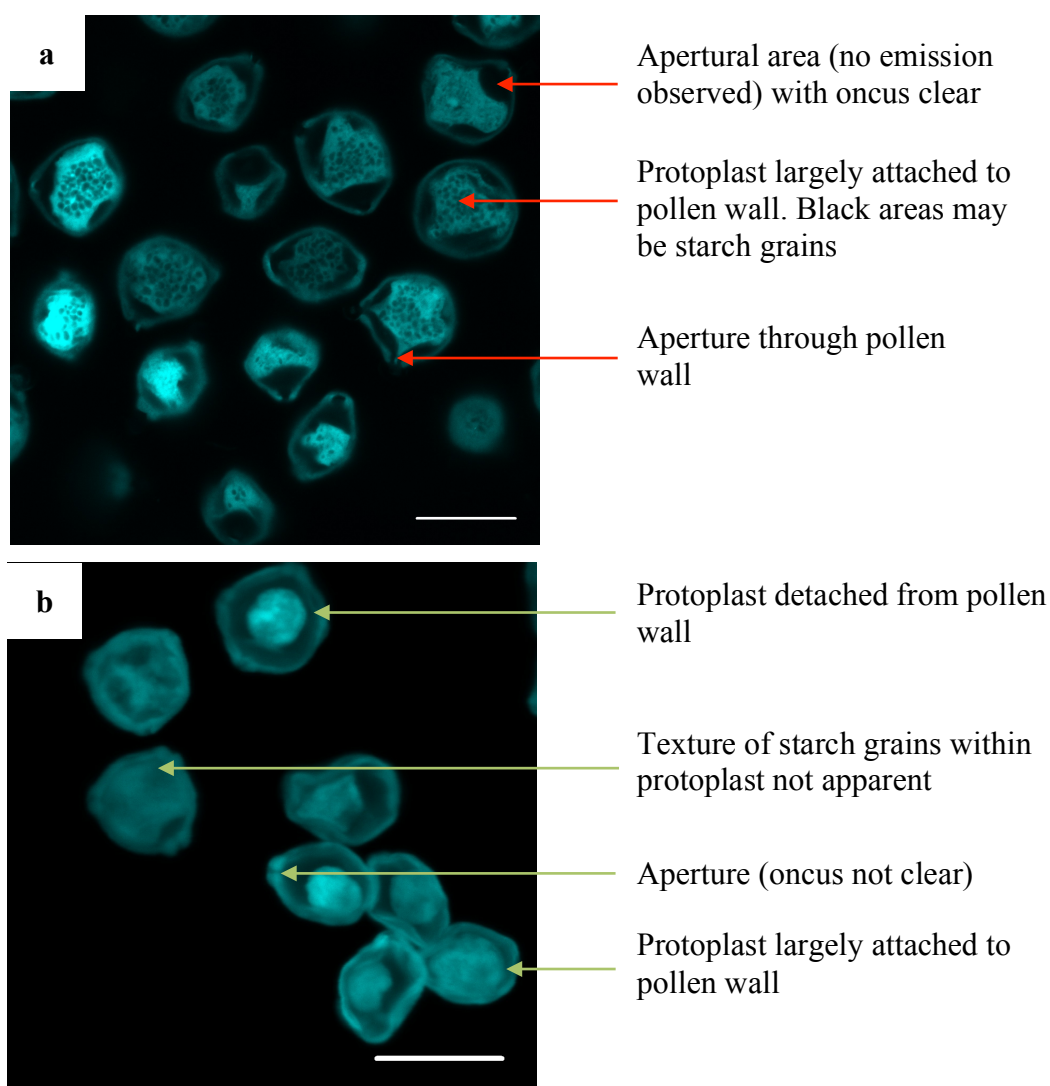


Figure 5.60: LSCM images of *Betula fontinalis* pollen (a) untreated and (b) enzyme-treated, excitation wavelength 405 nm.

Scale bars = 25 μm

5.5.1.3 LSCM of untreated pollen and spores, treated with Rhodamine B

Untreated *Betula fontinalis* and *Juglans nigra* pollen were treated with aqueous solutions of Rhodamine B (RhB) (1×10^{-3} to 1×10^{-6} mol dm $^{-3}$). The RhB-treated pollen was filtered under reduced pressure and washed with water to minimise the amount of RhB on the pollen's exterior exine surface. LSCM images of the samples treated with RhB (1×10^{-3} mol dm $^{-3}$) are shown in Figure 5.61 and Figure 5.62. Pollen treated with this concentration of RhB (the highest used) was selected for analysis to maximise the observed RhB emission. Compared to untreated *Betula fontinalis* and *Juglans nigra* pollen excited at 633 nm (Figure 5.54 and Figure 5.55 respectively),

RhB-treated pollen shows more intense emission at the longer excitation wavelengths (561 nm). The increased emission in RhB-treated pollen is not clearly specific to one structure within the pollen - the wall or protoplast - but is instead observed throughout the grains of both species.

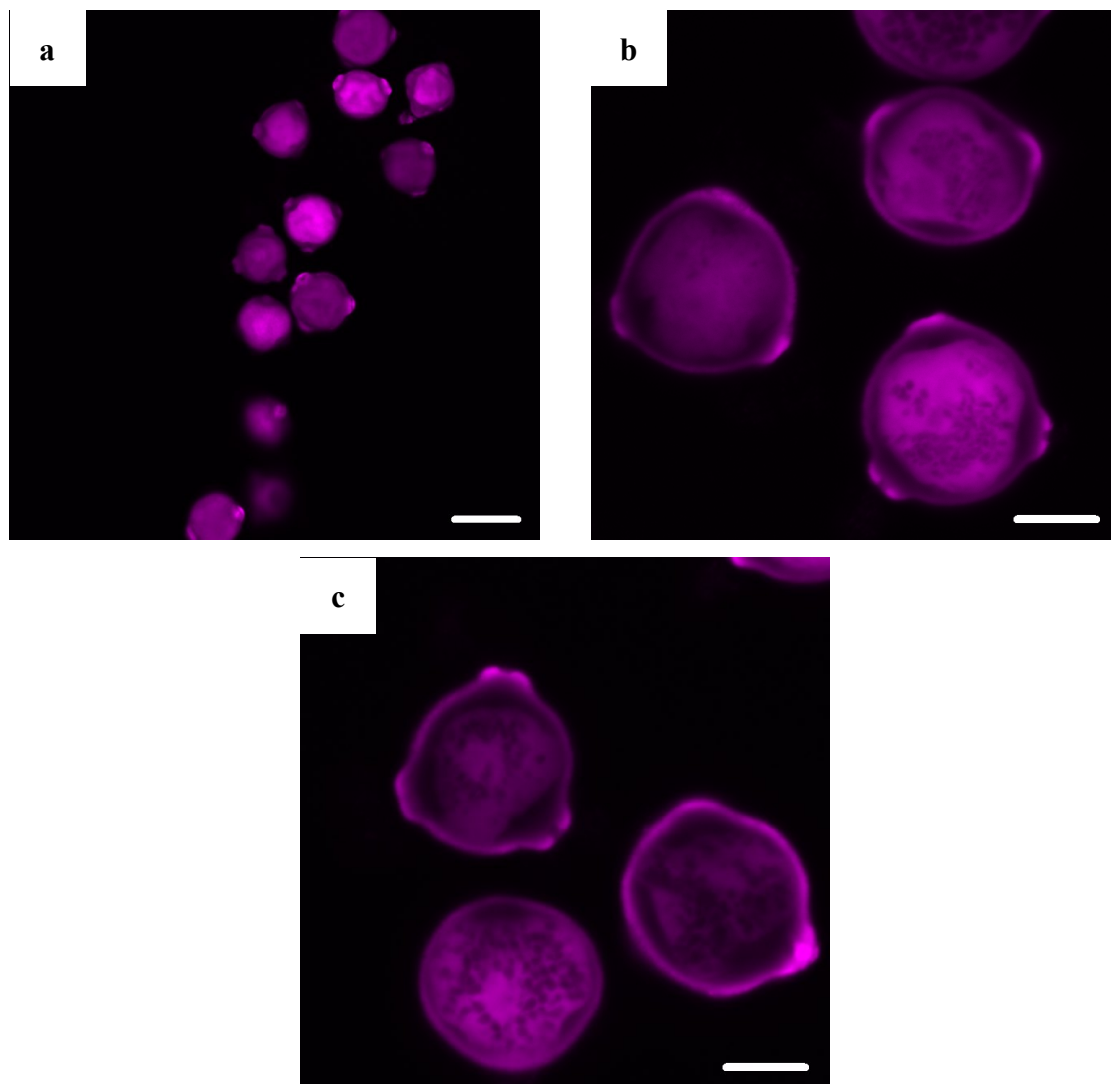


Figure 5.61: Laser scanning confocal micrographs of untreated *Betula fontinalis* pollen treated with an aqueous solution of RhB ($1 \times 10^{-3} \text{ mol dm}^{-3}$). Excitation wavelength 561 nm.

Scale bars: (a) = 25 μm ; (b) and (c) = 10 μm

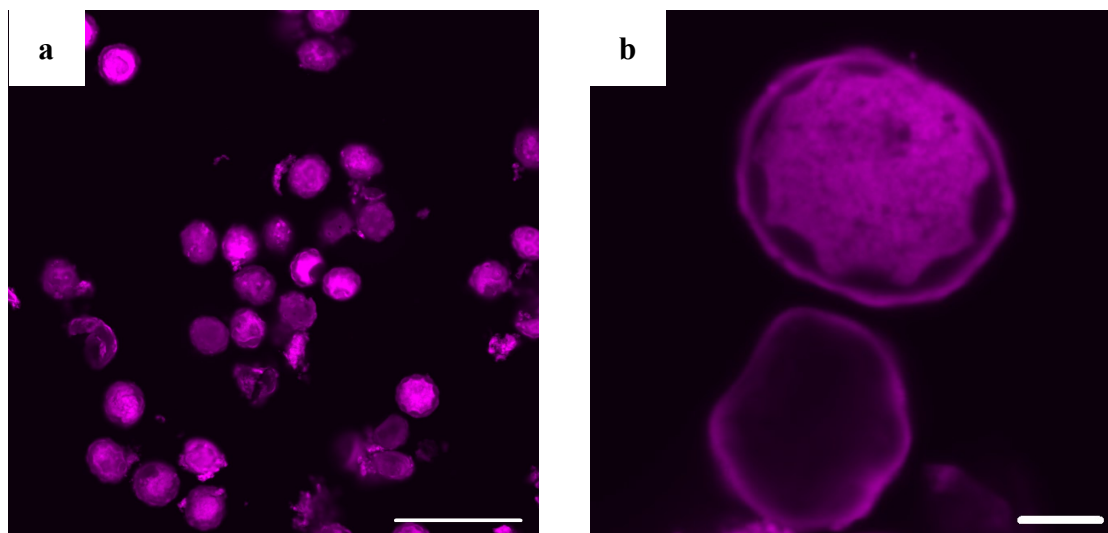


Figure 5.62: Laser scanning confocal micrographs of untreated *Juglans nigra* pollen treated with RhB (1×10^{-3} mol dm⁻³). Excitation wavelength 561 nm.

Scale bars: (a) = 100 μ m; (b) = 10 μ m

5.5.1.4 Single-track LSCM: summary of results

1. The 405 nm laser was found most suitable to inspect fluorescence arising from pollen, whereas excitation using the 561 nm laser was best to detect emission from RhB. These results support findings from spectrofluorometry.
2. Fluorescence was not consistent within each sample, or within each pollen grain or spore. One possible explanation is that individual pollen grains or spores within each sample were at different stages in their lifecycles. This would result in different chemical compositions and therefore varied emission.
3. The enzyme treatment proposed by Loewus *et al.* did not remove all non-sporopollenin material from the pollen species under investigation here. The degree to which non-sporopollenin material was removed varied from grain to grain. The resolution of the LSCM was insufficient to determine the effect of the enzyme treatment on the exine and intine and only the pollen wall as a whole could be commented on.

5.5.2 Multi-track LSCM of untreated and enzyme-treated *Betula fontinalis* pollen treated with aqueous and ethanolic solutions of Rhodamine B

In order to evaluate the effect of RhB on the quenching of sporopollenin's emission (see section 5.4.3) multi-track LSCM was performed. The samples prepared are summarised in Table 5.14. These samples were selected so that the effects of the enzyme-treatment, the solvent used and the concentration of RhB solution applied could all be examined. The concentrations of RhB solutions used were 1×10^{-3} , 10^{-4} , 10^{-5} and 10^{-6} mol dm⁻³. Excitation wavelengths (λ) of 405 and 561 nm were selected to excite sporopollenin and RhB respectively. Low ($\times 100$) and high ($\times 630$) magnification images are presented in an attempt to both demonstrate representative samples and highlight distinct components of the pollen grains. Within each Figure, LSCM settings, including the laser power and detector settings, were maintained between samples with the same magnification to enable images to be directly compared.

Table 5.14: Summary of samples prepared for multi-track LSCM

Pollen used	Treatment applied	
	RhB in water	RhB in ethanol
Untreated <i>Betula fontinalis</i>	✓	✓
Enzyme-treated <i>Betula fontinalis</i>	✓	✓

5.5.2.1 Enzyme-treated *Betula fontinalis* pollen, treated with aqueous solutions of Rhodamine B

LSCM images of enzyme-treated *Betula fontinalis* pollen, with and without the application of aqueous solutions of RhB, can be found in Table 5.15 and Table 5.16. Table 5.15 shows that emission resulting from excitation at 405 nm is seen from all samples, whether treated with RhB or not. Results from spectrofluorometry suggest that this emission is likely to be attributed to sporopollenin (Figure 5.27). Emission from enzyme-treated pollen excited at 405 nm is more intense than that from the same pollen treated with the higher concentrations of RhB used (1×10^{-3} and 1×10^{-4} mol dm⁻³). This indicates that RhB is able to quench pollen's autofluorescence and supports the findings from spectrofluorometry (see section 5.4.3). Quenching of emission from the

wall is observed at 1×10^{-3} and 1×10^{-4} mol dm⁻³ of RhB. However, quenching of emission from the protoplast is only seen at the highest concentration of RhB (1×10^{-3} mol dm⁻³). This indicates that at lower concentrations of RhB, insufficient quantities of the fluorochrome pass through the intine into the protoplast to facilitate quenching there. RhB is routinely used as a stain for LSCM and has been described as a suitable stain for the exine, being unable to pass into the cytoplasm.¹⁷⁹

When excited at 561 nm, enzyme-treated pollen without RhB does not emit at the LSCM laser and detector settings used (Table 5.16). Spectrofluorometry of enzyme-treated *Betula fontinalis* pollen shows that pollen does emit at these longer wavelengths, but more weakly than the shorter wavelength emission of sporopollenin (Figure 5.19). Therefore, the laser power used here may have been too weak to excite the long-wavelength components of pollen, meaning that a majority of the emission from excitation at 561 nm can be attributed to RhB. Enzyme-treated *Betula fontinalis* with the lowest concentration of RhB applied (1×10^{-6} mol dm⁻³) shows almost no emission from any part of the pollen grain. At higher concentrations of RhB (1×10^{-4} and 10^{-5} mol dm⁻³) emission is primarily observed from the pollen wall. Emission from both the protoplast and pollen wall is only seen at 1×10^{-3} mol dm⁻³ RhB. These results indicate that at lower concentrations of RhB (1×10^{-4} to 10^{-6} mol dm⁻³), little or no RhB passes through the intine to the protoplast to facilitate emission there. These findings are supported by similar results from excitation at 405 nm (Table 5.15).

Table 5.15: LSCM images of enzyme-treated *Betula fontinalis* pollen, with and without treatment with aqueous solutions of RhB. LSCM settings were maintained between samples of the same magnification. Excitation λ 405 nm.

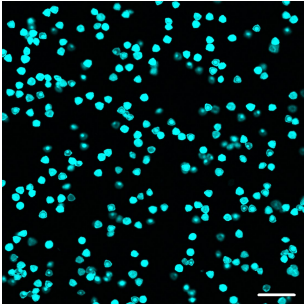
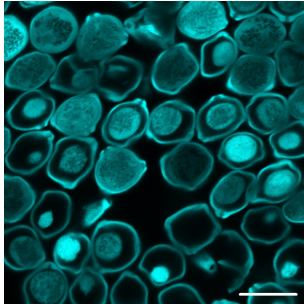
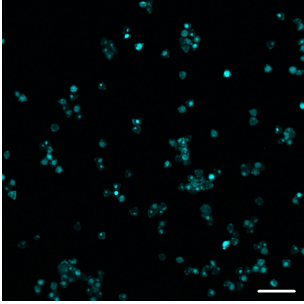
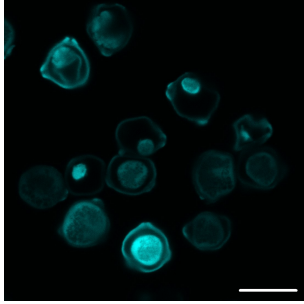
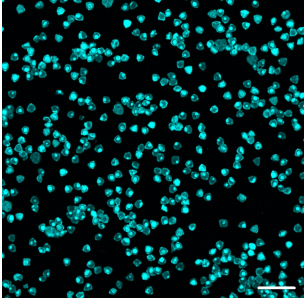
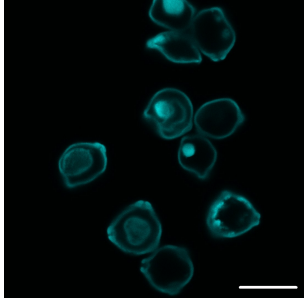
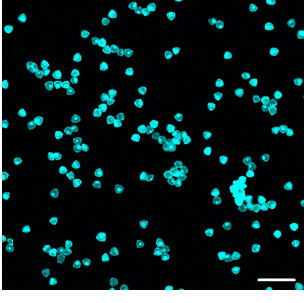
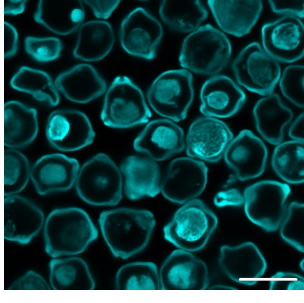
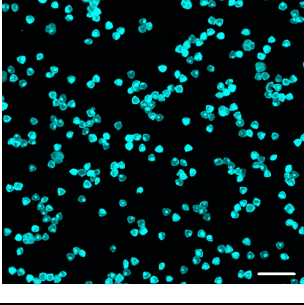
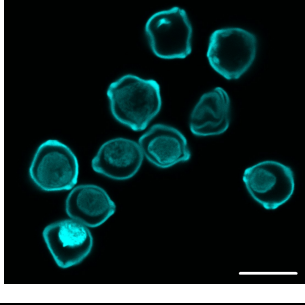
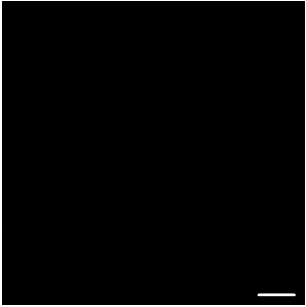
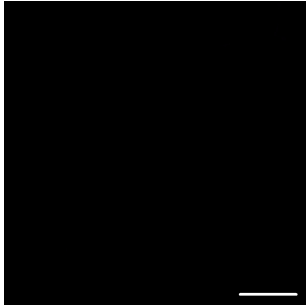
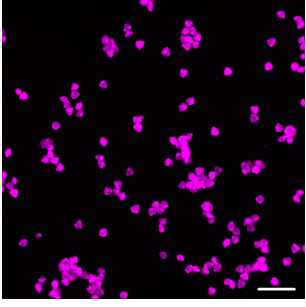
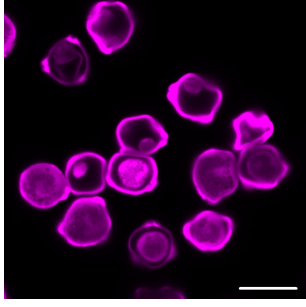
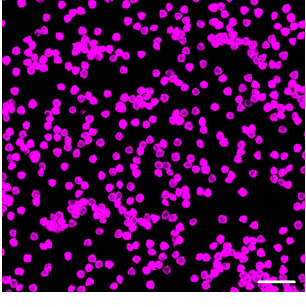
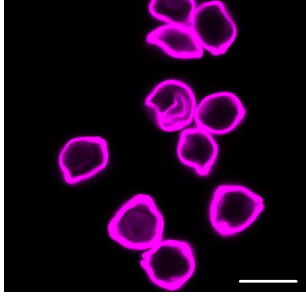
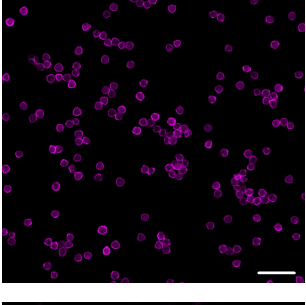
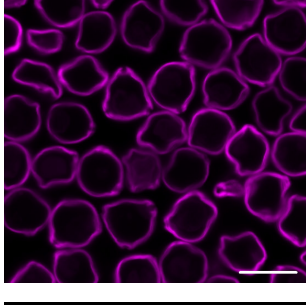
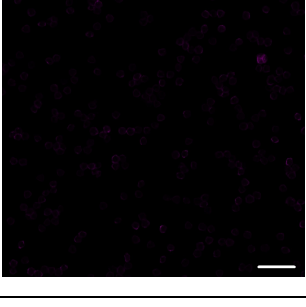
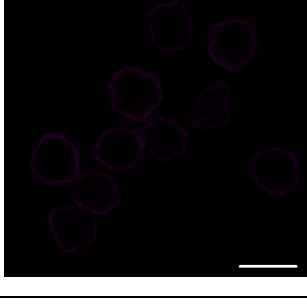
Concentration of RhB / mol dm ⁻³	× 100 magnification Scale bars = 100 μm	× 630 magnification Scale bars = 25 μm
No solution applied		
1×10^{-3}		
1×10^{-4}		
1×10^{-5}		
1×10^{-6}		

Table 5.16: LSCM images of enzyme-treated *Betula fontinalis* pollen, with and without treatment with aqueous solutions of RhB. LSCM settings were maintained between samples of the same magnification. Excitation λ 561 nm.

Concentration of RhB / mol dm ⁻³	× 100 magnification Scale bars = 100 μm	× 630 magnification Scale bars = 25 μm
No solution applied		
1×10^{-3}		
1×10^{-4}		
1×10^{-5}		
1×10^{-6}		

Enzyme-treated *Betula fontinalis* pollen, treated with aqueous solutions of RhB, was analysed by both LSCM and spectrofluorometry (see Figure 5.27 and Figure 5.28 for emission spectra). However, the excitation wavelengths and ranges over which emission were collected differed for each technique (see Table 5.17). This was largely due to the discrete laser frequencies available on the LSCM. In order to confirm whether the different excitation wavelengths used produced similar emission profiles over the ranges of wavelengths collected, measurements were taken on the spectrofluorometer using the LSCM excitation wavelengths and collection ranges summarised in Table 5.17 (Figure 5.63 and Figure 5.64). Untreated *Betula fontinalis* pollen was compared to the same pollen treated with an aqueous solution of RhB (1×10^{-3} mol dm⁻³).

Table 5.17: Excitation wavelength and range over which emission was collected for both spectrofluorometry and LSCM (applicable to all samples)

Spectrofluorometer		LSCM	
Excitation λ / nm	λ range collected / nm	Excitation λ / nm	λ range collected / nm
300	330 - 800	405	415 - 560
543*	570 - 800	561	564 - 758
548†	570 - 800		

Primarily used to observe emission from pollen

Primarily used to observe emission from RhB

* Excitation wavelength for pollen treated with aqueous solutions of RhB

† Excitation wavelength for pollen treated with ethanolic solutions of RhB

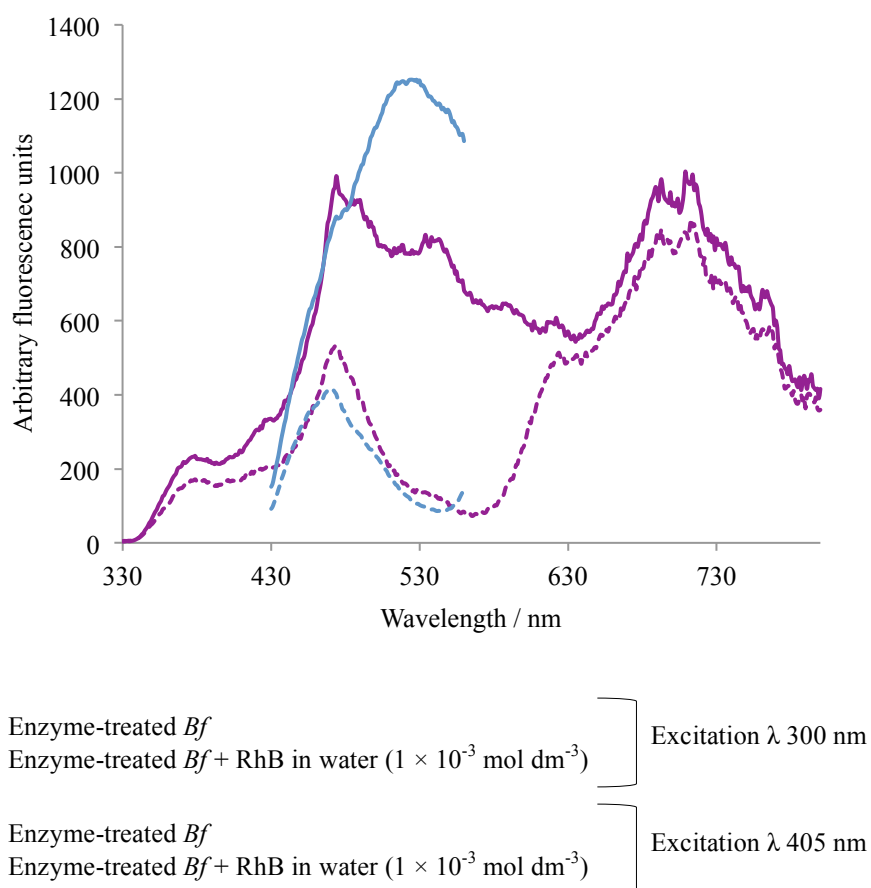


Figure 5.63: Emission spectra of enzyme-treated *Betula fontinalis* (*Bf*) pollen, and enzyme-treated *Bf* pollen treated with an aqueous solution of RhB (1×10^{-3} mol dm $^{-3}$) (excitation λ 300 and 405 nm)

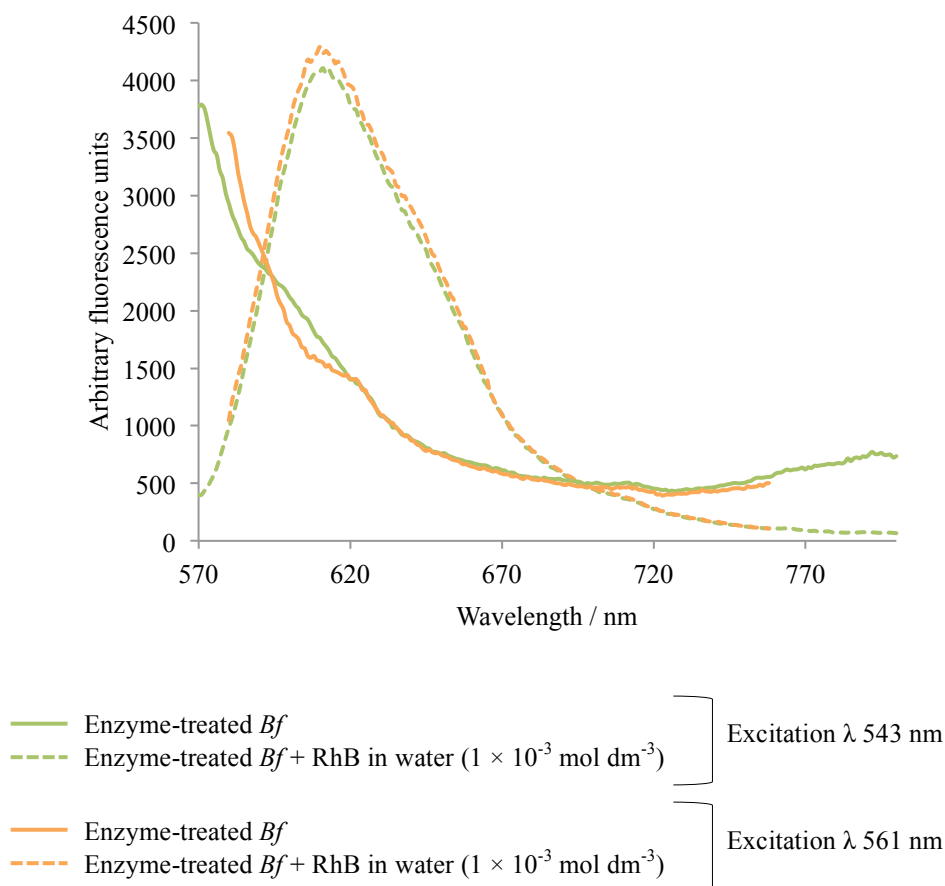


Figure 5.64: Emission spectra of enzyme-treated *Betula fontinalis* (*Bf*) pollen, and enzyme-treated *Bf* pollen treated with an aqueous solution of RhB (1×10^{-3} mol dm $^{-3}$) (excitation λ 543 and 561 nm)

Results comparing excitation at 300 and 405 nm show notable differences (Figure 5.63). In order to simulate the multi-track LSCM experiment, emission collected after excitation at 405 nm was collected over a much narrower range than after excitation at 300 nm. Spectrofluorometry shows that the intense emission peak from pollen between 630 – 800 nm was not observed during LSCM analysis. In addition, the pronounced quenching effect of pollen's emission observed after the addition of RhB between 500 – 600 nm is more easily observed after excitation at 300 nm than 405 nm. As these excitation wavelengths differ by 105 nm, it is unsurprising that such differences were seen. Therefore, quenching of pollen's emission in the presence of RhB is likely to be less obvious when observed by LSCM than by spectrofluorometry.

Spectra observed after excitation at 543 and 561 nm are very alike (Figure 5.64). Therefore, results from LSCM and spectrofluorometry using these excitation wavelengths are likely to be similar. This was predictable as these excitation

wavelengths only differ by 18 nm, compared to the 105 nm difference between the 300 and 405 nm excitation wavelengths.

5.5.2.2 Enzyme-treated *Betula fontinalis* pollen, treated with ethanolic solutions of Rhodamine B

Enzyme-treated *Betula fontinalis* pollen was treated with ethanolic solutions of RhB, and examined using multi-track LSCM after excitation at 405 and 561 nm (Table 5.18 and Table 5.19 respectively). These samples were compared to enzyme-treated pollen without the addition of RhB. After excitation at 405 nm, pollen without RhB shows emission from both the wall and the protoplast. Samples where RhB was applied show weaker emission from the pollen wall and no emission from the protoplast over all concentrations studied. These results suggest that when dissolved in ethanol, RhB was able to penetrate the wall of *Betula fontinalis* and quench emission from the protoplast. These findings are supported by spectrofluorometry (see Figure 5.29 for emission spectrum). Quenching of the protoplast's emission is only observed at higher concentrations of RhB (1×10^{-3} and 10^{-4} mol dm⁻³) in pollen treated with aqueous solutions of the fluorochrome (Table 5.15).

It is possible that compared to water; ethanol increases the penetration of RhB into pollen grains, allowing it to pass into the protoplast so that quenching can take place there. Recently published work has used ethanol to facilitate the uptake of a range of materials, including ibuprofen, yeast cells and dye materials into *Lycopodium clavatum* exine shells.^{58, 59, 74} Mackenzie *et al.* found that sunflower oil mixed with ethanol was absorbed more quickly into these shells than oil mixed with other solvents tested.⁷⁷ Although no explanation for this behaviour was offered, it does suggest that ethanol could be the optimum solvent to move materials, including RhB, into pollen grains.

Table 5.18: LSCM images of enzyme-treated *Betula fontinalis* pollen, with and without treatment with ethanolic solutions of RhB. LSCM settings were maintained between samples of the same magnification. Excitation λ 405 nm.

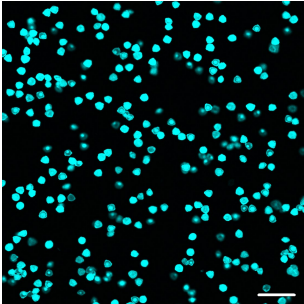
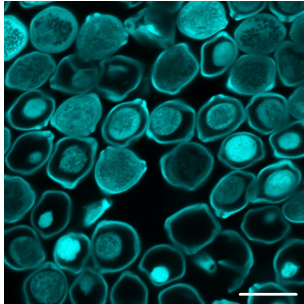
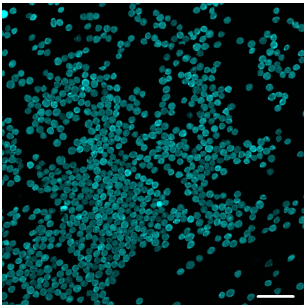
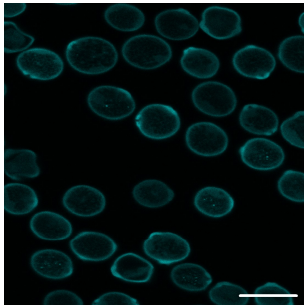
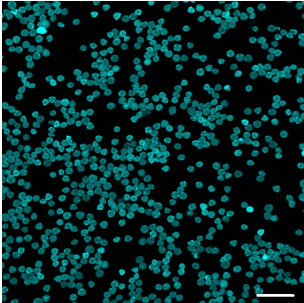
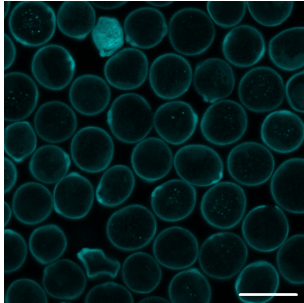
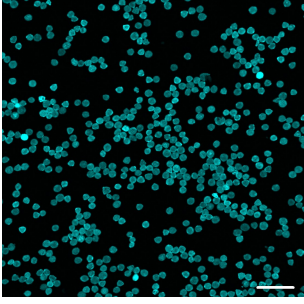
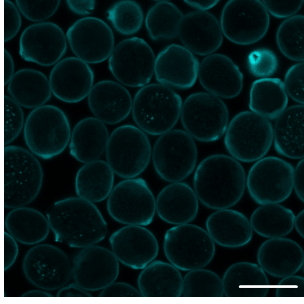
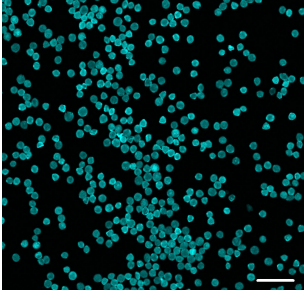
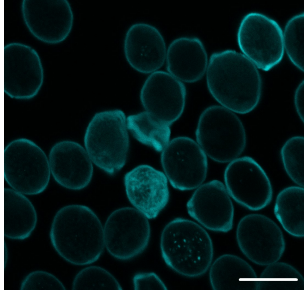
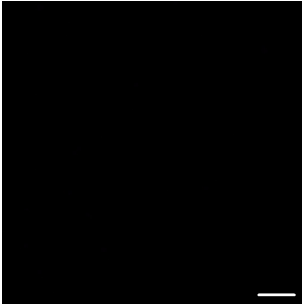
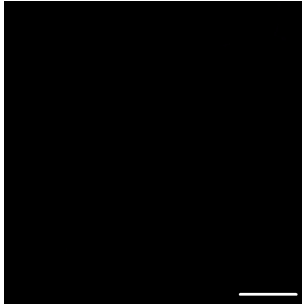
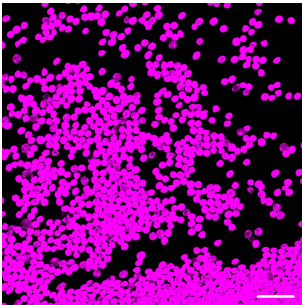
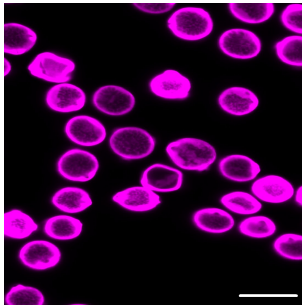
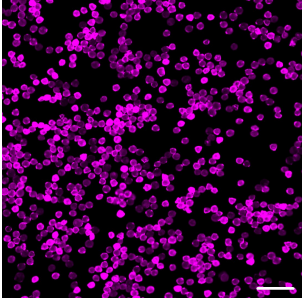
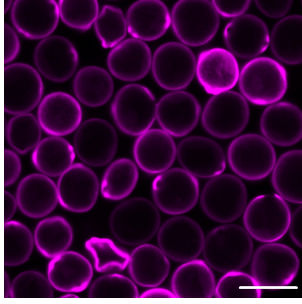
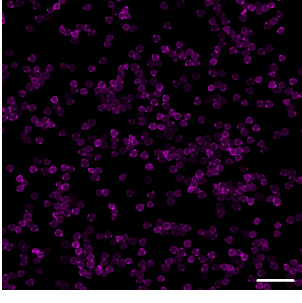
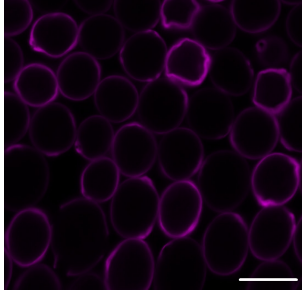
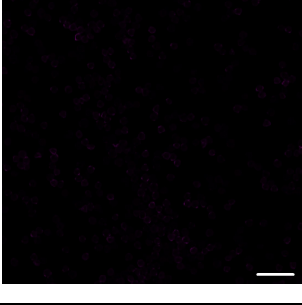
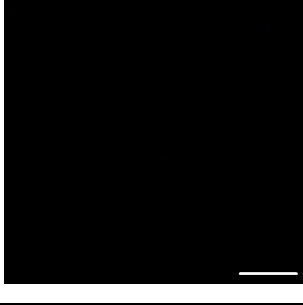
Concentration of RhB / mol dm ⁻³	× 100 magnification Scale bars = 100 μm	× 630 magnification Scale bars = 25 μm
No solution applied		
1×10^{-3}		
1×10^{-4}		
1×10^{-5}		
1×10^{-6}		

Table 5.19: LSCM images of enzyme-treated *Betula fontinalis* pollen, with and without treatment with ethanolic solutions of RhB. LSCM settings were maintained between samples of the same magnification. Excitation λ 561 nm.

Concentration of RhB / mol dm ⁻³	× 100 magnification Scale bars = 100 μm	× 630 magnification Scale bars = 25 μm
No solution applied		
1×10^{-3}		
1×10^{-4}		
1×10^{-5}		
1×10^{-6}		

An alternative explanation for the lack of emission from the protoplast of enzyme-treated pollen exposed to ethanolic solutions of RhB could be that the ethanol facilitates the movement of residual protoplast material, left over from the enzyme treatment, out of the grains. During the enzyme treatment used to produce the pollen for analysis, aqueous solutions were used to wash grains. Therefore, ethanol may remove more polar components of the protoplast that are less soluble in water. As a result, there could be less protoplast material to fluoresce. This explanation seems less likely as $\times 630$ magnification images taken after excitation at 561 nm indicate the presence of protoplast material (Table 5.19).

Not all grains emit with equal intensity after excitation at 561 nm (Table 5.18). This is especially clear in $\times 630$ magnification images of pollen treated with 1×10^{-4} , 10^{-5} and $10^{-6} \text{ mol dm}^{-3}$, where some grains clearly emit with greater intensity than others. Why some grains show such intense emission is not clear, although they could be at a different stage in their lifecycles compared to other grains in the same sample. As a result, they may have a different chemical composition, resulting in differing fluorescence. Roshchina demonstrated that fluorescence observed from pollen is influenced by a number of factors, including at which stage of its development a grain is observed at.⁴⁰

Enzyme-treated pollen treated with ethanolic solutions of RhB at concentrations of 1×10^{-3} , 10^{-4} and $10^{-5} \text{ mol dm}^{-3}$ fluoresces after excitation at 561 nm (Table 5.19). Emission is predominantly from the pollen wall and little emission from the protoplast is observed, especially at concentrations at or below $1 \times 10^{-4} \text{ mol dm}^{-3}$ RhB. Emission from the wall of RhB-treated pollen suggests that most RhB is bound to the pollen wall rather than to the protoplast. Limited emission is observed from the protoplast at the highest concentration of RhB ($1 \times 10^{-3} \text{ mol dm}^{-3}$), suggesting some binding there.

The resolution of the LSCM is insufficient to determine which wall layer (the exine or the intine) the RhB binds to, or whether both are equally preferred. This result contradicts the theory that ethanol increases the movement of RhB into the protoplast as, if this were the case, emission from RhB bound to the protoplast would be observed. However, these results support the idea that ethanol could remove protoplast material, thus decreasing emission from the protoplast, compared to that from enzyme-treated pollen treated with aqueous solutions of RhB.

5.5.2.3 Untreated *Betula fontinalis* pollen, treated with aqueous solutions of Rhodamine B

Untreated *Betula fontinalis* pollen was treated with aqueous solutions of RhB, and examined by LSCM after excitation at 405 and 561 nm (Table 5.20 and Table 5.21 respectively). After excitation at 405 nm, both the protoplast and wall of untreated pollen (without the addition of RhB) fluoresce. The addition of higher concentration RhB solutions (1×10^{-3} to 10^{-5} mol dm⁻³) quenches emission from the pollen wall, leaving only emission from the protoplast. This suggests that at sufficiently high concentrations, RhB is able to penetrate the wall of pollen grains to quench emission there, but is not able to reach pollen's protoplasts. This finding is supported by images collected after excitation at 561 nm, as emission from the walls of grains is more intense than from the protoplast, indicating preferential binding of RhB to the pollen wall. At the lowest concentration of RhB (1×10^{-6} mol dm⁻³) almost no quenching of the emission from the pollen wall is observed after excitation at 405 nm. This is due to the very limited binding of RhB to the wall of the pollen at this concentration, as supported by images collected after excitation at 561 nm. These results compare favourably to results from spectrofluorometry, which indicate that quenching of pollen's emission only occurs at higher concentrations of RhB (1×10^{-3} to 10^{-5} mol dm⁻³) (Figure 5.25).

After excitation at 561 nm, higher concentrations of RhB (1×10^{-3} and 10^{-4} mol dm⁻³) show emission from both the protoplast and wall, indicating that the fluorochrome bound to both of these structures. At 1×10^{-3} mol dm⁻³ emission is only seen from the wall, which suggests that at lower concentrations, insufficient RhB penetrates the protoplast to emit there. Emission from RhB is not seen at all at 1×10^{-6} mol dm⁻³.

An unusual finding is that after excitation at 405 nm, the overall intensity of emission from untreated pollen is weaker than from pollen treated with the two lowest concentrations of RhB (1×10^{-5} and 10^{-6} mol dm⁻³). This finding cannot be explained in terms of quenching, as untreated pollen should still show more intense emission than RhB-treated pollen. Although every effort was made to select random samples for LSCM analysis, it may be that the regions of the slide selected for analysis showed unusually low or high emission intensity.

Compared to enzyme-treated pollen, untreated pollen displays similar trends. However, ethanolic solutions of RhB may show greater penetration of the protoplast compared to the aqueous solutions applied to the same pollen samples.

Table 5.20: LSCM images of untreated *Betula fontinalis* pollen, with and without treatment with aqueous solutions of RhB. LSCM settings were maintained between samples of the same magnification. Excitation λ 405 nm.

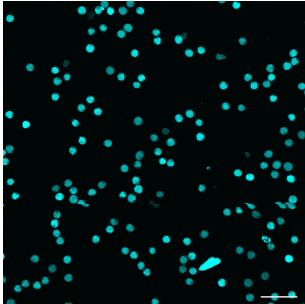
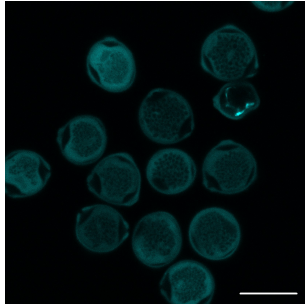
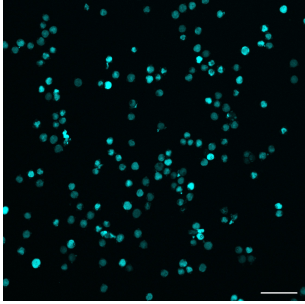
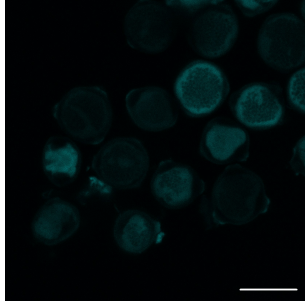
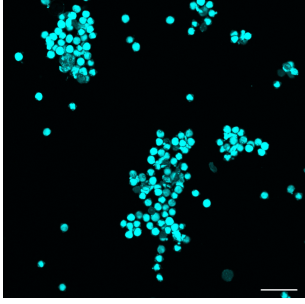
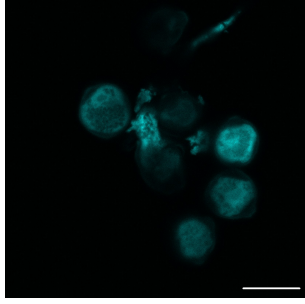
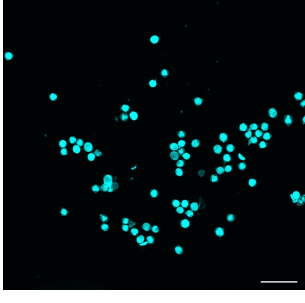
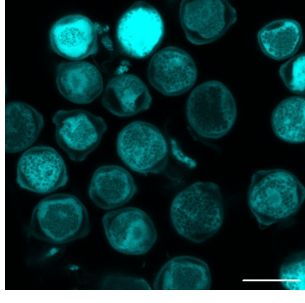
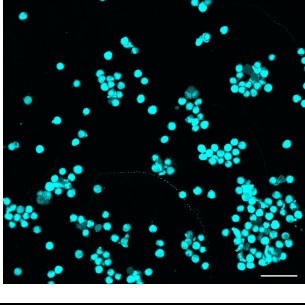
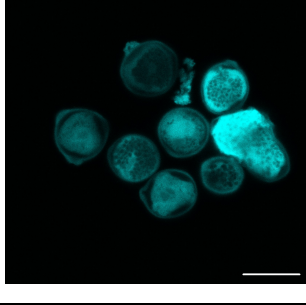
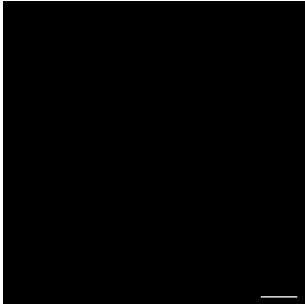
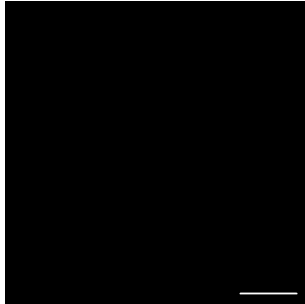
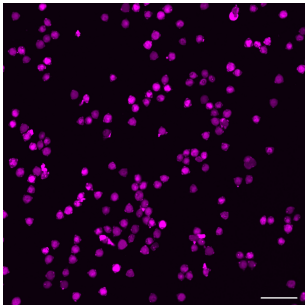
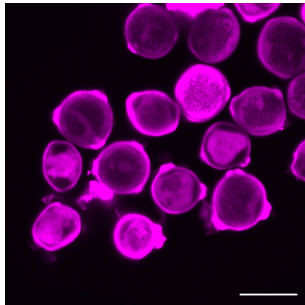
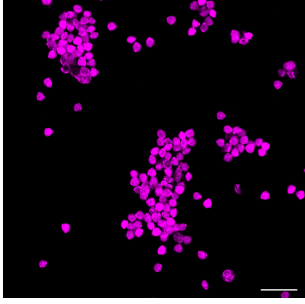
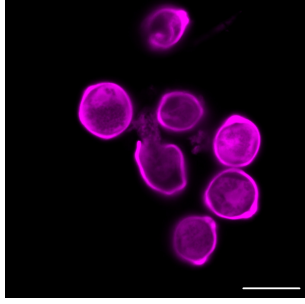
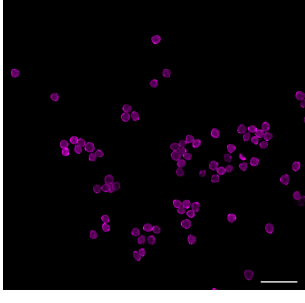
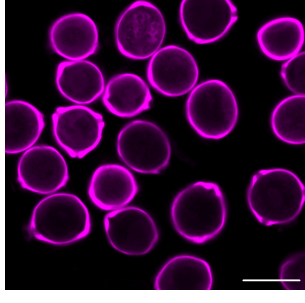
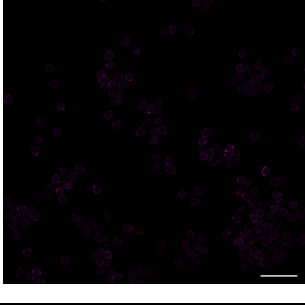
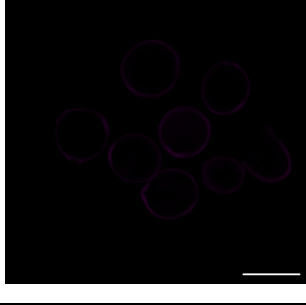
Concentration of RhB / mol dm ⁻³	× 100 magnification Scale bars = 100 μm	× 630 magnification Scale bars = 25 μm
No solution applied		
1×10^{-3}		
1×10^{-4}		
1×10^{-5}		
1×10^{-6}		

Table 5.21: LSCM images of untreated *Betula fontinalis* pollen, with and without treatment with aqueous solutions of RhB. LSCM settings were maintained between samples of the same magnification. Excitation λ 561 nm.

Concentration of RhB / mol dm ⁻³	× 100 magnification Scale bars = 100 μ m	× 630 magnification Scale bars = 25 μ m
No solution applied		
1×10^{-3}		
1×10^{-4}		
1×10^{-5}		
1×10^{-6}		

5.5.2.4 Untreated *Betula fontinalis* pollen, treated with ethanolic solutions of Rhodamine B

Untreated *Betula fontinalis* pollen was treated with ethanolic solutions of RhB. LSCM was used to examine these samples and excitation wavelengths of 405 and 561 nm were used (Table 5.22 and Table 5.23 respectively).

After excitation at 405 nm, emission from untreated pollen is similar to the same pollen treated with 1×10^{-3} to 10^{-5} mol dm⁻³ ethanolic solutions of RhB. Emission is slightly more intense from pollen treated with the lowest concentration solution (1×10^{-6} mol dm⁻³ RhB). These results are surprising, as after excitation at 300 nm, spectrofluorometry indicates emission from pollen treated with ethanolic solutions of RhB is quenched (Figure 5.65). As a result, weaker emission would be anticipated from RhB-treated samples. It may be that the random areas of the slides selected for analysis are not representative of the bulk sample. In addition, the excitation wavelength of the LSCM (405 nm) was different to that used for spectrofluorometry (300 nm), which may mean that quenching of pollen's emission was not effectively observed in this sample using the LSCM (see section 5.5.2.1 for a full discussion of this effect). This is in contrast to enzyme-treated pollen treated with ethanolic solutions of RhB, where quenching was observed by LSCM (Table 5.18).

Excitation at 561 nm induced no emission in untreated *Betula fontinalis* pollen (due to the absence of RhB), but very strong emission from pollen treated with the higher concentrations of RhB (1×10^{-3} and 10^{-4} mol dm⁻³). At 1×10^{-3} mol dm⁻³ RhB, emission is observed from both the protoplast and wall, but at 1×10^{-4} mol dm⁻³, emission from the protoplast is weaker. This suggests that at higher RhB concentrations, greater quantities of RhB penetrate the pollen grains and bind to their protoplasts. After treatment with 1×10^{-5} mol dm⁻³ RhB, only weak emission is seen from the pollen wall, indicating little binding of RhB there and no binding to the protoplast. No emission is present at the lowest RhB concentration (1×10^{-6} mol dm⁻³). These results don't correlate with observations made at 405 nm, as the presence of RhB (observed at 561 nm) should also quench pollen's emission at this wavelength. These results do support the suggestion that the areas of the slides selected for analysis at 405 nm were not representative of the bulk sample, especially at $\times 630$ magnification.

Table 5.22: LSCM images of untreated *Betula fontinalis* pollen, with and without treatment with ethanolic solutions of RhB. LSCM settings were maintained between samples of the same magnification. Excitation λ 405 nm.

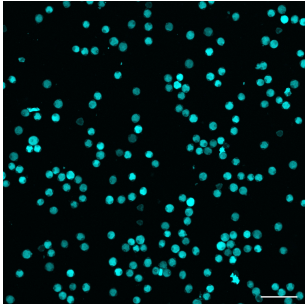
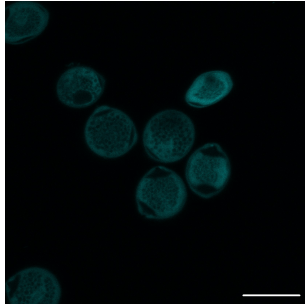
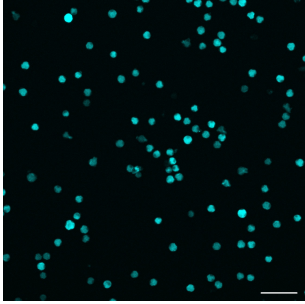
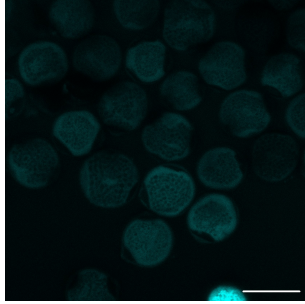
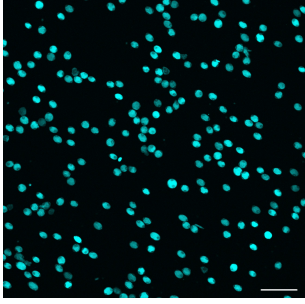
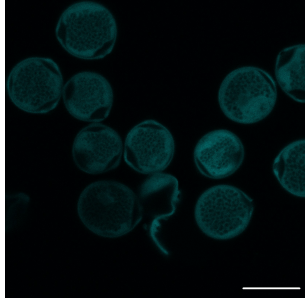
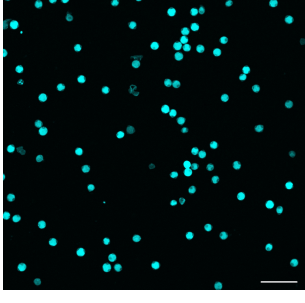
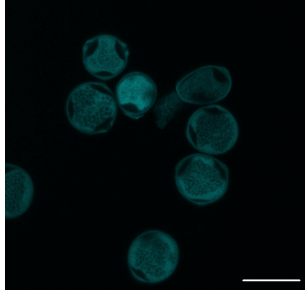
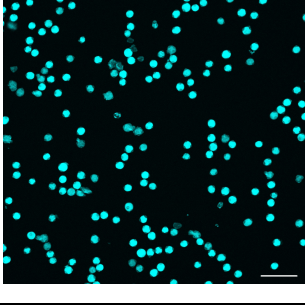
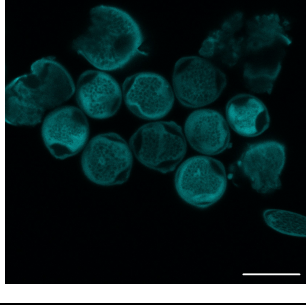
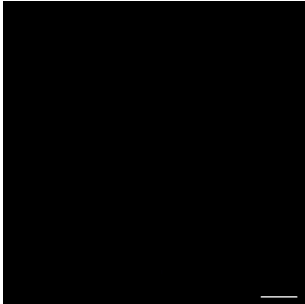
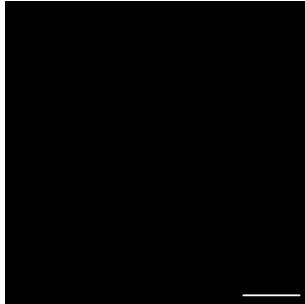
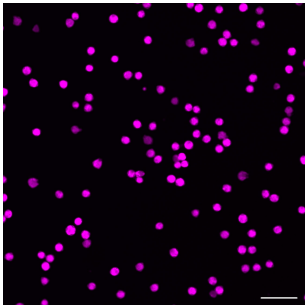
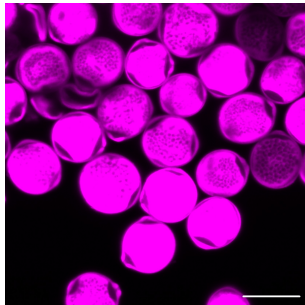
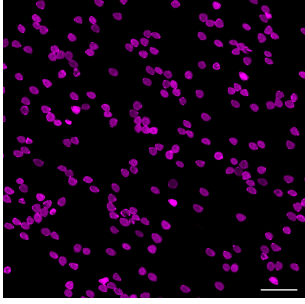
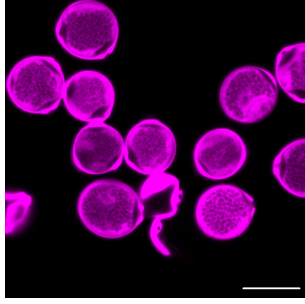
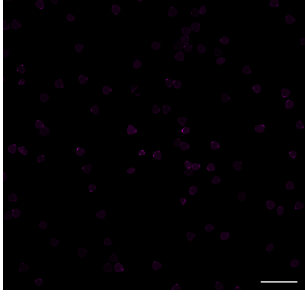
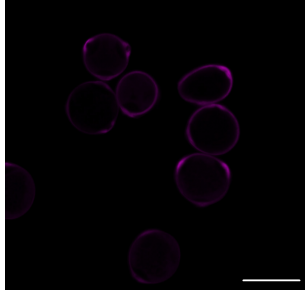
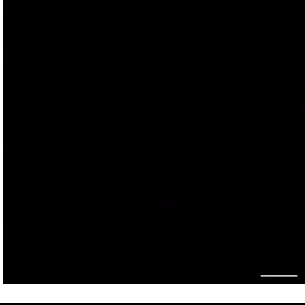

Concentration of RhB / mol dm ⁻³	× 100 magnification Scale bars = 100 μm	× 630 magnification Scale bars = 25 μm
No solution applied		
1×10^{-3}		
1×10^{-4}		
1×10^{-5}		
1×10^{-6}		

Table 5.23: LSCM images of untreated *Betula fontinalis* pollen, with and without treatment with ethanolic solutions of RhB. LSCM settings were maintained between samples of the same magnification. Excitation λ 561 nm.

Concentration of RhB / mol dm ⁻³	× 100 magnification Scale bars = 100 μm	× 630 magnification Scale bars = 25 μm
No solution applied		
1×10^{-3}		
1×10^{-4}		
1×10^{-5}		
1×10^{-6}		

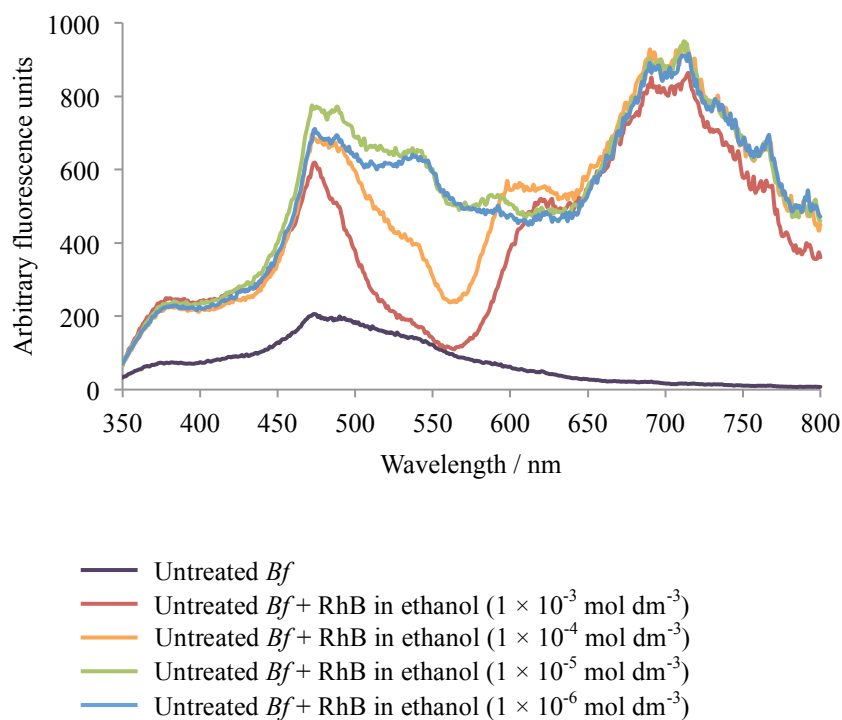


Figure 5.65: Emission spectra of untreated *Betula fontinalis* (*Bf*) pollen, treated with ethanolic solutions of RhB of varying concentrations (excitation λ 300 nm, 350 nm longpass filter)

5.5.2.5 Multi-track LSCM of untreated and enzyme-treated *Betula fontinalis* pollen treated with aqueous and ethanolic solutions of Rhodamine B: summary of results

1. Results from the samples analysed (see Table 5.14 for summary) indicate that multi-track LSCM is a suitable technique to evaluate the pollen species under investigation. The resolution of the LSCM was sufficient to allow comment on the protoplast and exine wall, but insufficient to differentiate between wall layers i.e. the exine and intine.
2. LSCM results are summarised in brief in Table 5.24. This table illustrates that enzyme-treated pollen, treated with aqueous solutions of RhB, showed the most successful binding or encapsulation of RhB (as measured by emission and quenching processes) over the range of concentrations studied. Even at the lowest concentration of RhB (1×10^{-6} mol dm⁻³), emission from the pollen's wall and protoplast was quenched, indicating some binding or encapsulation of RhB.

3. Findings were not always exactly analogous to spectrofluorometry. In particular, quenching of pollen's emission was not observed in untreated *Betula fontinalis* pollen, treated with ethanolic solutions of RhB. This anomaly may be explained by the differing excitation wavelengths and ranges over which emission was collected for LSCM and spectrofluorometry. Alternatively, it may indicate that representative samples were not selected for LSCM.
4. Table 5.24 illustrates that the difference between samples was not large. This finding is in contrast to spectrofluorometry, which shows greater variability between samples. As applied here, LSCM may be a less sensitive technique as the multi-track method applied collected emission over a narrower range than spectrofluorometry, meaning that some emission and quenching effects may have been missed. However, LSCM did allow the general location of RhB binding or encapsulation to be determined, which spectrofluorometry did not facilitate so readily.

Table 5.24: Summary of findings from LSCM

Concentration RhB	$1 \times 10^{-3} \text{ mol dm}^{-3}$				$1 \times 10^{-4} \text{ mol dm}^{-3}$				$1 \times 10^{-5} \text{ mol dm}^{-3}$				$1 \times 10^{-6} \text{ mol dm}^{-3}$			
	qp	qw	ep	ew	qp	qw	ep	ew	qp	qw	ep	ew	qp	qw	ep	ew
Enzyme-treated <i>Bf</i> + aqueous RhB																
Enzyme-treated <i>Bf</i> + ethanolic RhB																
Untreated <i>Bf</i> + aqueous RhB																
Untreated <i>Bf</i> + ethanolic RhB																

qp – quenching of protoplast's emission
qw = quenching of wall's emission

ep = emission from protoplast
ew = emission from wall

Observed after excitation at 405 nm

Observed after excitation at 561 nm

Observed

Not observed

5.6 Conclusions

Visual inspection of untreated pollen from *Betula fontinalis*, *Secale cereale*, *Juglans nigra*, *Taraxacum officinale* and *Ambrosia artemisiifolia*, indicated that species could not be identified by their appearance alone. Enzyme-treated *Betula fontinalis* and *Ambrosia artemisiifolia* pollen was indistinguishable from untreated pollen of the same species. However, all of these samples could be readily differentiated by spectrofluorometry. In comparison, *Lycopodium clavatum* spores could be distinguished both by eye and by spectrofluorometry as they turned from yellow to dark brown after base and acid treatment.

Distinct emission spectra were collected from all species, both before and after enzyme or base and acid treatments were applied. However, all pollen and spores possessed a strong emission peak at 470 nm, with a weaker band between 350 – 450 nm. These intense peaks were attributed to sporopollenin as they remained in the spectra even after pollen or spores were treated. The ratio of these peaks varied, suggesting that sporopollenin or its close environment, was altered by the treatments applied. Attempts were made to assign other peaks and bands, however spectra were too complex to draw any firm conclusions. Findings here could not support the hypothesis proposed by Sodeau *et al.*, that pollen or spores within the same botanical order display similar emission.⁹⁵

Both aqueous and ethanolic solutions of RhB of varying concentrations were applied to untreated and enzyme-treated *Betula fontinalis* pollen. The addition of RhB quenched emission from the pollen wall over the entire range of RhB concentrations studied. Quenching of the protoplast's emission only occurred at higher concentrations of RhB, indicating that at lower concentrations, RhB does not reach the protoplast in sufficient quantities to facilitate quenching. In all samples, RhB's peak emission shifted to longer wavelengths at higher RhB concentrations. The exact reason for this effect is difficult to pinpoint, although it is likely to be due to reabsorption or aggregation effects. Similar effects were observed when aqueous and ethanolic solutions of RhB were applied to untreated *Juglans nigra* pollen and *Lycopodium clavatum* spores.

Spectrofluorometry and LSCM should be considered complementary techniques to evaluate emission from pollen and spores (both with and without the addition of RhB

and/or other treatments). LSCM was able to highlight the general nature of binding or interaction of RhB with pollen or spores. However, the resolution available meant that only the overall pollen or spore wall could be scrutinised, rather than its individual components i.e. the exine and intine (pollen) or the exospore and endospore (spore). Spectrofluorometry allowed analysis of quenching effects as well as peak shifts and changes in peak ratios. Such investigations would not be possible using the LSCM in isolation.

Chapter 6:

Conclusions

6 Conclusions

6.1 Emptying pollen and spores

The primary aim of this thesis was to produce sporopollenin microcapsules from a range of species of pollen and spores. Published results indicate that spore microcapsules have desirable material properties and may overcome some manufacturing problems associated with current microcapsule technologies.

Several methods were attempted to prepare pollen and spore microcapsules, including base and acid treatment, acetolysis and treatments involving enzymes. Microcapsules were successfully produced from *Lycopodium clavatum* spores using a previously published base and acid protocol. This method was found to be unsuitable for all pollen species investigated. It was hypothesised that the lamellar structure of *Lycopodium clavatum*'s exospore imparted greater physical strength compared to the possibly weaker columellate and granular textures of the pollen exines.

Acetolysis is a standard palynological technique applied to pollen and spores to produce material for microscopy. It was investigated here as a method to produce microcapsules. Although, as predicted, it removed most non-sporopollenin material, the remaining sporopollenin exines (pollen) and exospores (spores) were dark brown. These would therefore be unsuitable for most microencapsulation applications where light-coloured microcapsules are desirable. In addition, this colour change indicated the likelihood that acetolysis altered sporopollenin's chemical structure, therefore possibly reducing some of its desirable material properties. Although it is possible to bleach acetolysed pollen and spores, this was not carried out as it would be likely to further change sporopollenin's structure.

A published method incorporating enzymes was applied to a range of pollen species. The published aim of this method was to generate material for analysis (rather than to produce microcapsules) but it was attempted here as it was considered 'gentler' compared to base and acid treatments and acetolysis. The enzyme treatment removed a portion of non- sporopollenin material from some grains, but left others damaged.

Therefore, it was considered an unsuitable method to produce microcapsules from the pollen species investigated. However, the selective nature of enzymes meant that this technique was the least likely of the three investigated for this thesis to alter sporopollenin's structure. Therefore, enzyme-treated *Betula fontinalis* pollen was compared to the same untreated pollen during fluorescence studies.

6.2 Attempted encapsulation of *Lactobacillus* bacteria

Enzyme-treated *Betula fontinalis* pollen was treated with suspensions of *Lactobacilli* in an attempt to encapsulate this bacterium. This work aimed to build on published results demonstrating the encapsulation of yeast cells. Light microscopy indicated that, if encapsulation was successful, it was very limited. Therefore, further optimisation of the method used to encapsulate bacteria is required. For example, applying a vacuum or putting the pollen under pressure prior to the application of bacteria, could increase levels of encapsulation. Alternatively, smaller bacteria or bacterial spores could be used, as *Lactobacillus* bacteria may have been too large to pass through the pores of this pollen. In addition, pollen grains with larger pores could be sought that may facilitate the motion of bacteria into grains.

6.3 Fluorescence studies

Pollen and spores are known to autofluoresce. Sporopollenin from both pollen and spores is thought to make up the most intense component of observed fluorescence emission, and this was confirmed in this thesis. Untreated pollen and spores from a range of species all appeared similar by visual inspection. Similarly, untreated pollen and enzyme-treated pollen could not be differentiated. However, the fluorescence emission of all species (untreated or enzyme-treated) was distinct, indicating the differing composition of each.

Untreated and enzyme-treated pollen and spores were treated with aqueous and ethanolic solutions of the fluorochrome, Rhodamine B (RhB). Different concentrations of solutions applied produced differently coloured grains. However, the same

concentration of RhB applied to a range of species resulted in particles that could not be differentiated by eye, but possessed different emission spectra.

Sporopollenin's emission was quenched by the addition of RhB, probably *via* the reabsorption of sporopollenin's emission by RhB. Additionally, in the presence of pollen and spores, RhB's emission shifted to longer wavelengths. It was considered that this was probably due to reabsorption or aggregation effects, although further investigations would be required to determine which of these effects is most likely.

The binding of RhB to untreated and enzyme-treated pollen was investigated using laser scanning confocal microscopy (LSCM). This confirmed that RhB bound preferentially to the pollen wall, rather than the protoplast. It is possible that RhB was unable to reach the protoplast of pollen grains in large enough quantities to bind there, thus explaining the higher concentration of RhB bound to the pollen wall. Sporopollenin's emission was quenched by RhB, providing further evidence that RhB was in close association with the sporopollenin exine. By applying a range of other fluorochromes, quenching effects as well as any preferential binding could be further investigated.

These results demonstrate that fluorescent pollen grains can be easily produced and their fluorescence quickly measured, either by spectrofluorometry or LSCM. Such fluorescent particles may find uses in security devices, where it would be useful for particles to appear similar by visual inspection, but different when analysed by spectrofluorometry.

In previously published work, *p*-coumaric acid and ferulic acid were proposed as proxies for sporopollenin. These structures are thought to be similar to monomers of sporopollenin. Solutions of these acids were combined with solutions of RhB and fluorescence patterns observed were similar to those observed in pollen treated with RhB. This suggests that these acids could be possible proxies. However, other materials, including riboflavin, have shown similar emission trends in the presence of RhB. Riboflavin is not thought to be structurally similar to sporopollenin. Therefore, fluorescent measurements indicate that *p*-coumaric acid and ferulic acid may be suitable proxies, but that these measurements should be evaluated in conjunction with other previously published analysis.

6.4 Concluding remarks and future work

Microcapsules were only successfully produced from spores. Therefore, further research is required to determine whether microcapsules can indeed be produced from pollen. This could be achieved by either developing new methods or further optimising existing methods. In addition, pollen and spores from a wider range of genera should be exposed to these treatments. This would provide further information on how treatments used to produce microcapsules influence pollen and spore structure. It would also allow the theory that lamellar wall structures impart greater strength to the exospore of spores to be fully evaluated.

Pollen and spores were combined with RhB to produce coloured, fluorescent particles. These fluorescent particles may find uses in commercial devices, where brightly coloured, micron-scale particles are required. Further work is required to determine how RhB interacts with pollen and spores. Methods to covalently bind RhB to pollen and spores should also be evaluated, as the pollen or spore to RhB interaction could be strengthened as a result. The fading of the RhB within these coloured particles should be measured and compared to that of standard RhB. If pollen and spores are found to reduce fading of the dye, these coloured particles could find a use in applications where the longevity of dyes is important, for example in outdoor displays.

Unfortunately, bacteria could not be successfully encapsulated. However, encapsulation could possibly be achieved with additional method development or the use of smaller bacteria, bacterial spores or pollen with larger pores.

Overall, pollen and spore microcapsules have great potential as alternatives to current microcapsule technologies. However, further work is required to optimise their production and develop their uses.

Chapter 7:

Experimental

7 Experimental

7.1 Materials

The suppliers of materials used are summarised in Table 7.1. Solvents were purchased from Fisher. A sample of Ruthenium Red was obtained from the Bioscience Technology Facility, The University of York. All reagents were used without further purification.

Table 7.1: Summary of materials used and associated suppliers

Supplier	Material	Abbreviation
Sigma Aldrich, UK	Acetic anhydride	
	<i>Ambrosia artemisiifolia</i> pollen	
	<i>Betula fontinalis</i> pollen	
	Bovine serum albumin	
	<i>p</i> -Coumaric acid	
	Cyclohexylamine	CHA
	Ferulic acid	
	Hydrochloric acid	HCl
	<i>Juglans nigra</i> pollen	
	4-Methylmorpholine <i>N</i> -oxide	MMNO
	<i>Ortho</i> -phosphoric acid (85 % solution)	
	Percoll	
	Rhodamine B	RhB
<i>Secale cereale</i> pollen		
	TWEEN 80	
Fluka, UK	Lactobacillus broth according to De Man, Rogosa and Sharpe	MRS broth
Acros Organics, UK	2-(<i>N</i> -Morpholino)ethanesulfonic acid buffer solution	MES buffer
Fisher, UK	Potassium hydroxide	
	Sodium hydroxide	
	Sulfuric acid	
Ascott Dairy Supplies, UK	Freeze-dried yogurt culture	
Apollo Scientific, UK	Cellulase	
	Macerase	
Merck4Biosciences, UK	Cellulase	
	Macerase	
Baldwin and Co., UK	<i>Lycopodium clavatum</i> spores	
Allergon, Sweden	<i>Ambrosia artemisiifolia</i> pollen	
	<i>Juglans nigra</i> pollen	
	<i>Secale cereale</i> pollen	
Agar scientific, UK	Formaldehyde	
	Glutaraldehyde	
	Osmium tetroxide	
	Spurr resin	

7.2 Methods

7.2.1 Acetolysis applied to *Lycopodium clavatum* spores and *Secale cereale*, *Juglans nigra* & *Betula fontinalis* pollen

Method based on the protocol provided by Carol Furness, Royal Botanic Gardens Kew, London, originally based on the method published by Erdtman.^{119, 180}

A fresh acetolysis mixture (9:1 ratio of acetic anhydride to sulfuric acid) was prepared. Pollen or spores (0.1 g of either *Lycopodium clavatum* spores or *Secale cereale*, *Juglans nigra* or *Betula fontinalis* pollen) were suspended in the acetolysis mixture (2 mL) without stirring and heated (90 °C) for 2 min. The suspension was centrifuged (1500 × g, 5 min) and the supernatant fraction discarded. The pollen was re-suspended in water (~ 10 mL) and centrifuged (1500 × g, 5 min). This washing was carried out a total of three times. Yields were not recorded as the masses of material used were very small; pollen and spores were recovered wet and material was only briefly retained for light microscopy.

7.2.2 Base and acid treatments

7.2.2.1 Standard base and acid treatment applied to *Lycopodium clavatum* spores and *Secale cereale* and *Juglans nigra* pollen

The method was based on the protocol published by Atkin *et al.*⁵⁷ The same method was applied to *Lycopodium clavatum* spores and *Secale cereale* & *Juglans nigra* pollen. The exact masses of each species used, the volumes of base and solvents are abbreviated with italicised letters. These abbreviations, as well as the percentage yields achieved, are summarised in Table 7.2. The published base and acid treatment was not completed for all species, and the point at which the method was halted for each species is indicated with an underlined phrase. The reasons for varying the method used for each species are discussed in section 3.4.

Pollen or spores (a g) were suspended in acetone (b mL) and stirred at reflux for 4 h. The suspension was filtered under reduced pressure and washed with acetone ($c \times d$ mL). The solids collected were suspended in potassium hydroxide (6 % (w/v), e mL) and stirred at reflux for 6 h. Solids were filtered under reduced pressure and washed with hot (~ 60 °C) water ($f \times g$ mL) (the method was stopped at this point for *Secale cereale* pollen). Solids were stirred at reflux in potassium hydroxide ((6 % (w/v), h mL) for a further 6 h, filtered under reduced pressure and washed with hot (~ 60 °C) water ($j \times k$ mL), followed by hot (~ 60 °C) ethanol ($j \times k$ mL). The solids were left to dry in air overnight (the method was stopped at this point for *Juglans nigra* pollen) and then stirred at reflux in *ortho*-phosphoric acid (85 %, 190 mL) for seven days. The suspension was cooled to ~ 100 °C and filtered under reduced pressure. The solids were washed with water (5×30 mL), acetone (1×30 mL), hydrochloric acid (2 mol dm^{-3} , 1×30 mL), sodium hydroxide (2 mol dm^{-3} , 1×30 mL), water (5×30 mL), acetone (1×30 mL) and ethanol (1×30 mL). The solids were filtered off under reduced pressure and left to air-dry overnight.

Table 7.2: Summary masses of each species used, the volumes of base and solvents applied and the percentage yields achieved

Quantity of reagent used	<i>Lycopodium clavatum</i>	<i>Secale cereale</i>	<i>Juglans nigra</i>
<i>a</i> / g	33.9	1.5	3.0
<i>b</i> / mL	93	15	9
<i>c</i> / mL	1	1	5
<i>d</i> / mL	100	20	5
<i>e</i> / mL	130	11	9
<i>f</i> / mL	–	1	1
<i>g</i> / mL	–	20	10
<i>h</i> / mL	90	–	9
<i>j</i> / mL	5	–	5
<i>k</i> / mL	30	–	3
Percentage yield	20.9	*	*

* Yield not recorded as the solids were bound to the sinter and only enough material for analysis could be recovered

7.2.2.2 Acid and base treatment applied to *Ambrosia artemisiifolia* pollen

Based on the method published by Fletcher *et al.*¹²⁴ *Ambrosia artemisiifolia* pollen (1.0 g) was stirred in acetone (3 mL) for 2 h. The solids were filtered under reduced pressure, washed with acetone (3 × 5 mL) and left to dry in air overnight. Solids were stirred at reflux in sodium hydroxide (1 % (w/v), 6 mL) for 1 h. The dark-orange suspension was partially filtered under reduced pressure and hydrochloric acid was added until pH 7 was achieved. The sticky nature of the product on the sinter meant that less than half of the total material could be filtered. This suspension was heated (without stirring) at reflux in ethanol (75 mL) for 1 h. The solids were filtered under reduced pressure and left to dry in air overnight. A 24 % yield was recorded.

7.2.3 Enzyme treatment applied to *Juglans nigra*, *Betula fontinalis* and *Secale cereale* pollen

This method is based on the protocol published by Loewus *et al.*⁶⁴ Pollen (0.25 g) was suspended in a solution of MMNO (60 % aqueous solution, 1.1 mL) and CHA (1.4 mL). After 10-15 min water (1.3 mL) was added and x pestle cycles were performed using a Potter-Elvehjem tissue grinder with a polytetrafluoroethylene (PTFE) pestle and glass mortar (the exact number of cycles performed on each species is recorded in Table 7.3). The suspension was left at room temperature for 2 h, diluted 3-fold with water and then centrifuged ($1500 \times g$, 5 min). The supernatant fraction was discarded and replaced with water (~ 20 mL in total). The mixture was shaken vigorously and re-centrifuged ($1500 \times g$, 5 min). This washing was repeated a total of five times. The supernatant fraction was discarded and replaced with MES buffer (pH 5.2, 6 mM, ~ 20 mL). The mixture was shaken vigorously and centrifuged ($1500 \times g$, 5 min). The supernatant fraction was discarded and Cellulysin (30 mg), Macerase (40 mg), bovine serum albumin (4 mg) and MES buffer (pH 5.2, 6mM, 3 mL) were added to the pellet. The suspension was stirred (27 °C, 2 h). Water (20 mL) was added and the suspension shaken vigorously and centrifuged ($1500 \times g$, 5 min). The supernatant fraction was discarded and replaced with an aqueous solution of sodium chloride (0.15 mol dm^{-3}). The mixture was shaken vigorously and centrifuged ($1500 \times g$, 5 min) (the method was stopped at this point for *Betula fontinalis* and *Secale cereale* pollen). The supernatant fraction was discarded and the pellet re-suspended in an aqueous solution of sodium chloride (0.15 mol dm^{-3} , 5 mL). This suspension was divided into two and added to two centrifuge tubes, each containing a two-step Percoll density gradient (each tube containing 2.5 mL each of 1.08 g mL^{-1} and 1.12 g mL^{-1} Percoll in aqueous sodium chloride solution (0.15 mol dm^{-3})). These were centrifuged ($1459 \times g$, 30 min) and the pellet collected. Yields were not recorded as they were very low (< 10 % of starting material) and the small, wet pellet could not be collected without also collecting a portion of the supernatant fraction. Sufficient material was recovered for analysis.

Table 7.3: Summary of the number of pestle cycles (x) applied to each species during enzyme treatment

Species	<i>Juglans nigra</i>	<i>Betula fontinalis</i>	<i>Secale cereale</i>
Number of pestle cycles (x) performed	10 or 30	10 or 30	10

7.2.4 Application of solutions of Rhodamine B to *Lycopodium clavatum* spores (untreated) and enzyme-treated *Betula fontinalis* pollen (untreated and enzyme-treated)

A summary of the samples prepared is presented in Table 7.4. Enzyme-treated *Betula fontinalis* pollen was prepared using the method outlined in section 7.2.3. Aqueous solutions of RhB (1×10^{-3} , 10^{-4} , 10^{-5} and 10^{-6} mol dm⁻³) were prepared and stored in the dark. Pollen or spores (100 mg) were stirred in the dark in a solution of RhB (5 mL) for 2 h. The suspension was filtered under reduced pressure and washed with water (4×25 mL). The solids were left to air-dry overnight and were stored in the dark. This method was repeated for each concentration of RhB used and was also carried out using ethanolic solutions of the same concentration (using ethanol to wash solids on the filter).

Table 7.4: Summary of pollen and spores treated with aqueous and ethanolic solutions of Rhodamine B

Species	Untreated	Enzyme-treated
<i>Lycopodium clavatum</i>	○◇	
<i>Betula fontinalis</i>	○◇	○◇

○ Pollen or spores treated with aqueous solutions of Rhodamine B

◇ Pollen or spores treated with ethanolic solutions of Rhodamine B

7.2.5 Preparation of saturated solutions of *p*-coumaric and ferulic acid (with and without Rhodamine B)

A saturated ethanolic solution of *p*-coumaric acid was prepared. Equal volumes of this solution were mixed with ethanolic solutions of RhB (1×10^{-3} , 10^{-4} , 10^{-5} and 10^{-6} mol dm⁻³). Solutions were stored in the dark prior to analysis. This was repeated with saturated ethanolic solutions of ferulic acid.

7.2.6 Addition of freeze-dried yogurt culture to enzyme-treated *Betula fontinalis* pollen

MRS broth powder (10.2 g) and TWEEN 80 (0.2 mL) were stirred at reflux in water (200 mL) until dissolved and the solution was then cooled to room temperature.¹³⁸ Freeze-dried yogurt culture (0.1 g) was added to a portion of this broth (50 mL) and the suspension was stirred at 30 °C for 2.5 h. Enzyme-treated *Betula fontinalis* pollen (17 mg, prepared as described in section 7.2.3) was added to a portion of the MRS broth containing the yogurt culture (5 mL). This suspension was stirred at 30 °C for 3 days then filtered under reduced pressure and washed with water (3×2 mL).

7.3 Techniques and analysis

7.3.1 Light microscopy

Light microscopy was carried out using an upright Zeiss Axioskop 40 microscope connected to a Lumenera INFINITYX 21 megapixel camera. Image capture and analysis was performed using Lumenera INFINITY capture software version 3.7.5.

7.3.1.1 Preparation of slides

Samples were suspended in water before being applied to glass slides. Suspensions were covered with glass cover slips. If water evaporated from the slide during analysis

(largely due to the heat of the microscope's halogen lamp), more water was applied to the slide. Water was introduced to the slide using a pipette and the water was taken up underneath the coverslip *via* capillary action (Figure 7.1). A filter paper 'wick' was applied to the edge of the coverslip to draw up any excess water. Where necessary, Ruthenium Red was used as a stain to highlight the intine of pollen grains. Where this was the case, an aqueous solution of Ruthenium Red (0.2 mol dm^{-3}) was prepared and applied in a similar fashion to the additional water.

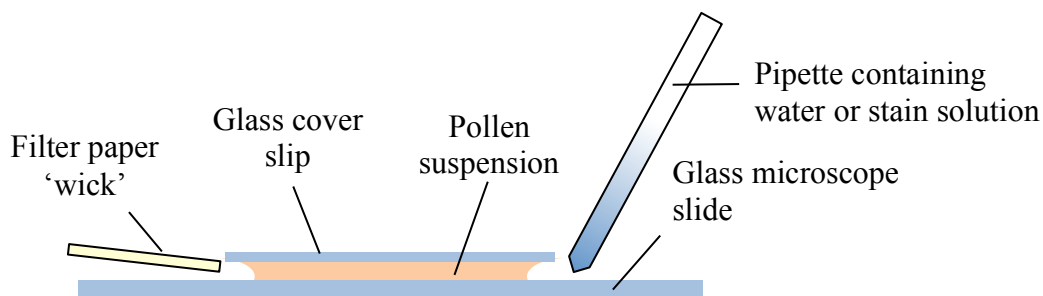


Figure 7.1: Schematic representation of the preparation of a microscope slide for light microscopy analysis and the application of water or a stain solution

7.3.2 Scanning electron microscopy

Scanning electron microscopy (SEM) was carried out on a JEOL JSM-6490LV.

7.3.2.1 Sample preparation

A double-sided adhesive strip was stuck to the top face of a conductive SEM stub. Pollen or spores to be analysed were dusted onto this tape with the aim of depositing a single layer of material. Stubs were coated with coated with gold/palladium using a sputter coater.

7.3.3 Transmission electron microscopy

Transmission electron microscopy (TEM) analysis was performed on a FEI Tecnai 12 BioTWIN, operated at 120 kV. Images were captured digitally using an Olympus MegaView III camera.

7.3.3.1 Preparation of sections

Sections for TEM analysis were prepared by Meg Stark of the Bioscience Technology Facility, The University of York. If solids did not settle to a pellet between each step, centrifugation was performed using a bench-top centrifuge, and the supernatant fraction was discarded. Pollen or spores were fixed in glutaraldehyde (2.5 %) and formaldehyde (4 %) in sodium phosphate buffer (100 mmol dm⁻³) for 7 h. Pollen or spores were washed in phosphate buffer (100 mmol dm⁻³) overnight. The solution was refreshed and the pollen or spores were washed for an additional 2 h. These were suspended in osmium tetroxide (1 %) in sodium phosphate buffer (100 mmol dm⁻³) for 2 h. Pollen or spores were dehydrated through an acetone series (25, 50, 70, 90 and 2 × 100 %), with each dehydration step taking 1 h, or if a step was left overnight, the mixture was cooled to 4 °C. Pollen or spores were infiltrated with a Spurr resin series (25, 50 and 75 %) in acetone, with each step taking 1.5 h, or if a step was left overnight, the mixture was cooled to 4 °C. Material was infiltrated with Spurr resin (100 %) over 6 h, with two resin changes being carried out during this time. The resin containing the pollen or spores was polymerised (70 °C, overnight). Sections (approximately 80 nm) were cut from the solid resin block using a Leica ultramicrotome. These were collected on copper grids with a Formvar/carbon support film and then stained.

7.3.3.2 Staining of sections

Preparation of uranyl acetate solution: A saturated solution of uranyl acetate was prepared in an ethanol/water (1:1) solution. This solution was stored in a tightly stoppered bottle in a refrigerator in the dark.

Preparation of Reynolds lead citrate: Lead nitrate (1.33 g) and sodium citrate (1.76 g) were each dissolved in recently boiled water (15 mL for each preparation). These

solutions were combined and shaken vigorously for one minute and then stirred gently for thirty minutes. Fresh, carbonate-free sodium hydroxide (8 mL, 1 mol dm⁻³) was added and the solution made up to 50 mL with recently boiled water. The solution was stored in syringes. All air was excluded and the syringes were sealed with lab film.

Staining of grids: Grids were floated on drops of uranyl acetate solution (one drop for each grid), covered to exclude light and left to stain for ten minutes. Grids were immersed in water to wash off excess stain and excess water was then removed by blotting grids on filter paper. Lead citrate solution was filtered through a Millipore filter (0.22 μm). Drops of the filtered solution were placed on a petri dish, adjacent to two pellets of sodium hydroxide (to prevent the precipitation of lead salts). Grids were floated on the drops of filtered lead citrate solution (one drop for each grid) for 10 min. Grids were immersed in water to wash off excess stain and then left to air dry. These were stored in a CO₂ free environment to prevent the precipitation of lead salts.

7.3.4 Laser scanning confocal microscopy

Laser scanning confocal microscopy (LSCM) was performed using a Zeiss LSM 710 on an Axio Observer.Z1 invert. Image collection and analysis was carried out using Zen 2009, produced by Zeiss. Single track mode was used, unless otherwise specified. To examine quenching effects, RhB-treated samples were examined in multi-track mode. This mode allows for the excitation and subsequent monitoring of more than one fluorochrome within a sample. Analysis is performed in series, as summarised in Figure 7.2. The laser strength and detector settings used were set for the RhB-treated sample and then maintained for the subsequent analysis of the equivalent sample without RhB.

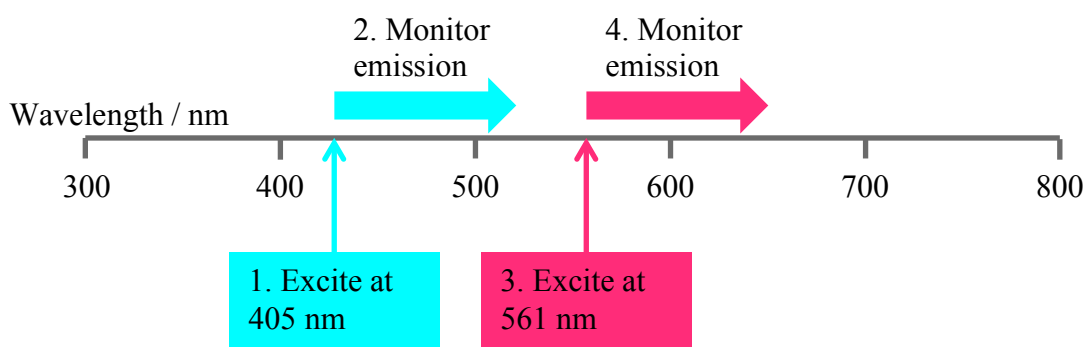


Figure 7.2: Summary of multi-track mode LSCM

7.3.4.1 Sample preparation

Samples of pollen and spores used were suspended in water. A square outline of vacuum grease (approximately 1.5×1.5 cm) was drawn onto the glass slide and a few drops of the pollen or spore suspension placed into this outline (Figure 7.3). A cover slip was placed over the suspension and grease outline, and gently pressed down, with the intention of leaving a single layer of spores or pollen grains between the slide and the cover slip.

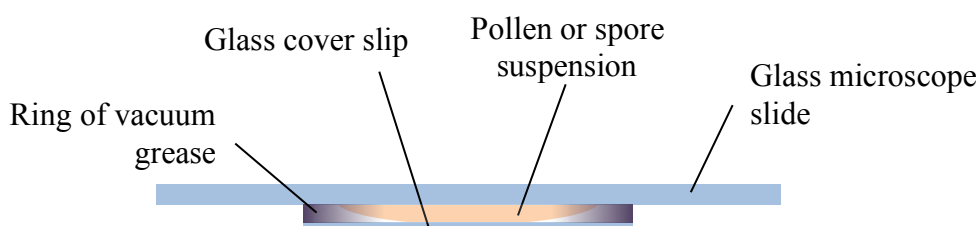


Figure 7.3: Schematic representation of the preparation of a microscope slide for laser scanning confocal microscopy

7.3.5 Spectrofluorometry

Spectrofluorometry was performed using a Hitachi F-4500 spectrofluorometer with a xenon lamp. Solid samples were analysed using a solid sample holder (part number 650-0161). During the analysis of some samples, a longpass filter (350 nm) was applied between the sample and the detector: see captions of emission spectra in section 5.4 for details of samples where this filter was used. This filter was added to avoid peaks in the spectrum resulting from scattering, rather than from the fluorescence of the sample.

7.3.5.1 Sample preparation

Liquid samples were analysed in a quartz cuvette, using a 90° excitation geometry (Figure 7.4). Solid pollen and spore samples were sandwiched between two square glass slides (approximately $2 \text{ cm} \times 2 \text{ cm}$) and secured along two edges using tape (Figure 7.5). These samples were inspected using a front-face excitation geometry (Figure 7.6).⁹⁷

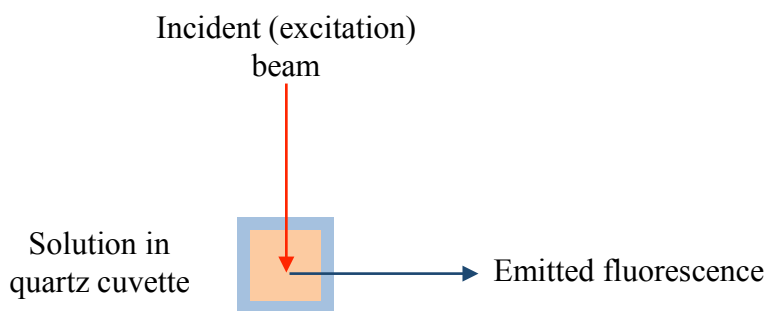


Figure 7.4: Schematic representation (aerial view) of 90 ° excitation geometry

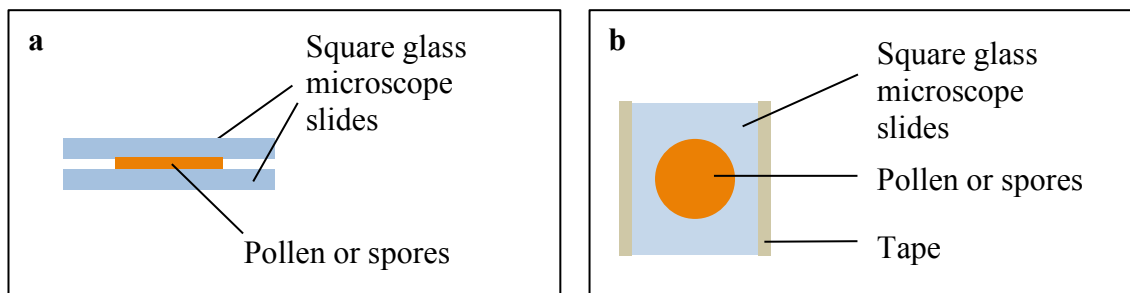


Figure 7.5: Schematic representation of the sample preparation required for front-face excitation fluorescence measurements

(a) side-on view and (b) aerial view

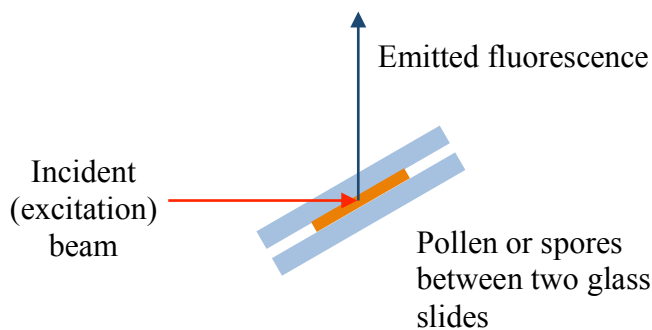


Figure 7.6: Schematic representation (aerial view) of front-face excitation geometry

Chapter 8:

Abbreviations

8 Abbreviations

Abbreviation	Definition
ALP	Alkaline phosphatase
<i>Bf</i>	<i>Betula fontinalis</i>
BSA	Bovine serum albumin
°C	Degrees Celsius
CA	<i>Para</i> -coumaric acid
CHA	Cyclohexylamine
cm	Centimetre
CRL	<i>Candida rugosa</i> lipase
DAPI	4',6-diamidino-2-phenylindole
dm	Decimetre
DNA	Deoxyribonucleic acid
ESI-QqTOF-MS	Electrospray ionisation coupled with quadrupole-quadrupole time-of-flight mass spectrometry
FA	Ferulic acid
FTIR	Fourier transform infrared
g	Gram
<i>g</i>	Relative centrifugal force
GC-MS	Gas chromatography-mass spectrometry
h	Hour
HOMO	Highest occupied molecular orbital
hPa	Hectopascal
IR	Infra-red
<i>Jn</i>	<i>Juglans nigra</i>
kb	Kilobar
kPa	Kilopascal
kV	Kilovolts
<i>Lc</i>	<i>Lycopodium clavatum</i>
LM	Light microscopy
LSCM	Laser scanning confocal microscope
LUMO	Lowest unoccupied molecular orbital
M	Molar

MALDI-ToF MS	Matrix-assisted laser desorption ionization time-of-flight mass spectrometry
MES	2-(<i>N</i> -morpholino)ethanesulfonic acid
mg	Milligram
min	Minutes
mL	Millilitre
mM	Millimolar
MMNO	4-Methylmorpholine <i>N</i> -oxide
mmol	Millimole
mol	Mole
MRI	Magnetic resonance imaging
MRS	De Man, Rogosa and Sharpe
NADH	Nicotinamide adenine dinucleotide
NADPH	Nicotinamide adenine dinucleotide phosphate
nm	Nanometre
NMR	Nuclear magnetic resonance
<i>p</i>	<i>Para</i>
PTFE	Polytetrafluoroethylene
RhB	Rhodamine B
RNA	Ribonucleic acid
rpm	Revolutions per minute
r.u.	Relative units
<i>Sc</i>	<i>Secale cereale</i>
SEM	Scanning electron microscope
sHRP	Streptavidin-horseradish peroxidase
TEM	Transmission electron microscope
UV	Ultra violet
v/v	Volume/volume
w/v	Weight /volume
w/w	Weight/weight
XPS	X-ray photoelectron spectroscopy
λ	Wavelength
μ l	Microlitre
μ m	Micrometre

Chapter 9:

References

9 References

1. E. Pacini and M. Hesse, *Flora*, 2005, **200**, 399-415.
2. R. B. Knox, *Pollen and Allergy*, Edward Arnold Ltd., London, 1979.
3. M. Hesse, in *Pollen and Pollination*, eds. A. Dafni and E. Pacini, Springer, Austria, 2000, pp. 1-17.
4. K. Krzywinski, K. Faegri, J. Iversen and P. E. Kaland, *Textbook of Pollen Analysis*, The Blackburn Press, Catldwell (N.J.), 2000.
5. S. Blackmore and I. K. Ferguson, eds., *Pollen and Spores: Form and Function*, Academic Press, London, 1986.
6. J. M. Osborn, G. El-Ghazaly and R. L. Cooper, *Plant Syst. Evol.*, 2001, **228**, 81-87.
7. B. Diethart, S. Sam and M. Weber, *Grana*, 2007, **46**, 164-175.
8. M. Weber and S. Ulrich, *Grana*, 2010, **49**, 83-90.
9. G. Erdtman, *An Introduction to Pollen Analysis*, Chronica Botanica Company, Waltham (M.A.), 1943.
10. G. Erdtman, *Pollenanalytische Untersuchungen von Torfmooren und marinen Sedimenten in Sudwest-Schweden*, Almqvist och Wicksells ; R. Friedlander und Sohn ; C. Kleincksieck, Stockholm; Berlin; Paris, 1921.
11. M. Hesse, H. Halbritter, M. Weber, R. Buchner, A. Frosch-Radivo and S. Ulrich, *Pollen Terminology: An illustrated handbook*, Springer, Austria, 2008.
12. J. B. Harborne and P. Group, *Phytochemical phylogeny: proceedings of the Phytochemical Society symposium, Bristol, April 1969*, Academic Press, 1970.
13. G. Shaw, in *Sporopollenin*, eds. J. Brooks, P. R. Grant, M. Muir, P. v. Gijzel and G. Shaw, Academic Press, London, UK, 1971, pp. 305-353.
14. F. A. Loewus, B. G. Baldi, V. R. Franceschi, L. D. Meinert and J. J. McCollum, *Plant Physiol.*, 1985, **78**, 652-654.
15. G. Shaw and A. Yeadon, *J. Chem. Soc. C*, 1966, 16-22.
16. M. G. Simpson, *Plant Systematics*, Elsevier/Academic Press, Burlington (M.A.), 2010.
17. J. R. Rowley, J. J. Skvarla and G. El-Ghazaly, *Can. J. Bot.*, 2003, **81**, 1070-1082.
18. J. M. Pettitt, *Protoplasma*, 1976, **88**, 117-131.
19. Z. Zivcova, E. Gregorova and W. Pabst, *J. Mater. Sci.*, 2007, **42**, 8760-8764.

20. M. F. Large and J. E. Braggins, *Rev. Palaeobot. Palynology*, 1990, **64**, 213-221.
21. J. Brooks and G. Shaw, *Grana*, 1978, **17**, 91-97.
22. John, *Journal fur chemie und physik*, 1814, **12**, 244-261.
23. Braconnot, *Annales de chimie et de physique*, 1829, **2**.
24. W. J. Guilford, D. M. Schneider, J. Labovitz and S. J. Opella, *Plant Physiol.*, 1988, **86**, 134-136.
25. K. E. Espelie, F. A. Loewus, R. J. Pugmire, W. R. Woolfenden, B. G. Baldi and P. H. Given, *Phytochemistry*, 1989, **28**, 751-753.
26. G. Shaw and D. C. Apperley, *Grana*, 1996, **35**, 125-127.
27. F. Ahlers, I. Thom, J. Lambert, R. Kuckuk and W. Rolf, *Phytochemistry*, 1999, **50**, 1095-1098.
28. A. R. Hemsley, W. G. Chaloner, A. C. Scott and C. J. Groombridge, *Ann. Bot.-Lon.*, 1992, **69**, 545-549.
29. M. Kawase and M. Takahashi, *Grana*, 1995, **34**, 242-245.
30. S. E. M. Moore, A. R. Hemsley, A. N. French, E. Dudley and R. P. Newton, *Protoplasma*, 2006, **228**, 151-157.
31. F. Zetzsche and K. Huggler, *Justus Liebigs Annalen der Chemie*, 1928, **461**, 89-109.
32. F. Zetzsche and O. Kälin, *Helv. Chim. Acta*, 1931, **14**, 517-519.
33. J. Heslop-Harrison, *Science*, 1968, **161**, 230-237.
34. J. Brooks and G. Shaw, *Nature*, 1968, **219**, 532-533.
35. K. Wehling, C. Niester, J. J. Boon, M. T. M. Willemse and R. Wiermann, *Planta*, 1989, **179**, 376-380.
36. M. V. Bhatt and S. U. Kulkarni, *Synthesis*, 1983, **1983**, 249-282.
37. J. W. de Leeuw, G. J. M. Versteegh and P. F. van Bergen, *Plant Ecology*, 2006, **182**, 209-233.
38. J. Rozema, R. A. Broekman, P. Blokker, B. B. Meijkamp, N. de Bakker, J. van de Staaij, A. van Beem, F. Ariese and S. M. Kars, *J. Photochem. Photobiol. B-Biol.*, 2001, **62**, 108-117.
39. P. Blokker, D. Yeloff, P. Boelen, R. A. Broekman and J. Rozema, *Anal. Chem.*, 2005, **77**, 6026-6031.
40. V. V. Roshchina, *International Journal of Spectroscopy*, 2012, **2012**, 14.
41. E. Dominguez, J. A. Mercado, M. A. Quesada and A. Heredia, *Sex. Plant Reprod.*, 1999, **12**, 171-178.

42. F. Zetzsche, P. Kalt, J. Liechti and E. Ziegler, *J. Prakt. Chem.*, 1937, **148**, 267-286.
43. W. J. Kress and D. E. Stone, *Grana*, 1982, **21**, 129-148.
44. J. Heslop-Harrison, in *International Review of Cytology, volume 107, Pollen: Cytology and Development*, eds. K. L. Giles and J. Prakash, Academic Press, London, UK, 1987, pp. 1-70.
45. A. Traverse, *Paleopalynology: Second Edition*, Springer London Limited, 2007.
46. S. Sengupta and J. R. Rowley, *Grana*, 1974, **14**, 143-151.
47. D. Southworth, *Grana Palynologica*, 1969, **9**, 5-15.
48. Y. L. Pan, S. C. Hill, R. G. Pinnick, J. M. House, R. C. Flagan and R. K. Chang, *Atmos. Environ.*, 2011, **45**, 1555-1563.
49. M. N. B. M. Driessen, M. T. M. Willemse and J. A. G. Van Luijn, *Grana*, 1989, **28**, 115-122.
50. P. van Gijzel, in *Sporopollenin*, eds. J. Brooks, P. R. Grant, M. Muir, P. v. Gijzel and G. Shaw, Academic Press, London, UK, 1971, pp. 659-685.
51. Graminex, Graminex manufacturing video, <http://www.graminex.com/video.php>, accessed 05.08.2012.
52. G. W. R. Halwas, *Pollen harvesting*, US 2006/0053686 A1, 2006
53. O. Durham, *Econ. Bot.*, 1951, **5**, 211-254.
54. S. Nilsson and J. Praglowski, *Grana*, 1978, **17**, 1-4.
55. A. R. Hemsley, A. C. Scott, P. J. Barrie and W. G. Chaloner, *Ann. Bot.-Lon.*, 1996, **78**, 83-94.
56. M. Hesse and M. Waha, *Plant Syst. Evol.*, 1989, **163**, 147-152.
57. S. Barrier, A. S. Rigby, A. Diego-Taboada, M. J. Thomasson, G. Mackenzie and S. L. Atkin, *LWT-Food Sci. Technol.*, 2010, **43**, 73-76.
58. S. Barrier, A. Diego-Taboada, M. J. Thomasson, L. Madden, J. C. Pointon, J. D. Wadhawan, S. T. Beckett, S. L. Atkin and G. Mackenzie, *J. Mater. Chem.*, 2011, **21**, 975-981.
59. A. Diego-Taboada, L. Maillet, J. H. Banoub, M. Lorch, A. S. Rigby, A. N. Boa, S. L. Atkin and G. Mackenzie, *J. Mat. Chem. B*, 2013, **1**, 707-713.
60. S. T. Beckett, G. Mackenzie and S. L. Atkin, *Exine shells*, GB 2010
61. E. Dominguez, J. A. Mercado, M. A. Quesada and A. Heredia, *Grana*, 1998, **37**, 93-96.
62. J. P. Joseleau, G. Chambat and B. Chumpitazihermoza, *Carbohydr. Res.*, 1981, **90**, 339-344.

63. H. Chanzy, B. Chumpitazi and A. Peguy, *Carbohydr. Polym.*, 1982, **2**, 35-42.
64. N. M. Tarlyn, V. R. Franceschi, J. D. Everard and F. A. Loewus, *Plant Sci.*, 1993, **90**, 219-224.
65. M. Rittscher and R. Wiermann, *Sex. Plant Reprod.*, 1988, **1**, 132-139.
66. S. Herminghaus, S. Gubatz, S. Arendt and R. Wiermann, *Z.Naturforsch.(C)*, 1988, **43**, 491-500.
67. K. S. Osthoff and R. Wiermann, *J. Plant Physiol.*, 1987, **131**, 5-15.
68. D. Southworth, *Am. J. Bot.*, 1988, **75**, 15-21.
69. A. Madene, M. Jacquot, J. Scher and S. Desobry, *Int. J. Food Sci. Tech.*, 2006, **41**, 1-21.
70. W. Wang, X. Liu, Y. Xie, H. a. Zhang, W. Yu, Y. Xiong, W. Xie and X. Ma, *J. Mater. Chem.*, 2006, **16**, 3252-3267.
71. H. Sohi, Y. Sultana and R. K. Khar, *Drug Dev. Ind. Pharm.*, 2004, **30**, 429-448.
72. S. S. Kuang, J. C. Oliveira and A. M. Crean, *Crit. Rev. Food Sci. Nutr.*, 2010, **50**, 951-968.
73. B. K. Green and L. Schleicher, *Oil-containing microscopic capsules and method of making them*, US2800457, 1957
74. S. A. Hamad, A. F. K. Dyab, S. D. Stoyanov and V. N. Paunov, *J. Mater. Chem.*, 2011, **21**, 18018-18023.
75. N. Kocak, M. Sahin and I. H. Gubbuk, *J. Inorg. Organomet. Polym. Mater.*, 2012, **22**, 852-859.
76. S. Gouin, *Trends Food Sci. Tech.*, 2004, **15**, 330-347.
77. S. T. Y. Beckett, S. L. H. Atkin and G. H. Mackenzie, *Dosage form*, US 7608270, 2009
78. S. L. H. Atkin, S. T. W. Beckett and G. H. Mackenzie, *Uses of sporopollenin*, US 2008/0188572 A1, 2008
79. M. F. Al-Omran, S. A. Al-Suwayeh, A. M. El-Helw and S. I. Saleh, *J. Microencapsulation*, 2002, **19**, 45-52.
80. M. Lorch, M. J. Thomasson, A. Diego-Taboada, S. Barrier, S. L. Atkin, G. Mackenzie and S. J. Archibald, *Chem. Commun.*, 2009, 6442-6444.
81. K. Kailasapathy, *Curr. Issues Intest. Microbiol.*, 2002, **3**, 39-48.
82. S. Cohen, T. Yoshioka, M. Lucarelli, L. H. Hwang and R. Langer, *Pharm. Res.*, 1991, **8**, 713-720.
83. R. W. Horobin and J. A. Kiernan, eds., *Conn's Biological Stains*, Taylor & Francis, Abingdon, UK, 2002.

84. H. Tutar, E. Yilmaz, E. Pehlivan and M. Yilmaz, *Int. J. Biol. Macromol.*, 2009, **45**, 315-320.
85. E. Yilmaz, M. Sezgin and M. Yilmaz, *J. Mol. Catal. B-Enzym.*, 2010, **62**, 162-168.
86. G. Shaw, M. Sykes, R. W. Humble, G. Mackenzie, D. Marsden and E. Pehlivan, *React. Polym.*, 1988, **9**, 211-217.
87. A. A. Gürten, M. Uçan, M. I. Abdullah and A. Ayar, *J. Hazard. Mater.*, 2006, **135**, 53-57.
88. M. Sahin, I. H. Gubbuk and N. Kocak, *J. Inorg. Organomet. Polym. Mater.*, 2012, **22**, 1279-1286.
89. S. Sayin, I. H. Gubbuk and M. Yilmaz, *J. Incl. Phenom. Macrocycl. Chem.*, 2013, **75**, 111-118.
90. S. Barrier, A. Lobbert, A. J. Boasman, A. N. Boa, M. Lorch, S. L. Atkin and G. Mackenzie, *Green Chem.*, 2010, **12**, 234-240.
91. J. White, *Pollen, Its Collection and Preparation for the Microscope*, Northern Biological Supplies, UK, 1999.
92. B. S. Weakley, *A Beginner's Handbook in Biological Transmission Electron Microscopy*, Churchill Livingstone, Edinburgh, 1981.
93. A. Hayat, *Principles and Techniques of Electron Microscopy: Biological Applications*, CRC Press, Cambridge, 1989.
94. S. W. Paddock, in *Confocal Microscopy: Methods and Protocols*, ed. S. W. Paddock, Humana Press, Totowa (N.J.), 1999, pp. 1-34.
95. D. J. O'Connor, D. Iacopino, D. A. Healy, D. O'Sullivan and J. R. Sodeau, *Atmos. Environ.*, 2011, **45**, 6451-6458.
96. R. Y. Tsien and A. Waggoner, in *Handbook of Biological Confocal Microscopy*, ed. J. B. Pawley, Plenum Press, New York, 1995, pp. 267-279.
97. A. Sharma and S. G. Schulman, *Introduction to Fluorescence Spectroscopy*, Wiley, New York, 1999.
98. A. J. Lawaetz and C. A. Stedmon, *Appl. Spectrosc.*, 2009, **63**, 936-940.
99. S. C. Hill, M. W. Mayo and R. K. Chang, US Army Research Laboratory, Adelphi (M.D.), 2009.
100. F. Garciasanchez, C. Carnero and A. Heredia, *J. Agric. Food. Chem.*, 1988, **36**, 80-82.
101. A. Sgarbossa and F. Lenci, *J. Fluoresc.*, 2013, **23**, 561-567.

102. P. Cariñanos, J. Emberlin, C. Galán and E. Dominguez-Vilches, *Aerobiologia*, 2000, **16**, 339-346.
103. K. Mitsumoto, K. Yabusaki and H. Aoyagi, *J. Biosci. Bioeng.*, 2009, **107**, 90-94.
104. D. Yeloff and C. Hunt, *Rev. Palaeobot. Palynology*, 2005, **133**, 203-219.
105. M. A. Palacios, E. Benito-Peña, M. Manesse, A. D. Mazzeo, C. N. LaFratta, G. M. Whitesides and D. R. Walt, *P. Natl. Acad. Sci. USA*, 2011, **108**, 16510-16514.
106. J. Wittborn, K. V. Rao, G. El-Ghazaly and J. R. Rowley, *Ann. Bot.-Lon.*, 1998, **82**, 141-145.
107. K. Uehara and S. Kurita, *Am. J. Bot.*, 1991, **78**, 24-36.
108. S. Sam, *Secale cereale in PalDat - a palynological database: Descriptions, illustrations, identification and information retrieval*, 2000 onwards, accessed 21.10.13.
109. P. Hoen, Glossary of Pollen and Spore Terminology, <http://www.pollen.mtu.edu/glos-gtx/glos-int.htm>, accessed 21.10.13.
110. A. Kalinowski, K. Winiarczyk and M. Radlowski, *Sex. Plant Reprod.*, 2002, **15**, 75-83.
111. H. Halbritter, *Juglans nigra in PalDat - a palynological database: Descriptions, illustrations, identification and information retrieval*, 2000 onwards, accessed 21.10.13.
112. G. L. Calzoni, A. Speranza, R. Caramiello, G. Piccone and P. Zannini, *Sex. Plant Reprod.*, 1990, **3**, 139-146.
113. H. Halbritter, S. Ulrich and S. Sam, *Ambrosia artemisiifolia in PalDat - a palynological database: Descriptions, illustrations, identification and information retrieval*, 2000 onwards, accessed 13.03.14.
114. H. Halbritter and B. Diethart, *Betula pendula in PalDat - a palynological database: Descriptions, illustrations, identification and information retrieval*, 2000 onwards, accessed 28.10.13.
115. H. Halbritter and B. Diethart, *Betula humilis in PalDat - a palynological database: Descriptions, illustrations, identification and information retrieval*, 2000 onwards, accessed 28.10.13.
116. S. Blackmore, J. A. J. Steinmann, P. P. Hoen and W. Punt, *Rev. Palaeobot. Palynology*, 2003, **123**, 71-98.
117. G. Erdtman, in *Handbook of Palynology: morphology - taxonomy - ecology*, Hafner Publishing Company, Copenhagen, 1969, pp. 213-216.

118. B. L. Yule, S. Roberts and J. E. A. Marshall, *Org. Geochem.*, 2000, **31**, 859-870.
119. C. Furness, personal communication, 2011
120. M. J. Balick and J. M. Beitel, *Econ. Bot.*, 1989, **43**, 373-377.
121. J. H. Wilce, *Am. Fern J.*, 1972, **62**, 65-79.
122. T. Reitsma, *Rev. Palaeobot. Palynology*, 1969, **9**, 175-202.
123. A. Diego-Taboada, P. Cousson, E. Raynaud, Y. Huang, M. Lorch, B. P. Binks, Y. Queneau, A. N. Boa, S. L. Atkin, S. T. Beckett and G. Mackenzie, *J. Mater. Chem.*, 2012, **22**, 9767-9773.
124. S. L. Atkin, S. Barrier, Z. Cui, P. D. I. Fletcher, G. Mackenzie, V. Panel, V. Sol and X. Zhang, *J. Photoch. Photobio. B*, 2011, **102**, 209-217.
125. M. Wilson, R. McNab and B. Henderson, *Bacterial Disease Mechanisms: An Introduction to Cellular Microbiology*, Cambridge University Press, Cambridge, 2002.
126. W. John, in *Aerosol Measurement: Principles, Techniques, and Applications*, eds. P. Kulkarni, P. A. Baron and K. Willeke, Wiley, Hoboken (N. J.), 2011, pp. 41-54.
127. D. Southworth, *J. Histochem.*, 1973, **21**, 73-80.
128. M. R. Bolick and S. Vogel, *Plant Syst. Evol.*, 1992, **181**, 171-178.
129. A. Huxley, M. Griffiths and M. Levy, eds., *The New RHS Dictionary of Gardening*, Macmillian, London, 1992.
130. P. Schols, K. Es, C. D'Hondt, V. Merckx, E. Smets and S. Huysmans, *Taxon*, 2004, **53**, 777-782.
131. M. Couderchet, J. Schmalfuss and P. Boger, *Pestic. Biochem. Physiol.*, 1996, **55**, 189-199.
132. K. Wilson and J. M. Walker, eds., *Principles and Techniques of Biochemistry and Molecular Biology*, Cambridge University Press, USA, 2010.
133. G. El-Ghazaly, R. Moate, M. Cresti, B. Walles, Y. Takahashi, F. Ferreira and G. Obermeyer, *Protoplasma*, 1999, **208**, 37-46.
134. C. A. Kim, M. J. Joung, S. D. Ahn, G. H. Kim, S.-Y. Kang, I.-K. You, J. Oh, H. J. Myoung, K. H. Baek and K. S. Suh, *Synth. Met.*, 2005, **151**, 181-185.
135. Y. C. Yuan, T. Yin, M. Z. Rong and M. Q. Zhang, *Express Polym. Lett.*, 2008, **2**, 238-250.
136. M. L. Harris, P. Morberg, W. J. M. Bruce and W. R. Walsh, *J. Biomech.*, 1999, **32**, 951-958.

137. J. G. Holt, ed., *Bergey's Manual of Determinative Bacteriology*, Williams & Wilkins, Baltimore, 1994.
138. J. C. De Man, M. Rogosa and M. E. Sharpe, *J. Appl. Bacteriol.*, 1960, **23**, 130-135.
139. J. C. Pommerville, *Fundamentals of Microbiology*, Jones & Bartlett Learning, Burlington (M.A.), 2013.
140. J. Marques, L. Amorim, M. Spósito, D. Marin and B. Appezzato-da-Glória, *Eur J Plant Pathol*, 2013, **136**, 35-40.
141. H. C. Huang and E. G. Kokko, *Phytopathology*, 1985, **75**, 859-865.
142. H. C. Huang, E. G. Kokko and R. S. Erickson, *Phytoparasitica*, 1997, **25**, 17-24.
143. H. C. Huang, E. G. Kokko and R. S. Erickson, *Bot. Bull. Acad. Sinica*, 1999, **40**, 101-106.
144. H. C. Huang, E. G. Kokko and J. W. Huang, *Rev. Mex. Fitopatol.*, 2003, **21**, 117-122.
145. E. Ricca and S. Cutting, *J. Nanobiotechnology*, 2003, **1**, 6.
146. L. H. Duc, H. A. Hong, N. Fairweather, E. Ricca and S. M. Cutting, *Infect. Immun.*, 2003, **71**, 2810-2818.
147. L. H. Duc and S. M. Cutting, *Expert Opin. Biol. Th.*, 2003, **3**, 1263-1270.
148. N. Q. Uyen, H. A. Hong and S. M. Cutting, *Vaccine*, 2007, **25**, 356-365.
149. G. Weber, *Biochem. J*, 1950, **47**, 114-121.
150. M. Sauer, J. Hofkens and J. Enderlein, *Handbook of Fluorescence Spectroscopy and Imaging: From Ensemble to Single Molecules*, Wiley, Weinheim, Germany, 2010.
151. G. Chichiricco and E. Pacini, *Plant Syst. Evol.*, 2008, **270**, 231-242.
152. K. F. Fang, Y. N. Wang, T. Q. Yu, L. Y. Zhang, F. Baluska, J. Samaj and J. X. Lin, *Flora*, 2008, **203**, 332-340.
153. J. L. Corriveau, N. O. Polans and A. W. Coleman, *Curr. Genet.*, 1989, **16**, 47-51.
154. J. S. Watson, M. A. Sephton, S. V. Sephton, S. Self, W. T. Fraser, B. H. Lomax, I. Gilmour, C. H. Wellman and D. J. Beerling, *Photochem. Photobiol. Sci.*, 2007, **6**, 689-694.
155. W. T. Fraser, M. A. Sephton, J. S. Watson, S. Self, B. H. Lomax, D. I. James, C. H. Wellman, T. V. Callaghan and D. J. Beerling, *Polar Res.*, 2011, **30**, 8312-8317.

156. S. H. Atkin, S. Y. Beckett and G. H. Mackenzie, *Whitened exine shells*, US 2011/0117148 A1, 2011
157. V. V. Roshchina, *J. Fluoresc.*, 2003, **13**, 403-420.
158. A. D. MacNaught and A. R. Wilkinson, *Compendium of Chemical Terminology: Iupac Recommendations*, Blackwell Scientific Publications, Oxford, 1997.
159. R. Wiermann and K. Vieth, *Protoplasma*, 1983, **118**, 230-233.
160. K. Lunau, *Plant Syst. Evol.*, 1995, **198**, 235-252.
161. A. N. Pisarevskii, S. N. Cherenkevich and V. T. Andrianov, *J. Appl. Spectrosc.*, 1966, **5**, 452-454.
162. E. V. Anslyn and D. A. Dougherty, *Modern Physical Organic Chemistry*, University Science Books, Sausalito (C.A), 2006.
163. V. Agranovski, Z. D. Ristovski, G. A. Ayoko and L. Morawska, *Aerosol Sci. Technol.*, 2004, **38**, 354-364.
164. U. Bundke, B. Reimann, B. Nillius, R. Jaenicke and H. Bingemer, *Atmos. Meas. Tech.*, 2010, **3**, 263-271.
165. W. Christian, G. Markus, P. Jutta, S. Monika and R.-G. Ute, *Nat. Protoc.*, 2013, **8**, 1535-1550.
166. R. F. Kubin and A. N. Fletcher, *J. Lumin.*, 1982, **27**, 455-462.
167. K. K. Rohatgi and G. S. Singhal, *J. Chem. Phys.*, 1966, **70**, 1695-1701.
168. K. K. Rohatgi, *J. Mol. Spectrosc.*, 1968, **27**, 545-548.
169. A. Penzkofer and W. Leupacher, *J. Lumin.*, 1987, **37**, 61-72.
170. Y. Lu and A. Penzkofer, *Chem. Phys.*, 1986, **107**, 175-184.
171. J. E. Selwyn and J. I. Steinfeld, *J. Chem. Phys.*, 1972, **76**, 762-774.
172. V. I. Yuzhakov, *Usp. Khim.*, 1992, **61**, 1114-1141.
173. M. E. Gal, G. R. Kelly and T. Kurucsev, *J. Chem. Soc. Farad. T. 2*, 1973, **69**, 395-402.
174. J. R. Lakowicz, *Principles of Fluorescence Spectroscopy*, Springer, New York, 2007.
175. J. Koziol, *Photochem. Photobiol.*, 1966, **5**, 41-54.
176. M. Sun, P. S. Song and T. A. Moore, *J. Am. Chem. Soc.*, 1972, **94**, 1730-1740.
177. M. A. Phelps, A. B. Foraker, W. Gao, J. T. Dalton and P. W. Swaan, *Mol. Pharmaceutics*, 2004, **1**, 257-266.
178. J. Mascarenhas, *Bot. Rev.*, 1975, **41**, 259-314.
179. C. J. Runions, K. H. Rensing, T. Takaso and J. N. Owens, *Am. J. Bot.*, 1999, **86**, 190-197.

180. G. Erdtman, *Handbook of Palynology: morphology - taxonomy - ecology*, Hafner Publishing Company, Copenhagen, 1969.